POLITECHNIKA GDAŃSKA

Imię i nazwisko autora rozprawy: Tomasz Ujazdowski

Dyscyplina naukowa: Automatyka, Elektronika, Elektrotechnika i Technologie Kosmiczne

ROZPRAWA DOKTORSKA

Tytuł rozprawy w języku polskim: Optymalizacja procesów biologicznych i zarządzanie pracą kilku reaktorów w oczyszczalni ścieków typu wsadowego.

Tytuł rozprawy w języku angielskim: Optimisation of biological processes and management of several reactors in a batch type wastewater treatment plant.

Promotor: *podpis*
Dr hab. inż. Robert Piotrowski, prof. uczelni
Promotor pomocniczy: *podpis*
Dr inż. Tomasz Zubowicz

Gdańsk, rok 2026

GDAŃSK UNIVERSITY OF TECHNOLOGY

The author of the doctoral dissertation: Tomasz Ujazdowski

Scientific discipline: Automation, Electronics, Electrical Engineering and Space Technologies

DOCTORAL DISSERTATION

Title of doctoral dissertation: Optimisation of biological processes and management of several reactors in a batch type wastewater treatment plant.

Title of doctoral dissertation (in Polish): Optymalizacja procesów biologicznych i zarządzanie pracą kilku reaktorów w oczyszczalni ścieków typu wsadowego.

Supervisor: *signature*
Dr hab. inż. Robert Piotrowski, prof. uczelni
Auxiliary supervisor: *signature*
Dr inż. Tomasz Zubowicz

Gdańsk, year 2026

POLITECHNIKA GDAŃSKA

OŚWIADCZENIE

Autor rozprawy doktorskiej: Tomasz Ujazdowski

Ja, niżej podpisany, oświadczam, iż jestem świadomy, że zgodnie z przepisem art. 27 ust. 1 i 2 ustawy z dnia 4 lutego 1994 r. o prawie autorskim i prawach pokrewnych (tj. Dz.U. z 2021 poz. 1062), uczelnia może korzystać z mojej rozprawy doktorskiej zatytułowanej:

Optymalizacja procesów biologicznych i zarządzanie pracą kilku reaktorów w oczyszczalni ścieków typu wsadowego.

do prowadzenia badań naukowych lub w celach dydaktycznych.[1]

Świadomy odpowiedzialności karnej z tytułu naruszenia przepisów ustawy z dnia 4 lutego 1994 r. o prawie autorskim i prawach pokrewnych i konsekwencji dyscyplinarnych określonych w ustawie Prawo o szkolnictwie wyższym i nauce (Dz.U.2021.478 tj.), a także odpowiedzialności cywilno-prawnej oświadczam, że przedkładana rozprawa doktorska została napisana przeze mnie samodzielnie.

Oświadczam, że treść rozprawy opracowana została na podstawie wyników badań prowadzonych pod kierunkiem i w ścisłej współpracy z promotorem dr. hab. inż. Robertem Piotrowskim, prof. uczelni, oraz promotorem pomocniczym dr. inż. Tomaszem Zubowiczem.

Niniejsza rozprawa doktorska nie była wcześniej podstawą żadnej innej urzędowej procedury związanej z nadaniem stopnia doktora.

Wszystkie informacje umieszczone w ww. rozprawie uzyskane ze źródeł pisanych i elektronicznych, zostały udokumentowane w wykazie literatury odpowiednimi odnośnikami, zgodnie z przepisem art. 34 ustawy o prawie autorskim i prawach pokrewnych.

Potwierdzam zgodność niniejszej wersji pracy doktorskiej z załączoną wersją elektroniczną.

Gdańsk, dnia …… ……..……..

podpis doktoranta

Ja, niżej podpisany, wyrażam zgodę na umieszczenie ww. rozprawy doktorskiej w wersji elektronicznej w otwartym, cyfrowym repozytorium instytucjonalnym Politechniki Gdańskiej.

Gdańsk, dnia …… ……..……..

podpis doktoranta

[1] Art. 27. 1. Instytucje oświatowe oraz podmioty, o których mowa w art. 7 ust. 1 pkt 1, 2 i 4–8 ustawy z dnia 20 lipca 2018 r. – Prawo o szkolnictwie wyższym i nauce, mogą na potrzeby zilustrowania treści przekazywanych w celach dydaktycznych lub w celu prowadzenia działalności naukowej korzystać z rozpowszechnionych utworów w oryginale i w tłumaczeniu oraz zwielokrotniać w tym celu rozpowszechnione drobne utwory lub fragmenty większych utworów.
2. W przypadku publicznego udostępniania utworów w taki sposób, aby każdy mógł mieć do nich dostęp w miejscu i czasie przez siebie wybranym korzystanie, o którym mowa w ust. 1, jest dozwolone wyłącznie dla ograniczonego kręgu osób uczących się, nauczających lub prowadzących badania naukowe, zidentyfikowanych przez podmioty wymienione w ust. 1.

POLITECHNIKA GDAŃSKA

STATEMENT

The author of the doctoral dissertation: Tomasz Ujazdowski

I, the undersigned, declare that I am aware that in accordance with the provisions of Art. 27 (1) and (2) of the Act of 4th February 1994 on Copyright and Related Rights (Journal of Laws of 2021, item 1062), the university may use my doctoral dissertation entitled:

Optimisation of biological processes and management of several reactors in a batch type wastewater treatment plant.

for scientific or didactic purposes.[1]

Gdańsk, …… ……..……..

signature of the PhD student

Aware of criminal liability for violations of the Act of 4th February 1994 on Copyright and Related Rights and disciplinary actions set out in the Law on Higher Education and Science (Journal of Laws 2021, item 478), as well as civil liability, I declare, that the submitted doctoral dissertation is my own work.

I declare, that the submitted doctoral dissertation is my own work performed under and in cooperation with the supervision of dr hab. inż. Robert Piotrowski, prof. uczelni, and the auxiliary supervision of dr inż. Tomasz Zubowicz.

This submitted doctoral dissertation has never before been the basis of an official procedure associated with the awarding of a PhD degree.

All the information contained in the above thesis which is derived from written and electronic sources is documented in a list of relevant literature in accordance with Art. 34 of the Copyright and Related Rights Act.

I confirm that this doctoral dissertation is identical to the attached electronic version.

Gdańsk, …… ……..……..

signature of the PhD student

I, the undersigned, agree to include an electronic version of the above doctoral dissertation in the open, institutional, digital repository of Gdańsk University of Technology.

Gdańsk, …… ……..……..

signature of the PhD student

[1] Art 27. 1. Educational institutions and entities referred to in art. 7 sec. 1 points 1, 2 and 4–8 of the Act of 20 July 2018 – Law on Higher Education and Science, may use the disseminated works in the original and in translation for the purposes of illustrating the content provided for didactic purposes or in order to conduct research activities, and to reproduce for this purpose disseminated minor works or fragments of larger works.

2. If the works are made available to the public in such a way that everyone can have access to them at the place and time selected by them, as referred to in para. 1, is allowed only for a limited group of people learning, teaching or conducting research, identified by the entities listed in paragraph 1.

POLITECHNIKA GDAŃSKA

OPIS ROZPRAWY DOKTORSKIEJ

Autor rozprawy doktorskiej: Tomasz Ujazdowski

Tytuł rozprawy doktorskiej w języku polskim: Optymalizacja procesów biologicznych i zarządzanie pracą kilku reaktorów w oczyszczalni ścieków typu wsadowego

Tytuł rozprawy w języku angielskim: Optimisation of biological processes and management of several reactors in a batch type wastewater treatment plant

Język rozprawy doktorskiej: angielski

Promotor rozprawy doktorskiej: dr hab. inż. Robert Piotrowski, prof. uczelni

Promotor pomocniczy rozprawy doktorskiej: dr inż. Tomasz Zubowicz

Streszczenie rozprawy w języku polskim:

Niniejsza rozprawa doktorska opisuje badania nad optymalizacją cyklu oczyszczania w sekwencyjnym reaktorze porcjowym oraz wprowadzeniem metod harmonogramowania zadań do biologicznej oczyszczalni ścieków typu wsadowego. Opracowany system sterowania oparto na strukturze hierarchicznej obejmującej trzy warstwy: sterowanie procesem, optymalizację procesu i zarządzanie procesem, ograniczonego do harmonogramowania pracy reaktorów. W każdej z warstw zdefiniowano i rozwiązano odpowiedni problem optymalizacji. Na potrzeby realizacji tych zadań wykorzystano zmodyfikowane modele procesów biologicznych oparte na strukturze osadu czynnego z uwzględnieniem modułów usuwania fosforu, wielowarstwowe modele sekwencyjnych reaktorów porcjowych oraz oryginalne modele opracowane na potrzeby zdefiniowania problemu harmonogramowania w rozważanej aplikacji. Zaproponowane rozwiązania obejmują między innymi: nieliniowe sterowanie predykcyjne stężeniem rozpuszczonego tlenu w fazach napowietrzania, zastosowanie stochastycznych algorytmów optymalizacji wielocelowej do wyznaczenia parametrów biologicznego cyklu oczyszczania ścieków dostosowanego do określonych warunków dopływowych, a także definicję i rozwiązanie problemu harmonogramowania zadań w kontekście zarządzania wieloma reaktorami porcjowymi na horyzoncie dwóch tygodni z uwzględnieniem zbiorników retencyjnych jako przestrzeni magazynowej. Wyniki badań potwierdzają skuteczność podejścia opartego na integracji harmonogramowania z optymalizacją procesową w zwiększaniu efektywności energetycznej i operacyjnej oczyszczalni ścieków.

Słowa kluczowe rozprawy doktorskiej w języku polskim:

harmonogramowanie zadań, optymalizacja wielocelowa, hierarchiczny system sterowania, odzyskiwanie zasobów wodnych, sekwencyjny reaktor porcjowy

POLITECHNIKA GDAŃSKA

DESCRIPTION OF DOCTORAL DISSERTATION

The Author of the doctoral dissertation: Tomasz Ujazdowski

Title of doctoral dissertation: Optimisation of biological processes and management of several reactors in a batch type wastewater treatment plant

Title of doctoral dissertation in Polish: Optymalizacja procesów biologicznych i zarządzanie pracą kilku reaktorów w oczyszczalni ścieków typu wsadowego

Language of doctoral dissertation: english

Supervisor: dr hab. inż. Robert Piotrowski, prof. uczelni

Auxiliary supervisior: dr inż. Tomasz Zubowicz

Summary of doctoral dissertation in English:

This doctoral dissertation presents research on the optimisation of the treatment cycle in a sequencing batch reactor and the introduction of task scheduling methods to a biological batch-type wastewater treatment plant. The developed control system is based on a hierarchical structure comprising three layers: process control, process optimisation, and process management, the latter limited to the scheduling of reactor operation. In each layer, a relevant optimisation problem was formulated and solved. To achieve these objectives, modified biological processes models were used, based on the activated sludge structure extended with phosphorus removal modules, as well as multilayer models of sequencing batch reactors and original models developed specifically to define the scheduling problem in the considered application. The proposed solutions include, among others, nonlinear predictive control of dissolved oxygen concentration during aeration phases, the application of stochastic multi-objective optimisation algorithms to determine the biological treatment cycle parameters adapted to specific inflow conditions, and the definition and solution of a scheduling problem for managing multiple batch reactors over a two-week horizon with retention tanks considered as storage space. The research results confirm the effectiveness of integrating scheduling with process optimisation in improving the energy and operational efficiency of the wastewater treatment plant.

Keywords of doctoral dissertation in English:

task scheduling, multi-objective optimisation, hierarchical control system, water resource recovery, sequencing batch reactor,

Pamięci mojego dziadka,
Mariana Ujazdowskiego...

Acknowledgments

I would like to express my gratitude to my supervisor, D.Sc. Robert Piotrowski, for his long-standing support, guidance, and collaboration throughout the course of my doctoral studies. His efficiency in handling formal matters and his help in smoothly managing the entire research process were invaluable.

My special thanks go to my co-supervisor, Ph.D. Tomasz Zubowicz, for his insightful discussions, support during conferences, and for countless helpful suggestions and constructive comments. I am also deeply grateful for the opportunity to collaborate on our joint research papers.

I would also like to thank D.Sc. Michał Grochowski, Head of the Department, for his continuous support to all doctoral students and for maintaining an open and friendly atmosphere in our research group.

My sincere thanks extend to all members of the Department of Intelligent Control and Decision Support Systems for creating a pleasant working environment, their advice, and the many inspiring conversations we shared over the nearly five years of my PhD journey.

I am deeply grateful to my Parents for their unwavering support, faith in my abilities, and for providing the conditions that allowed me to grow and pursue my ambitions. I love you and thank you for everything.

Dorotka, thank you for your patience, understanding, and presence. Your support has been truly invaluable.

Finally, warm and dry campfire wishes to the ŚPAM crew. Our friendship began during our studies, and together we made it through both degrees. You made the student years unforgettable, and I am truly glad that we still keep in touch. Our meetings always bring a moment of rest and laughter amidst the challenges of everyday life.

Preface

The challenges, variety of issues and unique nature of scientific research have long inspired me to continue my academic career. My particular interest in optimisation and control systems stems from their wide range of applications and the lack of monotony in the field.

The subject of my research on water resource recovery naturally stems from the scientific tradition of the Department of Intelligent Control Systems and Decision Support, where my supervisor and co-supervisor have established a strong research background in this area. Consequently, the study presented in this dissertation combines my interests in optimisation and control with the Department's expertise in wastewater treatment processes, forming the foundation for the research undertaken.

Over the five years of doctoral studies, I have had the opportunity to co-author twelve scientific papers, nine of which are directly related to the subject of this dissertation, while the remaining three resulted from additional research activities in the field of autonomous surface vehicles. This complements and expands on my current research interests.

The parts of this dissertation are based on research results that have been published or presented during the doctoral study period. These include peer-reviewed journal papers and conference papers. The respective publications contain selected results that are further elaborated, integrated, and extended in the present dissertation.

Financial support from the Gdańsk University of Technology by the DEC-43/2021/IDUB/I.3.3 grant under the Argentum Triggering Research Grants – Excellence Initiative – Research University programme is gratefully acknowledged. The funding enabled me to participate in several international conferences, providing valuable opportunities to broaden my scientific perspective and engage with the global research community.

Journal papers:

- Ujazdowski T., Piotrowski R. (2022). Task Scheduling – Review of Algorithms and Analysis of Potential Use in a Biological Wastewater Treatment Plant. *IEEE Access, 10*, 45230-45240 (ISSN: 2169-3536)
- Ujazdowski T., Zubowicz T., Piotrowski R. (2023). A comprehensive approach to SBR modelling for monitoring and control system design. *Journal of Water Process Engineering, 53*, 103774 (ISSN 2214-7144)
- Kolankowski M., Banach M., Piotrowski R., Ujazdowski T. (2023). A new approach to design control of dissolved oxygen and aeration system in SBR by applied backstepping control algorithm. *Acta Mechanica et Automatica, 17*, 605-612 (ISSN: 1898-4088)
- Ujazdowski T., Piotrowski R., Banach M. (2024). A stochastic approach for the solution of single and multi–objective optimisation problems of biological processes in sequencing batch reactor. *Journal of Process Control, 140*, 103266 (ISSN: 0959-1524)

- Ujazdowski T., Piotrowski R., Nocoń W., Stebel K., Pośpiech J. (2025). Design and comparison of PI and boundary-based predictive controller for control of aeration in activated sludge bioreactor–Simulation and laboratory research. *Journal of Process Control, 151*, 103446 (ISSN: 0959-1524)

Conference contributions:

- Ujazdowski T., Piotrowski R. (2022). Development of a decision model for solving the task scheduling of multiple Sequential Batch Reactors. Proc. of the 26th International Conference on Methods and Models in Automation and Robotics – MMAR 2022, August 22-25, 2022, Międzyzdroje, Poland
- Zubowicz T., Ujazdowski T., Klawikowska Z., Piotrowski R. (2024). An optimized dissolved oxygen concentration control in SBR with the use of adaptive and predictive control schemes. Proc. of the 22nd European Control Conference – ECC24, June 25-28, 2024, Stockholm, Sweden
- Ujazdowski T., Piotrowski R. (2024). Optimising sequencing batch reactor operation cycle planning using evolutionary algorithm. Proc. of the 28th International Conference on Methods and Models in Automation and Robotics – MMAR 2024, August 27-30, 2024, Międzyzdroje, Poland
- Ujazdowski T., Zubowicz T., Piotrowski R. (2025). Optimisation of the treated wastewater production cycle in SBR. Proc. of the 17th IFAC Symposium on Large Scale Complex Systems: Theory and Applications – LSS 2025, August 12-14, 2025, Dublin, Ireland

The wide range of topics related to control and optimisation covered in this study also allowed me to humbly appreciate the vastness of this field. In many ways, this illustrates the essence of the Dunning-Kruger effect, the more knowledge you acquire, the more clearly you see how much you still have to learn. This awareness can be both depressing and motivating, as there is always more that can be done.

Contents

List of Figures

List of Tables

List of Abbreviations

List of Major Symbols

Greek Symbols

α oxygen transfer coefficient or correction factor for wastewater quality

ε_k slack variable used to soften constraints at control interval k

ρ_ε penalty weight for constraint violation in the cost function

Σ_{SBR} SBR system model

Σ_{M} measurement subsystem (soft-sensor)

Σ_{DC} direct control subsystem (actuation interface)

Σ_{C} composite controller subsystem

Σ_{DO} aeration (DO) control subsystem

Σ_{P} pump control subsystem

Σ_{MIX} mixing control subsystem

Σ_{A} actuator subsystem

Σ_{PC} plant-wide control system

Σ_{in} input alphabet of the finite-state machine

$\phi_{i_{\mathrm{z}},i_{\mathrm{f}}}$ total flux of fraction i_{f} in layer i_{z}

$\boldsymbol{\chi}$ decision variable vector for the cycle optimisation

Roman Symbols

A reactor base area

$C_{i_{\mathrm{z}},i_{\mathrm{f}}}$ concentration of fraction i_{f} in layer i_{z}

$C_{\mathrm{in}\,i_{\mathrm{f}}}$ influent concentration of fraction i_{f}

C_{SO} dissolved oxygen (DO) concentration

$C_{\mathrm{SO\,sat}}(T)$ temperature-dependent saturation concentration of DO

$C_{\mathrm{in}}^{\mathrm{TN}}$, $C_{\mathrm{out}}^{\mathrm{TN}}$ influent and effluent total nitrogen concentrations

$C_{\mathrm{in}}^{\mathrm{TP}}$, $C_{\mathrm{out}}^{\mathrm{TP}}$ influent and effluent total phosphorus concentrations

$C_{\mathrm{in}}^{\mathrm{COD}}$, $C_{\mathrm{out}}^{\mathrm{COD}}$ influent and effluent COD concentrations

$DO(t)$ instantaneous dissolved oxygen concentration

$E(\mathcal{S})$ aggregated scheduling objective function

$E_{\mathrm{c}}(\mathcal{S})$ cost-related objective component

$E_{\mathrm{l}}(\mathcal{S})$ machine load balancing objective component

$E_{\mathrm{v}}(\mathcal{S})$ initial volume deviation objective component

$E_{\mathrm{p}}(\mathcal{S})$ penalty term related to constraint violation

$f_T(T)$ temperature correction factor from Arrhenius equation

$\mathcal{G}$ finite-state machine (FSM) representing the treatment cycle

$h(t)$ instantaneous height of liquid level in the reactor

h_{diff} immersion depth of diffusers

H prediction horizon length

i_{z} index of reactor layer (z direction)

i_{f} index of biochemical fraction

$i_{N,(\cdot)}$ nitrogen content coefficient of fraction $(\cdot)$

$i_{P,(\cdot)}$ phosphorus content coefficient of fraction $(\cdot)$

$\mathcal{J}$ set of all job types

J_k process type identifier in the k-th scheduled operation

J^* optimal value of the NMPC cost function

J_{y} output reference tracking component of the cost function

J_{u} control energy component of the cost function

$J_{\Delta u}$ control action variability component of the cost function

J_{ε} constraint violation component of the cost function

$J(\boldsymbol{z}_k)$ NMPC cost function to be minimised

$k_l a_{20}$ standard oxygen mass transfer coefficient at 20°C

$\mathbf{M}$ vector of control intervals defining the control horizon

$\mathcal{M}$ set of all machines

M_k reactor index assigned to the k-th scheduled operation

N number of reactive phase tuples within a cycle

n_{z} total number of layers in the reactor

n_{f} total number of biochemical fractions

$p(t)$ pressure in the aeration system or pipeline

p_{min} minimum opening pressure of diffusers

R_C number of aerobic phases in a cycle

S set of internal states (phases) of the FSM model

$\mathcal{S}$ set of scheduled operations over the time horizon

Q_{in} total influent flow rate

Q_{e} total treated effluent flow rate

Q_{w} total excess sludge outflow rate

Q_{mb} mixing flow rate due to bulk movement

Q_{sb} flow rate associated with sludge blanket displacement

$Q_{\mathrm{air}}(t)$ instantaneous airflow rate supplied to aeration system

$\bar{Q}_{\mathrm{air}}$ average airflow rate during a cycle

$Q_{\mathrm{air,ref}}(t)$ reference airflow rate for blower model

$r(\boldsymbol{a}, t)$ rate of production or consumption per unit volume

$r_{i_{\mathrm{f}}}(\boldsymbol{C}_{i_{\mathrm{z}}})$ reaction rate of fraction i_{f} in layer i_{z}

$R(t)$ respiration rate of microorganisms

$\overline{R}(t)$ modified respiration rate including DO limitation

R_{20} oxygen transfer rate at nominal temperature 20°C

$S_{(\cdot)}$ soluble fraction of component $(\cdot)$

SF switching function for continuous transition between layers

$T(t)$ temperature of wastewater at time t

T_{s} sampling period (algorithm time step)

T_k starting time of the k-th scheduled operation

$\boldsymbol{u}(t)$ control signal (manipulated variable) at time t

$\mathcal{U}_k$ sequence of control inputs over the control horizon starting at step k

$V_{i_{\mathrm{z}}}$ volume of layer i_{z} in the reactor

V_{CV} volume of control volume

$V_{\max}$ maximum reactor volume

$V_{\min\, i_{\mathrm{z}}}$ minimum volume of layer i_{z}

v_{s} settling velocity

v_{b} bulk velocity

v_{mb} mixing velocity in bulk flow

v_{sb} sludge blanket settling velocity

$X_{(\cdot)}$ particulate fraction of component $(\cdot)$

$\boldsymbol{x}(t)$ state vector at time t

$\mathcal{X}_k$ predicted state sequence over the horizon starting at step k

x_0 initial state at time k

$\mathbb{X}_{\mathrm{x}}$ admissible set for state variable

$\mathbb{X}_{\mathrm{u}}$ admissible set for control variable

$\mathbb{X}_{\mathrm{y}}$ admissible set for output variable

$\boldsymbol{z}_k$ decision variable vector for the NMPC quadratic programming problem

Other Symbols

$\cdot$ dot product operator

$\nabla\cdot$ divergence operator

$\mathrm{d}_{(\cdot)}$ total derivative operator

$\partial_{(\cdot)}$ partial derivative operator

Chapter 1

Introduction

This dissertation addresses the introduction of Task Scheduling (TS) to water resource recovery management in a biological Wastewater Treatment Plant (WWTP) application and examines the associated benefits and challenges. Overall, the dissertation addresses a broad spectrum of control engineering issues, from process control through process optimisation up to TS aspects related to the management of production processes at the Manufacturing Execution System (MES) layer.

The research problem aims to enhance the efficiency of wastewater treatment processes, leading to better outcomes for both the costs of the treatment process and the environment. The optimisation problems discussed are complex due to the non-linear, non-convex, and hybrid nature of the decision variables involved (binary, integer, and real). The complexity and specificity of the issue require a customised optimisation approach that considers the unique characteristics of wastewater treatment processes and their constraints. The results presented in this research work propose a hierarchical control structure containing optimisation layers.

To deliver comprehensive research documentation, this chapter is organised into five sections. Section 1.1 discusses a background problem, and consequently, a knowledge gap is identified. In Section 1.2, a problem is stated to fill the knowledge gap and the thesis and research objectives pursued to support the thesis are formulated. The justification and importance of the research are then discussed in Section 1.3. Following in Section 1.4, the methodology and the theoretical framework applied to accomplish the research objectives are given. Required sets of assumptions are given in Section 1.5.

1.1 State-of-the-Art

The multidisciplinary nature of the subject matter requires a clear identification of the framework within which the dissertation is set. The scope of the literature review is twofold. Firstly, it addresses the topic of biological wastewater treatment by introducing and explaining some of the treatment process concepts. Secondly, it looks at control strategies for such a process by examining trends and popular approaches. The structure of the state-of-the-art review itself follows the structure of the dissertation and the hierarchical, layered control system. This section presents the development of research in areas related to process modelling and the successively introduced control layers. The collection of discussed papers, in the order of their appearance, is presented with their breakdown in Fig. 1.1.

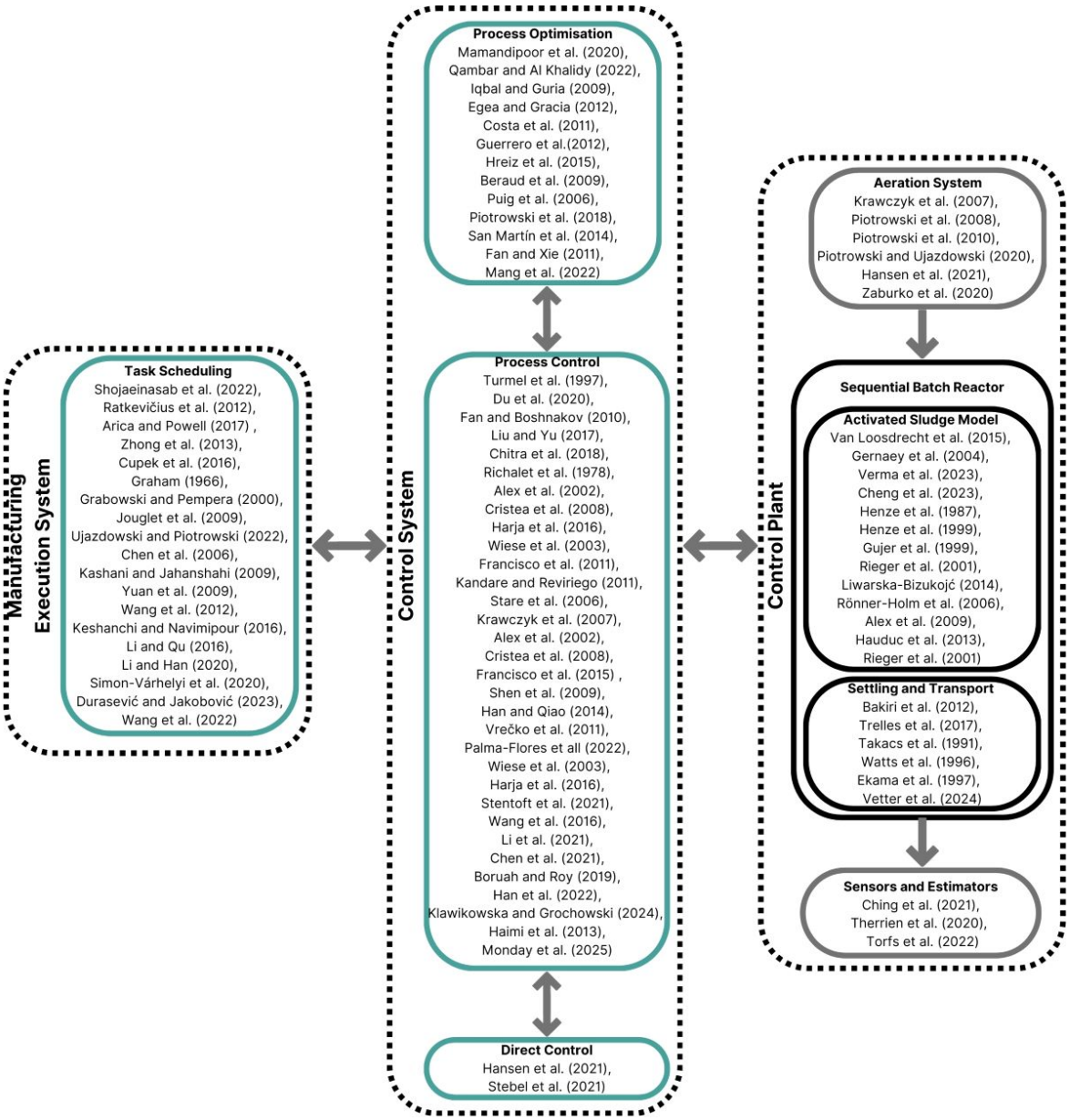

Figure 1.1: Literature review areas

The literature review is organised into three main subsections: Control Plant (Subsection 1.1.1), Control System (Subsection 1.1.2) and Manufacturing Execution System (Subsection 1.1.3). The first subsection provides an overview of the wastewater treatment process and focuses on modelling challenges. It includes research papers on Activated Sludge Model (ASM), Sequencing Batch Reactor (SBR), and the actuators as well as measurement devices relevant to the research problem. The second subsection addresses control and optimisation, outlining the decomposition of these aspects into control system layers. It briefly covers the direct control layer, followed by process control, which involves regulating the Dissolved Oxygen (DO) concentration. The process optimisation layer, meanwhile, is responsible for selecting the operating parameters of the SBR. The final subsection of the review discusses TS, which is presented in the literature as part of the MES framework.

1.1.1 Control Plant

The WWTP is a set of installations in which precisely defined mechanical, chemical, and biological processes purify water. Biological treatment removes organic compounds, nitrogen, and phosphorus. Too high content of organic compounds causes water die-off due to excessive oxygen consumption in water reservoirs. In turn, a concentration of nitrogen and phosphorus compounds that is too high leads to uncontrolled algal growth and water blooms. Li et al. (2015), highlight the importance of treatment processes noting that 3% of global electricity consumption is related to WWTP operation.

The WWTP design solutions can be classified into two groups based on processing principles, namely continuous-flow or batch-processing plants (Simon et al., 2006). Although continuous-flow plants are known to have lower installation costs and require less effort to operate, according to Dutta and Sarkar (2015), recent interest has been focused on batch processing facilities due to their flexibility in plant design and ability to treat not only municipal sewage but also industrial wastewater.

Among today's state-of-the-art technologies utilised in WWTPs, batch processing facilities, particularly those exploiting activated sludge technology through SBRs, play an increasingly important role. Hedayati Moghaddam and Sargolzaei (2015); Dionisi (2017); Masoudi et al. (2018) provides further information on this matter. Batch treatment technology has been advanced by the availability of measurement and automation solutions, resulting in improved efficiency. Ali et al. (2022) has found that using SBRs can lead to savings of more than 60% in operational costs associated with activated sludge processes.

Water Resource Recovery Facility (WRRF) is a modern term that reflects a shift in focus from treating wastewater as a waste product to recognising it as a valuable resource. A WRRF is a facility that not only treats wastewater but also recovers resources from it, such as water, energy, and nutrients. On the other hand, WWTP is a more traditional term that refers to a facility that primarily treats wastewater. A WWTP focuses on removing pollutants from wastewater to protect human health and the environment. The term WWTP typically implies a more fundamental level of treatment than a WRRF and may not include advanced treatment processes or resource recovery. The research problem under consideration is primarily concerned with treatment processes but extends them to management and optimisation problems, which fits the concept of water resource recovery more precisely.

Activated Sludge Model

Activated sludge refers to a flocculent culture of organisms that are developed under controlled conditions in aeration tanks or bioreactors as SBR. The literature provides various models to describe wastewater treatment's biological and chemical processes. These models incorporate different biological or chemical components depending on the approach taken in their development, described in detail by Van Loosdrecht et al. (2015).

Activated sludge systems began to develop in the 20th century when researchers started studying and describing the mechanisms of biological wastewater treatment. Early models primarily focused on describing the fundamental processes of organic pollutant degradation and nitrification, gradually becoming more complex and precise. Over time, additional mechanisms,

such as denitrification and biological phosphorus removal, were incorporated into the models, allowing for a more accurate representation of the actual processes occurring in WWTPs.

According to Gernaey et al. (2004), a key breakthrough came in the 1980s with the development of the ASM by the International Water Association (IWA). The ASM established a standard for describing the processes in activated sludge, including nitrification, denitrification, and organic matter degradation, making it a widely used tool in the design and optimisation of wastewater treatment plants.

In addition to the ASM, other models for biological wastewater treatment are also being developed. One example proposed by Verma et al. (2023) is the biofilm model, which describes treatment processes occurring in biofilm reactors, where microorganisms adhere to solid surfaces. Another approach is hybrid models, which combine various biological modelling techniques to better capture the complexity of processes occurring in different types of WWTPs. An example of such a system is the one described by Cheng et al. (2023).

The ASM family was initially introduced by Henze et al. (1987) among the well-known and extensively researched models. Over time, these models have undergone numerous extensions and modifications. Some components in the ASM are soluble fractions, while others belong to the group of solid particles known as particulate fractions. The behaviour of these components may involve sedimentation processes. For SBRs, the model equations typically account for anoxic and aerobic growth, respiration, and the storage of substrates as intracellular products.

In this study, two models from the ASM family were selected for review: the Activated Sludge Model no. 2d (ASM2d) (Henze et al., 1999) and the Activated Sludge Model no. 3 (ASM3) (Gujer et al., 1999) with Biological Phosphorus Removal (BioP) (Rieger et al., 2001), with additional modifications. Readers are referred to (Liwarska-Bizukojć, 2014) for more detailed insights into the ASMs and the variations among different versions.

Most of the existing literature focuses on flow-through WRRF. In contrast, the treatment process in SBRs is distinct due to the integration of sedimentation and activated sludge processes within a single reactor. Consequently, it can be inferred that this distinction impacts the process. Rönner-Holm et al. (2006) propose possible modifications to the ASM to model SBR WRRFs effectively. Furthermore, Alex et al. (2009) proposes implementing some of these modifications in the ASM3 model augmented with the BioP model.

The ASM2d represents the biological, chemical, and physical processes that occur in the activated sludge process and can be used to predict the performance of full-scale activated sludge plants. This model is based on the fundamental principles of mass balance, kinetics, and oxygen, nitrogen, phosphorus, and carbon transport in the activated sludge process. The model was described in the form of the Gujer matrix. It is a complex model describing 21 biological processes and 19 state variables, 8 of which describe soluble and 11 particulate fractions. Relative to the earlier version, this model is expanded to include phenomena accompanying phosphorus removal. The ASM2d model additionally introduces the growth of polyphosphate accumulating organisms under anoxic conditions, as described by Hauduc et al. (2013).

The ASM3 is a modified version of the Activated Sludge Model no. 1 (ASM1), which incorporates corrections to that model and additionally models storage of organic substrates as a new process. ASM3 includes the same basic processes as ASM2d, such as carbon oxidation,

nitrification and denitrification, but does not include phosphorus removal. The model consists of 13 fractions, 7 describing soluble and 6 particulate fractions. The model uses 12 processes representing hydrolysis, heterotrophic, and autotrophic organisms.

Rieger et al. (2001) propose a modified version of the ASM3 incorporating an additional BioP module to account for phosphorus transformations. The process equations of the ASM3 model were adjusted, and four new fractions related to phosphorus (one soluble and three particulate) were introduced. Additionally, eleven new process equations for the BioP module were integrated, and the Gujer matrix underwent modifications by incorporating updated coefficients following calibration.

The Lag Phase module is a proposal to improve the model with behaviour in the presence of the beginning of the aerobic phase after a prolonged anaerobic phase. Alex et al. (2009) provide details of this modification. Artificial enzymes affect the parameters of the maximum growth rate of heterotrophic organisms (aerobic growth and anoxic growth) and the maximum growth rate of autotrophic organisms. These artificial enzymes were implemented as additional system state variables; they are not part of the reactor influent and effluent fractions but are affected by sedimentation and mixing processes in the tank.

Settling and Transport

In an SBR, there are not only the biological and chemical processes described by the ASM but also the phenomena associated with sedimentation, which are closer to secondary settler models like those proposed by Bakiri et al. (2012). Due to the complexity of the models and SBR transport mechanisms, they are represented in the form of layered models. Two approaches can be distinguished: one with fewer layers of variable volume and the other with more layers of constant volume. In the first approach, during the sedimentation phase, where mixing is negligible and gravity is the dominant force, a sludge blanket is formed, observed and modelled, as described by Trelles et al. (2017). The second approach involves discretisation with constant volume along a single spatial dimension, which has been extensively discussed in the literature by Takacs et al. (1991) and Watts et al. (1996). Both groups employ sedimentation mechanisms described in the literature by various models.

Another phenomenon derived from secondary settling tanks is the sludge blanket, which forms the boundary between the solid-free medium and the sludge layer. A high concentration of suspended solids correlates with a sludge blanket (Ekama et al., 1997), indicating a particular height at which the sediment concentration changes rapidly. In variable volume models, this boundary is modelled by adjusting the boundary between the first and second layers. In models with fixed volume layers, the height of the sludge blanket is determined by considering the difference in Total Suspended Solids (TSS) concentrations between adjacent layers. The height of the sludge blanket can be used as an additional indicator to support the control of the treatment process, and an example of such a solution was proposed by Vetter et al. (2024).

Aeration System

Few studies have addressed the issue of the aeration system in SBR. One approach to this problem originates from research conducted at the department. It involves modelling the aeration system

based on electrical analogies. It was first presented in the Polish literature during the creation of the model for the Swarzewo installation in 2007 by Krawczyk et al. (2007). Subsequently, it was utilised in installations in Kartuzy (Piotrowski et al., 2008) and Nowy Dwór Gdański (Piotrowski et al., 2010). The structure of the aeration system model for control purposes was also employed to create a model for the aeration plant at Mątowskie Pastwiska (Piotrowski and Ujazdowski, 2020).

Another approach involves designing a control system utilising a non-linear model of the aeration system, as presented by Hansen et al. (2021). The article considers controlling both compressor scheduling and desired airflow. For control purposes, diffuser models were developed, represented by the relationship between airflow and pressure difference, and compressor models, represented by the relationship between pressure, power, and flow rate.

Another approach to modelling an aeration system is to use Computational Fluid Dynamics (CFD), as presented by Zaburko et al. (2020). The authors prepared a simulation that included two diffuser sections and an SBR tank. The paper shows the possibility of evaluating the aeration velocity based on the CFD model. In contrast to previous approaches, a mathematical description of the physical phenomenon was not used here. Furthermore, the study shows that diffuser shapes and velocity influence the amount of dissolved oxygen in the bioreactor and the behaviour of the suspended solids in the volume.

Sensors and Estimators

The topic of soft sensors in WWTPs was addressed in the systematic review paper by Ching et al. (2021). The review's authors highlighted the challenges faced in online monitoring of WWTP operations due to interference and failure of hardware sensors in harsh wastewater environments. The paper aimed to characterise the current status of WWTP soft sensors, analyse the advancements in their development methods and evaluate their relation to hardware technology. While a definitive state-of-the-art is challenging due to variations in different WWTPs, the review assessed the effectiveness of these methods in specific contexts based on the statistical properties of the dataset. It was found that neural networks have been the dominant methodology, but decision tree-based approaches have shown promise and robustness. The importance of adjunct statistical methods for handling multicollinearity and noise in WWTP datasets was emphasised. Furthermore, opportunities to enhance hardware sensor performance through soft sensor modelling were identified. The review, which covered 102 studies, concludes that the development and application of WWTP soft sensors have significantly increased, driven by the diverse target parameters for their development. The review also acknowledges advancements in the accuracy and durability of hardware sensors, emphasising the need for further improvements in response time for real-time monitoring and control in WWTPs.

These observations align with broader issues concerning data availability and measurement limitations in real WRRF. As noted by Therrien et al. (2020), measurement campaigns conducted on full-scale facilities remain difficult, costly and time-consuming, with some process variables unavailable for online monitoring. The authors argue that the development of advanced control and optimisation strategies for WRRFs is intrinsically linked to the accessibility of reliable data, which in turn motivates the creation of modelling approaches capable of providing high-quality

estimates of unmeasured variables. In this context, soft sensors constitute an essential layer within the data infrastructure required for WRRF operation. Similarly, Torfs et al. (2022) discuss the data-availability challenge from the perspective of the emerging transition towards digital twins in wastewater treatment field. Despite the growing interest in the concept, successful full-scale implementations remain rare.

1.1.2 Control System

Natural ecosystems have self-regulating properties. Rivers and, finally, the seas and oceans can handle a certain amount of incoming pollution. However, these processes are inefficient enough to deal with the increasing chemical pollution waste, as described by Mousavi and Khodadoost (2019). Responsible management of water resources associated with aversive degradation of aquatic environments requires regulation of the concentrations of substances discharged into the environment to prevent natural disasters and threats to the life and health of ecosystems. This enforces the need to control treatment processes, which can be implemented by simple or sophisticated methods.

A distinction can be made between the control layer focusing directly on the actuators (Direct Control), which may also involve hybrid control of individual process variables, and the process control layer (Process Control), which is responsible for regulating specific parameters and maintaining process variables within predefined operating ranges. Among the more advanced methods are those related to optimisation. These can concern the optimisation of the control of process variables or the optimisation of the parameters of the entire treatment process, for which process optimisation (Process Optimisation) is responsible.

Direct Control

In this case, the lowest layer of control, called the direct control layer, is the control of the aeration system. Depending on the treatment plant's design, such systems regulate the power of the blowers, the degrees of opening of the valves in the pipeline, or both simultaneously. From the perspective of higher control layers, e.g. DO concentration control, this layer is often treated as an actuator, is integrated into the facility model, or is ignored.

Hansen et al. (2021) propose using valve-controlled aeration system models for building controllers based on tabular flow characteristics from pressure corresponding to different valve opening degrees. The work presents so-called LookUp Table (LUT) controllers: one with feedforward control and another with feedforward and feedback control. The presented methods are compared to the traditional Proportional–Integral–Derivative (PID) control, tuned using the Zigler-Nichols method.

In some approaches, such control is combined with process control, as demonstrated by Stebel et al. (2021), where predictive on-off blower control was proposed to maintain the DO within a specified range. The authors used direct control of the actuator in a small, laboratory-scale installation, in a reactor-settling tank configuration.

Process Control

Many control methods have been applied to regulate the DO concentration in biological WWTPs, aiming to ensure the efficient execution of biological processes. Among the classic solutions, PID controllers dominated and were widely used due to their simplicity and ease of implementation (Turmel et al., 1997).

Kawail et al. (2006) propose two PID aeration control systems: one with feedback from the estimated ammonium nitrogen and the other using DO measurement. In recent years, research has continued to explore PID control, focusing on its application in new control structures, such as event-triggered control, as presented by Du et al. (2020).

Over time, it became evident that more advanced techniques, such as adaptive or fuzzy logic-based control, can better handle the non-linearity and variability of operating conditions in treatment plants. One such solution is the fuzzy controller developed by Fan and Boshnakov (2010) for DO control. Similarly, Liu and Yu (2017) proposed a strategy based on adapting PID controller parameters using fuzzy logic, while Chitra et al. (2018) introduced adaptive control for DO regulation in an experimental batch bioreactor.

Finally, Model Predictive Control (MPC) has gained significant recognition for its ability to predict future process states and optimally control the system based on a dynamic model. The subject of this dissertation focuses on optimisation solutions. Therefore, the following section provides a review of MPC applications in the context of WRRF, particularly focusing on DO concentration control.

MPC is based on optimising control on a specified time horizon using an object model. The first predictive controllers were developed in the 1970s by Richalet et al. (1978) in response to the increasing demand for control of multidimensional systems. Since then, measurement techniques, computing power and many other factors have developed. Technological evolution has also brought complex industrial problems, with economic and environmental factors forcing improvements in control techniques to ensure that losses are minimised while achieving design requirements.

The development of MPC in WWTP problems is significant; the first research works were concerned with the control of simplified systems based on selected measurements (Alex et al., 2002; Cristea et al., 2008; Harja et al., 2016); further works extended the systems with additional measurements or modelling of additional elements as (Wiese et al., 2003; Francisco et al., 2011; Kandare and Reviriego, 2011). At the same time as the development of control systems, models for control purposes were developed (Stare et al., 2006; Krawczyk et al., 2007). A review of the literature indicates that work on control in WWTPs is mainly concerned with flow-through-type WWTPs and the Benchmark Simulation Model no. 1 (BSM1) (Alex et al., 2002; Cristea et al., 2008; Francisco et al., 2011; Shen et al., 2009; Han and Qiao, 2014; Vrečko et al., 2011; Palma-Flores and Ricardez-Sandoval, 2022), only few publications are adapting the developed solutions for use in batch-type WWTPs (Wiese et al., 2003; Harja et al., 2016; Stentoft et al., 2021).

Alex et al. (2002), use of MPC to reduce peaks in ammonia nitrogen concentration for a flow-through treatment plant (BSM1), employing the ASM1 is presented. The system presented in the paper is applied to minimise the concentration ratio of one of the pollutants – Ammonium (NH_4).

Cristea et al. (2008) presents a similar problem where the application of MPC for BSM1,

ASM1 was developed. In addition to DO control, control was extended to include internal recycle flow. The paper presents a comparison of the control of a classical PID controller with the MPC for Nitrate (NO_3) and DO concentration measurements.

Another application of the MPC for BSM1 was presented by Francisco et al. (2011), where the control of both the DO concentration and the effluent ammonia concentration was implemented. The authors presented a solution for the automatic tuning of the MPC as a mixed sensitivity optimisation problem that considers both disturbance rejection and control effort objectives in the same function.

Kandare and Reviriego (2011) consider only aerobic reactors in WWTP. The authors developed adaptive predictive control of DO concentration, taking into account air pressure minimisation. This approach extends the measurement system with an additional measurement and provides the required oxygen, minimising energy consumption.

Further developments were related to the non-linear characteristics of the treatment processes. An example of such work is presented by Shen et al. (2009), where methods related to feedback by linear Dynamic Matrix Control, Quadratic Dynamic Matrix Control and Non-linear Model Predictive Control (NMPC). The research conducted in this paper also points to economic factors and presents the problem of increasing aeration costs while improving the quality of the treatment process. This paper also shows a development concerning the number of measurements, as the authors designed systems for up to five controlled variables, the concentration of NH_4, TSS, Biochemical Oxygen Demand (BOD), Chemical Oxygen Demand (COD) and Total Nitrogen (TN) in the effluent.

Vrečko et al. (2011) used a reduced non-linear mathematical process model based on a mass balance. Predictive control was compared to feedforward-PI and PI. The model was for a flow-through treatment plant, and the control was based on NH_4 concentration measurements.

A non-linear predictive DO control focusing on denitrification was presented by Han and Qiao (2014). The authors applied a non-linear model of a flow-through treatment system using a self-organising radial basis function. The control performances of this control system show that the NMPC method allows good performance in this application. Modelling of quality factors as well as entire treatment processes using neural networks is currently a developing trend (Wang et al., 2016; Li et al., 2021; Chen et al., 2021).

Another approach to consider the non-linear properties of the treatment process is proposed by Boruah and Roy (2019), who employed event-triggered NMPC. The authors used an approach in which the predictive control was not triggered cyclically, as in the classical approach, but only on certain conditions at defined control error levels. In their work, the controlled variables were DO and NO_3 concentration. The work used the BSM1 model. The event-driven triggering of the predictive control allowed the paper's authors to reduce calculations by up to almost 50% (compared to the classical NMPC approach).

Research on MPC in WWTP is also concerned with the system's behaviour under extreme, rare conditions. Francisco et al. (2015) consider an example of such work on large load disturbances. The authors conducted a study on the selection of measurements that provide effective control and then prepared two control strategies: multi-variable NMPC and decentralised NMPC with PI control for active constraints.

The next step in the development of non-linear predictive control was to extend control methods to include uncertainty consideration, like propose Palma-Flores and Ricardez-Sandoval (2022). The authors describe a method using power series expansions to create an optimisation model. The paper presents a detailed description of the method used as well as a comparison of control using PI controllers, linear MPC, as well as the proposed NMPC solution for four scenarios: effect of the control framework, impact of uncertainty, effect of tuning parameter, and effect of disturbance dynamics.

New research focuses on providing adequate robustness for predictive control. An example of such work is presented by Han et al. (2022), where a proposal for data-driven robust MPC is given for applications in WWTP (using BSM1). The model for fault-tolerant prediction of system behaviour was developed using a Fuzzy Neural Network. In this work, a combination of fuzzy logic together with neural networks was used to estimate DO concentration and nitrate nitrogen concentration.

Harja et al. (2016) propose DO concentration control for aerated bioreactor and settler treatment. Only organic matter removal was considered. In this case, the MPC output was the airflow control valve settings. In addition to the ASM1 model, a blower, pipeline and valve system model was used to represent the air delivery system to the tank. The expansion of the control object, which is the treatment plant tanks, by adding aeration system models (piping, blowers, diffusers) is also a developing trend.

Wiese et al. (2003) consider another approach to predictive control, where an operational system based on NH_4 and NO_3 measurements is presented for a treatment plant using SBR. The authors focused on determining the duration of the SBR cycle during rainfall. The control was implemented based on Case-Based Reasoning (CBR). Based on the measurements, the proposed algorithm finds similar cases that are known and available in the database. It generates a solution by adapting the solutions from the respective n cases.

An alternative way of development is to extend the objectives of predictive control by introducing ecological factors. Stentoft et al. (2021) present four WWTP management objectives related to minimising the amount of pollutants discharged into the reservoirs, minimising electricity consumption, minimising operating costs consisting of electricity and pollution taxes, and minimising the Global Warming potential. The control was designed for a biological reactor using the ASM1 model. The authors present the results of the MPC for these four different objectives, showing aeration patterns and dynamics of ammonium/nitrate concentrations in the biology tanks and the effluent.

The initial development of predictive control systems in WWTPs was related to the measurement of concentrations of single pollutants such as NH_4 and NO_3. With the evolution of computing techniques and the increased computing power of computers, control systems were extended to include additional measurements of pollutants such as Phosphate (PO_4) or multiple measurements simultaneously.

Methods have also been developed for the estimation of hard-to-measure parameters, described by Haimi et al. (2013). The organic compounds are still typically monitored by off-line laboratory measurements, of which the analysis of BOD requires several days, and COD analysis a few hours. As some parameters are not available online, modern research works are based on

estimates of qualitative parameters such as BOD, COD or TN. Estimates are based on available online sensors and additional measurements such as DO or Hydrogen potential (pH).

An alternative to the aforementioned control methods is a data-driven approach based on neural models and other Artificial Intelligence (AI) techniques. One example of such an application in the context of WWTP operation is presented in (Klawikowska and Grochowski, 2024), where control of oxygen transfer coefficients in three tanks was successfully designed using a reinforcement learning framework based on the BSM1 model.

Another AI-based method is described by Monday et al. (2025), who propose an Incremental Learning model for optimising air blower flow rates subject to treatment quality constraints. This line of research reflects a broader trend in the development of data-driven control strategies for WRRFs. However, despite their potential, machine learning techniques often face limitations in their applicability due to the lack of reliable long-term datasets and the difficulty of acquiring high-frequency, noise-free measurements. While such contributions demonstrate the potential of AI-based optimisation in wastewater treatment, research in this area remains limited.

Process Optimisation

Optimisation problems are commonly encountered in research, engineering, and everyday life. Any decision-making process that involves a choice based on existing criteria to gain benefits is an optimisation problem. In the field of optimisation, simple problems can be reduced to the fundamental task of finding the minimum or maximum value of a specific criterion. This criterion serves as a measure of performance or efficiency and guides the optimisation process. The objective is to improve the system or process being optimised by either minimising or maximising a selected criterion, while also accounting for various constraints that reflect the inherent nature of the process under consideration. These constraints may arise from physical limitations, resource availability, operational requirements, or regulatory standards. The interplay between the objective function and the constraints shapes the problem's complexity and guides the search for an optimal solution. The situation is even more complex in industrial process issues because there are always costs in addition to the quality of the final process result. Thus, two conflicting criteria arise, one to strive for the best possible outcome and the other to achieve the lowest possible process cost. A similar situation exists in WRRF, where simultaneously improving treated wastewater quality and reducing process costs naturally leads to the formulation of a Multi-Objective Optimisation (MOO) problem. Ensuring that a given oxygen trajectory is accurately tracked is one task. However, the question arises as to what this trajectory should be. The structure of the SBR cycle is known. Still, the quality of the treatment depends on the number of reaction phases, the length of the aerobic and anaerobic treatment stages, the number of chemicals added to improve the treatment process and the level of DO in the tank. The problem with conventional aeration tank control systems is that most treatment plants ignore the influent load and set the aeration blowers to a fixed DO concentration of 2.0 mg/l (Mamandipoor et al., 2020). These traditional operating systems are insensitive to influent conditions because they follow predetermined static treatment setpoints that ignore them. Modern research, such as considered by Qambar and Al Khalidy (2022), shows that varying oxygen levels according to reactor conditions gives better results and avoids excessive energy consumption for aeration. It

is, therefore, necessary to establish multiple variables for effective water treatment.

This introduces a second, higher-level optimisation layer responsible for shaping the SBR cycle and the DO characteristics during the aeration phases. This optimisation problem implies the selection of quality indicators, the development of an approach to estimate energy consumption and the satisfaction of constraints considered as water permits. Such an optimisation task can be Single-Objective Optimisation (SOO) with constraints or MOO, and the solution methods can be both deterministic and stochastic.

Optimisation entails exploring different configurations, settings, or parameters within the defined constraints to identify the optimal point, i.e. the solution to the problem that most closely meets the specified criteria. This search can be performed using various techniques, such as mathematical programming, evolutionary algorithms, or heuristic approaches. The choice of optimisation method depends on the problem's characteristics, complexity, and available resources. Optimisation methods can be broadly divided into exact (deterministic) methods, which aim to find precise solutions in a predictable manner, and stochastic methods, which use randomisation mechanisms and usually provide approximate solutions. In addition, there exists a class of deterministic approximate methods, which do not guarantee global optimality but are computationally efficient.

Optimising biological processes in a WWTP is complex yet highly significant for several key reasons. The primary objective of the optimisation is to achieve the lowest possible levels of pollutant indicators in the treated wastewater, meeting the values specified in the water permit. Simultaneously, minimising energy consumption in the treatment process is pursued. It is worth noting that the conditions in the reactor change depending on the characteristics of the wastewater inflow, which are determined by the daily cycle, weather conditions, or seasons. This variability requires dynamically adjusting the biological processes to remove pollutants effectively.

Furthermore, as mentioned earlier, the biological treatment process utilises particular microorganisms cultured in the SBR as activated sludge. Cultivating these microorganisms requires providing an appropriate environment characterised by specific physical and chemical factors. Among the fundamental technical indicators that determine the state and conditions in the treatment plant are pH, temperature, BOD, COD, TN, Total Phosphorus (TP), Food to Microorganisms (F/M) ratio, and Sludge Volume Index (SVI). Some of these components are also used to assess the quality of the treated wastewater, with COD, BOD, TN, and TP being the most commonly employed indicators.

Optimising biological processes started with flow-through WWTPs. Common optimisation objectives include biological and chemical indicators of treated wastewater quality related to regulatory permits. Another important optimisation objective is minimising energy consumption in the wastewater treatment process.

Iqbal and Guria (2009) present the optimisation of a WWTP from both single and multi-objective perspectives, making use of the Non-dominated Sorting Genetic Algorithm II (NSGA-II) algorithm and its single variant SGA-II. They were the first authors to apply MOO techniques to this field. The authors utilised a WWTP model consisting of an aeration tank and a settler. The optimisation objectives proposed by the authors were maximising the influent wastewater

flow rate, representing the plant throughput, minimising the discharge effluent BOD concentration, and minimising the plant operating cost. To achieve these objectives, the decision variables considered in the study included the mean cell residence time, hydraulic retention time, sludge recirculation ratio, and effluent overflow rate.

Following this, Egea and Gracia (2012) propose the use of advanced metaheuristics to optimise a benchmark treatment plant, showing that this approach is able to overcome the multimodality and noise problems that arise when dynamic operation is assumed. Similar methods for the optimisation of WWTP have been widely discussed by Costa et al. (2011), Guerrero et al. (2012) and Hreiz et al. (2015).

Costa et al. (2011) formulate a highly constrained two-objective problem in which minimising investment and operating costs and maximising effluent quality are simultaneously optimised. The authors used two conflicting objectives, leading to a set of Pareto optimal solutions reflecting different trade-offs between objectives. A population-based algorithm, an elite multi-objective genetic algorithm combined with a tournament technique, was used to solve the task.

Guerrero et al. (2012) propose a simulation study to design optimal control strategies for a WWTP with simultaneous biological removal of carbon, nitrogen and phosphorus. Three different control strategies were evaluated: open loop, optimised fixed setpoints for the ammonium and nitrate control loops and daily optimised setpoints. The authors used a wastewater treatment plant configuration consisting of two anaerobic reactors, one aerobic reactor and a settling tank, using ASM2d. A significant achievement of this study was introducing microbial-related failure risk (solids separation problems: swelling, foaming or rising sludge) as a component of a multi-criteria function for optimising control strategy setpoints in a wastewater treatment plant. This is the first use of such a risk assessment to achieve optimisation goals.

Another approach to multi-criteria dynamic optimisation of the operating strategy of a small wastewater treatment plant is considered by Hreiz et al. (2015). In addition, the burning of excess sludge to produce electricity to reduce operating costs was investigated. The authors focused on rigorous problem formulation and accurate modelling of phenomena to obtain physically relevant solutions. The mathematical problem has been formulated in such a way that the solution is less sensitive to (arbitrarily chosen) initial plant conditions.

A similar approach to MOO using the NSGA-II algorithm for the BSM1 flow-through treatment plant model is proposed by Beraud et al. (2009). As in the previous papers, the motivation behind using the genetic algorithm is to seek non-dominated solutions on the Pareto front. An additional strength of the paper is the extensive description of the mathematical model from both the settling tank and ASM aspects.

In contrast, the problems of biological optimisation concerning batch-type treatment plants have a much shorter history. Advanced control of biological processes in batch-type WWTP can involve determining or optimising specific process parameters, such as setting desired DO concentration trajectories. Parameters such as the duration of aerobic and anaerobic phases, the number of aerobic and anaerobic phases, or the volume of influent wastewater introduced into the reactor may also undergo optimisation.

One of the first approaches to SBR cycle optimisation was presented by Puig et al. (2006). The solution presented is based on the dynamic calculation of phase lengths based on the occurrence

of the ammonia valley phenomenon. The authors used pH and Oxygen Uptake Rate (OUR) measurements to vary the SBR cycle to provide conditions for carbon and nitrogen removal. This approach did not yet use the definition of an optimisation problem but dynamically reacted to changes in the treatment process.

A further approach, presenting a thorough view of the optimisation problem, was described by Piotrowski et al. (2018). The authors used an SBR model with the biochemical part modelled by ASM2d. The optimisation problem in this paper was to minimise energy consumption by minimising aeration duration under hard constraints in the form of water permits. The paper tests the effectiveness of five optimisation methods: two non-deterministic and three deterministic. Of the non-deterministic optimisation methods, the following were selected: $(\mu + \lambda)$ Evolutionary Strategy and the Simulated Annealing (SA) algorithm. The following deterministic optimisation methods were selected: Sequential Quadratic Programming, the Direct Method and the Branch and Bound (B&B) algorithm.

San Martín et al. (2014) consider another solution dedicated to SBRs. The authors proposed a mechanism to optimise the number of switches for two-state aeration control. Instead of DO concentration trajectories, a discrete trajectory of blower states (on/off) in the aeration system is determined. The problem considered is to calculate the number of switches and the individual length of each aerobic and anoxic phase. As in previous work for SBRs, energy minimisation was applied with non-linear constraints originating from the water permit.

Another approach to optimise biological processes in SBRs is the use of pattern recognition, as described by Fan and Xie (2011). The authors used pattern recognition to regulate the biological nitrogen and phosphorus removal process in an SBR reactor. In this way, the duration of each reaction phase was reduced to the exact time required for the existing loading conditions. The simulation results presented show that the treatment process cycle can be significantly shortened while ensuring compliance with the integrated discharge standard. As described by Beraud et al. (2009), who used observation of the pH index and measurement of DO. Furthermore, the authors implemented a control based on a fuzzy controller operating on the fuzzy premises of the aforementioned measurements.

Mang et al. (2022) consider the SBR inflow was optimised to achieve higher nitrogen removal efficiency. The optimisation was performed using the Technique of Order Preference by Similarity to the Ideal Solution (TOPSIS) with the entropy weighting method. The results indicated that the three-stage reactor filling was effective by providing the required carbon source in the anaerobic phase for nitrate removal, which improved the denitrification process.

Historically, the focus has primarily been on flow-through WWTPs, for which MOO methods have been developed, often using sludge recirculation to ensure appropriate conditions. Less research has been conducted on SBRs, initially focusing on responding dynamically to reactor processes based on measurements of additional parameters. Subsequently, studies began to optimise the duration of aerobic/anoxic phases, followed by the filling and number of fillings during the cycle. The advancement of research on SBR optimisation leads to a comprehensive understanding of the reactor cycle. The described papers encompassed topics such as energy minimisation, compliance with water regulations, and ensuring suitable conditions within the reactor for the microorganisms involved in the treatment process.

1.1.3 Manufacturing Execution System

The MES, as described by Shojaeinasab et al. (2022), are sophisticated software platforms designed to monitor, control, and optimise production processes in real-time within industrial settings. Widely recognised in industries for their ability to bridge the gap between Enterprise Resource Planning (ERP) (Ratkevičius et al., 2012) and control systems. The MES enable seamless management of production, ensuring higher efficiency, quality control, and real-time data acquisition. The MES typically cover a broad range of functionalities, from scheduling and dispatching to performance analysis and production tracking. Arica and Powell (2017) propose a taxonomy to characterise MES, highlighting key aspects such as decision support logic. Regarding real-time scheduling, the authors discuss optimisation-driven decision support, incorporating rule-based techniques introduced by Zhong et al. (2013). Arica and Powell also describe simulation-driven scheduling approaches, including multi-agent systems, with an example provided by Cupek et al. (2016). In commercial industries, MES has become an indispensable tool for optimising production workflows and reducing operational costs.

However, WRRF does not typically operate as a profit-driven enterprise. Instead, their primary goal is to ensure the treatment and safe discharge of wastewater, often under the governance of municipal or public utilities. Due to the non-revenue nature of WRRFs, advanced industrial structures like MES are rarely implemented, even though they demonstrate significant advantages in terms of operational efficiency and resource management. WRRFs could greatly benefit from such systems to enhance their process optimisation capabilities, but their adoption has been slow.

By introducing optimisation issues through the SBR management layer, we can consider tariff costs of electrical energy to minimise not only electricity consumption but also the overall cost of energy. This introduces a new layer of optimal management for multiple treatment processes, which allows for the integration of the TS problem. This approach is akin to MES frameworks (as scheduling is often placed as an important part of such a system, according to Shojaeinasab et al. (2022)), where operational decisions are optimised based on both technical and economic considerations, adapting industrial methodologies to the specific needs of WRRF operations. Thus, embedding the TS problem within the broader scope of the MES provides a structured approach for energy cost optimisation in wastewater treatment.

Task Scheduling

The TS issues are optimisation problems that aim to establish a sequence for tasks (also called jobs) execution, considering various factors such as time constraints, operation prioritisation, and interdependencies between tasks dictated by technological requirements. These issues originated with the job-shop scheduling problem, first discussed by Graham (1966). Since then, various TS problems have emerged, such as flow-shop scheduling explored by Grabowski and Pempera (2000) and Jouglet et al. (2009).

In various industries, a task represents a specific process that leads to the completion of a final product. In the realm of information technology, a task could involve executing calculations within a particular program or algorithm, either on a single processor or in a computing cloud environment. In fields like electronics and automation, tasks typically correspond to technological

processes. Additionally, tasks can pertain to ensuring the required energy supply for performing operations by system components, giving rise to Energy Harvesting issues. Furthermore, certain industries encounter Crew Scheduling problems, where tasks are defined based on the number of personnel needed to achieve a particular objective.

Optimisation problems related to plant operations and real-world industrial scenarios often fall under the category of NP-hard problems. Consequently, there is a contemporary emphasis on the development of non-deterministic algorithms to tackle these challenges effectively (Ujazdowski and Piotrowski, 2022b). Given the scarcity of papers on TS topics in the WRRF area, several noteworthy papers that illustrate the evolution of this field and the breadth of its applications will be presented at the outset. Particular attention will be devoted to the algorithms utilised in these studies.

Chen et al. (2006) consider TS in a grid environment by mapping the scheduling problem into a graph optimisation challenge. They propose a Particle Swarm Optimisation (PSO)-based algorithm, where each task-resource assignment is encoded as a particle, and the algorithm seeks the longest path in the task-resource graph. Their approach proves effective for solving TS problems, allowing for dynamic global optimisation adjustments during runtime, as the algorithm can be modified according to the resource status.

A popular approach to solving TS problems is the use of the SA algorithm, which strikes a good balance between exploration and exploitation. Kashani and Jahanshahi (2009) proposes applying SA in distributed systems. The authors compare this method with Tabu Search and the classic Genetic Algorithm (GA). The comparison demonstrates the strengths and weaknesses of each approach, showing how SA can efficiently navigate large solution spaces while preventing premature convergence in distributed scheduling environments.

Another example of an application area is the short-term hydrothermal generation scheduling problem presented by Yuan et al. (2009). The authors propose modifications to the cultural algorithm, introducing the Enhanced Cultural Algorithm, which replaces the GA with Differential Evolution. The proposed algorithm addresses the complexity of hydraulic networks, scheduling time dependencies, non-linear relationships, and water transport delays. The goal is to determine the optimal water release for hydro and thermal power generation over short horizons. The authors' experiments demonstrate the effectiveness of the proposed algorithm in solving this highly constrained optimisation problem.

Wang et al. (2012) consider the Artificial Bee Colony algorithm in the theoretical application for the flexible job-shop scheduling problem. The authors developed specialised encoding and decoding schemes, as well as effective search operators such as hybrid initialisation, crossover, mutation, local search, and population updating.

Another notable contribution relating to the cloud environment is an algorithm proposed by Keshanchi and Navimipour (2016) for assigning subtasks to processors. The authors employed a hybrid approach that integrates local search with population-based search, widely recognised as a Memetic Algorithm (MA). In this method, a GA was applied to prioritise subtasks during the exploration phase, while a simple Hill Climbing algorithm was used for local exploitation, allowing for more efficient optimisation in subtask allocation. This approach illustrates the effective use of metaheuristic techniques in TS challenges.

Li and Qu (2016) explore the use of the Cultural Genetic Algorithm to address scheduling issues in cloud computing. The authors highlight the applicability of TS in minimising time span, reducing costs, and maintaining load balance in resource utilisation after task completion. Similar to the approach of Keshanchi and Navimipour (2016), the proposed algorithm builds on the foundation of GA, but extends it by incorporating a belief space and a non-uniform mutation operator to enhance solution diversity. Li and Qu also present encoding and decoding mechanisms, as well as details on adapting the algorithm to TS problems.

Li and Han (2020), similar to Wang et al. (2012), proposes the application of the Artificial Bee Colony algorithm for solving the TS problem. The application addresses the Hybrid Flow-shop Scheduling problem and relates to the area of cloud computing. Key contributions include embedding eight perturbation structures to enhance the balance between exploration and exploitation, an adaptive perturbation structure, and a deep-exploitation function. Experimental results confirm the algorithm's robustness and efficiency, with future work focusing on improving local search, stability, and expanding the algorithm's application to dynamic cloud environments.

WRRFs are systems in which economic factors are not the predominant priority and, therefore, have not yet been the subject of TS algorithms, which are mainly used to optimise production. However, the growing trend to reduce pollution and improve environmental sustainability opens the way to introduce the scheduling problem to this type of facility and improve its performance by applying an additional layer of facility management.

This introduces another layer and extends the perspective from the treatment process to the management of multiple treatment processes. Assuming more than one SBR exists, the filling and aeration times and durations of the SBRs need to be optimised to meet the expected pollutant removal requirements from the water system.

Only a few works deal with scheduling in WRRF. The initial publications on the matter were published a couple of years ago (Simon-Várhelyi et al., 2020; Wang et al., 2022), indicating the topic's nascent stage of development and a significant knowledge gap at the intersection of the WRRF and TS control fields.

Simon-Várhelyi et al. (2020) proposed a WWTP scheduling strategy based on temporarily storing wastewater during the day and processing it during the night, for BSM1-based flow-through plant. This approach aimed to reduce electrical costs only by assuming lower energy costs at night, without considering peak-off tariffs. The authors presented several scenarios for the storage and scheduling algorithm, but it was not explained how the initial storage conditions were determined. However, this is a preliminary idea and approach to WWTP scheduling, requiring more thorough research and case studies.

The application of scheduling for SBRs was presented by Wang et al. (2022), who proposed two scheduling strategies for one day of operation of four reactors with very short treatment phases. The approach took into account peak and off-peak tariffs but did not take into account storage capacity as considered by Simon-Várhelyi et al. (2020). The solution presented promising results, and the authors pointed out the existing gap in TS studies for WWTP or WRRF. However, the studies presented are very limited in scope and have strong restrictions; for example, the assumption of constant sewage inflows can be considered a major drawback of the approach considered.

Literature studies in the area of scheduling further indicate a gap in knowledge regarding heuristic methods for solving the Unrelated Parallel Machine Scheduling Problem (UPMSP) according to Durasević and Jakobović (2023), the features of which are exhibited by the problem under consideration. The complexity of the UPMSP is significant, as it belongs to the class of NP-hard problems. This implies that finding an optimal solution within a reasonable time frame using deterministic methods is impractical due to the exponential growth of the solution space with the increase in problem size. The NP-hard nature of UPMSP makes traditional deterministic approaches inefficient and often ineffective, as they would require extensive computational resources and time, rendering them impractical for real-world applications. Therefore, the application of heuristic methods is crucial, as they provide approximate solutions within acceptable time frames and resource constraints, making them suitable for tackling the inherent complexities and variability of UPMSP.

In summary, the state-of-the-art review highlights three specific gaps that motivate this dissertation. First, most advanced control and optimisation solutions have been developed for flow-through WWTPs, and only a limited number of studies address batch-type SBR systems in a systematic way, particularly when sedimentation and aeration are integrated in a single reactor. Second, while MOO and predictive control have been explored at the process level, they are rarely combined with explicitly optimised, variable DO trajectories and have not been embedded in a hierarchical structure that links single-reactor optimisation with the coordinated operation of multiple reactors. Third, the potential of TS methods and MES-like management concepts for multi-SBR facilities remains largely unexplored, despite clear analogies to scheduling problems in production systems. These gaps define the context and necessity of the research presented in this dissertation.

1.2 Problem Formulation and Research Objectives

The contribution of this research work is to address identified gaps in knowledge regarding the applicability of scheduling strategies in the context of wastewater treatment and the optimisation of operational parameters in SBRs. The state-of-the-art review also indicates the need for solutions that consider variable reference values for DO concentration trajectories and phase structures for a single SBR. Most of the solutions discussed pertain to flow-through WWTPs, which differ in process and operational conditions from batch plants. Additionally, there is a lack of studies addressing the characteristics of WRRFs in relation to TS problems, in particular the absence of a scheduling layer applying TS methods to coordinate the operation of multiple SBRs under energy tariff and process constraints. In light of the gaps in knowledge identified in Section 1.1, the following main thesis is formulated:

T. *The introduction of a task scheduling layer for managing water resource recovery in biological wastewater treatment plants, embedded within a hierarchical control structure, enables a reduction of operational costs for multi-reactor facilities while maintaining compliance with legal requirements and effluent quality standards.*

In order to verify the thesis, two research objectives were defined as follows:

O 1. *To design an operator decision support system for biological processes in a single sequencing batch reactor by formulating and solving constrained multi-objective optimisation problems for a batch-type wastewater treatment plant. The system shall determine, among others, the number and duration of aerobic and anaerobic phases and the associated dissolved oxygen reference trajectories.*

O 2. *To design a system for the efficient and cost-aware management of several sequencing batch reactors by formulating and solving a task scheduling problem over a given time horizon, taking into account energy tariffs, storage capacity and job availability associated with wastewater inflows.*

The first objective concerns the process optimisation layer, where algorithms are developed to optimise the treatment process to meet quality criteria. This layer provides reference trajectories for the processes.

The second objective acts as a MES layer, where optimisation of the management of several reactors is carried out, providing cycle start times, allocation of reactors and cycle parameters, taking into account the operational factors of the entire treatment facility.

To achieve these objectives, the following Research Tasks (RTs) were carried out:

RT 1. *Preparation of the simulation environment: SBR and aeration system models for control design purposes.*

RT 2. *Synthesis of NMPC based on DO concentration control.*

RT 3. *Analysis of the potential use and development of MOO in an SBR phases optimisation.*

RT 4. *Development of a management system for several SBRs by solving the TS problem.*

RT 1: *Preparation of the simulation environment: SBR and aeration system models for control design purposes.*

This RT focused on the development of a simulation environment supporting the design and verification of advanced control and optimisation algorithms for SBR-based WRRFs. Utility models describing biological and biochemical processes were developed using the ASM3 model and its modifications, complemented by a dynamic model of the aeration system accounting for oxygen transfer and actuator limitations. The resulting environment enabled the generation of SBR operating schedules and the evaluation of water quality indicators, and provided a modelling basis for subsequent control and optimisation tasks.

RT 2: *Synthesis of NMPC based DO concentration control.*

This RT addressed the development and implementation of a NMPC strategy for control DO concentration in an SBR. The NMPC algorithm was formulated using a non-linear process model and explicit actuator constraints related to the aeration system. The control objective was defined as the accurate tracking of a DO reference trajectory while minimising energy consumption associated with aeration. The developed control system constituted a lower-level control layer supporting the optimisation tasks considered in subsequent research stages.

RT 3: *Analysis of the potential use and development of MOO in an SBR phases optimisation.*

This RT investigated the optimisation of biological process phases within a single SBR, with particular emphasis on multi-objective formulations. The optimisation problem was defined using mixed decision variables describing phase sequencing, phase durations, and DO set-points, and was solved using constrained MOO approaches. The objectives included minimisation of operational costs and improvement of treated effluent quality, leading to Pareto-optimal solutions in the multi-objective case. The outcomes of this task provided decision-support information for operators and constituted an upper-level optimisation layer above the DO control system.

RT 4: *Development of a management system for several SBRs by solving the TS problem.*

This RT focused on the formulation and solution of a TS problem for a WRRF comprising multiple SBRs. The facility was modelled as a multi-machine system processing batch treatment tasks subject to technological constraints, inflow availability, and energy tariff variations. Simplified reactor models, derived from the results of RT 3, were employed to ensure computational tractability over extended scheduling horizons. The developed scheduling model enabled the generation of coordinated reactor operation schedules aimed at reducing energy costs and supporting operator decision-making.

1.3 Justification of the Research Problem Undertaken in the Context of the State-of-the-Art

The research problem under consideration has significant environmental, economic, and social implications in the field of wastewater treatment and control engineering. WRRFs play a key role in water management and directly impact the environment and, thus, society.

The development of civilisation is accompanied by population growth, technological progress and, consequently, an increase in pollution generation. Until the late 18th century and the first industrial revolution, interest in environmental issues was negligible. The situation changed in the 1990s when awareness of environmental degradation and the desire to protect it gained public recognition. Today, as humanity faces the urgent challenges of climate change, pollution and declining biodiversity, environmental protection has become a critical issue. Governments, industry and individuals are actively seeking ways to mitigate and reverse the impact of human activity on the environment. In this context, green technologies, renewable energy sources, and responsible resource management are more critical than ever.

The research topic raised, related to improving water quality and increasing the efficiency of the treatment process, corresponds to the sixth Sustainable Development Goal of ensuring access to water and sanitation for all through the sustainable management of water resources described by Lee et al. (2016). The effects of climate change increase the pressure on the environmental sustainability of these systems.

Wastewater treatment systems are key urban infrastructures that remove harmful pollutants from used water, thereby preventing their release into the environment and protecting human health. As such, they are part of the group of Critical Infrastructure Systems (CIS) that are considered essential to the functioning of modern society. The reliable operation of wastewater

treatment systems is critical to maintaining a safe and healthy living environment for communities, as untreated or inadequately treated wastewater can spread disease and adversely affect ecosystems.

Biological treatment takes advantage of the metabolic reactions of living organisms to reduce the quantity of biological matter and consequently lower the level of nitrogen and phosphorus-based pollutants, leading to water recovery, details provided by Keller et al. (2001) and Wu et al. (2007). Among the state-of-the-art technologies used at WRRF today, there are batch treatment systems, especially those based on activated sludge technology inside SBR, as described by, among others: Coats and Wilson (2017), Cornejo et al. (2019) and Dutta and Sarkar (2015). It has been found that well-controlled SBR can lead to savings of more than 60% in the operating costs associated with activated sludge processes (Ali et al., 2022).

Requirements for the quality of treated wastewater are set out in the European Council Directive (1991). However, these are only legal requirements and are a general example - a required minimum level of wastewater treatment not adapted to current needs and circumstances.

Additionally, it was observed that most solutions in the literature focus on continuous-flow treatment plants, which differ significantly in both processes and operational conditions from batch-type plants. In the case of SBRs, the model represents an aerobic and anaerobic tank and a settling tank. The aeration phase is initiated according to a predetermined schedule, and even within a single treatment cycle, the reactor's conditions vary at the start of each aeration phase. This creates a need for adaptive mechanisms or models that respond to biological and chemical changes between cycles, where incoming wastewater may have varying characteristics, and within cycles as conditions change between aeration phases.

The effectiveness of treatment in SBRs depends on several factors, including the number of reaction phases, the duration of aerobic and anaerobic stages, and the amount of chemicals added to enhance the process or aeration efficiency. Modern research like Mamandipoor et al. (2020) and Qambar and Al Khalidy (2022) shows that varying oxygen levels tailored to reactor conditions give better results and avoid unnecessary energy consumption. It is, therefore, necessary to establish multiple variables for effective water treatment. The dissertation aims to fill the gap in multi-objective solutions that optimise process costs and the treated effluent quality. This includes selecting the optimal number and duration of aerobic-anaerobic sequences in SBR.

Another approach to achieving these benefits is assigning operation cycles with varying parameters tailored to real-time conditions. A key element in this optimisation is improving the operating schedule of the WRRF through solving the TS problem. While TS methods have been successfully applied in various industries, the literature review reveals a lack of models specifically addressing scheduling issues in SBR management or even in broader WWTP contexts. Furthermore, there is a scarcity of methods for establishing optimal schedules in this area that account for both efficiency and economic considerations. This gap highlights the need to develop new scheduling models and methods to enhance their management and operational efficiency in the context of SBRs.

Today, optimisation methods are not widely used in the management layers of the WRRF. Numerous papers in the literature describe the improvement of WRRF operations, considering different levels of control. Still, they apply to other control layers or do not refer to SBRs. Fur-

thermore, spreadsheet-based scheduling methods are still widely used. However, these techniques are limited to generating schedules for simple processes and often produce sub-optimal results. WRRF operators usually do not have the capacity or do not feel the need to update schedules once they have been adopted. In addition, current methods of managing multiple reactors do not consider the cost of electricity at peak and off-peak tariffs. WRRFs are systems in which economic factors are not the predominant priority and, therefore, have not yet been the subject of TS algorithms, mainly used to optimise production. However, the growing trend to reduce pollution and improve environmental sustainability opens the way to introduce the TS problem to this type of facility and improve its performance by applying an additional layer of facility management.

1.4 Research Methodology

The dissertation uses tools from various theoretical disciplines in a synergistic manner. For the design of control systems, it is important to have a good knowledge of the dynamics of the control system and its operation. Within the framework of this research work, knowledge of the dynamics of the facility is aggregated from previous research results (carried out by a research team of which the author is part) and presented in the form of a utility model of a bioreactor based on ASM2d and ASM3 with BioP. Utility models were developed in the form of Partial Differential Equations (PDEs) and based on the use of fundamental laws of physics related to the principles of conservation of mass. On the other hand, the aeration system was developed based on an electrical analogue model tuned to data from the Swarzewo WWTP.

The optimal control system was designed according to the following scheme: formulation of the optimisation problem (decision variables, constraints, and objective function), selection of the optimisation algorithm, and implementation of the algorithm. Subsequently, simulation tests were carried out on the prepared utility models for different WWTP operating scenarios. The proposed scheme applies to the control design at all considered levels of the hierarchy, as illustrated in Fig. 1.2.

The optimisation methods and tools were used to effectively handle the inherent complexities arising from the dynamic nature of the process as part of the RT 3. This involved the pursuit of algorithms to solve the optimisation problem. Particular emphasis was placed on exploring algorithms within the Evolutionary Algorithm family, given their potential suitability for tackling the complex challenges posed by the problem at hand. The selected methods were carefully evaluated and compared to determine their effectiveness and applicability in optimising the phases of the biological processes within the SBR. Examples of decision variables may include the number of alternating sequences of aerobic reaction and anaerobic reaction, the duration of the aerobic reaction, and the required level of DO concentration.

Real-world scheduling problems belong to the class of NP-hard problems and require the use of non-deterministic algorithms to find solutions effectively. In the context of solving these problems (as RT 4), suitable non-deterministic algorithms were sought. Examples of objective functions that can be used to evaluate solutions in a scheduling problem include makespan, load balancing (equal distribution of jobs across machines) and production cost minimisation.

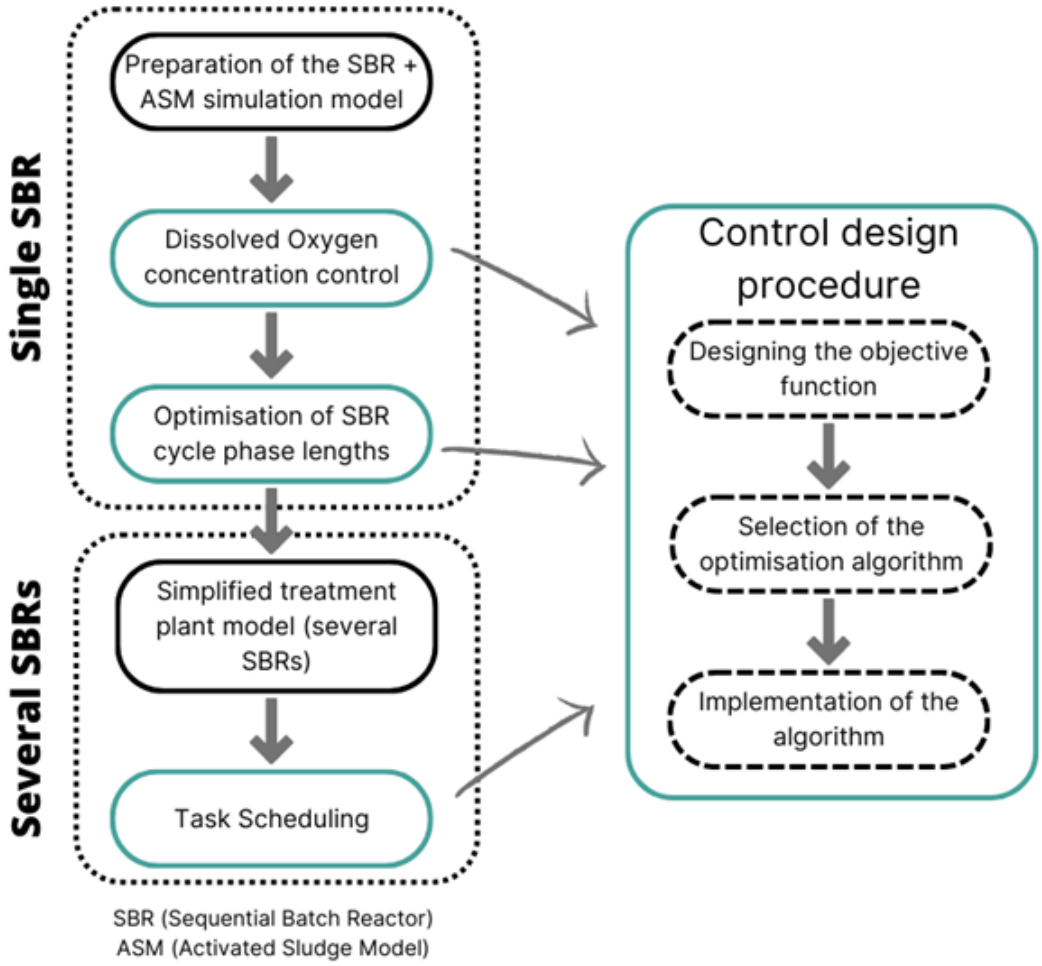

Figure 1.2: Control system design stages

Analysis of the algorithms' performance was carried out through simulations using a variety of scenarios, providing a wide range of operational conditions. The scenarios for verifying the effectiveness of control systems were developed using experience and knowledge of the control system's behaviour and relate only to the system's normal operating condition.

The algorithms under consideration were implemented and verified using the Python and MATLAB platforms. Python provides access to libraries for numerical computation (such as numpy and pandas) and evolutionary algorithms (such as the LEAP - Library for Evolutionary Algorithms). However, MATLAB offers the advanced simulation tool Simulink, which is suitable for modelling, control and optimisation of complex systems.

1.5 Assumptions

This section brings together the assumptions made in the dissertation. These concern both the modelling aspects and the simplifications used for optimisation and task scheduling issues.

Assumption 1.1. *The wastewater influent pumped into SBR is mechanically treated.*

This implies that coarse solids, grit, and other large debris, that could cause mechanical

interference, have been removed prior to entering the SBR. What follows from the technological layout of a typical batch-type WWTP.

Assumption 1.2. *No chemical enhancers are added during the SBR cycle to improve the treatment process.*

This implies that processes occurring under the effect of chemical enhancers (e.g. the use of coagulants or iron salts) are not taken into account. This assumption reduces the complexity of the problem by focusing on biological treatment.

Assumption 1.3. *The plant is considered to operate under normal operating state and conditions.*

The model being constructed neglects phenomena required for process diagnostics, which fall outside the scope of this work. This also implies that the actuators and measuring devices are fully operational.

Assumption 1.4. *The solid particles are small (with respect to the container) and have the same density.*

This implies that the geometry of particulate matter contained in the SBR is negligible and does not affect the physical and chemical phenomena being modelled.

Assumption 1.5. *The solid and fluid components of the suspension are incompressible in their pure state.*

The change in pressure does not affect the Control Volume (CV).

Assumption 1.6. *The suspension is fully mixed before settling.*

This impacts the selection of initial conditions for the spatially distributed processes included in the SBR.

Assumption 1.7. *The number of physical dimensions is reduced to a single axis aligned with the direction of gravity.*

This implies that all body forces present in the model (gravity, mixing, inflow/outflow) are considered in only one dimension.

Assumption 1.8. *The density of a component in a mixture can be defined as the concentration of that component in the mixture.*

Considering that the medium contained in the SBR is a mixture of soluble (S) and particulate (X) matter, characterised by different fractions interacting through chemical and biochemical reactions, the density (ρ) can be interpreted in terms of the mass concentration (C) for each fraction representing a pure biochemical compound.

Assumption 1.9. *During aeration or wastewater inflow to the SBR, mixing occurs spontaneously and the medium stored is well-mixed.*

This implies that the medium is well-mixed during the aeration phase and during refilling and that the fraction concentrations in the different layers of the model are the same. Therefore, the DO measurement and respiration estimation can only come from one layer because it is representative of the whole model.

Assumption 1.10. *There is no mass transfer between the solid and the fluid during sedimentation.*

This implies that the particulate and fluid phases are treated separately in the modelling of the sedimentation process.

Assumption 1.11. *Deterministic phase execution.*

Phase durations and transitions are assumed to be executed deterministically according to the design. This assumption stems from the preliminary nature of research in this field and the lack of fundamental considerations available in the existing literature. Consequently, the scope of this research is limited to the fundamental complexity of the problem.

1.6 Work Outline

This dissertation consists of eight chapters (including an Introduction and a Summary) and three Appendices (labelled A to C). The appendices complement the dissertation by presenting additional derivations to support the contributions presented in the main body. Chapter 2 describes the facility, which serves as a case study, and the technical conditions of this plant and the processes occurring there. Chapter 3 is a collection of the models used in the dissertation. These models were developed as part of RT 1–RT 4 and are required to develop the control system. Chapter 4 provides a control system architecture as an introduction to Chapters 5–6, which describe the successive layers of the system and correspond respectively to RT 2–RT 4. The numerical results obtained for the considered and designed system, based on simulation models of the plant, are presented and discussed in Chapter 7. The dissertation is summarised in Chapter 8, which furthermore indicates possible perspectives for future research.

Chapter 2

Description of Case Study Plant

A detailed description of the selected biological WWTP is presented in this chapter, including its processes and operational parameters, which serve as a reference for research and modelling. The description covers both the technical aspects of the plant and the characteristics of its processes, which will allow a better understanding of the problems and challenges of optimising control as well as management in such an environment.

The case-study facility is located in northern Poland, in the Swarzewo village area. It is managed by the Water and Sewage Company (Spółka Wodno-Ściekowa) 'Swarzewo' (see Fig. 2.1). This facility was modernised in 2018 and is a mechanical-biological-chemical treatment plant. It treats approximately 5000 m^3/d under standard conditions, increasing to nearly 14 000 m^3/d during the holiday season due to the high tourist traffic in the region. Industrial plants connected to the Swarzewo WWTP include Dagoma, BMC, Pomech, Bowil, Jantar, and PPiUR 'Szkuner'. Thus, it treats mixed wastewater from residential areas as well as from industrial establishments.

Wastewater treatment is a multistage process involving successive mechanical, biological, and chemical operations. It is assumed that the initial mechanical treatment processes are performed according to a strict technological order and are continuous, i.e., there is no need to schedule them. These processes use screens, grit chambers, or sand traps. Biological treatment takes place with the help of microorganisms that make up the activated sludge. The removal of different compounds requires different conditions in the SBR. It is worth mentioning that activated sludge in an SBR requires a regular feed of wastewater to sustain the life processes of the microorganisms. Furthermore, the efficiency of treatment also depends on the age of the sludge: excessively young sludge may not have a sufficiently developed population of microorganisms, whereas overly aged sludge exhibits reduced biological activity. As mentioned in Section 1.1, treatment with the SBR has considerable flexibility to adapt the operational parameters to the requirements of the treatment process.

The research considers SBRs with the following five distinct processing phases for the treatment of wastewater: filling (P-1), biological reactions (aerobic, anaerobic, refilling) (P-2), settlement (P-3), decantation (P-4), and an idle stage (P-0), as shown in Fig. 2.2.

In the first phase (P-1), untreated wastewater is added to the SBR, which already contains activated sludge from the previous batch of sewage. Typically, this process starts with about 25%–35% of the total volume of the reactor, which consists of activated sludge and residues from the previous cycle. In many cases, the reactor is not filled to capacity, but the influent

Figure 2.1: Biological part of the WWTP in Swarzewo (Ujazdowski and Piotrowski (2022b))

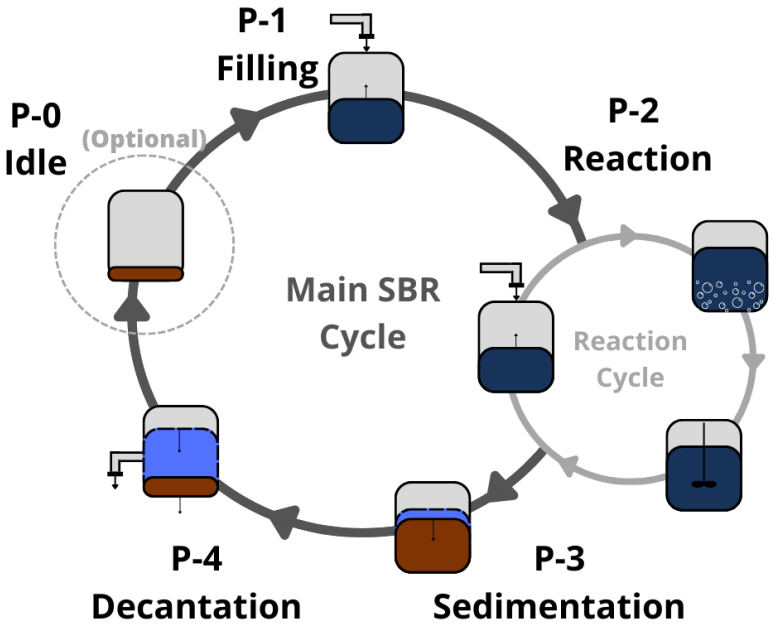

Figure 2.2: SBR Main Cycle

is refilled during the reaction phase. Next, the biological reaction phase (P-2) begins, which involves aeration and mixing that encourage the growth of microorganisms and the development of biological processes related to the treatment of sewage. This is the longest phase of the process. After the reaction phase, the treated wastewater accumulates in the upper part of the reactor, while the activated sludge, microorganisms, and remaining particulates settle at the bottom of the tank in the settlement phase (P-3). The fourth phase is decantation (P-4), which involves discharging the clarified treated effluent into a natural water reservoir, e.g. sea, river or lake. This is followed, if necessary, by the removal of excess sludge. The storage and treatment of excess sludge is a separate, extensive subject of the treatment process. Finally, the reactor enters an idle phase (P-0), which is the shortest and the least important from the perspective of the treatment process phases and is simply a waiting period before starting the next cycle. Although the specifics of each phase may vary in duration or other aspects depending on the particular case and any process optimisation, the basic characteristics of the cycle and processing phases remain consistent according to Keller et al. (2001) and Ujazdowski and Piotrowski (2022a).

Looking at the biological treatment process of SBR, it can be observed that the wastewater medium introduced into the SBR during the filling phase is retained in the reaction and settlement phases, with the decantation step taking place in the last phase (as shown in Fig. 2.2). During these stages, the essential life-sustaining elements of nitrogen and phosphorus in the molecular forms present in the wastewater medium are utilised as nutrients to promote the growth of microorganisms. This approach takes advantage of the metabolic reactions of living organisms to reduce the quantity of biological matter and consequently lower the level of nitrogen and phosphorus-based pollutants, leading to water recovery.

Nitrogen removal takes place through nitrification and denitrification. Nitrification, the initial stage, occurs under aerobic conditions and involves the conversion of ammonium nitrogen, formed during ammonification, into nitrate (III) and then into nitrate (V) with the assistance of nitrifying bacteria such as *Nitrosomonas* and *Nitrobacter*. This process has been described in detail by Silverstein and Schroeder (1983). On the other hand, denitrification is the process in which nitrate (V) is reduced to atmospheric nitrogen as described by Wu et al. (2007). This enzymatic process leads to a decrease in the nitrogen concentration within the wastewater. Notably, denitrification takes place under anaerobic conditions, where the absence of oxygen enables the conversion of nitrate (V) into its gaseous form, thus facilitating the removal of nitrogen from the wastewater.

From the perspective of this dissertation, these reactions are represented in the selected ASM models and contribute to key effluent indicators such as TN. The structure and timing of aerobic and anoxic phases in the SBR cycle, as well as the DO trajectories applied during aeration, directly influence the extent of nitrification and denitrification and thus become natural decision variables for optimisation and control.

The reduction of phosphorus compounds in the wastewater treatment process can take place in two ways: biologically or chemically. Dephosphatation is the process of biological phosphorus removal. It occurs in two stages, similar to the nitrogen removal process, but it starts with an anaerobic phase. During anaerobic conditions in the reactor, Polyphosphate-accumulating organisms (PAO) used in the phosphorus removal process, such as *Candidatus Accumulibacter*

phosphates bacteria, release polyphosphates into the wastewater and take up volatile fatty acids, leading to an increase in phosphorus concentration in the medium. This release of polyphosphates allows the bacteria to store energy in the form of polyhydroxyalkanoates. Subsequently, in the aerobic phase, these bacteria oxidise the stored polyhydroxyalkanoates and use them as an energy source to take up large quantities of phosphate from the wastewater, which is then stored intracellularly as polyphosphate. This enables them to satisfy their vital functions and allows for an increase in the biomass comprising these bacteria. The second part of this process is so intensive that it draws more phosphorus from the wastewater than is produced in the anaerobic phase, thus allowing a reduction in the amount of phosphorus in the treated wastewater. Details of the phosphorus treatment process are given by Kuba et al. (1997).

In the context of the present work, these phenomena are modelled using the BioP extensions for ASM3, and the resulting TP in the effluent is another of the quality indicators considered in optimisation tasks. The ability to alternate anaerobic and aerobic conditions within the SBR cycle makes the design of phase sequences and aeration patterns a powerful lever for enhancing biological phosphorus removal.

Generally, the biological treatment process can be supported by the dosing of coagulants. This is a common practice, but it increases the cost of the treatment process and consumes chemical resources. The chemical method involves binding phosphorus by precipitating sludge in the form of insoluble salts of metal phosphates such as iron, aluminium or calcium. These substances are delivered to the wastewater in the form of soluble salt substances. The Swarzewo facility employs this chemical method for phosphorus reduction, using ferrous sulfate (II) for phosphate coagulation. The dissertation considers increasing the efficiency of the biological treatment process. Therefore, based on the Assumption 1.1 and Assumption 1.2, only the biological part of WRRF is considered.

The risk of inadequate treatment, or of discharging pollutants directly into natural receivers, bypassing the process, is increased concentrations of pollutants in the water, which can manifest itself differently depending on the composition of the wastewater. High concentrations of organic compounds in the water can be harmful as they cause a depletion of oxygen in water reservoirs, leading to water die-off. Similarly, high levels of nitrogen and phosphorus compounds can result in the uncontrolled growth of algae and water blooms. Uncontrolled algal growth can also harm aquatic organisms by reducing the amount of light, oxygen, and nutrients available in the water.

Swarzewo WWTP consists of six SBRs (three small: SBR1 – SBR3 and three large: SBR4 – SBR6). Small tanks have a capacity of about 5000 m^3 and a diameter of 30 m. The large ones, on the other hand, have a capacity of about 6500 m^3, and their diameter is 34 m. All tanks have the same height of 7 m. In addition, the Swarzewo facility includes a retention tank and a stormwater retention lagoon, which provide an additional buffer during excessive inflow to the plant. The retention tank's dimensions are the same as those of the large SBR, and it is connected via a pump system to the mechanical treatment installation and the SBRs. The lagoon is square-shaped, with a side length of 60 m and a depth of approximately 4.5 m, resulting in a total capacity of 16 200 m^3. After the treatment process, the contents of the SBR reactors flow into one of two stabilisation ponds, where sedimentation of the remaining activated sludge occurs, along with further wastewater treatment by algae and zooplankton. One stabilisation

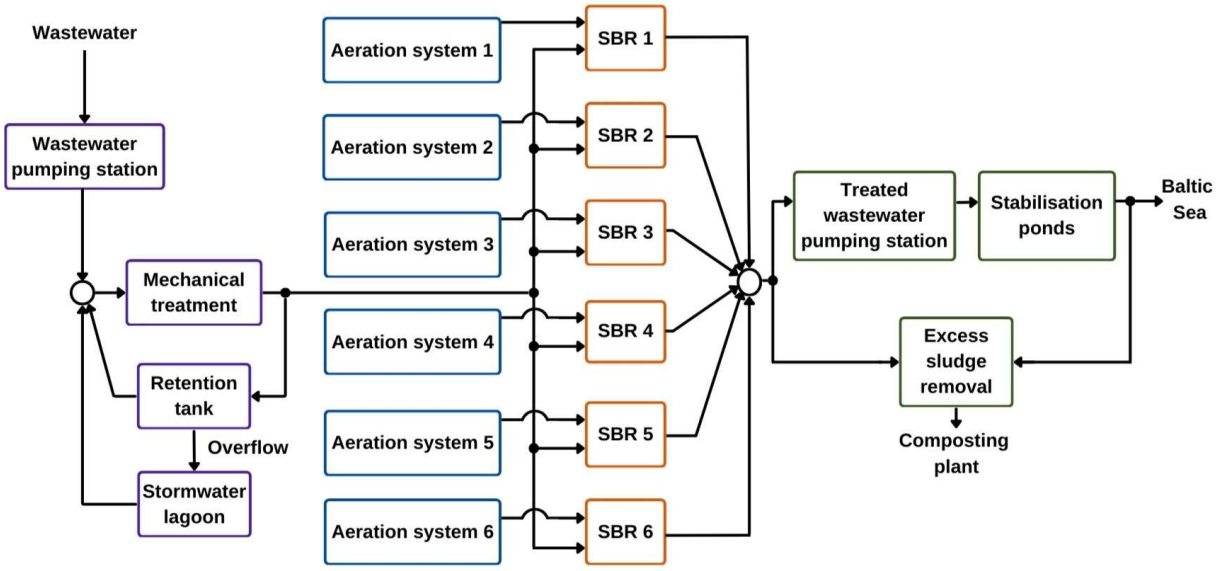

Figure 2.3: Technological scheme of the WWTP in Swarzewo

pond measures 90 m by 60 m, while the other is 115 m by 70 m. Both ponds have a depth of 2.5 m. The clarified wastewater is then discharged into the open sea. The geometric and volumetric parameters used in the subsequent analyses are summarised in tabular form in Chapter 7.

Unlike flow-through systems, this type of facility does not include elements such as a secondary clarifier, sludge recirculation system, or division of aeration chambers into anaerobic, anoxic, and aerobic zones. The operating cycle of the treatment plant in the SBR system necessitates batch wastewater treatment. Each reactor is equipped with essential components, such as an aeration grid for activated sludge bacteria, mixers for mixing wastewater and bacteria, and automatic gates for controlling the inflow of raw wastewater, the outflow of treated wastewater, and the removal of excess sludge. Additionally, the system has a control and measurement apparatus to monitor the process.

Air is supplied to the reactors from the aeration system. Each reactor has its own installation. The technological scheme is shown in Fig. 2.3. Depending on the size of the reactor, blowers with a capacity of 115 kW (for small SBR) or 150 kW (for large SBR) are used. The blowers are from the same manufacturer and have similar operating characteristics but different power outputs. This arrangement allows for separate control of the phases of each of the reactors. The aeration system also includes diffuser installations. Each small reactor has two branches, with the left branch consisting of 616 diffusers and the right branch consisting of 600 diffusers. The diffusers open when the pressure exceeds 2 kPa. In large reactors, both branches have 900 diffusers each, and the diffusers open when the pressure exceeds 1.5 kPa. Under Assumption 1.3, full availability of the actuators and their normal operation are considered.

The amount of pollution in summer is even three times higher than in other seasons. In summer, the quality requirements for treated wastewater also change. Information on acceptable pollutant concentration levels in treated wastewater is presented in European and Polish standards. The values compliant with the water permit for the Swarzewo treatment plant are presented in Table 2.1.

The cost of wastewater treatment is closely linked to electricity prices. Currently, there is a

Table 2.1: Maximum pollutant concentrations in effluent

Pollutant load factor	Maximum permitted value	Unit
Chemical oxygen demand (COD)	125	g O_2/m^3
Total nitrogen (TN)	10 (from July 1 to August 31) 15 (for the rest of the year)	g N/m^3
Total phosphorus (TP)	1 (from July 1 to August 31) 2 (for the rest of the year)	g P/m^3

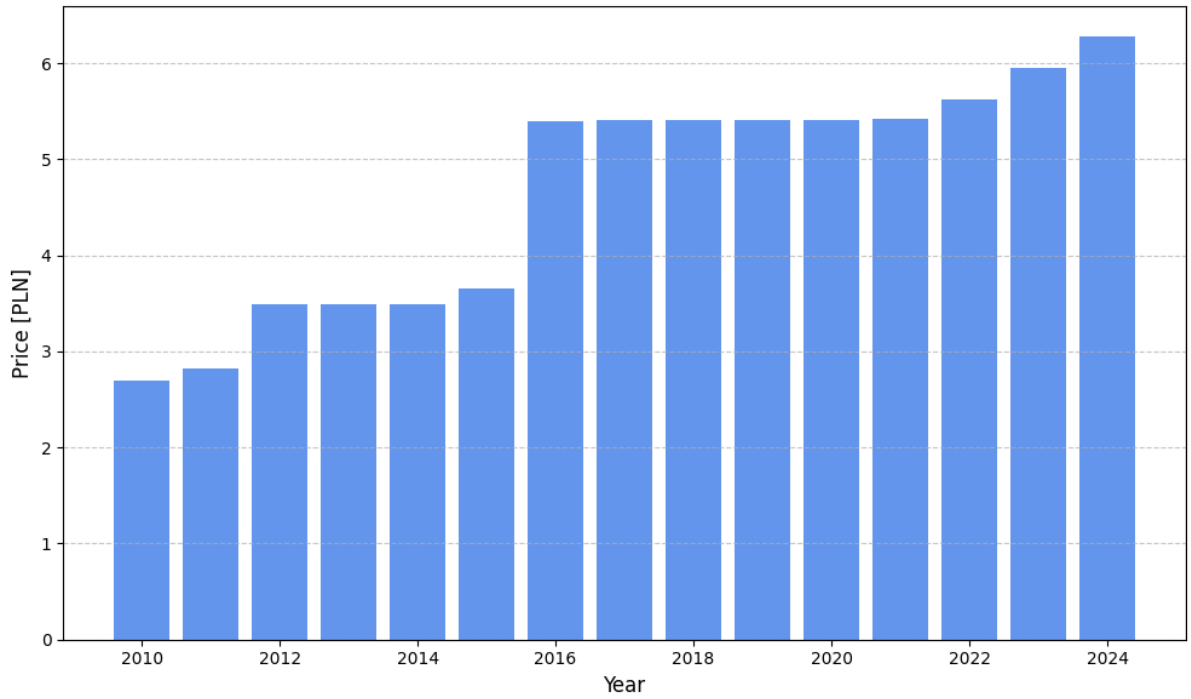

Figure 2.4: Price for wastewater treatment of 1 m^3 – Swarzewo Wastewater Treatment Plant

noticeable increase in the cost of electricity due to the current situation in European markets. Consequently, the overall cost of the treatment process has increased substantially, as illustrated in Fig. 2.4. Data presented by the Water and Sewage Company 'Swarzewo' (Spółka Wodno-Ściekowa "SWARZEWO", 2025) shows that the price of treating 1 m^3 of wastewater since 2010 has increased from PLN 2.69 to PLN 6.28. Which, with a standard inflow, currently exceeds 30 000 PLN per day.

The Swarzewo WWTP exhibits several features that make it particularly suitable as a case study for advanced control, optimisation and scheduling. First, the facility comprises six SBRs of two different sizes, a retention tank and a stormwater lagoon, which together form a multi-reactor system with non-trivial hydraulic interactions. Second, the plant treats mixed municipal and industrial wastewater, and the daily inflow varies significantly. Third, the plant operates under increasingly strict effluent quality constraints and faces substantial growth in electricity costs, which motivates energy-aware operation. These characteristics align closely with current research directions in energy-efficient WRRF operation.[1]

[1] See, for example, recent works on scheduling and optimisation in WWTPs (Simon-Várhelyi et al., 2020; Wang et al., 2022).

Chapter 3

Models for Control Design Purposes

Models are an integral part of control system design. They can serve as simulations of real-world systems for testing and verifying algorithms or be part of a control strategy as model-based control. Models are also used for estimation, prediction, and data filtering. In the subsequent chapters, the case study plant is represented by a detailed simulation environment that integrates biological, hydraulic and aeration-system models. This environment can be interpreted as a digital twin of the Swarzewo WWTP in the sense of recent digital twin concepts for WRRFs: it is a virtual replica of the physical facility that enables the testing of control strategies, optimisation algorithms and scheduling policies under realistic scenarios and constraints. Digital twins are increasingly recognised as a key tool for real-time optimisation and decision support in wastewater treatment, particularly in the context of energy efficiency and regulatory compliance. Positioning the Swarzewo plant within this framework underscores the practical relevance of the proposed hierarchical control and TS solutions.[1]

This chapter collects and describes the models used in this dissertation, developed mainly within RT 1. Starting with the biological reactor model in Section 3.1, which is the SBR and its modules, used later as a control plant simulation. Next, Section 3.2 introduces models applied in control algorithms, including the DO model and aspects of oxygen transfer, as well as the related issue of respiration estimation. Further in Section 3.3, a simplified SBR model for optimisation tasks is presented. Then, the mathematical description of several SBRs and additional tanks representing a WRRF for TS purposes is found in Section 3.4. The chapter concludes with the influent model described in Section 3.5.

3.1 Sequencing Batch Reactor Model

The SBR exhibits strongly coupled hydraulic, biochemical, and settling phenomena, which motivates a structured modelling approach. On the basis of a general understanding of this system and its operational principles, it is possible to extract some key information about it. The SBR is represented as a tank with fixed, known geometric dimensions, typically featuring one influent and two effluent streams (treated effluent and waste sludge). The incoming medium consists of various biochemical substances, divided into soluble and particulate, as outlined in Assumption 1.8.

[1] See, for example, recent works on digital twins for WWTPs (Therrien et al., 2020; Torfs et al., 2022)

The activated sludge in the reactor enables biochemical reactions between the various substances, termed fractions, which in turn lead to either production or consumption, as described by the ASM framework in Subsection 3.1.1. In SBR processes, flocs, small clusters of bacteria and organic matter, play a significant role. They form due to microbial activity within the sludge, aggregating into larger structures that facilitate sedimentation. This process is known as flocculation. The ASM distinguishes between several fractions describing the different groups of microorganisms involved in floc formation, including heterotrophic and autotrophic biomass, and PAO.

The flocculation initiates the process of sedimentation, where solid particles settle due to gravity[2]. In the reactor, stratification occurs, whereby larger particles settle to the bottom, resulting in an increase in the concentration of nitrogen and phosphorus. Furthermore, the formation of a sludge blanket, which serves as a boundary between the denser lower zone and the clearer upper zone of the SBR, is observed. This phenomenon and its mathematical models are further detailed in Subsection 3.1.2.

The simulation model, designed to validate control algorithms, also incorporates the Measurement System (Subsection 3.1.3) and Actuator System (Subsection 3.1.4) for air supply and oxygen dispersion. This extension of the model beyond the reactor provides a comprehensive representation of the technological peripherals associated with the system. Therefore, including the measurement and aeration subsystems yields an integrated plant model suitable for closed-loop simulation and controller evaluation. This section was developed based on research work published in (Ujazdowski et al. (2023)).

Considering the aforementioned phenomena, creating a model for an SBR requires accounting for temporal and spatial changes in the modelled quantities. To achieve this, the fundamental principles of mass conservation are applied, resulting in models based on PDEs. Given the medium's heterogeneous nature, there are complex interactions among its components, including chemical reactions and biological processes involving activated sludge. Some substances are transformed into others as a result of these interactions. These interactions necessitate careful selection of state variables to ensure that the model is suitable for monitoring and control applications.

A phenomenological approach was used to derive the model. By introducing a concept familiar from modelling in, among other things, thermodynamics, i.e. the $V_{\mathrm{CV}}(t)$ denotes a CV in which the distribution of a substance is considered. Each point in this volume, denoted by $\boldsymbol{a}$, contains this substance with a known spatial density, which can be expressed as $\rho(\boldsymbol{a}, t)$. This density represents the mass of the substance per unit volume at a given location and moment. It is also assumed that at any point $\boldsymbol{a}$, there can be production or consumption of a substance - in other words, a substance can be generated or consumed at a given CV. The change in this mass is described by $r(\boldsymbol{a}, t)$, which represents the rate of production or consumption of the substance per unit volume. Taking these processes into account, the mass balance equation allows a description

[2] The sedimentation process is effective in the context of compact sludge flocs. Additionally, filamentous flocs, characterised by a substantial surface area in relation to their mass, can disrupt the process of sedimentation. The composition of the bacteria is a determining factor, with the reactor control and the F/M ratio also playing a significant role. In cases of poorly conducted processes, the addition of a flocculant to enhance sedimentation may be required.

of the change in the total mass of a substance inside a CV, taking into account chemical reactions and substance flows:

$$\mathrm{d}_t \int\limits_{V_{\mathrm{CV}}(t)} \rho(\boldsymbol{a},t)\,\mathrm{d}\,V = \int\limits_{V_{\mathrm{CV}}(t)} r(\boldsymbol{a},t)\,\mathrm{d}\,V, \tag{3.1}$$

where: $\mathrm{d}_{(\cdot)}$ denotes a derivative operator with respect to $(\cdot)$ and $\mathrm{d}\,V$ is and infinitesimal element of CV.

Then, by virtue of the Leibniz integral rule, it is possible to split the change in total mass in volume into a term describing the change in density ρ in CV over time. The second term takes into account the mass flux through the surface area surrounding CV:

$$\mathrm{d}_t \int\limits_{V_{\mathrm{CV}}(t)} \rho(\boldsymbol{a},t)\,\mathrm{d}\,V = \int\limits_{V_{\mathrm{CV}}(t)} \partial_t\rho(\boldsymbol{a},t)\,\mathrm{d}\,V + \int\limits_{A_{\mathrm{CS}}(t)} \rho(\boldsymbol{a},t)\boldsymbol{u}_{\mathrm{CS}}\cdot\boldsymbol{n}\,\mathrm{d}\,A, \tag{3.2}$$

where: $\partial_{(\cdot)}$ denotes a partial derivative operator with respect to $(\cdot)$, $\mathrm{d}\,A$ at each t is an infinitesimal area element of $A_{\mathrm{CS}}(t)$, namely the Control Surface (CS) – surface enclosing the CV, $\boldsymbol{u}_{\mathrm{CS}}$ is the velocity vector of points on CS, $\boldsymbol{n}$ is a unit CS normal vector pointing outward, $\cdot$ signifies the dot product, so that the term $\boldsymbol{u}_{\mathrm{CS}}\cdot\boldsymbol{n}$ yields the expansion velocity of CS.

Replacing the Left-Hand Side (LHS) of (3.1) with the Right-Hand Side (RHS) of (3.2) results in:

$$\int\limits_{V_{\mathrm{CV}}(t)} \partial_t\rho(\boldsymbol{a},t)\,\mathrm{d}\,V \quad + \int\limits_{A_{\mathrm{CS}}(t)} \rho(\boldsymbol{a},t)\boldsymbol{u}_{\mathrm{CS}}\cdot\boldsymbol{n}\,\mathrm{d}\,A, = \int\limits_{V_{\mathrm{CV}}(t)} r(\boldsymbol{a},t)\,\mathrm{d}\,V. \tag{3.3}$$

Then, by applying Gauss' (Ostrogradsky) theorem, which involves transforming the surface integral of a vector field into the volume integral of the divergence of that field, a formula can be written:

$$\int_{A_{\mathrm{CS}}(t)} \rho(\boldsymbol{a},t)\boldsymbol{u}_{\mathrm{CS}}\cdot\boldsymbol{n}\;\mathrm{d}\,A = \int_{V_{\mathrm{CV}}(t)} \nabla\cdot(\rho(\boldsymbol{a},t)\boldsymbol{u}_{\mathrm{CS}})\;\mathrm{d}\,V. \tag{3.4}$$

With this notation, the density- and velocity-dependent surface integral of the mass flux is equivalent to the volume integral of the mass divergence, allowing the equation (3.3) to be written in Euler form:

$$\partial_t\rho(\boldsymbol{a},t) + \nabla\cdot(\rho(\boldsymbol{a},t)\boldsymbol{u}_{\mathrm{CS}}) - r(\boldsymbol{a},t) = 0, \tag{3.5}$$

where $\nabla\cdot$ signifies the divergence. Moreover, the term $\rho(\boldsymbol{a},t)\boldsymbol{u}_{\mathrm{CS}}$ yields the mass flux.

Upon applying the Leibniz (product) rule to the secondary term in (3.5), the resulting equation can be expressed thus:

$$\partial_t\rho(\boldsymbol{a},t) + \nabla\rho(\boldsymbol{a},t)\cdot\boldsymbol{u}_{\mathrm{CS}} + \rho(\boldsymbol{a},t)\nabla\cdot\boldsymbol{u}_{\mathrm{CS}} = r(\boldsymbol{a},t), \tag{3.6}$$

where the second term in the LHS represents the transport mechanism of the medium, and the third term allows the change in the CV under consideration to be taken into account. The term in the RHS of the equation is used to address sources, sinks and reaction interactions with the

biochemical species that constitute the medium in the CV.

Considering the definition $\nabla \stackrel{\text{def}}{=} (\partial_x, \partial_y, \partial_z)$ and $\boldsymbol{u}_{\text{CS}} \stackrel{\text{def}}{=} (v_x, v_y, v_z)$, by the virtue of Assumption 1.7, the notation (3.6) can be simplified. This is achieved by focusing solely on processes occurring along the z-axis, effectively reducing the complexity of the problem to one dimension. Consequently, this leads to:

$$\partial_t \rho(z,t) + v_z \partial_z \rho(z,t) + \rho(z,t) \partial_z v_z = r(z,t). \tag{3.7}$$

The simplified continuity equation (3.7) provides the basis for the derivation of SBR. In order to enhance the legibility of the subsequent considerations, the dependence of the variables on (z,t) has been omitted.

The following setup is presented to derive the model of the system under consideration from the general model. The modelling approach to the quantitative properties of SBR was originally proposed by Alex (2011) and is available, for example, in the off-the-shelf simulation software #SIMBA by ifak - Institut für Automation und Kommunikation e. V. (2024). The resulting model corresponds to a commercial application and has been implemented in the MATLAB Simulink environment. The implementation in the fast prototyping environment was specifically chosen to allow the model to be extended with additional modules, thereby increasing its adaptability for both research and practical applications. Furthermore, this section presents a comprehensive description of SBR modelling tailored to developing monitoring and control systems. This setup has been illustrated in Fig. 3.1.

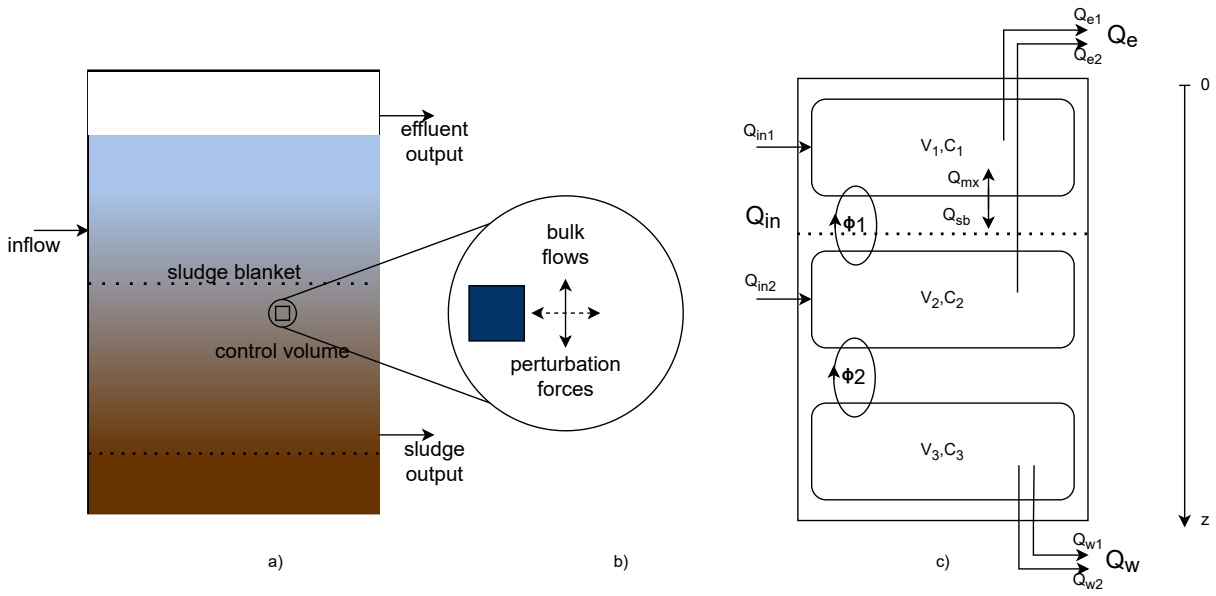

Figure 3.1: a) technological model; b) control volume; c) layer structure

Considering the technological layout and operating principles, the SBR's CV is divided (discretised) into three layers ($i_z \in \overline{1, n_z}$ and $n_z = 3$). The two layers from the top are characterised by a variable volume (V_1, V_2). In contrast, the layer at the bottom of the reactor, which represents the dense sludge, is considered as a constant volume (V_3). The SBR has a fixed maximum volume ($V_{\max}$) while the actual volume results from the mass balance of influents (Q_{inf}) and effluents (Q_{eff}). In addition, two other factors influence the variability of layers. Firstly, the

sedimentation of particles, in other words, the height of the sludge blanket, with the settling velocity (v_{sb}), is the result of gravity and friction. Secondly, the bulk flow occurs in the model as a consequence of considering mixing (Q_{mb}) in the reactor. This is the flow observed during the operation of the mixer or during the filling or aeration phase of the reactor. The value of the $Q_{\mathrm{mb}} = Av_{\mathrm{mb}}$, where v_{mb} is set equal to the maximum settling velocity, which serves to counteract the effects of gravity and A is reactor base area. This value is used to imitate the rise of a sludge blanket during mixing or filling.

Given that Assumptions 1.4 – 1.6 hold, the described setup provides the basis for establishing volumetric balance within the SBR and its constituent layers, hence, $\forall i_{\mathrm{z}}$:

$$\mathrm{d}_t V_{i_{\mathrm{z}}} = Q_{\mathrm{inf}\, i_{\mathrm{z}}} - Q_{\mathrm{eff}\, i_{\mathrm{z}}}, \tag{3.8}$$

where the characterisation of the RHS terms depends on i_{z} as described in the following lines.

The dependence on i_{z} is related, among other things, to the influent of the reactor, which is distributed between the upper and middle layers. This is the instantaneous process shown in the static model:

$$Q_{\mathrm{in}\, i_{\mathrm{z}}} = \kappa_{i_{\mathrm{z}}} Q_{\mathrm{in}}, \tag{3.9}$$

where: $\kappa_1 \overset{\mathrm{def}}{=} \kappa(SVI, V_1)$ and $\kappa_2 \overset{\mathrm{def}}{=} 1 - \kappa(SVI, V_1)$ with $\kappa(SVI, V_1)$ being a proportionality coefficient defining a clear water fraction in the wastewater inflow Alex (2011).

Furthermore, it is considered that the outflow of treated wastewater Q_{e} acts not only on the top layer but also on the middle layer. This happens only in the boundary scenario of emptying the reactor, during which a minimum volume has been reached through the top layer. For this purpose, flows $Q_{\mathrm{e}\,1}$ and $Q_{\mathrm{e}\,2}$ are introduced, which divide the outflow. To ensure a smooth transition between them, a switching function (SF) proposed by Alex (2011) is applied. This function introduces a continuous approximation, defined as:

$$\mathrm{SF}(x, \mathrm{ub}, \mathrm{lb}) = \begin{cases} 0 & \text{for } x \leq \mathrm{lb}, \\ a + bx + cx^2 + dx^3 & \text{for } \mathrm{lb} < x < \mathrm{ub}, \\ 1 & \text{for } x \geq \mathrm{ub}, \end{cases} \tag{3.10}$$

where ub and lb denote the upper and lower bounds, respectively, and the coefficients are:

$$a = \frac{\mathrm{lb}^2(3 \cdot \mathrm{ub} - \mathrm{lb})}{(\mathrm{ub} - \mathrm{lb})^3}, \quad b = \frac{-6 \cdot \mathrm{ub} \cdot \mathrm{lb}}{(\mathrm{ub} - \mathrm{lb})^3}, \quad c = \frac{3(\mathrm{ub} + \mathrm{lb})}{(\mathrm{ub} - \mathrm{lb})^3}, \quad d = \frac{-2}{(\mathrm{ub} - \mathrm{lb})^3}.$$

Using SF, the outflows $Q_{\mathrm{e}\,1}$ and $Q_{\mathrm{e}\,2}$ can be expressed as:

$$Q_{\mathrm{e}\,1} = \mathrm{SF}\left(\frac{V_1}{V_{\max}}, 2V_{\min 1}, V_{\min 1}\right) Q_{\mathrm{e}}, \tag{3.11a}$$

$$Q_{\mathrm{e}\,2} = \left[1 - \mathrm{SF}\left(\frac{V_1}{V_{\max}}, V_{\min 1}, 2V_{\min 1}\right)\right] \mathrm{SF}\left(\frac{V_2}{V_{\max}}, 2V_{\min 2}, V_{\min 2}\right) Q_{\mathrm{e}}. \tag{3.11b}$$

where: $V_{\min 1}$, $V_{\min 2}$ denote the minimum volume of the first and second layers, respectively.

The total treated effluent (Q_{e}) is calculated as the sum of these components:

$$Q_{\mathrm{e}} = Q_{\mathrm{e}\,1} + Q_{\mathrm{e}\,2}. \tag{3.12}$$

Excess sludge can also be discharged from the reactor, as mentioned in Chapter 2. Since the excess sludge outflow (Q_{w}) is located at the bottom of the SBR, it forces the flow of medium from the upper layers. The third layer is a constant volume layer, so the outflow from this layer is balanced by the inflow from the middle layer. Analogous to the outflow Q_{e}, a flow $Q_{\mathrm{w}\,1}$ can be introduced in the upper layer, occurring if the reactor continues to empty despite the minimum volume of the middle layer being reached:

$$Q_{\mathrm{w}\,1} = \mathrm{SF}\left(\frac{V_1}{V_{\max}}, V_{\min 1}, 2V_{\min 1}\right)\left[1 - \mathrm{SF}\left(\frac{V_2}{V_{\max}}, 2V_{\min 2}, V_{\min 2}\right)\right] Q_{\mathrm{w}}, \tag{3.13a}$$

$$Q_{\mathrm{w}\,2} = \mathrm{SF}\left(\frac{V_2}{V_{\max}}, 2V_{\min 2}, V_{\min 2}\right) Q_{\mathrm{w}}. \tag{3.13b}$$

The total excess sludge outflow (Q_{w}) is given by the sum of these components:

$$Q_{\mathrm{w}} = Q_{\mathrm{w}\,1} + Q_{\mathrm{w}\,2}. \tag{3.14}$$

In summary, the inflow to the top layer ($i_{\mathrm{z}} = 1$) consists of the clean water component of influent ($Q_{\mathrm{in}\,1}$) and Q_{sb}, representing the change in sludge blanket height through sedimentation. The effluent from this layer accounts for the treated medium outflow ($Q_{\mathrm{e}\,1}$), mixing flow (Q_{mb}), and the emergency sludge removal ($Q_{\mathrm{w}\,1}$). Meanwhile, the middle layer ($i_{\mathrm{z}} = 2$) volume changes with inflow of more concentrated pollutants ($Q_{\mathrm{in}\,2}$), the emergency sludge removal ($Q_{\mathrm{w}\,1}$) and mixing flow (Q_{mb}). The outflow from this layer includes excess sludge removal ($Q_{\mathrm{w}\,1}$ and $Q_{\mathrm{w}\,2}$), emergency treated medium outflow ($Q_{\mathrm{e}\,2}$), and the flow related to changes in the sludge blanket height (Q_{sb}). Therefore, it follows that for the top layer ($i_{\mathrm{z}} = 1$):

$$Q_{\mathrm{inf}\,1} = Q_{\mathrm{in}\,1} + Q_{\mathrm{sb}}, \tag{3.15a}$$

$$Q_{\mathrm{eff}\,1} = Q_{\mathrm{w}\,1} + Q_{\mathrm{e}\,1} + Q_{\mathrm{mb}}, \tag{3.15b}$$

in case of the middle layer ($i_{\mathrm{z}} = 2$):

$$Q_{\mathrm{inf}\,2} = Q_{\mathrm{in}\,2} + Q_{\mathrm{w}\,1} + Q_{\mathrm{mb}}, \tag{3.16a}$$

$$Q_{\mathrm{eff}\,2} = Q_{\mathrm{w}\,1} + Q_{\mathrm{w}\,2} + Q_{\mathrm{e}\,2} + Q_{\mathrm{sb}}, \tag{3.16b}$$

and in case of the bottom layer ($i_{\mathrm{z}} = 3$):

$$Q_{\mathrm{inf}\,3} = Q_{\mathrm{w}\,1} + Q_{\mathrm{w}\,2}, \tag{3.17a}$$

$$Q_{\mathrm{eff}\,3} = Q_{\mathrm{w}\,1} + Q_{\mathrm{w}\,2}. \tag{3.17b}$$

By virtue of the Assumption 1.8, and knowing that the number of fractions is n_{f} it follows that, $\forall i_z$, additional n_f equation of the form (3.7) is required. Dividing the layer into fractions and understanding that each fraction represents a pure biochemical species, it can be assumed

that density (ρ) can be interpreted in terms of mass concentration (C). Therefore, the density of a component in a mixture can be defined as the concentration of the component in the mixture.

Once the flows occurring in the reactor and their consequences (impact on the volume) have been presented, the fluxes affecting the concentrations of substances should also be considered. The second term on the LHS of (3.7) represents the overall flux between the SBR layers. This flux comprises two components: the settling flux due to gravity (precipitation of particles, ϕ_{s}) and the bulk flux caused by the volumetric movement of water along the reactor walls, ϕ_{b}. It can be expressed as $\forall i_{\mathrm{z}}$:

$$\phi_{i_{\mathrm{z}},i_{\mathrm{f}}} = \phi_{\mathrm{s}\,i_{\mathrm{z}},i_{\mathrm{f}}} + \phi_{\mathrm{b}\,i_{\mathrm{z}},i_{\mathrm{f}}}, \tag{3.18}$$

where:

$$\phi_{\mathrm{s}\,i_{\mathrm{z}},i_{\mathrm{f}}} = v_{\mathrm{s}\,i_{\mathrm{z}}} C_{i_{\mathrm{z}},i_{\mathrm{f}}}, \tag{3.19}$$

and:

$$\phi_{\mathrm{b}\,i_{\mathrm{z}},i_{\mathrm{f}}} = v_{\mathrm{b}\,i_{\mathrm{z}}} C_{i_{\mathrm{z}},i_{\mathrm{f}}}, \tag{3.20}$$

with: v_{b}, v_{s} being the vertical bulk flow and settling velocities, respectively.

Then, by examining the third term on the LHS side of (3.7), it represents the rate of change in the concentration of a substance per unit volume. Specifically, in the context of the considered spatially discretised system, this term is expressed as the product of the concentration $C_{i_{\mathrm{z}},i_{\mathrm{f}}}$ at a given layer i_{z} and fraction i_{f}, divided by the volume $V_{i_{\mathrm{z}}}$ of that layer, and the time derivative of the volume $V_{i_{\mathrm{z}}}$, it reads $\forall i_{\mathrm{z}}$, i_{f} : $\dfrac{C_{i_{\mathrm{z}},i_{\mathrm{f}}}}{V_{i_{\mathrm{z}}}} \partial_t V_{i_{\mathrm{z}}}$.

The RHS of (3.7) represents biological or chemical reactions that cause changes in concentration between different fractions. These changes are consistent with the mass balance within the reactor. Whereby the change in one component depends on the concentrations of all substances in the layer under consideration ($\boldsymbol{C}_{i_{\mathrm{z}}} \overset{\mathrm{def}}{=} [C_1, C_2, \ldots, C_{n_{\mathrm{z}}}]^T$). Hence, $\forall i_{\mathrm{z}}, i_{\mathrm{f}} : r_{i_{\mathrm{f}}}(\boldsymbol{C}_{i_{\mathrm{z}}}) \in \mathbf{r}(\boldsymbol{C}_{i_{\mathrm{z}}})$. A detailed description has been provided in the Subsection 3.1.1.

Considering the presence of inflows and outflows within the tank, the RHS of (3.7) must be extended to account for external sources and sinks. These contributions are represented as external inflows and outflows, given by:

$$\phi_{\mathrm{inf}\,i_{\mathrm{z}},i_{\mathrm{f}}} = \frac{Q_{\mathrm{inf}\,i_{\mathrm{z}}}}{A} C_{\mathrm{in}\,i_{\mathrm{f}}}, \tag{3.21}$$

$$\phi_{\mathrm{eff}\,i_{\mathrm{z}},i_{\mathrm{f}}} = \frac{Q_{\mathrm{eff}\,i_{\mathrm{z}}}}{A} C_{i_{\mathrm{z}},i_{\mathrm{f}}}. \tag{3.22}$$

Then, based on the definition of a derivative, the influence of the second (transport) term in (3.7) for the i_{z}th layer can be approximated (spatially discretised along the z-axis) by the ratio of the change in mass flux ($\Delta\phi$) to the change in layer height (Δz). This flux variation results from the inflows and outflows in each layer and is determined by the processes described in (3.15) – (3.17). Furthermore, in the event that Assumption 1.6 is deemed valid and that sedimentation and bulk flows at the reactor boundaries are negligible (equal to 0), the SBR

model can be derived from (3.8) and (3.15) – (3.17), $\forall i_\mathrm{f}$:

$$\partial_t V_1 = Q_{\mathrm{in}1} + Q_{\mathrm{sb}} - Q_{\mathrm{w}1} - Q_{\mathrm{e}1} - Q_{\mathrm{mb}}, \tag{3.23a}$$

$$\begin{aligned}\partial_t C_{1,i_\mathrm{f}} = {} & (Q_{\mathrm{in}1} C_{\mathrm{in}\,i_\mathrm{f}} - (Q_{\mathrm{w}1} + Q_{\mathrm{e}1} + Q_{\mathrm{mb}} + Q_{\mathrm{s}1} + Q_{\mathrm{m}1} + \partial_t V_1) C_{1,i_\mathrm{f}} \\ & + (Q_{\mathrm{sb}} + Q_{\mathrm{m}1}) C_{2,i_\mathrm{f}}) \frac{1}{V_1} + r_{i_\mathrm{f}}(\boldsymbol{C}_1),\end{aligned} \tag{3.23b}$$

$$\partial_t V_2 = Q_{\mathrm{in}2} + Q_{\mathrm{mb}} - Q_{\mathrm{w}2} - Q_{\mathrm{e}2} - Q_{\mathrm{sb}}, \tag{3.23c}$$

$$\begin{aligned}\partial_t C_{2,i_\mathrm{f}} = {} & (Q_{\mathrm{in}2} C_{\mathrm{in}\,i_\mathrm{f}} + (Q_{\mathrm{mb}} + Q_{\mathrm{s}1} + Q_{\mathrm{m}1} + Q_{\mathrm{w}1}) C_{1,i_\mathrm{f}} \\ & - (Q_{\mathrm{w}1} + Q_{\mathrm{w}2} + Q_{\mathrm{e}2} + Q_{\mathrm{s}2} + Q_{\mathrm{m}1} + Q_{\mathrm{m}2} + Q_{\mathrm{sb}} + \partial_t V_2) C_{2,i_\mathrm{f}} \\ & + Q_{\mathrm{m}2} C_{3,i_\mathrm{f}}) \frac{1}{V_2} + r_{i_\mathrm{f}}(\boldsymbol{C}_2),\end{aligned} \tag{3.23d}$$

$$\partial_t V_3 = 0, \tag{3.23e}$$

$$\partial_t C_{3,i_\mathrm{f}} = ((Q_{\mathrm{s}2} + Q_{\mathrm{w}1} + Q_{\mathrm{w}2} + Q_{\mathrm{m}2}) C_{2,i_\mathrm{f}} - (Q_{\mathrm{w}1} + Q_{\mathrm{w}2} + Q_{\mathrm{m}2}) C_{3,i_\mathrm{f}}) \frac{1}{V_3} + r_{i_\mathrm{f}}(\boldsymbol{C}_3), \tag{3.23f}$$

where $Q_{\mathrm{m}1}$ and $Q_{\mathrm{m}2}$ implement the bulk flow between layers 1 and 2, and layers 2 and 3, respectively.

The total number of equations considered while using this modelling approach is given by $n = 3(n_\mathrm{f} + 1)$. Furthermore, it is important to note that the gravitational sedimentation represented by the v_s has no impact on the soluble fractions. However, it is still affected by the movement of the sludge blanket, represented by the v_{sb}. Conversely, the change in particulate fraction concentration is influenced by gravitational sedimentation but not by the movement of the sludge blanket. These effects are implemented by:

$$Q_{\mathrm{s},i_\mathrm{z}} = \begin{cases} 0 & \text{, for soluble matter} \\ A v_{\mathrm{s}\,i_\mathrm{z}} & \text{, for particulate matter} \end{cases}, \tag{3.24}$$

and:

$$Q_{\mathrm{sb}} = \begin{cases} A v_{\mathrm{sb}} & \text{, for soluble matter} \\ 0 & \text{, for particulate matter} \end{cases}. \tag{3.25}$$

The numerical values of the aforementioned parameters, including those related to reactor geometry and mass flows, are presented in the Experiment Setup (Section 7.1) of Chapter 7.

3.1.1 Reaction Term

The biochemical processes occurring in the reactor, described by the ASM, indicate the rate of production or consumption of a substance. In the equations of the previous section, it is represented by $\boldsymbol{r}(\boldsymbol{C}_{i_\mathrm{z}}) \overset{\mathrm{def}}{=} [r_1(\boldsymbol{C}_{i_\mathrm{z}}),\, r_2(\boldsymbol{C}_{i_\mathrm{z}}),\, \ldots, r_{n_\mathrm{f}}(\boldsymbol{C}_{i_\mathrm{z}})]^T$, which can be referred to as a reaction term. The ASM models are presented in the form of a Petersen–Gujer matrix, which, through a matrix of coefficients, relates biological and chemical processes to represent changes in the concentrations of the substances considered in the model.

The reaction model is considered in each layer of SBR, in its Petersen–Gujer form. The detailed procedure for obtaining the coefficient of change of fraction concentration for a unit

volume is to calculate a column-wise summation of the product of stoichiometric coefficients and process rates:

$$\boldsymbol{r}(\boldsymbol{C}_{i_\mathrm{z}}) = \sum_{i_\mathrm{p}=1}^{n_\mathrm{p}} p_{i_\mathrm{p}}(\boldsymbol{C}_{i_\mathrm{z}}) g_{i_\mathrm{p},i_\mathrm{f}}, \forall i_\mathrm{f} \in [1, n_\mathrm{f}] \tag{3.26}$$

where: $p_{i_\mathrm{p}}(\boldsymbol{C}_{i_\mathrm{z}})$ denotes the i_pth process rate, $g_{i_\mathrm{p},i_\mathrm{f}}$ is the stoichiometric coefficient weighting the impact of i_pth process on the i_fth fraction, n_f denotes the number of model fractions, n_p denotes the number of processes.

As mentioned in Subsection 1.1.1, the structure of the reaction term for the SBR model is a combination of ASM3 (Gujer et al. (1999)) with the BioP module (Rieger et al. (2001) and an additional element introducing the lag-phase (Alex et al. (2009)). This combination is referred to as Activated Sludge Model no. 3 extended (ASM3e). The following paragraphs discuss the details of each component of ASM3e.

Each model module is distinctly represented in the Petersen–Gujer matrix notation, with stoichiometric parameter values taken from the source literature. For soluble fractions, parameters of ASM3 are denoted as gASM3S, while those for particulate matter are gASM3X. The process kinetics are represented as pASM3. The BioP module extends ASM3 by incorporating phosphorus transformations through additional phosphorus-related fractions parameters noted as gBIOPS and gBIOPX and corresponding process equations pASM3.

To combine the module with ASM3, the required stoichiometric coefficients for the alkalinity and suspend solids fractions have been calculated according to Gujer and Larsen (1995). The modified gASM3S, gASM3X parameters are represented respectively as gASM3PS, gASM3PX. It is worth mentioning that the BioP module tends to overestimate TP since it does not include anaerobic decay and maintenance of PAO, according to Hauduc et al. (2013).

The last module of the model addresses the inactivity of microorganisms during significant shifts in environmental conditions, particularly at the onset of the aerobic phase following a prolonged anaerobic period; the lag phase module incorporates additional artificial particulate fractions representing enzymes X_EH and X_EA. Their parameters are represented by gLAG. Corresponding processes for the growth and decay of these enzymes denote pLAG. As mentioned in the introduction, these enzymes, while not part of reactor influent or effluent, are subject to sedimentation and mixing.

Introducing matrix notation by defining stoichiometric elements for all modules as shown in the Fig. 3.2 $\mathbf{G} \equiv [g_{i_\mathrm{p},i_\mathrm{f}}] \in \mathbb{R}^{n_\mathrm{p} \times n_\mathrm{f}}$ and process rates $\boldsymbol{p} \overset{\mathrm{def}}{=} \left[p_1(\boldsymbol{C}), p_2(\boldsymbol{C}), \ldots, p_{n_\mathrm{p}}(\boldsymbol{C})\right]$ leads to:

$$\boldsymbol{r}(C_{i_\mathrm{z}}) = \boldsymbol{p}^T \boldsymbol{G} \tag{3.27}$$

This notation allows for a simple implementation of these models in a matrix form in almost any programming environment. Additionally, Petersen–Gujer matrix can be written as a sparse matrix to make computer calculations more efficient.

Furthermore, the effect of temperature on the process rates is introduced into the model using the Arrhenius law. The temperature correction factors are defined as follows:

$$f_{T1} = e^{(-0.04(20-T))}, \tag{3.28a}$$

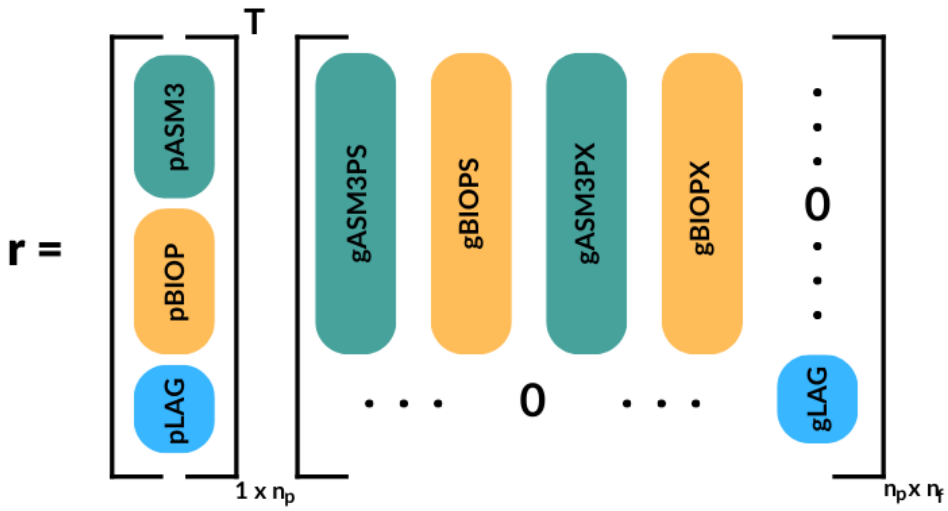

Figure 3.2: ASM3e Petersen–Gujer matrix

$$f_{T2} = e^{(-0.07(20-T))}, \tag{3.28b}$$

$$f_{T3} = e^{(-0.105(20-T))}, \tag{3.28c}$$

where T denotes the temperature, while f_{T1}, f_{T2}, f_{T3} are the temperature correction factors corresponding to heterotrophs, decay and hydrolysis processes, and autotrophic organism growth and respiration, respectively.

Including the temperature correction factors, as defined by (3.28), extends the representation of process rates. This modification accounts for the dynamic impact of temperature on reaction kinetics. Consequently, the updated process rates used in (3.27) can be expressed as $\boldsymbol{p} \overset{\text{def}}{=} \left[p_1(\boldsymbol{C}, T, p_2(\boldsymbol{C}, T, \ldots, p_{n_\text{p}}(\boldsymbol{C}, T\right]$.

The complete list of fractions and their corresponding labels utilised in ASM3e is specified in Table 3.1.

3.1.2 Sludge Blanket Model

The sludge blanket represents the observable stratification in SBR due to the concentration of solid particles. As a reminder, this is modelled by changing the boundary between the first and second layers, which can be interpreted as the ratio of the volume of these layers to the volume of the reactor. The height of the sludge blanket is, therefore, a function of the settling velocity (v representing both v_{sb} and v_s). In general, the value of the settling velocity is a variable quantity in space and time (depending on the local properties of the medium). In the context of treatment processes, this dependency is typically introduced by representing the v as a function of TSS and SVI.

Table 3.2 presents the models of the settling velocity dynamics known to affect the height of the sludge blanket. The first model (Takacs et al. (1991)) was employed by Alex et al. (2011) in the SBR modelling. The following models were introduced into the literature by: Daigger and Roper (1985), Wahlberg and Keinath (1988), Akça et al. (1993), Ozinsky and Ekama (1995), Daigger (1995). Collectively, these were described by Trelles et al. (2017) in a review of sludge settling prediction models.

Table 3.1: Fractions of the ASM3e

Fraction	**Symbol**	**Description**	**Unit**
$C_{(\cdot),1}$	S_{O}	Dissolved oxygen	g O_2/m^3
$C_{(\cdot),2}$	S_{S}	Readily biodegradable substrate	g COD/m^3
$C_{(\cdot),3}$	S_{NH}	Nitrogen	g N/m^3
$C_{(\cdot),4}$	S_{NO}	Nitrate and nitrite nitrogen	g N/m^3
$C_{(\cdot),5}$	$S_{\mathrm{N_2}}$	Dinitrogen	g N/m^3
$C_{(\cdot),6}$	S_{ALK}	Alkalinity	mole HCO_3^-/m^3
$C_{(\cdot),7}$	S_{I}	Soluble inert organic matter	g COD/m^3
$C_{(\cdot),8}$	X_{I}	Particulate inert organic matter	g COD/m^3
$C_{(\cdot),9}$	X_{S}	Slowly biodegradable substrate	g COD/m^3
$C_{(\cdot),10}$	X_{H}	Heterotrophic biomass	g COD/m^3
$C_{(\cdot),11}$	X_{STO}	Organic storage products	g COD/m^3
$C_{(\cdot),12}$	X_{A}	Autotrophic biomass	g COD/m^3
$C_{(\cdot),13}$	X_{TSS}	Particulate material as model component	g TSS/m^3
$C_{(\cdot),14}$	$S_{\mathrm{PO_4}}$	Inorganic soluble phosphorus	g P/m^3
$C_{(\cdot),15}$	X_{PAO}	Phosphorus-accumulating organisms	g COD/m^3
$C_{(\cdot),16}$	X_{PP}	Cell-internal inorganic storage product of PAO	g P/m^3
$C_{(\cdot),17}$	X_{PHA}	Cell-internal organic storage products of PAO	g COD/m^3
$C_{(\cdot),18}$	X_{EH}	Virtual enzyme level of heterotrophic biomass	g COD/m^3
$C_{(\cdot),19}$	X_{EA}	Virtual enzyme level of autotrophic biomass	g COD/m^3

Table 3.2: Settling velocities models

No.	Authors	Model equation ($TSS[kg/m^3], SVI[mL/g], v[m/h]$)
1	Takacs et al. (1991)	$v = \frac{1}{24} \cdot 380 \cdot e^{-(0.1184+0.0017 \cdot SVI) \cdot TSS}$
2	Daigger et al. (1985)	$v = 7.8e^{-(0.148+0.0021SVI)TSS}$
3	Wahlberg et al. (1998)	$v = (15.3 - 0.0615SVI)e^{-(0.426+3.841 \cdot 10^{-3}SVI - 5.43 \cdot 10^{-5}SVI^2)TSS}$
4	Akça et al. (1993)	$v = 28.1SVI^{-0.2667}e^{-(0.177+0.014SVI)TSS}$
5	Ozinsky et al. (1995)	$v = 8.53e^{-0.00165SVI}e^{-(0.2+9.1 \cdot 10^{-4}SVI)TSS}$
6	Daigger (1995)	$v = 6.5e^{-(0.165+0.00159SVI)TSS}$

Based on Table 3.2, three general structures of settling velocity models can be identified, each varying by the degree of polynomials used in their formulation. Models no. 1, 2, 6 have a shared structure assuming a numerical base settling velocity and an exponential function from the result of multiplying the TSS concentration with a linear SVI function. Models no. 3, 4, and 5 modify this structure by adding SVI dependency in the base velocity, with model no. 2 also introducing a non-linear SVI component in the exponential term. Differences in parameters reflect calibration for diverse datasets and WRRFs. Fig. 3.3 visualises the relationship between settling velocity and TSS concentration.

The implemented models share a comparable dynamic profile. Of particular note are models 1 and 3, which show significantly higher sedimentation velocities. The potential process optimisation with the use of these models will result in a shorter sedimentation phase. The remaining models present minimal variation, indicating they can be employed as alternatives.

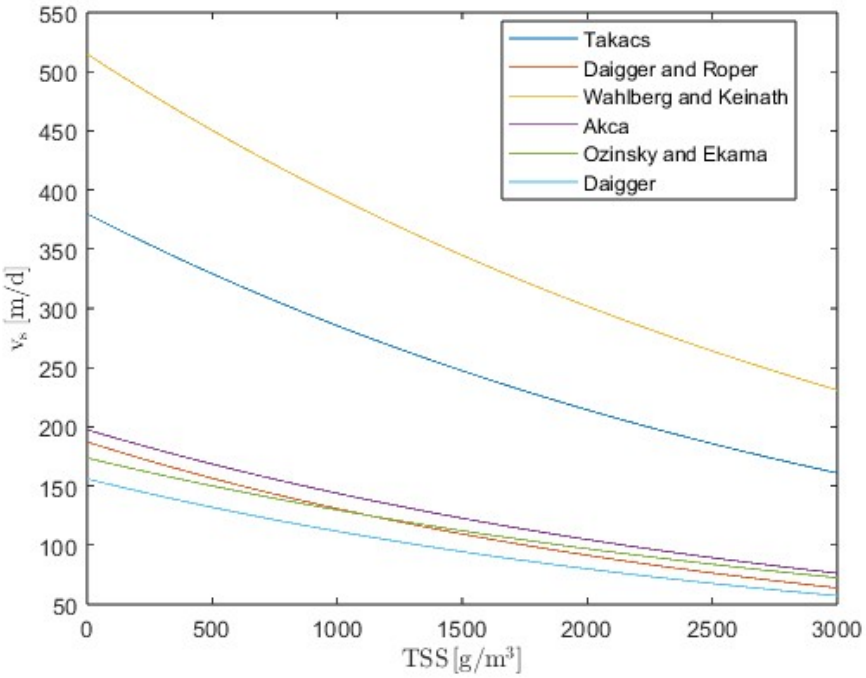

Figure 3.3: Settling velocity models

3.1.3 Measurement System

In contemporary practice, the measurements used in WWTPs can be divided into two main categories (Haimi et al. (2013)). The first category is measurements related to the pollution rate of wastewater, which are usually difficult to measure, expensive and/or time-consuming. Next are secondary measurements related to processes that are not directly quality-related. These measurements are used in control systems and are often easy to measure in comparison to the former group.

The first category includes measurements of: NO_3, TN, PO_4, TP, NH_4, TSS, COD. The second category of measurements typically includes pressure, temperature, flow rate, level measurements, conductivity, turbidity, pH, and DO. A list of important quality parameters for discharged wastewater is provided in Table 3.3.

Nitrate - NO_3

The first parameter that indicates water pollution and can be measured online is nitrate. Measurement is based on Ultraviolet (UV) absorption spectroscopy. Nitrate in wastewater is produced during aeration and released to the atmosphere later in anaerobic processes. Excessive concentrations of nitrogen compounds in the discharged effluent can result in water blooms. It directly represents one of the fractions of ASM3e (S_{NO}).

Total Nitrogen - TN

TN represents the sum of all nitrogenous compounds in wastewater, including organic nitrogen, ammonia, nitrite, and nitrate. It is a key indicator of pollution and eutrophication potential.

Table 3.3: Physico-chemical measurement of parameters for wastewater monitoring discharges (Adapted from Quevauviller et al. (2007))

Parameters	Main principles	Other principles
NH_4	Ion-selective electrode	UV spectrophotometry (after photooxidation)
	Colorimetry	(Ionic chromatography)
	Titrimetry	(Chemiluminescence)
BOD	Respirometry	(UV spectrophotometry)
COD	Titrimetry (after oxidation)	UV spectrophotometry
	Colorimetry (after microwave oxidation)	Photometry infra-red (after catalytically oxidation)
Conductivity	Electrical	
DO	Electrochemistry	Luminescence
Heavy metals	Electrochemistry	UV photometry (cold steam method) for mercury
NO_3	UV spectrophotometry	(Ion selective electrode)
Organic matter	UV spectrophotometry	
		NDIR[2] photometry
PAH[1]	Fluorimetry	Optical: light intensity reflection (UV spectrophotometry)
pH	Electrochemistry	Electronic (ISFET[3])
PO_4	Colorimetry	UV spectrophotometry (Ionic chromatography)
		Titrimetry
TOC[2]	NDIR[4] photometry (after oxidation)	UV spectrophotometry
TN	Colorimetry (after digestion)	UV spectrophotometry (after photooxidation) (Chemiluminescence)
TP	Colorimetry	UV spectrophotometry
Turbidity	Nephelometry	UV spectrometry

[1] PAH - Polycyclic Aromatic Hydrocarbons
[2] NDIR - Non-Dispersive Infra-Red
[3] ISFET - Ion-Sensitive Field Effect Transistor
[4] TOC - Total Organic Carbon

TN is calculated based on the concentrations of nitrogen species present in the reactor, making it an ideal soft sensor derived from modelled ASM3 fractions, according to Gujer et al. (1999):

$$\begin{aligned} TN = & \underbrace{S_{\mathrm{NH}} + S_{\mathrm{NO}} + S_{\mathrm{N_2}} + i_{N,SS} \cdot S_{\mathrm{S}} + i_{N,SI} \cdot S_{\mathrm{I}}}_{\text{Soluble (S)}} \\ & + \underbrace{i_{N,XI} \cdot X_{\mathrm{I}} + i_{N,XS} \cdot X_{\mathrm{S}} + i_{N,BM} \cdot (X_{\mathrm{H}} + X_{\mathrm{PAO}} + X_{\mathrm{PHA}})}_{\text{Particulate (X)}}, \end{aligned} \tag{3.29}$$

where $S_{(\cdot)}$ denotes soluble fraction, $X_{(\cdot)}$ is particulate fraction, $i_{N,(\cdot)}$ signifies nitrogen component of $(\cdot)$ and BM stands for biomass.

Phosphate - PO_4

The component responsible for water blooms is phosphorus compounds. Phosphate can also be determined using online instrumentation through the colourimetry method. The consequences of too high Phosphate concentrations are increased algal growth and oxygen depletion up to anoxia in the deeper regions. It directly represents one of the fractions of BioP (S_{PO4}).

Total Phosphorus - TP

TP encompasses all phosphorus forms, such as orthophosphates, polyphosphates, and organic phosphorus. This parameter is essential for assessing nutrient loads that may contribute to algal blooms. TP is estimated from phosphorus-related fractions, serving as a reliable model-based soft sensor. Similar to TN, it is derived from the ASM model on the basis of Rieger et al. (2001):

$$\begin{aligned} TP = & \underbrace{i_{P,SS} \cdot S_{\mathrm{S}} + i_{P,SI} \cdot S_{\mathrm{I}} + S_{\mathrm{PO_4}}}_{\text{Soluble (S)}} \\ & + \underbrace{X_{\mathrm{PP}} + i_{P,XI} \cdot X_{\mathrm{I}} + i_{P,XS} \cdot X_{\mathrm{S}} + i_{P,BM} \cdot (X_{\mathrm{H}} + X_{\mathrm{PAO}} + X_{\mathrm{PHA}})}_{\text{Particulate (X)}}, \end{aligned} \tag{3.30}$$

where $i_{P,(\cdot)}$ signifies phosphorus component of $(\cdot)$.

Ammonium - NH_4

One of the most commonly employed quality parameters is the measurement of NH_4. Ammonium nitrogen can be determined in real-time using online instrumentation and is commonly used in WWTPs. There are several methods for measuring NH_4, one of which is easily implemented in online instrumentation is ion selective electrodes, which rely on ammonia gas sensing. NH_4 in ASM3e model is represented directly by (S_{NH}) fraction.

Total Suspended Solids - TSS

TSS indicate the concentration of solid particles suspended in wastewater. This parameter impacts treatment efficiency and sludge settleability. It can be calculated from ASM3e using particulate organic matter and biomass fractions, providing a reliable indicator of process performance. However, in ASM3e, TSS is represented by a separate fraction (X_{TSS}).

Chemical Oxygen Demand - COD

Another indicator is COD, which quantifies the oxygen required to oxidise both organic and inorganic matter in wastewater, reflecting pollutant loads. Using ASM3e, COD can be derived from soluble and particulate fractions:

$$COD = \underbrace{S_{\mathrm{S}} + S_{\mathrm{I}} - S_{\mathrm{O}} - \frac{64}{14} S_{\mathrm{NO}} - \frac{24}{14} S_{\mathrm{N_2}}}_{\text{Soluble (S)}} + \underbrace{X_{\mathrm{I}} + X_{\mathrm{S}} + X_{\mathrm{H}} + X_{\mathrm{STO}} + X_{\mathrm{PAO}} + X_{\mathrm{PHA}}}_{\text{Particulate (X)}}. \tag{3.31}$$

Dissolved Oxygen - DO

An essential measurement from the perspective of the control system that does not directly relate to the quality of the treated wastewater is the measurement of DO concentration. This parameter can be monitored by an online DO sensor (electrochemical or optical) to maintain effective treatment. Electrochemical DO sensors measure the concentration of DO in wastewater based on the electrical current produced. However, optical DO (luminescence) sensors measure the concentration of DO in wastewater based on the luminescence quenching in the presence of oxygen.

The control system developed uses the sensor model proposed by Czyżniewski et al. (2023). The model is a classical current output loop (4–20 mA) sensor that considers the influence of quantisation processes, measurement noise and the conversion of analogue signals to digital. These factors were used to evaluate the impact of DO measurement quality.

Respiration Rate

An important parameter related to the aeration process is respiration, i.e. the rate of oxygen uptake by microorganisms. There are devices capable of measuring the respiration of wastewater, but these are advanced, expensive devices and, therefore, rarely used. However, a soft sensor for respiration can be proposed based on other process parameters, based on the estimation methods as presented by Spanjers and Vanrolleghem (1995). Further details on the estimation of respiration can be found in Subsection 3.2.2.

Other Measurements

Additional measurements include pressure, temperature, flow rate, level measurements, conductivity, turbidity, and pH. These are well-known devices used in many other industries, which is why no more space has been devoted to them. It is also relevant to consider measurements related to actuators, such as the measurement of pressure in the air supply line to the tank. While these measurements are of technological importance, they are not significant in the context of this work.

3.1.4 Actuator System

The SBR is supplied with air via an aeration system (see Fig. 3.4), which serves as the actuator system for the DO controller. The aeration system comprises three principal components: a diffuser unit, a pipeline and an air blower. The diffusers situated at the base of the tank provide a uniform distribution of air, which is pumped into the pipeline by the blower. The aeration flow rate (Q_{air}) is the control signal that exerts the most significant influence on the DO concentration as a controlled variable. The desired Q_{air} is achieved by holding the necessary pressure within the pipeline. This pressure was modelled on the basis of hydrostatic pressure, which is related to the reactor fill height and the diffusers' minimum opening pressure:

$$p = \frac{(h(t) - h_{\text{diff}}) \cdot \rho \cdot g}{1000} + p_{\min}, \tag{3.32}$$

where: p is the pressure in the pipeline [kPa], $h(t)$ is the height of medium level in the SBR [m], $h_{\text{diff}} = 0.5\,\text{m}$ is the immersion depth of diffusers, $\rho = 1150\,\text{kg/m}^3$ is the medium density, $g = 9.81\,\text{m/s}^2$ is the gravitational acceleration, $p_{\min}$ is the minimum opening pressure of the diffusers [kPa].

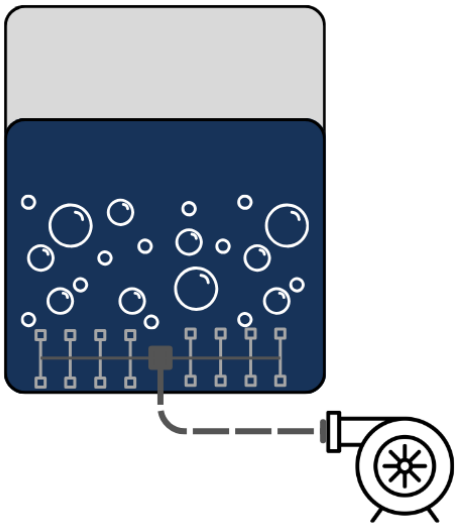

Figure 3.4: SBR aeration system

It is common practice for SBR-equipped WWTPs to utilise valve-based airflow control. This is frequently linked to the utilisation of blowers that lack the capacity to modify their operational speed in a variable manner. The utilisation of valves serves to regulate the flow, which in turn results in additional losses. The Swarzewo treatment plant serves as a distinctive case study, employing variable-speed blowers in its operational configuration. As discussed earlier in Chapter 2, in this case, there are separate installations for each reactor. A distinction is made between two types of aeration systems depending on the size of the reactor. Thus, two aeration system models with different parameters had to be developed. In considering the pressure model described by (3.32), the distinction can be attributed to the parameter representing the minimum opening pressure of the diffusers - $p_{\min}$. Blowers, on the other hand, have different (but similar) operating characteristics depending on their power. Smaller blowers (AT150) are used in smaller reactors, while larger blowers (AT200) are used in correspondingly larger reactors. Fig. 3.5 and Fig. 3.6 illustrate the complete relationship between airflow, pressure and blower speed. The operating range of the blower is limited by overheating and surge.

Models for both blowers have been developed based on their performance characteristics. A LUT approach was utilised, where specific operational points were tabulated from the manufacturer's data. To estimate values between these predefined points, interpolation methods were applied, ensuring a smooth and accurate approximation of the blower's behaviour across its operating range. In addition to the blower models included in the actuator system, inverse models were developed for direct control of the aeration, also using the LUT. Details of such a blower and aeration system modelling were provided by Piotrowski and Ujazdowski (2020). This approach balances computational efficiency with the precision necessary for integration into control system simulations and optimisation tasks.

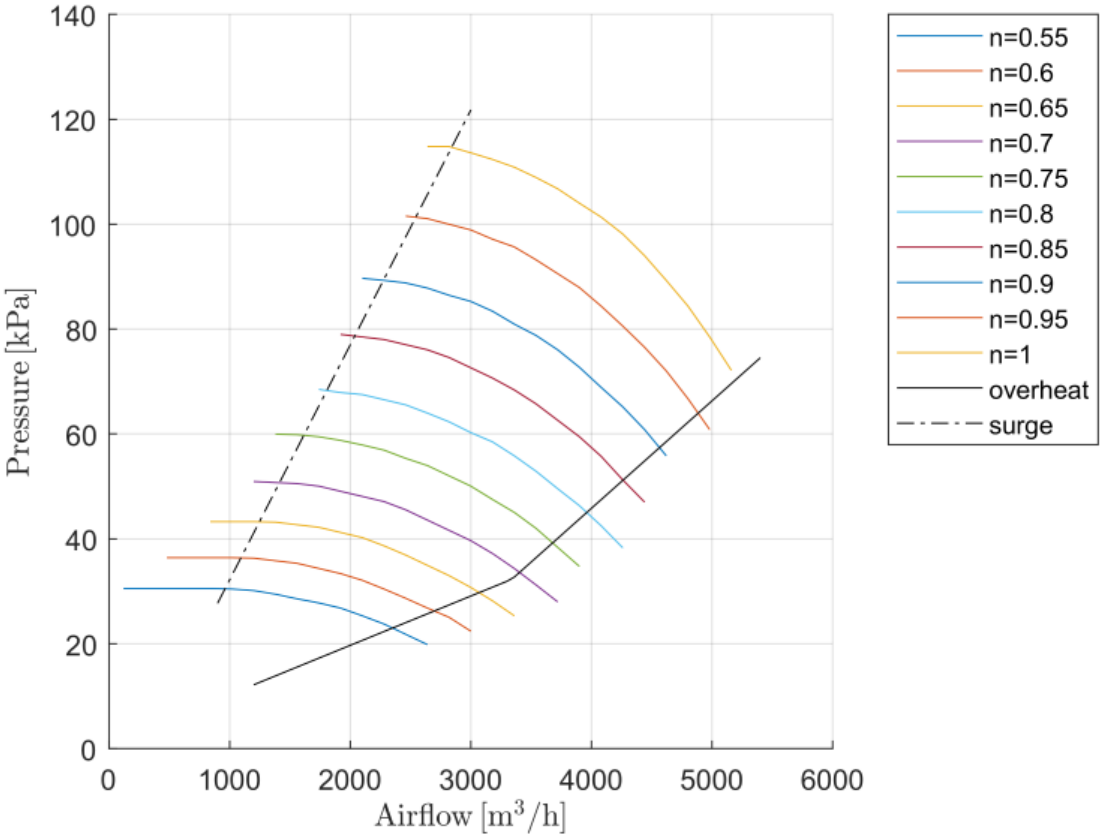

Figure 3.5: Operating characteristics of the AT150 blower (Aerzen USA Corporation, 2025)

Limitations, such as modelling the overheating and surge of the blower, were included in the inverse model. The equations of the limitations for AT150 blower are:

$$p_1(t) = 0.0094 \cdot Q_{\text{air, ref}}(t) + 0.8792, \tag{3.33a}$$

$$p_2(t) = 0.0205 \cdot Q_{\text{air, ref}}(t) - 36.1888, \tag{3.33b}$$

$$p_3(t) = 0.0448 \cdot Q_{\text{air, ref}}(t) - 12.6264, \tag{3.33c}$$

and for AT200 blower:

$$p_4(t) = 0.0074 \cdot Q_{\text{air, ref}}(t) + 0.2675, \tag{3.34a}$$

$$p_5(t) = 0.0159 \cdot Q_{\text{air, ref}}(t) - 36.1816, \tag{3.34b}$$

$$p_6(t) = 0.0403 \cdot Q_{\text{air, ref}}(t) - 5.2320, \tag{3.34c}$$

where $p_1(t)$, $p_2(t)$, $p_3(t)$, $p_4(t)$, $p_5(t)$, and $p_6(t)$ are pressure limit functions. The overheat limitation is active if the pressure in the aeration system, $p(t)$, is less than $p_1(t)$ or $p_2(t)$, for AT150 and less than $p_4(t)$, or $p_5(t)$ for AT200. The surge limitation is active if $p(t) > p_3(t)$ and $p(t) > p_6(t)$, respectively.

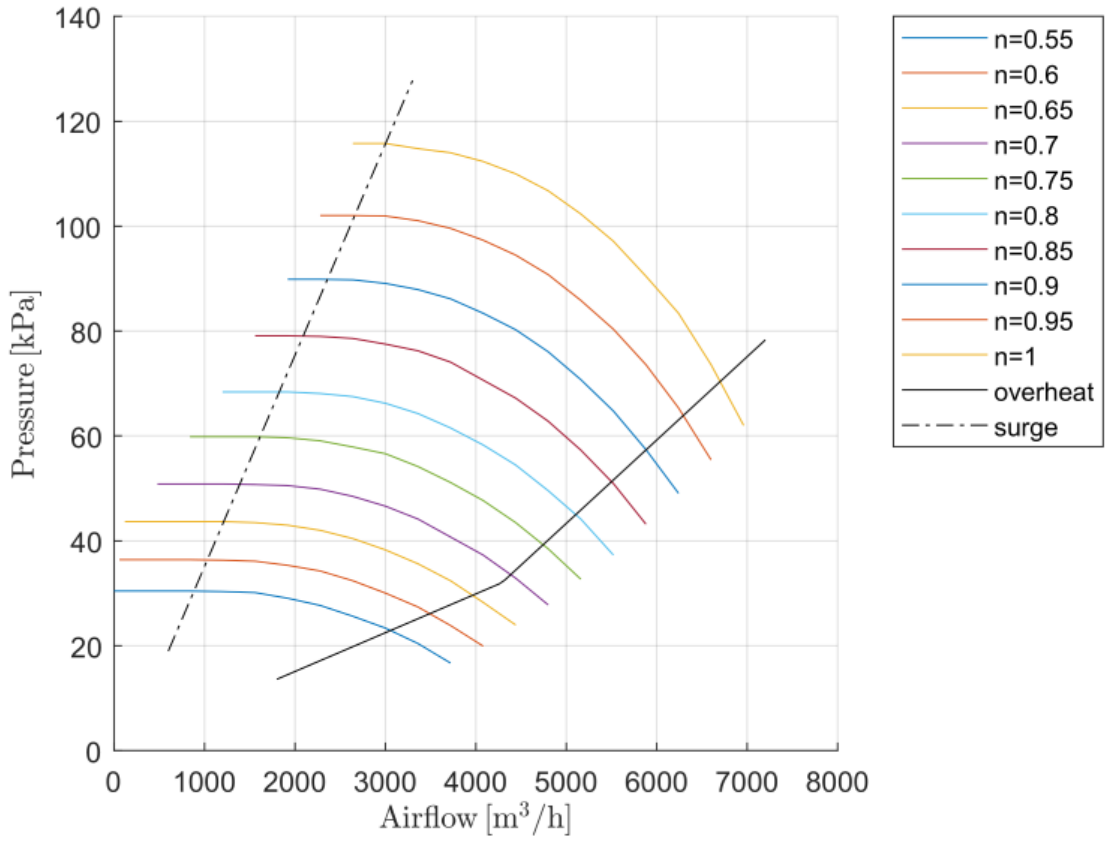

Figure 3.6: Operating characteristics of the AT200 blower (Aerzen USA Corporation, 2025)

3.2 Dissolved Oxygen Model

The dynamics of DO play a vital role in the treatment process. The literature documents a multitude of forms and methods of modelling this phenomenon. Appendix A outlines a straightforward derivation of the DO dynamic model based on mass balance.

The DO model described in this section is designed for use in process control algorithms for state estimation and prediction. The model incorporates several key components, including a complex aeration intensity factor that describes how much of the oxygen supplied by the diffusers at the bottom of the reactor in the form of bubbles is taken up by the reactor contents (dissolves in the water). This factor is further elaborated upon in Subsection 3.2.1. Additionally, the model accounts for the effect of oxygen saturation, a temperature-dependent variable that influences the rate of oxygen dissolution. Another crucial element is the estimation of respiration, which represents the rate of oxygen consumption by microorganisms. The model described utilises data on variables such as temperature, the height of the effluent in the reactor, and the mass flow rate of air through the actuator system. It assumes the use of the respiration estimation described in Subsection 3.2.2. As the modelling of biological phenomena lies outside the scope of this dissertation, the reader is referred to Section 3.6 of (Olsson and Newell (2005)) book for modelling details on the choice of phenomena modelled or the approach to their description.

Let the dynamics of DO in a discrete variable volume of SBR containing an immersed probe

be of the form:

$$\begin{aligned} \mathrm{d}_t\, C_{\mathrm{SO}} = f_T(T(t))\, \alpha\, k_l a_{20}\ (h(t))\, Q_{\mathrm{air}}(t) \\ (C_{\mathrm{SO\,sat}}(T(t)) - C_{\mathrm{SO}}(t)) - \overline{R}(t) + \overline{\Phi}_{\mathrm{m}}(t), \end{aligned} \tag{3.35}$$

where $T(t)$ signifies temperature at t; $f_T(T(t)) \stackrel{\mathrm{def}}{=} 1.024^{(T(t)-20)}$ accounts for Arrhenius equation; α is the oxygen transfer coefficient; $k_l a_{20}$ denotes the aeration rate dependent on the airflow ($Q_{\mathrm{air}}(t)$) and height of medium level ($h(t)$) in the SBR, $C_{\mathrm{SO\,sat}}(T(t))$ signifies cubic approximation of temperature-dependent DO saturation level, $\overline{R}(t) \stackrel{\mathrm{def}}{=} \frac{DO(t)}{K+DO(t)} R(t)$ is the rate of respiration ($R(t)$) to account for the impact of biological species on the DO balance in ASM3e, $\overline{\Phi}_{\mathrm{m}}(t)$ represents the impact of internal mixing flows from neighboring SBR layers (Ujazdowski et al. (2023)).

The DO model described here has been successfully applied by Zubowicz et al. (2024).

3.2.1 Oxygen Transfer Model

The oxygen transfer model addresses the dynamics of oxygen dissolution into water, corrected for variable temperatures using the temperature factor $f(T(t))$ as shown in (3.35). The model takes the form of:

$$k_l a_{20}(h(t)) \stackrel{\mathrm{def}}{=} R_{20}\, \frac{h(t) - h_{\mathrm{diff}}}{C_{\mathrm{SO\,sat}}(20)\, V_{\max}}, \tag{3.36}$$

where: R_{20} representing the oxygen flow at nominal temperature, $C_{\mathrm{SO\,sat}}(20$ signifies cubic approximation of saturation level at nominal temperature, h_{diff} the immersion depth of diffusers, and $V_{\max}$ as the maximum tank volume.

As emphasised by Olsson and Newell (2005), the oxygen transfer model was developed for clean water. The standard parameter $k_l a$, used extensively, does not adequately represent oxygen transfer in wastewater. In the literature on WRRF issues, a correction factor, α, is frequently introduced to adjust for wastewater characteristics. According to Jiang et al. (2023), many researchers assume a fixed $\alpha = 0.5$. However, studies show that α varies with organic load, typically between 0.25 and 0.7. In some cases, values close to clean water conditions $\alpha = 0.8$ are assumed. Jiang proposed an equation for α based on soluble COD denoted as sCOD:

$$\alpha(sCOD) = 0.7704 \cdot e^{-0.035 sCOD}, \tag{3.37}$$

with constraints ensuring α remains within $[\underline{\alpha}, \overline{\alpha}] = [0.25, 0.8]$.

The complete oxygen transfer model incorporating $\alpha \stackrel{\mathrm{def}}{=} \alpha(sCOD)$ is:

$$\alpha\, k_l a_{20}\, (h(t)) = 0.7704 \cdot e^{-0.035 sCOD(t)} R_{20}\, \frac{h(t) - h_{\mathrm{diff}}}{C_{\mathrm{SO\,sat}}(20)\, V_{\max}} \tag{3.38}$$

This approach adjusts oxygen transfer predictions to reflect real wastewater characteristics while ensuring accuracy across a range of operating conditions.

3.2.2 Respiration Estimator

Respiration is a slow-variable process describing oxygen consumption due to microbial activities and biochemical transformations. In this dissertation, it is used in differential models, so the

respiration rate, denoted by $R(t)$, is actually considered.

Respiration is often treated as an external disturbance because measuring equipment (respirometers) is expensive. In literature, respiration measurement is typically considered a soft sensor based on black-box models. For example, this approach has been used by Puig et al. (2006) and Stebel et al. (2021), who proposed simple models based on the calculation of the DO derivative. Nevertheless, recent research papers put forth a more sophisticated methodology for estimating respiration rates, as outlined by Czyżniewski et al. (2023). The authors present a synthesis of observers for respiration rate estimation, employing methods based on sliding mode and an adaptive approach to the Luenberger observer.

The scope of the dissertation does not address the estimation issues. Thus, the availability of $R(t)$ was assumed and determined directly from the ASM3 + BioP model. The procedure for determining the respiration from the Petersen–Gujer matrix is presented in Appendix B.

3.3 Model for Optimisation

The model used for optimisation represents a simplified version of the SBR model derived in Section 3.1. The simplifications employed concentrate on the key elements of the process that are critical for optimisation while excluding less significant phenomena to reduce the computational complexity.

Considering that the objective of optimisation is to improve the performance of the reaction phase of the SBR cycle, the sedimentation phase is excluded from the model. The optimisation approach is thus limited to the processes occurring during the reaction phase, where biological and chemical transformations take place.

Moreover, for optimisation, the reactor is assumed to operate as a perfectly mixed system during the mixing, reaction, and filling phases. This assumption eliminates the need to account for spatial concentration gradients and, therefore, neglects the processes of sedimentation and sludge blanket formation. Based on these assumptions, the model is further reduced to a single-layer representation:

$$\partial_t V = Q_{\text{in}} - Q_{\text{w}} - Q_{\text{e}}, \tag{3.39a}$$

$$\partial_t C_{i_{\text{f}}} = (Q_{\text{in}} C_{\text{in}\,i_{\text{f}}} - (Q_{\text{w}} + Q_{\text{e}} + \partial_t V) C_{i_{\text{f}}}) \frac{1}{V} + r_{i_{\text{f}}}(\boldsymbol{C}), \tag{3.39b}$$

During the reaction phase, whether aerobic or anaerobic, there are no inflows or outflows from the system. Considering only the reactive term $r(z,t)$ from (3.7) as active in the RHS of (3.39) results in:

$$\partial_t V = 0, \tag{3.40a}$$

$$\partial_t C_{i_{\text{f}}} = r_{i_{\text{f}}}(\boldsymbol{C}), \tag{3.40b}$$

Furthermore, the model excludes the dynamics of sensors, actuators, and the operation of the control system. For optimisation purposes, it is assumed that the DO concentration is maintained at a reference value – DO_{ref}. This assumption eliminates additional control-related complexities.

3.4 Model for Task Scheduling

In terms of general notation, the TS problem is understood through the two main sets and the interdependencies between them. The first set includes tasks (**J**), which, as already mentioned in the State-of-the-Art section, are called jobs. They represent a mathematical interpretation of an industrial process or computation on a computer processor and may consist of a sequence of sub-jobs represented by an additional set of operations (**O**). The second most important set is (**M**) – machines, the equipment on which the jobs are executed. Whereby it is assumed that each machine can process at most one job at a time and that each job can be processed on at most one machine at a time. The solution to the problem thus defined is the start and end times of the jobs and their assignment to machines.

TS covers a wide range of problems, which can vary considerably in terms of their nature and complexity. To address this diversity, Graham et al. (1979) proposed a classification framework based on three fields, denoted as $\alpha \,|\, \beta \,|\, \gamma$. This structured approach allows for a systematic description of scheduling problems and their unique characteristics. In this scheme, the α represents the machine environment and is described in Subsection 3.4.1. The second field β represents additional problem constraints and characteristics. Selected interpretations and features are described in Subsection 3.4.2. Finally, the γ field represents the criteria that are optimised. However, they are not part of the model and are therefore described much further (in Chapter 6).

3.4.1 Water Resource Recovery Facility as Machine Environment

The field α is defined by recognising the features of the process flow, the number of machines and the characteristics of the machines. The combination of these three elements constitutes the machine environment.

Starting from the process flow characteristics, a distinction can be made between single-stage and multi-stage processes. Based on the description of the facility presented in Chapter 2, it is intuitive to conclude that the biological batch-type WRRF can be classified as a multi-stage system that manages a set of production jobs (treatment processes) using multiple machines (facility infrastructure).

However, some processes (especially those involving mechanical treatment) do not require scheduling, and their performance is, in some ways, passive. Furthermore, if we assume that only treated wastewater is the product in consideration, then, based on the Assumptions 1.1–1.3 and with regard to the biological aspect of the cycle, the process can be reduced to jobs that are exclusively processed on SBRs, which are now understood to be the only machines in the system. However, this reasoning is not sufficient to distinguish the problem as single-stage or multi-stage.

Each job is a technological process described by operations performed in a restrictive technological order. Based on the description of the SBR cycle (see Chapter 2 and Figure 2.2), the following can be regarded as operations: filling, anaerobic reaction, refilling, aerobic reaction, sedimentation, decantation. The idle phase thus remains a state in which the machine is not assigned any job. In addition, we understand that operations cannot be processed simultaneously. It can, therefore, be assumed that a single job consists of operations performed in a fixed

sequence on a single machine. This allows the cycle to be seen as a whole with a more complex structure, reducing the problem to a single stage. Further details on this approach are provided in Subsection 3.4.2.

Another component that should be considered is the number of machines. Batch treatment plants usually consist of more than one reactor; in the case under consideration, there are six reactors. Thus, the problem under discussion is a multi-machine problem described in the literature as parallel machines.

In Chapter 2, attention is given to two sizes of reactors utilised in the facility. It is important to note that, once initiated, the process cannot be transferred between reactors. This implies that each job must be processed in a designated machine, with each machine having the capacity to perform only a single batch concurrently. This establishes that the machines are independent of one another and do not interact. This observation serves to define a machine environment, with the concept of unrelated machines representing a final element in the definition.

To summarise, the machine environment denoted by the α, in this case, is regarded as a single-stage process with unrelated parallel machines. This type of problem is considered in the literature as UPMSP (Durasević and Jakobović (2023)).

The WRRF can also be interpreted in other ways. For instance, it can be regarded as a singular machine executing a single or multi-stage process, thereby extending the problem to batch scheduling (see Wahl et al. (2024)). Following this perspective, reactors are not viewed as machines in themselves but rather as a means to execute treatment process operations in parallel, akin to threads in a processor. Similarly, the problem can include additional operations such as combustion of excess sludge, biofuel collection or maintenance of actuators, or even downtime associated with infrastructure modernisation. Implying the applicability of other features of the problem, as well as algorithmic solutions designed for other machine environments. However, the remainder of this dissertation adopts the interpretation of biological treatment processes using SBRs as UPMSP.

3.4.2 Problem Features and Additional Constraints

Any scheduling problem, regardless of the machine environment to which it relates, may have a set of special features and constraints that form part of the β field. The number of features may be zero or more and is determined by the problem, its requirements, and the designer's decisions. Some features are implied by the assumed machine environment or are mutually exclusive. The following subsection briefly describes the known features and how they can be implemented in the assumed machine environment. An additional subdivision into time, job and machine features has been introduced.

Time Constraints

These features of the problem relate to the time constraints of the schedule.

- *Setup times*: this feature means that switching from one job to another on the machine requires a configuration operation of a certain duration. This operation prepares the machine for the next job and can be related to the machine, the already completed job or the upcoming job. It may be related to the machine settings, machine cleaning, or other similar operations.

  In the case of the SBR control problem, *setup times* might relate to transitions between operating cycles in which excess sludge removal occurs, or take into account the required reactor pauses before the next fill, allowing the activated sludge to settle completely.

- *Release times*: jobs are not always available from the start of the scheduling horizon. Instead, each job has an associated release time that specifies when it becomes available for processing. Machines cannot execute a job before release time, making this constraint particularly relevant in dynamic scheduling environments.

  In the SBR context, this feature may be related, for example, to the availability of sufficient wastewater volume to initiate a cycle due to the occurrence of inflow, reaching the minimum reactor volume, the filling level of retention tanks, or to the completion of previous phases of the operation cycle.

- *Due date*: this feature refers to the specific time by which a job should ideally be completed, typically treated as a soft constraint. Jobs may be completed after their due dates, albeit at a penalty or reduced performance measure.

  For SBR systems, *due date* may represent a preferred completion time of a cycle or phase, driven by operational requirements or effluent quality objectives.

- *Deadline*: in this case jobs must be completed before a specified time. Unlike due dates, deadlines represent hard constraints, and schedules failing to meet them are considered infeasible.

  In SBR operation, *deadline* constraints may correspond to a hard requirement to complete a phase or cycle before a critical event, such as the next influent occurrence or exceeding allowable hydraulic capacities. It may also be associated with planned discharges from industrial facilities that have additional treatment requirements.

- *Common due date and common deadline*: all jobs may share a common due date or deadline by which they must be completed. This refers to situations where the entire set of jobs must, or should, be completed in a given time frame, rather than there being individual time constraints for each job.

  In the context under consideration, this feature may apply to an entire set of reactors or cycles that should be completed within a specified time interval, e.g., within an operating day, which may be related to the aspects mentioned for *due date* and *deadline*.

Job-Related Features

The features described below relate to the interpretation of the jobs and the process properties that directly influence the form of the jobs.

- *Batch scheduling*: jobs can be grouped into batches for scheduling, with two main approaches: serial and parallel. In a serial approach, jobs within the same batch are processed sequentially, often without additional setup time, allowing for faster execution. In a parallel approach, multiple jobs within a batch are executed simultaneously on a machine, with the batch's execution time determined by the longest processing time among its jobs. Problems of this type are very different from classic TS and are often classified separately in the literature as the batch scheduling problems.

  In the context of SBR, *batch scheduling* may reflect the cyclical operation of reactors, where individual phases can be treated as batch jobs (performed for the same volume of wastewater).

- *Job sizes*: feature unique to the batch scheduling problems. Jobs are assigned sizes that reflect the space they occupy within a batch. If unspecified, all jobs are assumed to be of equal size, typically normalised to one unit.

  For SBR systems, *job size* may be interpreted as the volume of wastewater processed during a given phase, constrained by reactor capacity.

- *Precedence constraints*: specific jobs must follow a predefined execution order, meaning that specific jobs cannot start until their predecessors are completed.

  In SBR operation, this feature arises directly from process technology, where phases such as filling, reaction, settling, and decanting must follow a strict sequence.

- *Auxiliary resources*: this feature refers to some jobs that require additional resources during setup or execution. These resources, such as workers or materials, may be renewable (replenished over time) or non-renewable (finite and depleted once used). Job execution cannot commence unless the necessary resources are available.

  In the context of SBR operation, *auxiliary resources* may include, for example, the available wastewater volume, chemical enhancers, blowers, pumps, electricity, or operating personnel required to perform specific phases of the cycle.

- *Changing processing times*: job processing times are not always constant. They may increase due to deterioration effects or decrease with learning effects or additional resources, such as improved worker efficiency. It is usually assumed to be a constant factor or a time-dependent variable taken into account in long schedules.

  In SBR systems, phase processing times may vary depending on biological conditions (like sludge age), temperature, pollutant load, or the applied control strategy.

Machine-Related and Miscellaneous Constraints

The last group of additional problem features relates to machines but has an indirect impact on time constraints or job features.

- *Machine eligibility*: under this assumption, not all machines are suitable for processing every job. There are permission constraints, which define a subset of machines capable of performing given jobs.

  In the case of SBR, not each reactor may be capable of performing all tasks, e.g. due to differences in volume, technological equipment, or current operational status.

- *Machine capacities*: in batch scheduling scenarios, the capacity of machines affects the size of batches they can process. This means that there can be different batch sizes, and some machines may be able to process larger batches than others.

  Reactor capacity in SBR systems can directly limit the maximum batch volume, affecting the size of jobs that can be processed within a cycle.

- *Dedicated machines*: some machines are better equipped to perform specific jobs, resulting in these jobs being completed more quickly in comparison to other machines. However, this does not preclude them from being performed by other machines as *machine eligibility* does.

  In the context under consideration, some reactors may be better suited to specific types of wastewater, for example, due to different mixing or aeration systems, or the availability of chemical assistance.

- *Machine availability*: machines are not always operational due to scheduled maintenance or unexpected breakdowns. If the periods of unavailability are deterministic, schedules can be planned around them. If stochastic, schedules must adapt dynamically to machine downtime.

  The availability of SBRs may be limited by planned technological interruptions, cleaning operations, or failures, which must be accounted for in the schedule.

- *Machine maintenance*: many scheduling problems (mainly related to production lines) take into account the occurrence of maintenance. Maintenance activities are required to ensure machine functionality, either preventively to maintain desired performance or correctively to address failures. Maintenance periods may be fixed and immutable or flexibly allocated when machines are idle.

  This feature may include the maintenance of reactors, actuators and measuring devices, which may necessitate the temporary shutdown of the reactor.

- *Machine speed*: sometimes machines can operate at different speeds to enhance job processing times. However, higher speeds often incur additional costs, such as increased resource consumption or energy usage.

  In SBR systems, *machine speed* may correspond to aeration or mixing intensity, influencing the rate of biological processes.

- *Machine deterioration*: over time, machine performance may degrade, slowing job execution or reducing capacity. Maintenance (considered as *machine maintenance*) is necessary to restore machine performance to its nominal state. This feature is similar to *changing processing times*, but machine-oriented rather than whole process-oriented.

  Machine deterioration in the context of SBR operation may relate to the degradation of technological elements, such as air diffusers, which may lead to reduced process efficiency and longer phase times.

- *Rework processes*: faulty jobs may need reprocessing on machines, potentially multiple times. These rework constraints are often stochastic, as it is not always known in advance which jobs will require rework.

  In SBR systems, *rework processes* may occur when effluent quality criteria are not met, requiring extension or repetition of reaction phases.

- *Load and transport*: jobs may need to be transported and loaded onto machines using vehicles with limited capacity. The introduction of this related logistics feature has the effect of introducing additional delay times for the start of the jobs, which need to be taken into account in the scheduling process. It can also potentially be associated with available storage space or transport costs.

  Load and transport does not naturally occur in SBR operation. However, it is possible to consider adapting this feature of the problem to include pumping stations or the times associated with filling or emptying reactors.

Selected β Features and Constraints

First of all, in terms of time constraints, there is an excess sludge removal phase in the SBR cycle, which can be considered as preparation of the reactor for the next cycle. As there is no need to change the SBR settings between cycles, the excess sludge removal can be considered as part of the cycle, extending the duration of each task without having to be considered as a constraint in terms of *setup times*.

The biological treatment processes do not usually take into account *deadlines* and *due dates*, but the volume of reactors, retention ponds or auxiliary ponds, such as the stormwater retention lagoon mentioned in Chapter 2, should be taken into account. The presence of these tanks and the assumption of a continuous inflow of wastewater to the plant is linked to the consideration of job availability, which can be interpreted in different ways.

In the system considered, there is a retention tank and a stormwater lagoon, which act as storage in the scheduling problem and provide a buffer between the influent to the treatment plant and the SBRs. The inclusion of this buffer makes it possible to reduce the problem of continuous filling to a discrete problem and thus differentiate the batches of wastewater. This is one of the features that allow the SBR cycle to be treated as a single-stage process in its entirety.

The formulation of this problem can be approached through time constraints on the availability of jobs, i.e. *release times*, or through the availability of jobs depending on the resources in the storage space, i.e. in this case, the reservoirs, by introducing *auxiliary resources*. In this

interpretation of the problem, wastewater is a non-linearly renewable resource that continuously flows into the reservoirs.

Considering another characteristic (*changing processing times*), it can be assumed that over the long time horizon of normal operation of the treatment plant, there are no phenomena that affect the processing rate of the treatment cycles. In addition, there are no dependencies between SBR cycles, so there is no need for *precedence constraints*.

Adopting an understanding of the treatment plant as UPMSP precludes the use of the *batch scheduling* feature, which also implies the exclusion of *job sizes* and *machine capacities*. In the approach under consideration, each reactor operating cycle is treated as a single job. Furthermore, the process control layer in this work is considered as a separate control layer (which is discussed in more detail in later chapters), so the scheduling process does not directly integrate individual phases of the cycle. This abstraction significantly reduces the complexity of the scheduling problem. Conversely, the batch scheduling problem approach would require treating individual phases of the cycle as separate jobs, which could provide a more detailed representation of the process and constitutes a promising area for future research.

Then, moving on to the constraints and features associated with machines and knowing that there are reactors of different sizes capable of processing different batch sizes (not to be confused with *job sizes*), it is possible to introduce a subdivision of the job set into those intended for specific reactor types. This approach introduces a feature of the *machine eligibility* problem. In the exceptional situation where the volume of SBRs involved would be k-times, then one could consider introducing a *dedicated machines* approach so that a certain batch could be executed by a large SBR or by two cycles of another reactor.

Further machine features, such as *machine availability* and *machine maintenance*, are beyond the scope of biological treatment, and thus of this work, and are not considered. However, in real-world problems, these features should be considered individually for each WRRF.

A treatment cycle may consist of several sub-cycles of reactions, as mentioned in Chapter 2, affecting the quality of the treatment and the energy consumption. The number of aeration cycles can therefore be interpreted as a change in machine mode by introducing the *machine speed* feature. Similarly to *changing processing times*, *machine deterioration* is not considered in this formulation of the scheduling problem.

Another feature is related to malfunctioning jobs and their repetition. *Rework processes*, however, are generally not applicable in the WRRF context. If a treatment process does not achieve the desired performance, corrective actions are typically implemented during operation, for example, through chemical enhancement or adjustment of control parameters, rather than by repeating the entire treatment cycle. In practice, treated wastewater is usually pumped from the reactors to downstream units, such as stabilisation ponds or receiving waters, and the plant layout often does not allow the same wastewater batch to be routed back to the reactors for re-treatment. Moreover, a comprehensive assessment of treatment quality is not always available online and is commonly based on laboratory analyses performed at discrete time intervals, rather than on a cycle-by-cycle basis. As a result, the concept of repeating a job, as assumed in *rework processes*, is not directly applicable to the considered system.

The last feature considered in the dissertation is *load and transport*. In the present study,

it was assumed that filling and emptying are parts of the cycle, so this time was transferred to the job duration. In addition, in exceptional situations, *load and transport* can be applied to treatment processes if significant amounts of slurry tankers arrive at the facility.

3.4.3 Sequential Batch Reactor Cycle as Job in Task Scheduling Problem

Assigning an SBR cycle to a reactor, understood as allocating a job to a machine, is one issue. In WRRF problems, however, it is important to evaluate the quality of the treatment process, which significantly depends on the concentration of harmful substances in the influent, so it is necessary to determine what the efficiency of a cycle is. The SBR model described at the beginning of this chapter cannot be used effectively in a TS problem due to its computational complexity. The TS problem requires the assignment of multiple SBR cycles over a given time horizon, and the optimisation problem requires the recalculation of multiple schedules. It is thus imperative to develop a model of reduced computational complexity that incorporates the distinctive characteristics of the SBR and aligns with the standard notation employed in scheduling problems.

In the case under consideration, the set of all job types is denoted as $\mathcal{J}$ and is partitioned into two disjoint subsets: $\mathcal{J} = J_{\text{small}} \cup J_{\text{large}}$, $J_{\text{small}} \cap J_{\text{large}} = \emptyset$. Similarly, the set of all machines is denoted by $\mathcal{M}$, and it is divided into two disjoint subsets: $\mathcal{M} = \mathcal{M}_{\text{small}} \cup \mathcal{M}_{\text{large}}$, $\mathcal{M}_{\text{small}} \cap \mathcal{M}_{\text{large}} = \emptyset$. The subset $\mathcal{M}_{\text{small}}$ represents machines eligible for executing tasks from J_{small}, while $\mathcal{M}_{\text{large}}$ represents machines dedicated to tasks from J_{large}, ensuring a clear division based on capacity and job requirements.

A feasible schedule is then defined by two key decision variables: the start times of tasks, represented as $T = \{T_1, T_2, \ldots, T_K\}$, and the assignment of tasks to machines, expressed as $A = \{(j, m) \mid j \in \mathcal{J}, m \in \mathcal{M}\}$. Each task $j \in \mathcal{J}$ must start at a specific time T_j and be processed on one eligible machine $m \in \mathcal{M}$. The solution must ensure that tasks assigned to the same machine do not overlap in time and that the processing respects the eligibility constraints defined by the task–machine partitioning.

The parameters of each assigned job are needed to evaluate the schedule obtained by the optimisation algorithm. Statistical job models were developed based on data obtained from the SBR cycle optimisation process, as illustrated in Fig 3.7.

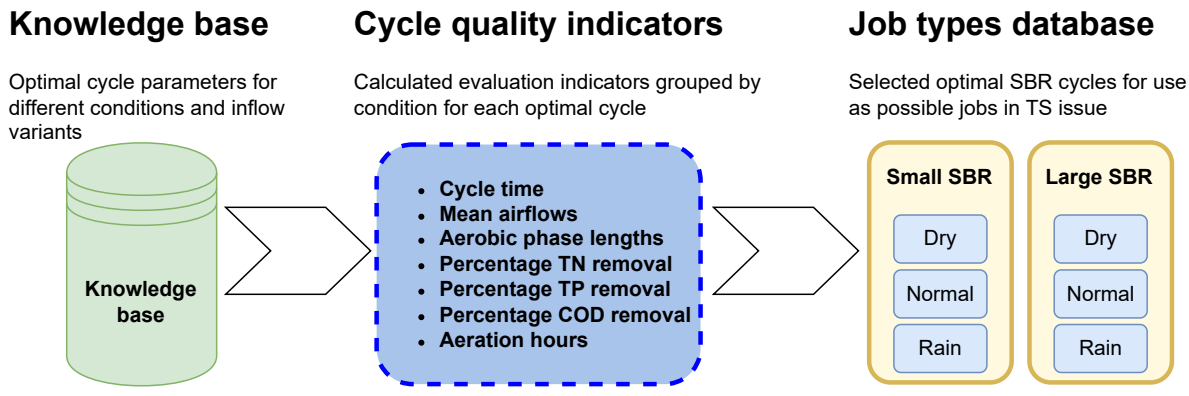

Figure 3.7: Job set design scheme

Quality Indicators (QIs) were calculated for whole groups of scenarios, obtaining statistical values for rain, normal and dry influent types. These calculations are carried out separately for small and large reactors so as to separate the sets of jobs for small and large reactors. In the end, six jobs described by the following QIs were obtained: the vector of average airflows [m^3/d], the vector of aerobic phase durations [d], the total duration of aerobic phases [d], the TN removal efficiency percentage, the TP removal efficiency percentage and the COD removal efficiency percentage. Additional parameters include the total duration of each cycle and the operational vector of actuators, which indicates the hours of equipment operation within a cycle.

The mathematical formulations for these QIs are given as follows. The average airflow during a cycle is defined as:

$$\bar{Q_{\text{air}}} = \frac{1}{R_C} \sum_{n=1}^{R_C} \int_{t_{\text{q}n}^{\text{start}}}^{t_{\text{q}n}^{\text{stop}}} Q_{\text{air}}(t)\, \mathrm{d}t, \tag{3.41}$$

where $\bar{Q_{\text{air}}}$ denotes the average airflow, $Q_{\text{air}}(t)$ represents the instantaneous airflow, R_C number of aerobic phases in a cycle and $t_{\text{q}n}^{\text{start}}$ and $t_{\text{q}n}^{\text{stop}}$ signify the start and end times of phase n, respectively.

The total duration of the aerobic phases is given by:

$$T_{\text{aer}} = \sum_{n=1}^{N} \left(t_n^{\text{stop}} - t_n^{\text{start}} \right), \tag{3.42}$$

where T_{aer} is the total aerobic time, and t_n^{start} and t_n^{stop} denote the start and stop times of the n-th aerobic phase.

The TN removal efficiency is expressed as:

$$R_{\text{TN}} = \left(1 - \frac{C_{\text{out}}^{\text{TN}}}{C_{\text{in}}^{\text{TN}}} \right) \cdot 100, \tag{3.43}$$

where R_{TN} represents the nitrogen removal efficiency, and $C_{\text{out}}^{\text{TN}}$ and $C_{\text{in}}^{\text{TN}}$ denote the total nitrogen concentrations in the effluent and influent, respectively.

Similarly, the TP removal efficiency is given as:

$$R_{\text{TP}} = \left(1 - \frac{C_{\text{out}}^{\text{TP}}}{C_{\text{in}}^{\text{TP}}} \right) \cdot 100, \tag{3.44}$$

where R_{TP} is the phosphorus removal efficiency, with $C_{\text{out}}^{\text{TP}}$ and $C_{\text{in}}^{\text{TP}}$ representing the phosphorus concentrations in the effluent and influent, respectively.

The COD removal efficiency is described as:

$$R_{\text{COD}} = \left(1 - \frac{C_{\text{out}}^{\text{COD}}}{C_{\text{in}}^{\text{COD}}} \right) \cdot 100, \tag{3.45}$$

where R_{COD} indicates the COD removal efficiency, and $C_{\text{out}}^{\text{COD}}$ and $C_{\text{in}}^{\text{COD}}$ denote the COD concentrations in the effluent and influent, respectively.

The procedure for developing the knowledge base is illustrated in Fig. 3.8. This data-driven approach is based on research outcomes outlined in Chapter 5.

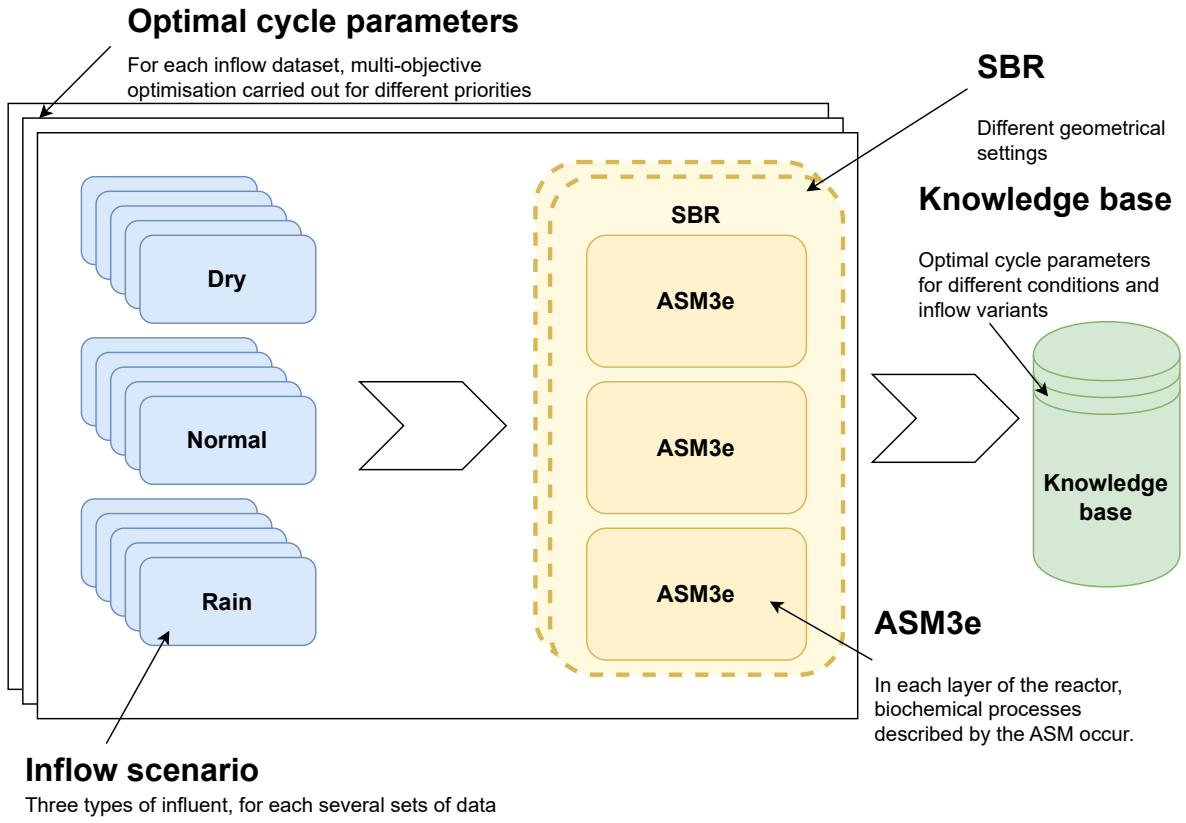

Figure 3.8: Knowledge base design scheme

3.5 Influent Model

In the context of wastewater treatment projects, the quality of the influent can be considered a key factor influencing the final outcomes. The aeration requirements and the effectiveness in removing pollutants are determined by the fraction distribution, which in turn is driven by sludge production that is directly linked to the influent load. Consequently, the dynamics of pollutant inflow into a biological treatment plant have an impact on both short- and long-term process dynamics. Therefore, the evaluation of the system is significantly influenced by the characteristics of the wastewater inflow into the SBR. The preparation of the wastewater influent characteristics was based on the Benchmark Simulation Model no. 2 (BSM2) influent modelling approach, as presented by Gernaey and Jeppsson (2014). A diagram of the influent model is shown in Fig 3.9.

The model was modified by introducing ASM3 + BioP fractions instead of ASM2d fractions. The considered outputs are the daily flow (Q), temperature (T), COD, TN and TP profiles. The original influent model was designed for flow-through treatment plants, so in order to adapt it to the single SBR used in Chapter 5, the influent was reduced by one-third without changing the pollutant concentration.

The model takes into account diurnal behaviour, the weekend pattern, which consists of a lower average flow rate and lower pollutant loads during weekends compared to normal weekdays, seasonal changes to model increased infiltration in the rainy season compared to the dry season, holiday periods during which lower average wastewater flow rates are maintained over a period of several weeks, temperature dynamics, and rain events.

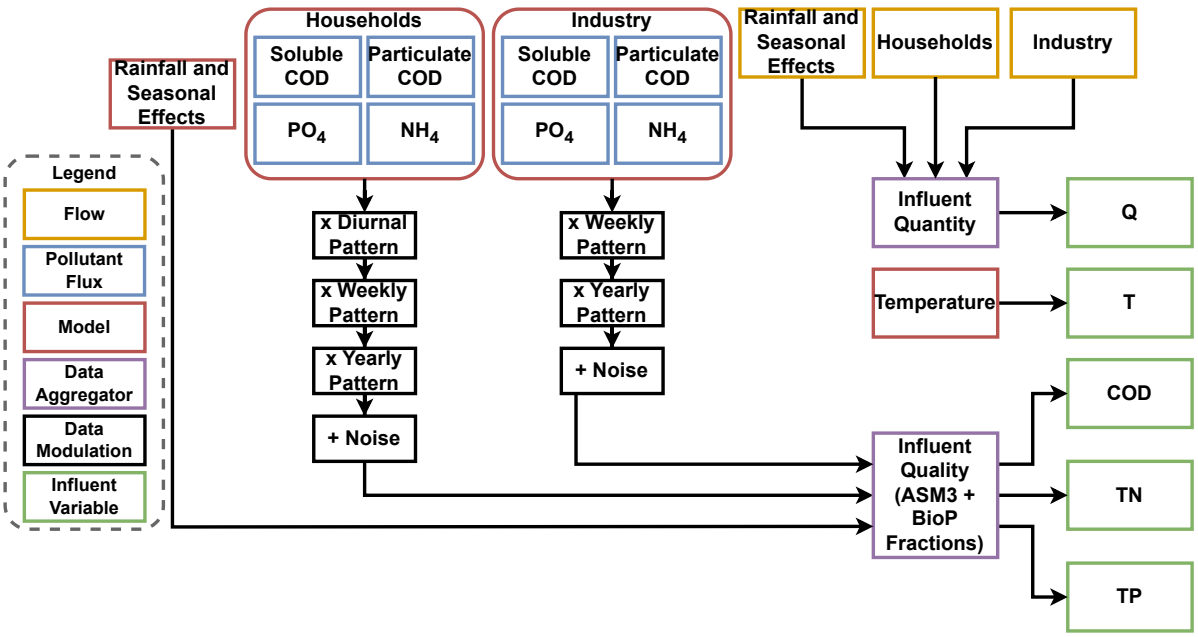

Figure 3.9: General overview of the influent model

To illustrate, the weekend effect entails a slight reduction in household wastewater production, amounting to an 8% decrease on Saturdays and 11% on Sundays, when compared to typical weekdays. Then, the temperature model shows the diurnal and seasonal temperature dynamics that affect the process according to the dependencies mentioned in the previous sections. Moreover, the model employs two seasonal categories and uses a seasonal correction infiltration model to generate a dry-weather seasonal effect and a wet-weather seasonal effect. These two seasonal corrections are then merged with rainfall, allowing the net infiltration contribution to be calculated.

The described model provides influent data for up to 18 months. From this, a full year has been selected, and the data is divided into day-length sequences. Three types of inflow scenarios-dry, normal, and rainy-were then identified as to which of the corresponding inflow sequences belong. In this way, a dataset with variable parameters throughout the year was obtained. To illustrate the variability of inflow data, a sample inflow month is presented in Fig. 3.10, and additional analysis of inflow data is included in Chapter 7.

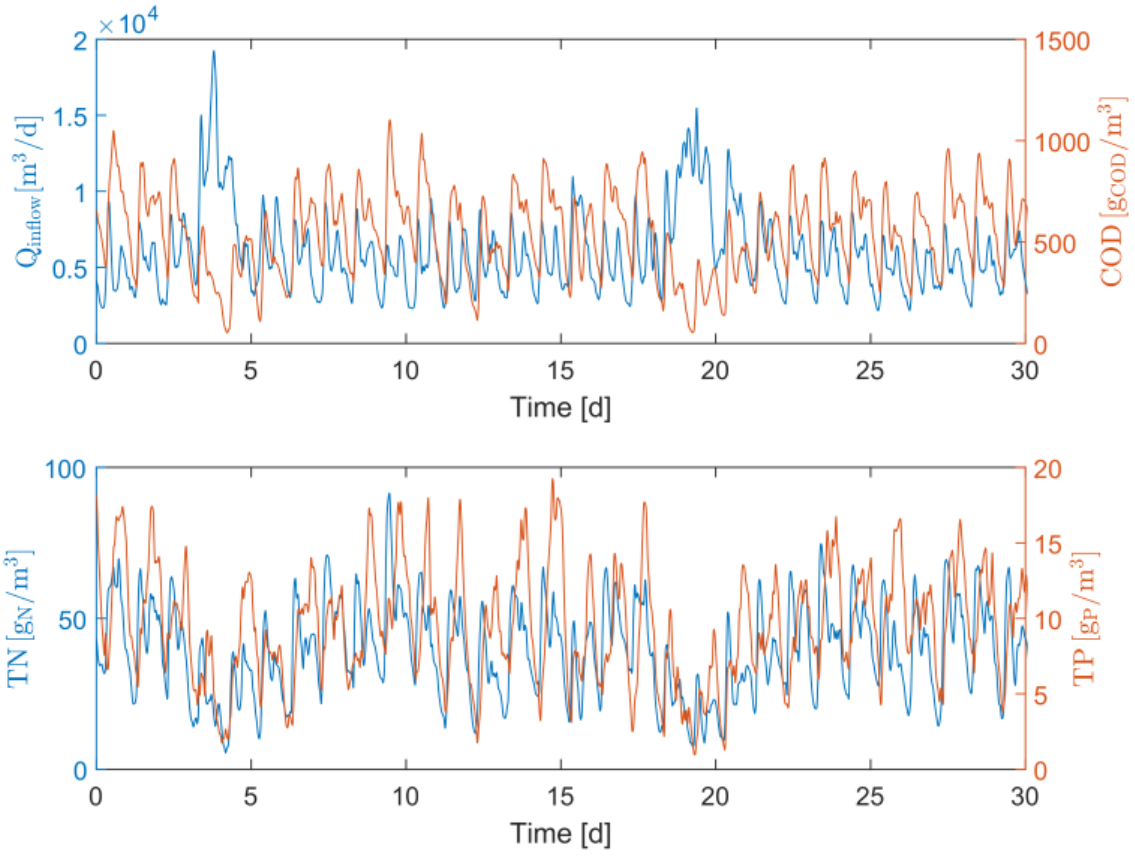

Figure 3.10: Example monthly influent

Chapter 4

Control System Architecture

Control of a given plant can be defined as the intentional and orderly influence of a controller on a plant to achieve the desired operational or functional objectives of the system. When considering the problem of WRRF control, it is therefore necessary to outline the fundamental purpose of the control system being designed. This purpose is to process the inflow of wastewater so that the effluent of treated water meets the standards set by water-related legislation.

The complexity arises both from the nature of the process itself (non-linear, dynamic and highly dependent on external conditions) and from the need to take into account variable operational objectives and numerous technological and environmental constraints. Treatment plants operating in batch mode (SBR) are additionally characterised by the cyclical nature of their operation, which necessitates the use of specific control strategies tailored to the individual phases of the technological cycle. Under such conditions, the design of an effective control system requires not only precise process modelling but also the appropriate division of control tasks to ensure that various aspects of plant operation can be managed in a coordinated and efficient manner.

This chapter focuses on the architectural decomposition of the control system and on the formal specification of information interfaces between decision layers. At this stage, the mathematical objects introduced do not represent concrete control laws or optimisation algorithms; rather, they define abstract input–output relations that characterise how information and commands are exchanged across the hierarchy.

The purpose of this abstraction is to decouple architectural design from controller and optimiser synthesis. Lower layers are responsible for fast, safety-critical execution of control commands, while higher layers operate on slower time scales and generate references, schedules, and operational policies. The formal mappings introduced in this chapter, therefore, specify what information is required and produced by each layer, not how the corresponding control or optimisation problems are solved. Detailed controller design, optimisation formulations, and scheduling algorithms are developed in the subsequent chapters, where the abstract interfaces defined here are instantiated with specific models and solution methods.

The structure of this chapter is as follows. Section 4.1 provides a detailed examination of the layered control structure and the underlying motivation for its utilisation in the context of the problem under consideration. In the subsequent Section 4.2, the formulation of the control problems within each layer is introduced, focusing on the interactions between the layers.

4.1 Motivation for Hierarchical Control

Starting from the fundamental purpose of the WRRF, which determines the way the whole system operates, and complementing it with economic factors, the tasks carried out by the control system in a facility can be organised in a hierarchical manner. Thus, the objectives to be considered when designing the control framework include: ensuring operational safety, maintaining the required quality of the treated effluent and optimising resource consumption and operating costs. Each of these aspects represents a separate but related criterion that should be considered at the appropriate level of the control hierarchy. The fulfilment of the listed sub-objectives enables the overarching goal of operating the treatment plant to be achieved. By dividing tasks according to these criteria, responsibilities can be allocated to the individual layers of the control system, from the top level, which focuses on optimal planning of operations, through the intermediate level ensuring the coordination and quality of technological processes, to the direct level responsible for the safety and operational stability of the implementing equipment. This approach provides the basis for the application of a hierarchical, layered control structure that enables the effective management of a complex and multidimensional wastewater treatment process.

Hierarchical layered control systems are a commonly used approach to controlling advanced and complex industrial processes. By introducing a decomposition of the system (either temporal or functional), the complexity of the control problem for the entire process under consideration can be reduced to several smaller issues. The advantages of this approach are presented in detail by Tatjewski (2007). Furthermore, the discussed control structures have already been successfully applied in flow-through treatment plants, as in (Brdys et al., 2008), where predictive control was implemented in hierarchical structures developed on the basis of functional decomposition. In short, it can be said that reducing the complexity of the control problem facilitates the effective design of both overarching optimisation strategies and local control tasks, adapted to the specifics of the individual process components.

Based on the three economic objectives of the control system – safety, process quality, and cost optimisation – specific functions are assigned to the individual system layers. The direct control layer is responsible for executing defined control commands via actuators, and for preventing the release of untreated wastewater or contaminants into the environment (e.g., by avoiding reactor overflows). Above this lies the process control layer, where the treatment process must comply with desired quality and regulatory standards. These are typically verified by monitoring bodies, for instance, through sample analysis. At this level, the control problem can be framed as a constraint satisfaction task, upon which cost minimisation objectives may be placed. In this study, the cost-oriented objective is extended to incorporate environmental considerations, which may at times conflict with purely economic goals. This reflects the need for solutions that promote more effective wastewater treatment outcomes. Once the plant is operating reliably and in accordance with process objectives, optimisation and planning tasks can be addressed at both the process control level and above. This relates directly to the main contribution of this dissertation: the process optimisation and TS layers introduced as part of the proposed architecture, which include MES-level coordination and planning capabilities. Finally, system layers result from both the aforementioned decomposition and associated economic objectives.

The layers of the designed system correspond to levels 1 to 3 of the five-level automation

pyramid (see Fig. 4.1), in accordance with the ISA-95 standard (Scholten, 2007). With the main effort related to optimisation tasks and economic aspects located at level 3 and partly at level 2. To the best of the author's knowledge, levels 3 and 4 have not been applied to facilities such as WRRF to date.

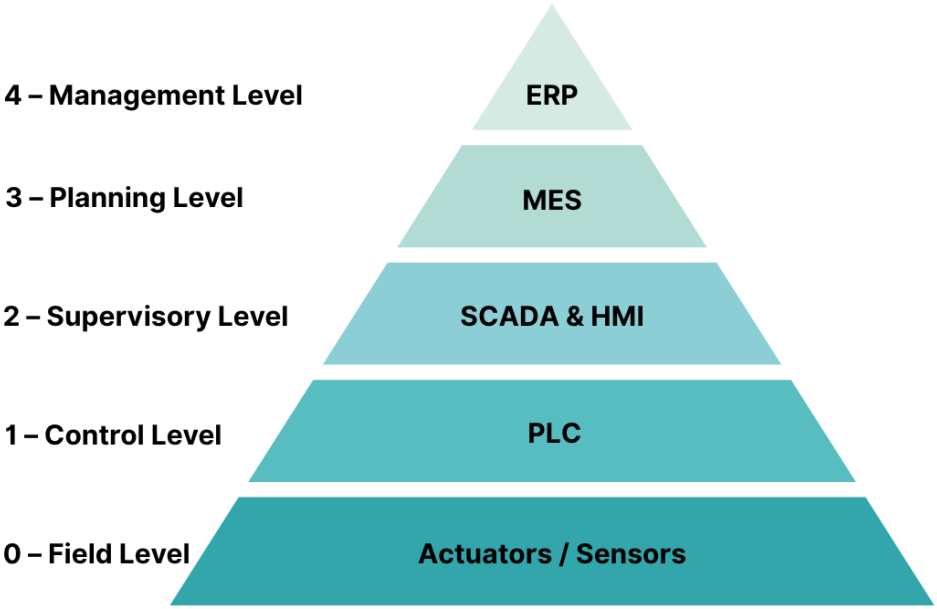

Figure 4.1: Automation pyramid

4.2 Formulation of Control Layers

The following formal definitions specify the abstract interfaces of the hierarchical control architecture. Let Σ_{WRRF} denote a biological batch-type WRRF as a hybrid dynamical system, which comprises a set of processing units modelled as Σ_{SBR}. These units correspond to individual SBRs. By virtue of Assumption 1.1 and Assumption 1.3 the analysis is restricted to the biological treatment stage, i.e., the mechanical stage and emergency modes are excluded.

To facilitate the analysis and design of the control framework, a clear distinction is made between two subsystems:

- Control System, which refers to the lower layers of control (levels 1 and 2) implemented within each individual SBR unit. It encompasses the logic and mechanisms responsible for the safe, stable, and efficient operation of a single reactor. This includes immediate equipment control, local process regulation, and real-time optimisation of internal operating parameters. In addition, it also takes into account offline optimisation of process parameters.

- MES, coordinates the operation of the entire WRRF. Its role is to manage the use of multiple SBR units while taking into account constraints such as inflow variability, resource availability, legal discharge limits and environmental goals. At this level, the system generates schedules for individual SBRs and optimises the distribution of loads across all available reactors.

This decomposition is illustrated in Fig. 4.2, where the vertical structure represents a hierarchical arrangement of decision layers ranging from low-level control to high-level scheduling.

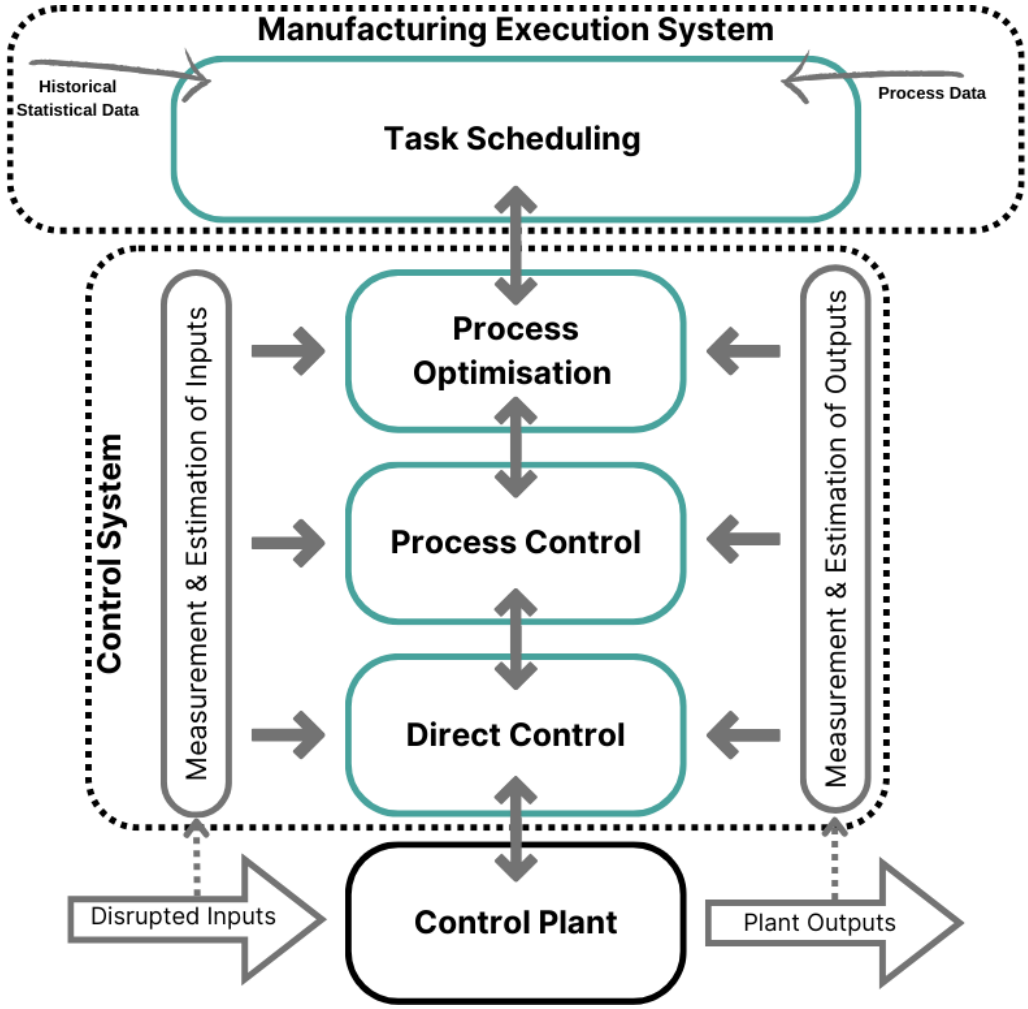

Figure 4.2: System architecture

To define Σ_{SBR}, let $\mathbb{R}^n$ denote the n-dimensional real vector space with standard operations (addition $+$, scalar multiplication $\cdot$), and let $\mathbb{T} \subset \mathbb{R}$ represent an open time interval. Let $\{n_{\text{x}}, n_{\text{u}}, n_{\text{d}}, n_{\text{y}}, n_{\text{c}}\} \subset \mathbb{Z}_+$ be the dimensions of the state, actuation input, disturbance input, measured output, and controlled output spaces, respectively. Then, for all $t \in \mathbb{T}$, the vectors:

$$\boldsymbol{x}(t) \in \mathbb{X}_{\text{x}} \subset \mathbb{R}^{n_{\text{x}}}, \quad \overline{\boldsymbol{u}}(t) \in \mathbb{X}_{\overline{\text{u}}} \subset \mathbb{R}^{n_{\text{u}}}, \quad \boldsymbol{d}(t) \in \mathbb{X}_{\text{d}} \subset \mathbb{R}^{n_{\text{d}}}, \quad \boldsymbol{y}(t) \in \mathbb{X}_{\text{y}} \subset \mathbb{R}^{n_{\text{y}}}, \quad \boldsymbol{c}(t) \in \mathbb{X}_{\text{c}} \subset \mathbb{R}^{n_{\text{c}}},$$

are time-dependent signals corresponding to the state, control input, disturbance, measured output, and controlled output, respectively. A mathematical model of the SBR system is defined as follows:

$$\Sigma_{\text{SBR}} : \begin{cases} \boldsymbol{h}_{\mathbf{x}} : \mathbb{X}_{\text{x}} \times \mathbb{X}_{\overline{\text{u}}} \times \mathbb{X}_{\text{d}} \to \mathbb{R}^{n_{\text{x}}} \\ \boldsymbol{h}_{\mathbf{y}} : \mathbb{X}_{\text{x}} \times \mathbb{X}_{\overline{\text{u}}} \times \mathbb{X}_{\text{d}} \to \mathbb{X}_{\text{y}} \\ \boldsymbol{h}_{\mathbf{c}} : \mathbb{X}_{\text{x}} \times \mathbb{X}_{\overline{\text{u}}} \times \mathbb{X}_{\text{d}} \to \mathbb{X}_{\text{c}} \end{cases}, \tag{4.1}$$

where $\boldsymbol{h}_{\mathbf{x}}$, $\boldsymbol{h}_{\mathbf{y}}$, and $\boldsymbol{h}_{\mathbf{c}}$ denote the dynamics, measurement, and control output functions, respectively.

The measurement system providing soft-sensor outputs is defined as:

$$\Sigma_{\mathrm{M}} : \mathbb{X}_{\mathrm{y}} \times \mathbb{X}_{\mathrm{d}} \to \mathbb{X}_{\mathrm{y_m}}, \tag{4.2}$$

where $\mathbb{X}_{\mathrm{y_m}}$ denotes the space of estimated (measured) outputs. Then, in the subsequent sections, each control layer is introduced in a bottom-up fashion: from direct control and process control, through process optimisation, and finally to the task scheduling problem.

Based on these abstract interfaces, the functionality of each control layer is described next, progressing from direct control to task scheduling.

4.2.1 Direct Control

The direct control layer is the only one that exerts an immediate influence on the physical system. It executes low-level control commands at the actuator level, ensuring that equipment operates in accordance with instructions.

Key actuators include the feed pump, mixer, aeration system, decantation pump, and excess sludge pump. These are characterised by the flow rates associated with the corresponding physical processes: feed (Q_{in}), mixing (Q_{m}), decantation (Q_{e}), sludge removal (Q_{w}), and aeration (Q_{air}). The interface between the control signals and actuator commands is formalised as:

$$\Sigma_{\mathrm{DC}} : \mathbb{X}_{\mathrm{u}} \to \mathbb{X}_{\overline{\mathrm{u}}}, \tag{4.3}$$

where $\mathbb{X}_{\overline{\mathrm{u}}} \subseteq \mathbb{X}_{\mathrm{u}}$, and $\boldsymbol{u}(t) \in \mathbb{X}_{\mathrm{u}}$ for all $t \in \mathbb{T}$.

This layer is usually implemented using PLC-based automation systems, which activate the actuators by sending binary switching signals or setting control values, such as motor speeds or valve positions. These signals are issued based on process recipes and logic programmed into the PLCs and often include basic fail-safe mechanisms.

A detailed consideration of the design and implementation of this layer, including instrumentation and low-level control logic, lies outside the scope of this research.

4.2.2 Process Control

There are three control loops in the process control layer that are essential for this study. The first loop determines the operation of the pump during the filling and decantation phases. The second controls the aeration process by regulating the DO concentration in the SBR. The third activates the mixer. The pump and mixer control systems are realised using on–off (switched) control strategies and thus operate through the direct control layer. The aeration control system, being continuous and more complex, is discussed in Chapter 5. It receives a reference DO trajectory from the higher layer and computes the required $Q_{\mathrm{air}} \in \mathbb{X}_{\mathrm{u}}$.

The control of pumps and the mixer is considered an engineering implementation task, whereas DO control constitutes a significant research challenge. The overall decomposition of the control system is formalised as:

$$\Sigma_{\mathrm{C}} := \Sigma_{\mathrm{DO}} \oplus \Sigma_{\mathrm{P}} \oplus \Sigma_{\mathrm{MIX}}, \tag{4.4}$$

where $\oplus$ denotes the parallel (or block-diagonal) composition of subsystems. Each subsystem $\Sigma_i \in \{\Sigma_{\mathrm{DO}}, \Sigma_{\mathrm{P}}, \Sigma_{\mathrm{MIX}}\}$ represents a controller that maps measurement and reference signals to actuation commands, and shares a common functional structure:

$$\Sigma_i : [\mathbb{X}_{\mathrm{y_m}} \times \mathbb{X}_{\mathrm{r}}] \to \mathbb{X}_{\mathrm{u}}. \tag{4.5}$$

Consequently, the composite controller Σ_{C} also realises a function of the same type:

$$\Sigma_{\mathrm{C}} : [\mathbb{X}_{\mathrm{y_m}} \times \mathbb{X}_{\mathrm{r}}] \to \mathbb{X}_{\mathrm{u}}, \tag{4.6}$$

where $\boldsymbol{y}_{\mathrm{m}}(t) \in \mathbb{X}_{\mathrm{y_m}} \subset \mathbb{X}_{\mathrm{y}}$ is the measurement vector and $\boldsymbol{r}(t) \in \mathbb{X}_{\mathrm{r}} \subset \mathbb{X}_{\mathrm{c}}$ is the reference signal at time t.

Therefore, the plant-wide controller Σ_{PC} is given by the serial composition:

$$\Sigma_{\mathrm{PC}} := \Sigma_{\mathrm{A}} \circ \Sigma_{\mathrm{C}} \circ \Sigma_{\mathrm{M}}, \tag{4.7}$$

where $\circ$ denotes function composition.

As mentioned earlier, the main focus of this work within the process control layer concerns the aeration process. Since the control of pumps and the mixer is not treated as a research problem, the plant-wide controller can be simplified to the following form:

$$\Sigma_{\mathrm{PC}} := \Sigma_{\mathrm{A}} \circ \Sigma_{\mathrm{DO}} \circ \Sigma_{\mathrm{M}}. \tag{4.8}$$

The objective is to design a control law for the aeration process Σ_{DO}, a component of the plant-wide controller Σ_{C}. This controller maps the soft-sensor outputs and reference signals into actuation signals. The reference signals $\boldsymbol{r}(t) \in \mathbb{X}_{\mathrm{r}}$ may be assigned either manually by the plant technologist or automatically as the outcome of an optimisation process, as considered in this work.

4.2.3 Process Optimisation

The process optimisation layer is responsible for determining the optimal configuration of phase sequences and operational intensities within the SBR cycle, subject to dynamic system behaviour and external constraints. This layer addresses the question of when and how intensively to activate various subprocesses (particularly aeration) to ensure treatment objectives are met under varying influent conditions.

As outlined earlier, the SBR reactor performs the functions of both aerobic and anaerobic treatment, as well as settling. The sequence of phases within a single cycle includes non-aerated (e.g., filling, anoxic) and aerated phases. Notably, even within the same treatment cycle, different aeration phases begin under varying conditions, owing to biological and chemical transitions. These variations are further amplified between cycles due to fluctuating influent characteristics. Hence, the optimisation layer must incorporate mechanisms capable of adapting to these changes both within and across cycles.

This temporal variability motivates a computational approach to SBR optimisation and con-

trol, formalised using a hybrid automaton abstraction. Let the structure of the water treatment cycle in a Σ_{SBR} be represented as a Finite State Machine (FSM):

$$\mathcal{G} \stackrel{\text{def}}{=} (S,\, \Sigma_{\text{in}},\, \phi,\, s_0,\, \lambda)\,, \tag{4.9}$$

where S denotes the set of internal states (phases), s_0 initial state, Σ_{in} the finite input alphabet encoding event triggers (timers and sensor thresholds), and λ the structured output function governing actuation. The FSM is driven by a transition function ϕ, which determines the phase evolution in response to events.

However, the individual cycle parameters used to determine the occurrence of state-switching events of the described machine (for example, reaching the required phase length) remain undefined. The optimisation problem is thus formulated over the decision variable vector:

$$\boldsymbol{\chi} \stackrel{\text{def}}{=} \left[(r,\, T_{\text{o}},\, T_{\text{a}})_1\,,\, \ldots,\, (r,\, T_{\text{o}},\, T_{\text{a}})_N\right]^T, \tag{4.10}$$

where r denote the DO concentration intensity, T_{o} and T_{a} denote the durations of the aerobic and anoxic phases. The number of tuples N corresponds to the sequence of reactive phases within a given cycle.

These decision variables are subject to constraints imposed by the process dynamics, control architecture, and physical actuation capabilities. The task of the optimisation layer is to search the space of the problem feasible set to identify the optimal $\boldsymbol{\chi}^*$ that ensures the desired process performance, such as energy efficiency or effluent quality.

It remains challenging to adapt cycle parameters continuously to influent or reactor state due to the limitations of biological and chemical parameter measurement devices. This approach is not only impractical but also not cost-effective. However, offline optimisation can be carried out on the basis of statistical influent data for various scenarios.

Finally, the optimisation task consists of determining the cycle structure understood as an FSM, the treatment cycle parameters such as phase durations, and the DO concentration levels in each aeration segment. This establishes a direct link between the process optimisation and the process control layer.

The detailed implementation of this layer is presented in Section 5.3, which explores MOO strategy for determining the optimal sequencing and operational setpoints of the SBR cycle, taking into account varying influent scenarios and performance trade-offs.

4.2.4 Task Scheduling

The process planning problem is formalised in the MES framework as a TS problem over the set of subsystems Σ_{SBR}, where each task represents a wastewater treatment cycle to be executed. The objective of the scheduling problem is to determine the allocation of tasks to specific reactors (i.e. machine assignment) and to establish the corresponding start times for each execution. Formally, each scheduled operation can be defined as a tuple $\tau_k = (J_k,\, T_k,\, M_k)$, where J_k indicates the type of process treatment cycle, T_k denotes the starting time, and M_k refers to the reactor index assigned to the task. The complete schedule is then represented as a finite set $\mathcal{S} = \{\tau_1, \tau_2, \ldots, \tau_K\}$, which must satisfy mutual exclusivity constraints (i.e. no overlapping tasks

on the same reactor), sequencing constraints, and optional concurrency limitations.

In this setting, the process planning problem is formulated as a TS problem, where each Σ_{SBR} operates under temporal and spatial constraints. Each tuple τ_k encodes the time slot and reactor allocation for a single execution of a treatment cycle. The set $\mathcal{S}$ encodes the global coordination plan, ensuring feasibility with respect to shared infrastructure and inter-reactor constraints.

Each J_k corresponds to a specific instance of an SBR treatment cycle, by providing goals to be achieved by the SBR control system through process optimisation layer obtained by offline optimisation as indicated in Section 3.4. Then, the TS algorithm as described in Chapter 6, provides the sequence ($\mathcal{S}$) of operation of all reactors in the facility over the indicated time horizon. Finally, this layer of the system provides information on the type of cycle structure, its parameters and the switching time for the FSM that is part of the Σ_{SBR}. Furthermore, based on Assumption 1.11, the cycle is executed deterministically, which means that production planning is directly transferred to execution.

Chapter 5

Control System - Process Control & Optimisation

The purpose of this chapter is to provide a comprehensive overview of the considered control system in terms of the process control and process optimisation layers. In Chapter 4, these layers were positioned as elements of the control system corresponding to Levels 1 and 2 of the automation pyramid. The scope of this chapter in relation to the overall system architecture is highlighted in Fig. 5.1 for clarity.

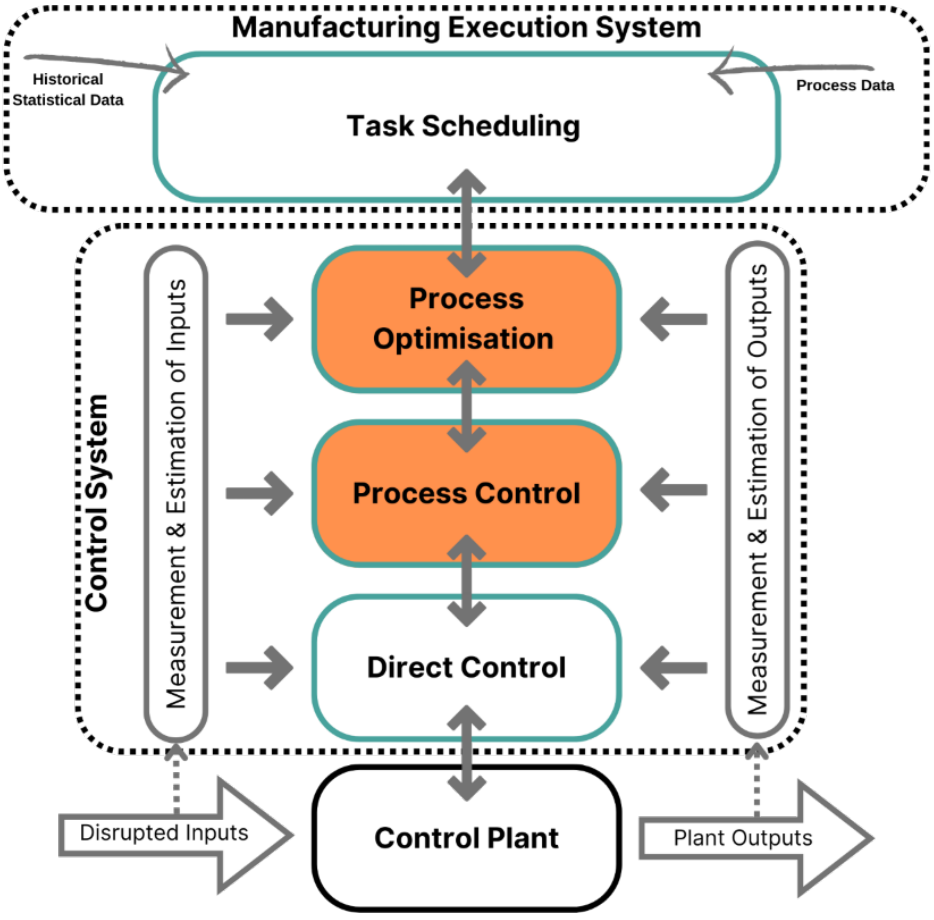

Figure 5.1: System architecture: Process Control & Optimisation

This chapter addresses two main research tasks. First, Section 5.1 presents the DO concentration control system developed under RT 2, including a proposal for the implementation of NMPC as an optimising control strategy supporting various control approaches. Second, Section 5.2 discusses the approach to representation of SBR operation cycle and its execution in the considered framework, which serves as an element bridging offline cycle optimisation and the realisation of corresponding cycle phases and associated processes. Subsequently, Section 5.3 presents the optimisation of the SBR cycle using MOO methods implemented under RT 3.

A detailed process handling pipeline is shown in Fig. 5.2. Among the system components, a data acquisition module has been introduced to support scenario-specific optimisation. This module enables the collection of both historical data and synthetic influent data obtained from the influent model (Section 3.5). The considered cycle optimisation process applies to specific influent conditions and can thus be extended to similar influent patterns. All considered control and optimisation formulations assume normal plant operation as defined in Assumption 1.3, which consequently also implies the full functionality of all actuators and measurement devices.

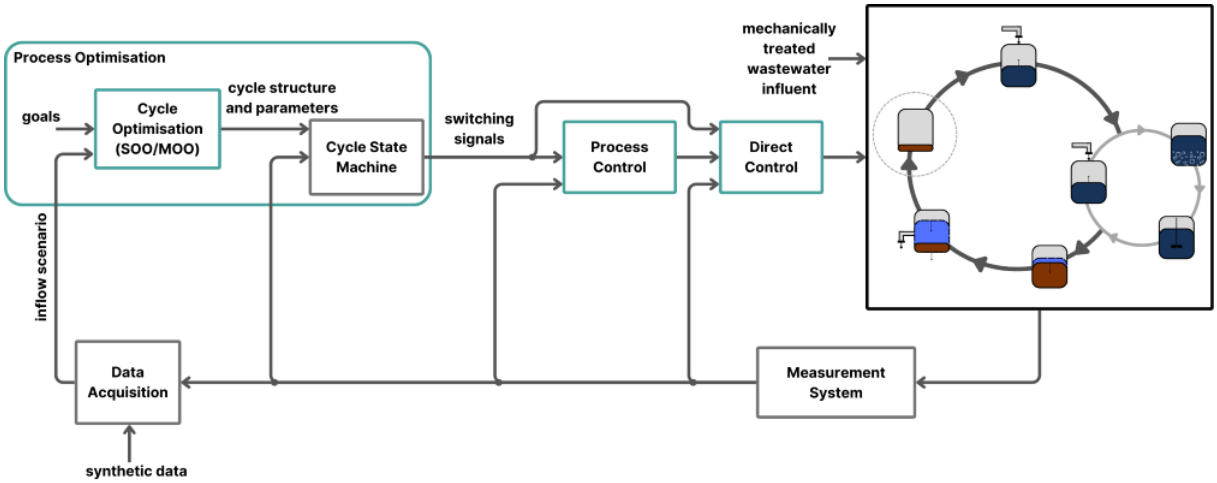

Figure 5.2: Block diagram of SBR cycle optimisation

5.1 Process Control - NMPC-Based Control

The objective of this section is to present a systematically designed NMPC-based DO control framework that is explicitly compatible with hierarchical and optimisation-driven operation of SBR systems. Therefore, the main intention is to present a complete and reproducible controller design procedure, augmented with architectural and algorithmic features that enable direct integration with higher-level optimisation and scheduling layers. Another approach to control using model-based DO control strategies was published in Zubowicz et al. (2024), where a more straightforward form of predictive control was compared with an adaptive approach based on a model – Direct Model Reference Adaptive Control (DMRAC).

The standard designation of controller inputs and outputs has been taken, so for this chapter, u is understood as the control output, also known as the manipulated variable, y is the controlled output, and x stands for the state variable. The aeration process under consideration can be expressed in standard non-linear state-space form to support predictive control design

and constraint handling:

$$\begin{aligned} \dot{\boldsymbol{x}}(t) &= f\big(\boldsymbol{x}(t), \boldsymbol{u}(t), \boldsymbol{d}(t)\big), \\ \boldsymbol{y}(t) &= g\big(\boldsymbol{x}(t), \boldsymbol{u}(t), \boldsymbol{d}(t)\big), \end{aligned} \tag{5.1}$$

where $\boldsymbol{d}(t)$ denotes unmeasured disturbances, $f(\cdot)$ stands for the non-linear state function and $g(\cdot)$ is an output function.

By formulating the controller's task to find the optimum control sequence over the prediction horizon with known constraints, segments that require further explanation are identified. The prediction horizon will be introduced in Subsection 5.1.1 as an explanation of the presence of signal sequences in the controller description, followed by Subsection 5.1.2 describing the optimisation task supplemented by the cost functions and constraints. Furthermore, the final part of Subsection 5.1.2 introduces an additional modification to the controller used during the initialisation of the algorithm. The controller under consideration, illustrated in Fig. 5.3, is applied in closed-loop control as the execution mechanism for supervisory reference trajectories, ensuring constraint satisfaction and dynamic feasibility at the process level. Whereby the actuator system is understood to be the part of the direct control layer responsible for the aeration process itself. The schematic of the controller itself is shown in Fig. 5.4, where elements such as Zero-Order Hold (ZOH), weights, and initial guess are described in the following subsections.

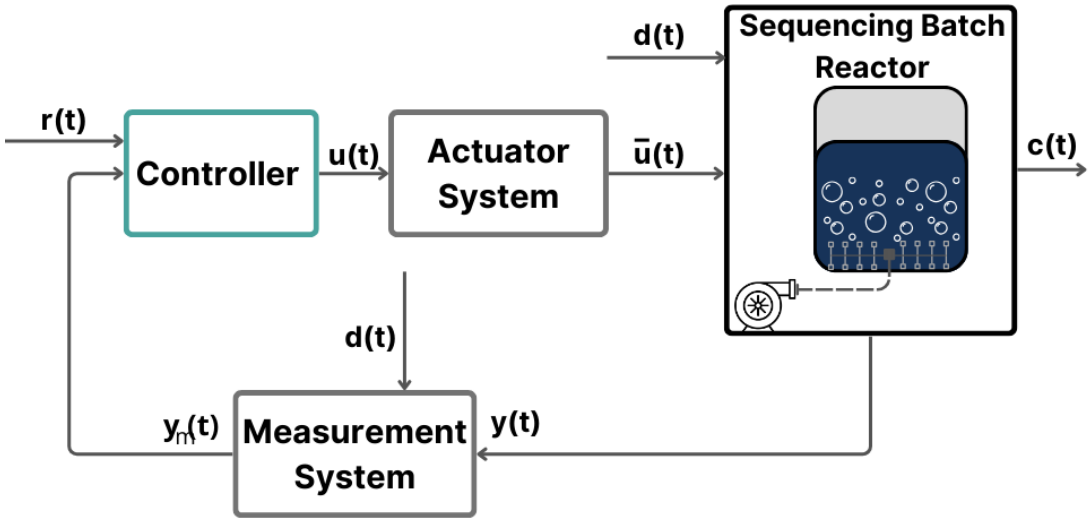

Figure 5.3: Block diagram of DO concentration control

5.1.1 Prediction Horizon and Control Sequence

The main feature that makes the NMPC algorithm highly effective is its ability to anticipate future system behaviour using a process model, taking into account both current measurements and expected disturbances, allowing proactive and constraint-aware control actions to be made over a defined horizon. The algorithm under consideration is based on a non-linear process model in discrete form and is executed in discrete time with a fixed step T_s. The designed algorithm is used to maintain a reference DO level, so DO concentration in SBR is a state variable ($x(k)$) in the model. The DO dynamics model was presented in Section 3.2. It indicates that the variables under consideration include measurements such as DO ($C_{\mathrm{SO}}(t)$), temperature ($T(t)$), reactor fill

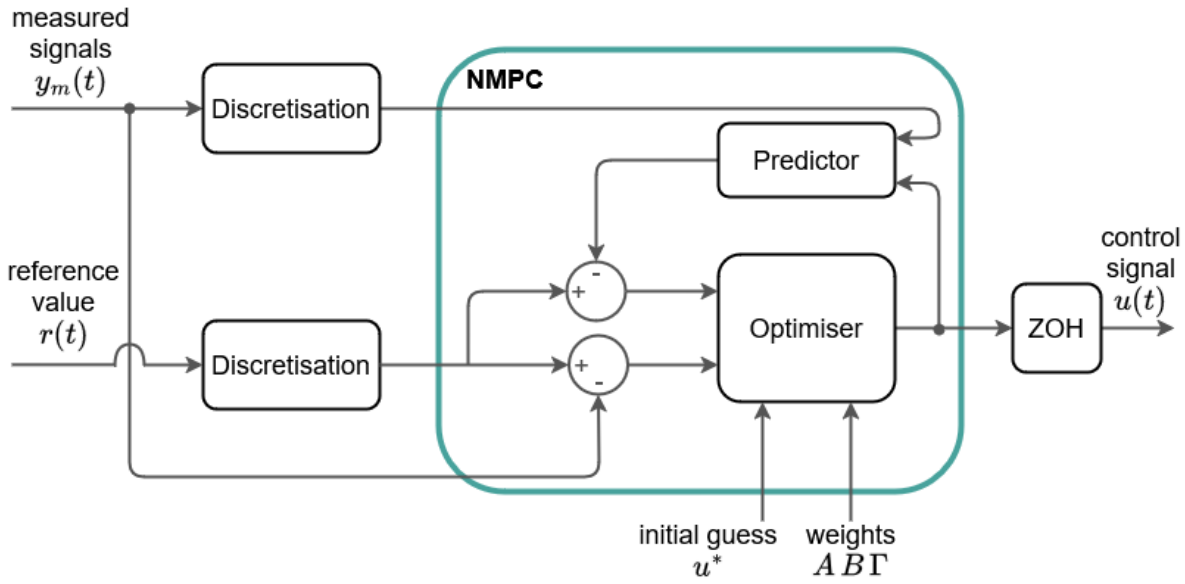

Figure 5.4: Controller scheme - NMPC

level ($h(t)$) and respiration rate ($\overline{R}(t)$), here included as an estimate of respiration ($\hat{R}$) based on Subsection 3.2.2. It also introduces unmeasurable disturbances such as $\overline{\Phi}_{\mathrm{m}}(t)$ and takes into account one manipulated variable – airflow ($Q_{\mathrm{air}}(t)$) – denoted in this chapter as u. However, the model described requires discretisation.

The prediction of the state variable is performed for a number of steps equal to the prediction horizon (H). The floating time window of prediction starts at the current time and has a fixed length equal to the product of T_{s} and H, where T_{s} is the algorithm time step. Signals such as temperature and respiration rate are slowly varying processes, while the reactor fill level is constant during the aeration phase. From a prediction perspective, these become model parameters defined at time k. State variables, as well as disturbances, in turn, take the form of sequences over a prediction horizon H and are given by:

$$\mathcal{D}_k = [\boldsymbol{d}(k|k)^T \ \boldsymbol{d}(k+1|k)^T \ \ldots \ \boldsymbol{d}(k+H-1|k)^T]^T, \tag{5.2a}$$

$$\mathcal{X}_k = [x(k|k) \ x(k+1|k) \ \ldots \ x(k+H-1|k)]^T. \tag{5.2b}$$

Furthermore, the control signal is subject to the same considerations. The $Q_{\mathrm{air}}(t)$ is determined in the optimisation process. In the form of the predictive algorithm used, operating in discrete time, the decision variable takes the form of a sequence corresponding to the control intervals on the control horizon $\mathbf{M}$.

$$\mathcal{U}_k = [u(m_1|k)\, u(m_2|k) \ \ldots \ u(m_M|k)], \tag{5.3}$$

The control horizon takes the form of a vector of natural numbers $\mathbf{M} = [m_1, m_2, \ldots, m_M]$. They represent the control intervals. The length of the control horizon is the sum of the control

intervals and must not exceed the length of the prediction horizon:

$$\sum_{i=1}^{M} m_i \leq H \tag{5.4}$$

At the end of the last interval, the algorithm holds the controller output constant for the remaining prediction horizon steps. Using the control horizon in this form reduces computational complexity. Only the first element of $\mathcal{U}_k$ is applied to plant through an actuator, as:

$$u(t) = \mathcal{L}_{\text{ZOH}} \left\{ u^*(m_1|k) \right\}, \tag{5.5}$$

where $(\cdot)^*$ is optimal realization of $(\cdot)$, $\mathcal{L}_{\text{ZOH}}$ denotes a signal reconstruction using ZOH digital to analogue converter.

Following this, a discrete form of a process model can be introduced to determine (5.2b). Assuming that there is only one output in the adopted model corresponding to the state variable and by discretising (3.35), the model used in NMPC takes the form:

$$\begin{cases} x(k|k) & = x_0, \\ y(k|k) & = x(k|k), \\ x(k+1|k) & = x(k|k) + T_{\text{s}} f_T(T(k|k)) \alpha k_l a_{20}(h(k|k)) u(k|k) \left(C_{\text{SO sat}}(T(k|k)) - x(k|k) \right) \\ & \quad - T_{\text{s}} \hat{R}(k|k) + v(k|k), \end{cases} \tag{5.6}$$

where x_0 is the initial state interpreted as the DO measurement at time k, $(x(k|k),\, u(k|k)) \equiv (C_{\text{SO}}(t),\, Q_{\text{air}}(t))|_{t=kT_{\text{s}}}$ denote the internal model state and control input, $T(k|k)$ is the measured temperature, $h(k|k)$ is the medium level, $\hat{R}(k|k)$ is the respiration rate estimate, and $v(k|k)$ accounts for modelling uncertainties due to structural and parameter errors. The output is denoted by $y(k|k)$.

The $v(k|k)$ term aggregates the impact of transforming (3.35) into (5.6). This disturbance was introduced into the model as an additional state variable inspired by Thangavel et al. (2019), where the authors presented a so-called model-error model to handle structural plant-model mismatch. Thus, the element $\overline{\Phi}_{\text{m}}(t)$ is replaced by the difference between the current DO measurement and the prediction of the state variable $(x(k))$, understood as the prediction error, projected over the entire prediction horizon:

$$v(k|k) = C_{\text{SO}}(k|k) - x(k|k), \tag{5.7a}$$

$$v(k+p|k) = v(k|k) \quad \forall p \in \{1, \ldots, H\} \tag{5.7b}$$

5.1.2 Optimisation Problem Formulation

As previously mentioned, the NMPC algorithm solves a constrained, non-linear, optimisation problem at each time step, generating a sequence of optimal control actions based on the current state and the predicted future behaviour of the system. The optimisation problem takes the

form of:

$$\text{NMPC} := \begin{cases} J^* = \min\limits_{\boldsymbol{z}_k} J(\boldsymbol{z}_k) \\ \text{subject to:} \\ x(k+p|k) \in \Omega_{\text{x}}, \quad y(k+p|k) \in \Omega_{\text{y}}, \\ u(k+p|k) \in \Omega_{\text{u}}, \quad \Delta u(k+p|k) \in \Omega_{\Delta\text{u}}, \\ p \in \{1, \ldots, H\}, \quad x(k+H|k) = x_{\text{H}}, \end{cases} \tag{5.8}$$

where J^* represents the optimal value of the objective function $J(\boldsymbol{z}_k)$, minimised over the decision variable vector $\boldsymbol{z}_k$; the explicit form of $J(\boldsymbol{z}_k)$ and the definition of the $\boldsymbol{z}_k$ are provided later in this section; $x(k+p|k)$, $u(k+p|k)$, and $y(k+p|k)$ are the state, control input, and output predictions at step $k+p$, constrained to belong to the admissible sets Ω_{x}, Ω_{u}, and Ω_{y}, which are introduced and detailed in the subsequent part of this section and are assumed to be subsets of corresponding open sets $\mathbb{X}_{\text{x}}$, $\mathbb{X}_{\text{u}}$, and $\mathbb{X}_{\text{y}}$; $\Delta u(k+p|k)$ is an additional variable representing the control variation and is limited by the admissible set $\Omega_{\Delta\text{u}}$; $p \in \{1, \ldots, H\}$ is the step-index within the prediction horizon, and $x(k+H|k) = x_{\text{H}}$ is the terminal state constraint, ensuring the system's behaviour adheres to desired terminal conditions.

The stability of the control can be examined on the basis of the classical approach (Tatjewski (2007)) by taking the simplified notation of the cost function ($h(x,u)$) and knowing that $h(x,u) \geq 0$ and $h(x,u) = 0$ if and only if $x = 0$ and $u = 0$.

Cost Function

The general formulation of NMPC can be represented as an optimisation problem that seeks to minimise a cost function subject to system dynamics and constraints. In the system under consideration (in accordance with the motivation for hierarchical control presented in Chapter 4), two main, classic control objectives can be distinguished at this layer. Firstly, the quality of control is responsible for achieving the desired DO dynamics, and thus influencing the ecological factors related to the quality of the treatment process. Secondly, the economic factor related to the cost of the process is directly linked to the electricity consumed by the blowers. Moreover, from a pragmatic standpoint, the minimisation of control variability is regarded as an objective, which impacts the stability of biochemical processes and decreases the wear and tear of actuators. The resulting MOO problem was reduced to a SOO using the aggregation method. Thus, the basic equation for the developed cost function can be written as follows:

$$J(\boldsymbol{z}_k) = A \cdot J_{\text{y}}(z_k) + B \cdot J_{\text{u}}(z_k) + \Gamma \cdot J_{\Delta\text{u}}(z_k) + J\epsilon(z_k), \tag{5.9}$$

where $J_y(z_k)$ represents the output reference tracking term, $J_{\text{u}}(z_k)$ corresponds to control energy, $J_{\Delta\text{u}}(z_k)$ is control action variability, $J\epsilon(z_k)$ denotes constraint violation and A, B, Γ are the weights of the individual control strategies. Vector z_k represents the decision variable for the Quadratic Programming (QP) problem assuming control intervals for the entire prediction horizon:

$$z_k^T = [u(k|k)\ u(k+1|k)\ \ldots\ u(k+H-1|k)\ \epsilon_k], \tag{5.10}$$

assuming that u takes values from $\mathcal{U}_k$ on the intervals defined by $\mathbf{M}$:

$$u(k+i|k) = \begin{cases} u(m_1|k), & \text{for } i < m_1, \\ u(m_j|k), & \text{for } \sum_{l=1}^{j-1} m_l \leq i < \sum_{l=1}^{j} m_l, \\ u(m_M|k), & \text{for } \sum_{l=1}^{M} m_l \leq i. \end{cases} \tag{5.11}$$

For output reference tracking, the NMPC controller aims to keep selected plant outputs at or near specified reference values. It uses the following performance measures:

$$J_y(z_k) = \sum_{p=0}^{H-1} [\frac{1}{s_{\mathrm{y}}}(r(k+p|k) - y(k+p|k))]^2, \tag{5.12}$$

where y is dependent on control z_k based on equation (5.6).

The term corresponding to control energy is then expressed as the sum over the prediction horizon of the squares of the scaled control signal:

$$J_{\mathrm{u}}(z_k) = \sum_{p=0}^{H-1} \left(\frac{1}{s_{\mathrm{u}}} u(k+p|k)\right)^2. \tag{5.13}$$

Similarly expressed is the control action variability term, which takes the values of the control signal change:

$$J_{\Delta \mathrm{u}}(z_k) = \sum_{p=1}^{H-1} \left(\frac{1}{s_{\Delta \mathrm{u}}} \cdot (u(k+p|k) - u(k+p-1|k))\right)^2. \tag{5.14}$$

Constraint violation constitutes the remaining part of the cost function. An NMPC controller employs a dimensionless, non-negative slack variable, ε_k, which quantifies the worst-case constraint violation. The corresponding performance measure is:

$$J_\varepsilon(z_k) = \rho_\varepsilon \varepsilon_k^2, \tag{5.15}$$

where ε_k is a dimensionless slack variable at control interval k and ρ_ε denotes the constraint violation penalty weight.

The weighting coefficients determine the relative prioritisation of tracking performance, energy efficiency, and control smoothness, thereby encoding the operational control strategy. The weights for each control strategy $A\,B\,\Gamma$ can be selected based on the assumptions made during design or can be selected through a procedure of tuning the controller parameters or optimising them. In this research work, the selection of weights for the strategy was based on experiments conducted in Chapter 7 to analyse the system's behaviour for different weights.

The selection of weights for the normalised cost functions enables the determination of the control strategy, with the position of the point in space dictating whether the controller should seek the optimal hold on the set point or perhaps also reduce the cost of control. This is especially relevant for SBR conditions because, for repeated aeration phases, each successive phase requires a different air supply to maintain the same DO level, and the same is also valid for long-term aeration phases. Furthermore, fluctuations in the microorganism population within the biological reactor render it more cost-effective to maintain DO levels in relation to cycle time.

Constraints

The state variable, as well as the manipulated variable, are assumed to take scalar values and are constrained to the ranges $\Omega_x = [\underline{x}, \overline{x}]$ and $\Omega_u = [\underline{u}, \overline{u}]$, respectively. In addition, for the manipulated variable, a limitation is applied to the rate of change of the signal, which is constrained to the range $\Omega_{\Delta u} = [\underline{\Delta u}, \overline{\Delta u}]$. The constraint on the state variable reflects the nature of the process, whereas the constraints on the manipulated variable and its rate of change are related to the actuator's capabilities. Based on equation (5.6), the output constraints $\Omega_y = [\underline{y}, \overline{y}]$ are assumed to coincide with the state constraints, i.e., $\Omega_y = \Omega_x$.

The NMPC implementation includes a slack variable and the scaling of the variables to a normalised form, through which the constraints take a modified form:

$$\frac{\underline{y}}{s_{\mathrm{y}}} - \varepsilon_k \underline{V}_{\mathrm{y}} \leq \frac{y(k+p \mid k)}{s_{\mathrm{y}}} \leq \frac{\overline{y}}{s_{\mathrm{y}}} + \varepsilon_k \overline{V}_{\mathrm{y}}, \tag{5.16a}$$

$$\frac{\underline{u}}{s_{\mathrm{u}}} - \varepsilon_k \underline{V}_{\mathrm{u}} \leq \frac{u(k+p-1 \mid k)}{s_{\mathrm{u}}} \leq \frac{\overline{u}}{s_{\mathrm{u}}} + \varepsilon_k \overline{V}_{\mathrm{u}}, \tag{5.16b}$$

$$\frac{\underline{\Delta u}}{s_{\Delta \mathrm{u}}} - \varepsilon_k \underline{V}_{\Delta \mathrm{u}} \leq \frac{\Delta u(k+p-1 \mid k))}{s_{\Delta \mathrm{u}}} \leq \frac{\overline{\Delta u}}{s_{\Delta \mathrm{u}}} + \varepsilon_k \overline{V}_{\Delta \mathrm{u}}, \tag{5.16c}$$

where V denotes dimensionless Equal Concern for Relaxation (ECR) values used to soften the constraints, ε_k is a scalar quadratic programming slack variable, s_{y} denotes the scale factor for plant output in engineering units, s_u is the scale factor for the control value in engineering units, and $s_{\Delta \mathrm{u}}$ is the scale factor for the control value in engineering units.

The introduction of slack variables and the scaling of optimisation variables serve two complementary purposes. Firstly, scaling is applied to improve the numerical conditioning of the underlying QP problem by bringing all optimisation variables and constraints to comparable magnitudes. Secondly, the use of a slack variable allows the constraint set to be softened in a controlled manner, ensuring feasibility of the optimisation problem under model mismatch, disturbances, or transient operating conditions. By penalising the slack variable in the cost function, constraint violations are discouraged but not strictly prohibited, which improves robustness and prevents infeasibility of the NMPC optimisation problem. In this case, the V parameters are dimensionless controller parameters analogous to the cost function weights but used to soften the constraints implicitly used in the adopted simulation environment. Taking all ECR values as zero means applying hard constraints[1].

Initial Guess of Manipulated Variable

The aerobic reaction phase follows long-lasting anaerobic conditions that bring the DO concentration close to zero. To mitigate prolonged transient behaviour at the onset of aerobic phases, an informed initialisation strategy for the manipulated variable is employed. It allows a predetermined value to be applied in the first step of the controller, mimicking the start-up state of the system.

[1] In the conducted simulation studies, no violations of hard constraints were observed for the considered operating conditions.

This value can be determined from the model equation (3.35), taking the average measurement of respiration in the first aeration phase and assuming that the operating point for known temperature and height has been reached. Assuming that the derivative of DO is equal to zero and substituting under the parameters and variables of equation (3.35) the values shown in Table 5.1, we obtain $u^* = 64\ 220\ \mathrm{m}^3/\mathrm{d}$.

Table 5.1: Parameter values used for initial manipulated variable guess

Parameter	**Value**	**Unit**
R_{20}	16	$\mathrm{g\,O_2/m^4}$
$C_{\mathrm{SO\,sat}}$	8.63736	$\mathrm{g\,O_2/m^3}$
h_{diff}	0.5	m
$V_{\max}$	4948	$\mathrm{m^3}$
α	0.8	–
$\hat{R}$	700	$\mathrm{g\,O_2/m^3}$
h	5.985	m
T	20	°C

5.2 Cycle Representation and Execution Logic

In conventional operation, cycle structures and parameters are manually configured by the technologist (see Table 5.2) and further used as fixed over many cycles of operation. In contrast, the proposed framework replaces this static configuration with data-driven cycle optimisation.

Table 5.2: Structure and parameters of an example SBR cycle

lp.	Phase name	Phase switching condition	Duration (T_{d}) [hours]
1	Idle	$T_{\mathrm{p}} \geq T_{\mathrm{d}}$	1.20
2	Filling 1	$V_{\mathrm{m}} \geq 0.86 V_{\max}$	–
3	Aerobic 1	$T_{\mathrm{p}} \geq T_{\mathrm{d}}$	3.71
4	Anaerobic 1	$T_{\mathrm{p}} \geq T_{\mathrm{d}}$	2.66
5	Filling 2	$V_{\mathrm{m}} \geq 0.96 V_{\max}$	–
6	Aerobic 2	$T_{\mathrm{p}} \geq T_{\mathrm{d}}$	3.97
7	Anaerobic 2	$T_{\mathrm{p}} \geq T_{\mathrm{d}}$	1.63
8	Filling 3	$V_{\mathrm{m}} \geq 0.98 V_{\max}$	–
9	Aerobic 3	$T_{\mathrm{p}} \geq T_{\mathrm{d}}$	4.80
10	Anaerobic 3	$T_{\mathrm{p}} \geq T_{\mathrm{d}}$	0.24
11	Sedimentation	$T_{\mathrm{p}} \geq T_{\mathrm{d}}$	0.77
12	Decantation	$T_{\mathrm{p}} \geq T_{\mathrm{d}}$	1.00
13	Reactor emptying	$V_{\mathrm{m}} \leq 0.60 V_{\max}$	–

T_{d} denotes the preset duration of the selected phase, T_{p} is the elapsed time of the current phase, V_{m} is the current reactor volume, and $V_{\max}$ is the maximum reactor volume.

A cycle defined in this manner can be implemented as a sequence of actuator switching actions and, naturally, represented as a finite-state machine. A state machine is responsible for phase transitions and monitoring the process flow. It takes the cycle structure and parameters as input and provides discrete actuator commands and continuous reference trajectories to the process control layer. The optimisation method introduced in Section 5.3 replaces the predefined cycle pattern with patterns obtained by solving the optimisation problem for the selected influent data. Furthermore, the selection of optimisation objectives gives a range of possible cycle realisation scenarios for a given influent data. This is of particular relevance in the context of MOO, wherein the decision-maker has the capacity to determine whether further reduction of selected pollutants is necessary, for instance, based on the status of local water bodies.

A Moore state machine is defined by its finite set of states, input and output alphabet, and a state transition function. In the case under consideration, the states refer to the phases of the SBR cycle. Table 5.3 provides an overview of the states, denoted as:

$$S = \{S_I, S_F, S_O, S_A, S_S, S_D, S_E\}. \tag{5.17}$$

Considering the description of the cycle in Chapter 2, each operation of filling or refilling the SBR with wastewater is assumed to be defined by three factors: duration, operating costs and volume of wastewater transported from the pumping station to the SBR. Sedimentation and reaction operation under anaerobic conditions are defined solely by duration. Meanwhile, the operation of the reaction under aerobic conditions is represented by duration and energy consumption for the operation of the blowers. Decanting and excess sludge removal are analogous to filling the SBR, utilising only energy resources. However, the costs associated with sludge removal are outside the scope of this consideration.

The inputs to the system, which trigger transitions between states, are collectively referred to as the input alphabet, defined in Table 5.4 and represented as:

$$\Sigma_{\text{in}} = \{\text{a, b, c, d, e, f, g, h, i, j, k}\}, \tag{5.18}$$

where the inputs are either time-based transitions (e.g., a, d, e) or volume-based transitions (e.g., b, g, j).

Next, the transition function, denoted as ϕ, specifies how the state changes in response to the current state and input, according to:

$$\phi : S \times \Sigma_{\text{in}} \to S. \tag{5.19}$$

Therefore, the output function, λ, maps each state to a unique output vector, representing the system's operational parameters in that state:

$$\lambda : S \to \Sigma_{\text{out}}. \tag{5.20}$$

The state transitions are detailed in Table 5.5, where each row maps the current state and input symbol to the subsequent state and output vector. Assuming this understanding, the output alphabet (Σ_{in}) is defined in the Output column of Table 5.5. This binary state vector

($\boldsymbol{b} \in \{0,1\}^n$) indicates the ON (1) or OFF (0) status of the reactor feed, mixer, aeration, decantation and excess sludge removal actuators with related control layers, respectively.

Finally, Fig. 5.5 shows the diagram of the state machine under consideration.

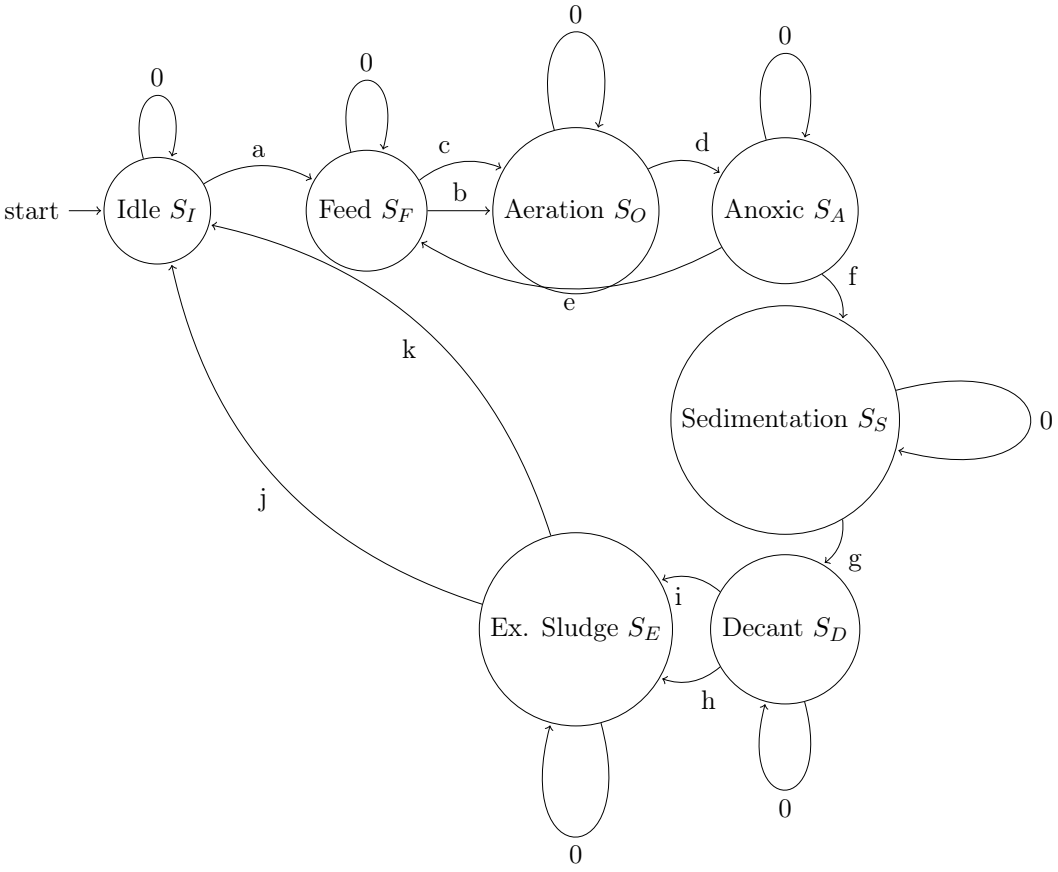

Figure 5.5: Cycle State Machine: Diagram

Recognising that the SBR's phase transitions are event-driven in a state- and input-dependent manner, the similarities of these operational characteristics to a manufacturing system become apparent.

At each discrete time step t, the state machine:

1. receives an input: $\sigma_t \in \Sigma_{in}$,
2. is in a current state: $q_t \in Q$,
3. transitions to the next state via: $q_{t+1} = \phi(q_t, \sigma_t)$,
4. produces an output consisting of: $\lambda(q_t) = (\mathbf{b}_t)$.

Table 5.3: Cycle State Machine: States

Index	Name	Symbol	Description
0	Idle	S_I	Waiting phase for the start of the cycle, during which the actuators are switched off and the volume of the tank is only activated sludge. The phase has a defined duration, after which a change of state takes place.
1	Feed	S_F	During this phase, the tank is filled to the indicated volume. The phase can occur several times during one cycle if there are so-called refills. During this phase, the feed pump system is switched on and the occurrence of a mixing process (not necessarily associated with the operation of the mixer) is considered. A phase has a defined duration and a set volume. A change of state occurs when the first condition is met.
2	Aeration	S_O	Part of the reaction phase in which aerobic processes occur. During this phase, the aeration system is switched on. Depending on the type of diffuser system, mixing is carried out by the aeration process or an external mixer. The phase has a defined duration, after which a change of state takes place.
3	Anoxic	S_A	Part of the reaction phase in which anoxic processes occur. During this phase, the aeration system is switched off. Mixing is carried out by external mixer. The phase has a defined duration, after which a change of state takes place. This is the final stage of the reaction phase, after which the process can proceed to the sedimentation stage, or to the next reaction phase.
4	Sedimentation	S_S	A phase similar to Idle, but implemented for a full reactor. The phase has a defined duration, after which a change of state takes place.
5	Decant	S_D	During this phase, the tank is emptied, through a system of pumps discharging the treated effluent. The phase has a defined duration and a fixed volume. A change of state occurs when the first condition is met.
6	Ex. Sludge	S_E	The excess sludge discharge phase is carried out after the decantation process is completed. The phase has a defined duration and a fixed volume. A change of state occurs when the first condition is met.

Table 5.4: Cycle State Machine: Alphabet

Symbol	Name	Description
0	No change	The machine remains in the current phase.
a	Idle Duration	Change of state from Idle to Feed as a result of reaching the set phase duration
b	Feed Duration	Change of state from Feed to Aeration as a result of reaching the set phase duration. * The filling time is assumed to be a safety condition, occurring only as a result of a small inflow of pollutants, resulting in the start of the cycle for an partially filled. **Consideration is being given to starting the reaction phase with an aeration sub-phase, in line with previous research results on optimising the sequence of the reaction phase.
c	Feed Max Volume	Change of state from Feed to Aeration as a result of reaching the set phase volume.
d	Aeration Duration	Change of state from Aeration to Anoxic as a result of reaching the set phase duration.
e	Anoxic Duration	Change of state from Anoxic to Feed as a result of reaching the set phase duration. * Occurs if the cycle involves more than a single reaction phase.
f	Anoxic Duration Last Reaction	Change of state from Anoxic to Sedimentation as a result of reaching the set phase duration. * Indicates the end of the reaction phase.
g	Sedimentation Duration	Change of state from Sedimentation to Decant as a result of reaching the set phase duration.
h	Decant Duration	Change of state from Decant to Ex. Sludge as a result of reaching the set phase duration.
i	Decant Min Volume	Change of state from Decant to Ex. Sludge as a result of reaching the minimum set volume for the completion of this phase.
j	Ex. Sludge Duration	Change of state from Ex. Sludge to Idle as a result of reaching the set phase duration.
k	Ex. Sludge Min Volume	Change of state from Ex. Sludge to Idle as a result of reaching the minimum set volume for the completion of this phase.

Table 5.5: Cycle State Machine: Transitions

Current state	Input	Next state	Output
S_I	0	S_I	[0 0 0 0 0]
	a	S_F	
S_F	0	S_F	[1 1 0 0 0]
	b	S_O	
	c	S_O	
S_O	0	S_O	[0 1 1 0 0]
	d	S_A	
S_A	0	S_A	[0 1 0 0 0]
	e	S_F	
	f	S_S	
S_S	0	S_S	[0 0 0 0 0]
	g	S_D	
S_D	0	S_D	[0 0 0 1 0]
	h	S_E	
	i	S_E	
S_E	0	S_E	[0 0 0 0 1]
	j	S_I	
	k	S_I	

5.3 Process Optimisation - Multi-Objective Optimisation

Application of an approach based on a MOO algorithm responds to emerging regulatory, environmental, and sustainability-driven performance criteria in modern WRRF. It aligns with the sixth Sustainable Development Goal, which aims to ensure access to water and sanitation for all through the sustainable management of water resources (Setty et al. (2020)). Legal water restrictions (European Council Directive (1991)) have long-established pollution standards; however, significant climate-focused policy changes are beginning to emerge in the EU, such as those outlined by Popp (2024). Implementing these changes in water resource management requires appropriate tools.

The employment of MOO allows constraints on selected QI to be transferred to the minimisation task, thereby resulting in a more responsive environment than that achieved through process optimisation using SOO. This section considers the inclusion of TP, TN and COD estimates in the upper reactor layer during the decantation phase in the optimisation process, thus providing an estimate of the performance of the entire treatment cycle.

As the name suggests, MOO assumes the existence of more than one objective function. These functions are often conflicting, and the optimisation problem is defined in a multidimensional objective space, where each solution is represented as a vector of objective function values. Unlike SOO, which aims to find decision variable values that yield extreme (minimum or maximum) objective function value while satisfying imposed constraints, MOO seeks to optimise all components of the objective function vector simultaneously.

Therefore, the solution of a MOO problem takes the form of a set of solutions that constitute

a subset of the decision variable space. In practice, this set is narrowed down by introducing constraints or infeasibility conditions for the obtained solutions. Therefore, the implementation of constraints allows to define a set of feasible solutions, which constitutes a subset of the space of decision variables.

In case when optimisation algorithm yields a set of feasible solutions such that no objective can be improved without worsening at least one other, the resulting set constitutes the Pareto-optimal solutions. This set, known as the Pareto front, represents optimal trade-offs between objective functions. In practice, selecting a specific solution from this set requires additional preference-based methods, such as weighting schemes, compromise programming, or interactive methods that incorporate the subjective priorities of the decision-maker. Details on optimality concepts in MOO problems, as well as explanations of terms specific to this type of optimisation, are presented in Chapter 3 of the book (Sekulski (2012)).

As a reminder, as discussed in the State-of-the-Art section, MOO has primarily been applied to continuous-flow WWTPs, where decision variables typically include concentrations of fractions in aerobic and anaerobic tanks, aeration, or recirculation rates. However, such optimisation does not directly translate to batch treatment plants, where phase durations and reaction cycle structures play a more significant role.

In the considered case, MOO was implemented without introducing the number of reaction cycles as a decision variable. Instead, a separate optimisation was performed for one reaction cycle ($R_C = 1$) and for three reaction cycles ($R_C = 3$). Fixing the number of reaction cycles reduces the dimensionality of the optimisation problem while remaining consistent with established operational practice at WWTP, where the single reaction phase approach is popular in the literature, while the normal operating manner of the Swarzewo facility is three reaction cycles. Each reaction cycle has its own duration of phases and desired level of DO concentration. This assumption is another reason for adopting a fixed number of reaction cycles to avoid changing the number of decision variables during the solution of the optimisation problem. Moreover, the research studies conducted as part of Section 5.1 have demonstrated that subsequent aeration phases demand a reduced aeration level to sustain a DO_{ref}. Further details can be found in Chapter 7.

Therefore, the set of decision variables $\boldsymbol{\chi} \stackrel{\text{def}}{=} [\boldsymbol{\chi}_{\text{r}}, \boldsymbol{\chi}_{\text{l}}]$, where r is in the range from 1 to R_C, and l is in the range from $R_C + 1$ to $3R_C$. The decision variables used in the MOO are summarised in Table 5.6.

Table 5.6: Decision variables for the MOO problem.

Symbol	Description	Type	Unit
$\boldsymbol{\chi}_{\text{r}}$	DO concentration set point, $DO_{\text{ref}}(t)$	Real	g O_2/m^3
$\boldsymbol{\chi}_{\text{l}}$	Duration of aerobic phase	Real	d
$\boldsymbol{\chi}_{\text{l}+1}$	Duration of anaerobic phase	Real	d

It is important to note that the indicated decision variables directly represent the parameters of the state machine responsible for executing optimal control. The length of the aeration phase will determine the activation times of the aeration system (including NMPC) and the intensity of aeration.

The MOO objective functions are presented in Subsection 5.3.1, while the constraints on decision variables are described in Subsection 5.3.2. The algorithms selected for finding the solution set of MOO, as well as the method for selecting a solution from this set, are discussed in Subsection 5.3.3. The preliminary results obtained during the development of this section were presented in a conference publication (Ujazdowski and Piotrowski (2024)).

Remark: The studies on SOO presented in Appendix C were carried out as part of a series of publications Kolankowski et al. (2023); Banach et al. (2023); Ujazdowski et al. (2024). These investigations are not discussed in detail in the main body of this research work due to the use of SBR models different from those adopted elsewhere in the thesis and the lack of direct comparability with the results presented in the main chapters. Nevertheless, they illustrate that SOO strategies were considered within the broader research context and provide background for understanding the development towards multi-objective approaches.

5.3.1 Objective Functions

The four objective functions were proposed as elements of a vector of objective functions for MOO of the SBR operating cycle:

$$\begin{aligned} f_1(\boldsymbol{\chi}) &= \frac{\sum_{i=1}^{\mathrm{R_C}}(\chi_i \cdot \chi_{\mathrm{R_C}+2i-1}))}{DO_{\mathrm{norm}} \cdot t_{\mathrm{norm}}} \\ f_2(\boldsymbol{\chi}) &= \frac{TP_{\mathrm{mean}}(\boldsymbol{\chi})}{TP_{\mathrm{norm}}} \\ f_3(\boldsymbol{\chi}) &= \frac{TN_{\mathrm{mean}}(\boldsymbol{\chi})}{TN_{\mathrm{norm}}} \\ f_4(\boldsymbol{\chi}) &= \frac{COD_{\mathrm{mean}}(\boldsymbol{\chi})}{COD_{\mathrm{norm}}} \end{aligned} \tag{5.21}$$

where TP_{norm} represents the TP concentration scaled relative to a reference value, set at 2 g P/m^3; TN_{norm} denotes the corresponding TN concentration, with a reference value of 18 g N/m^3; COD_{norm} indicates the scaled COD, referenced to 125 g COD/m^3; t_{norm} represents the relative time duration, expressed as $\frac{5}{24}$ days; and DO_{norm} signifies the DO concentration, relative normalised against 2 g O_2/m^3.

The first objective function represents an abstract measure of electricity consumption during the aeration process. It is formulated as the sum of the products of the DO_{ref} value for each phase and the corresponding aeration phase duration. The remaining three objective functions are defined based on water quality regulations for the key treatment performance indicators: TP, TN, and COD. Each objective function is expressed as the ratio of the average estimated concentration of a given indicator during the decanting phase to its permissible value specified in the water rights permit. This formulation allows for an intuitive interpretation of the results, where values below 1 indicate compliance with the standard, whereas values exceeding 1 signify a violation of the regulatory limit. The exception is ($f_1(\boldsymbol{\chi})$), for which the indicated 'norm' values are the average phase length and DO level used in the case study plant.

Therefore, the MOO problem can be stated as follows:

$$\begin{aligned} \mathcal{F}^* = \arg\min_{\boldsymbol{\chi}\in\chi} F(\boldsymbol{\chi}) = \begin{bmatrix} f_1(\boldsymbol{\chi}) & f_2(\boldsymbol{\chi}) & f_3(\boldsymbol{\chi}) & f_4(\boldsymbol{\chi}) \end{bmatrix}^T \\ \text{subject to:} \quad lb_i \leqslant \chi_i \leqslant ub_i, \quad \text{for} \quad (1 \leqslant i \leqslant L). \end{aligned} \tag{5.22}$$

where $f_i(\boldsymbol{\chi})$, $i \in 1,2,3,4$, represent the objective functions, $\boldsymbol{\chi} \in \mathcal{X}$ denotes a decision variable vector within the L-dimensional solution space $\mathcal{D}$, and lb_i and ub_i define the lower and upper bounds of the feasible region, respectively. Inequality and equality constraints are not considered in this case.

As mentioned, since the problem involves multiple conflicting objectives, the solution is not a single optimal point but rather a set of trade-off solutions known as the Pareto front. The set of non-dominated solutions can be expressed as:

$$\mathcal{F}^* = \{F(\boldsymbol{\chi}) \mid \boldsymbol{\chi} \in \mathcal{X}_\mathrm{P}\}. \tag{5.23}$$

The Pareto dominance is defined as follows: A solution $\boldsymbol{\chi}'$ dominates another solution $\boldsymbol{\chi}''$, denoted by $\boldsymbol{\chi}' \prec \boldsymbol{\chi}''$, if:

$$\forall i \in B, \quad f_i\left(\boldsymbol{\chi}'\right) \leqslant f_i\left(\boldsymbol{\chi}''\right) \wedge \exists k \in B : f_k\left(\boldsymbol{\chi}'\right) < f_k\left(\boldsymbol{\chi}''\right), \tag{5.24}$$

where B is defined as the number of objective functions.

5.3.2 Constraints

The constraints were established based on theoretical process characteristics and validated through simulation studies. The lower bounds for the variables $\boldsymbol{\chi}_\mathrm{l}$ correspond to the minimum durations of aerobic and anaerobic phases within a cycle, selected considering both the DO dynamics and the aeration system response. The upper bounds on duration, on the other hand, are based on the practical capacity needs of the treatment plant. The theoretical lower limit of $\boldsymbol{\chi}_\mathrm{r}$, representing the DO_ref value, is $0.5\,\mathrm{g\ O_2/m^3}$, whereas its theoretical upper limit is constrained by the saturation DO level – DO_sat. However, the applied constraints are stricter than theoretical bounds. This deliberate tightening of limits significantly reduces the feasible solution space, thereby improving computational efficiency and accelerating the optimisation process.

The constraints on the length of the aerobic/anaerobic phases are considered separately for the different cycle structures and depend on the number of reaction cycles – $\mathrm{R_C}$. The following formulas describe the constraints:

$$\mathbf{lb} \leq \chi \leq \mathbf{ub} \tag{5.25a}$$

$$\chi = \begin{bmatrix} \chi_\mathrm{r} & \chi_\mathrm{l} \end{bmatrix} \tag{5.25b}$$

$$\mathbf{lb} = \begin{bmatrix} 1 & \begin{cases} \frac{4}{24}, & \text{if } \mathrm{R_C} = 1 \\ \frac{0.5}{24}, & \text{if } \mathrm{R_C} = 3 \end{cases} \end{bmatrix} \tag{5.25c}$$

$$\mathbf{ub} = \begin{bmatrix} 3 & \begin{cases} \frac{10}{24}, & \text{if } \mathrm{R_C} = 1 \\ \frac{4}{24}, & \text{if } \mathrm{R_C} = 3 \end{cases} \end{bmatrix} \tag{5.25d}$$

where **lb** denotes lower bound vector and **ub** is upper bound vector.

5.3.3 Selection and Deployment of Optimal Cycles

The set of feasible solutions for the considered optimisation problem is strictly defined by upper and lower bounds on the decision variables. However, since the decision variables are continuous and the objective functions exhibit non-linear dependencies, solving this problem is inherently challenging. Finding exact solutions to such a problem involves significant computational complexity. Therefore, this study employs stochastic methods, which can provide near-optimal solutions but do not guarantee exact optimality.

A schematic representation of the proposed process optimisation system is provided in Fig. 5.6. The MOO problem is solved for a given influent scenario by calling in each iteration a simplified SBR model. In the following, the stochastic algorithm used to obtain the set of solutions is described, and then the mechanism for selecting the cycle structure as a ready-to-use solution for the cycle state machine is explained.

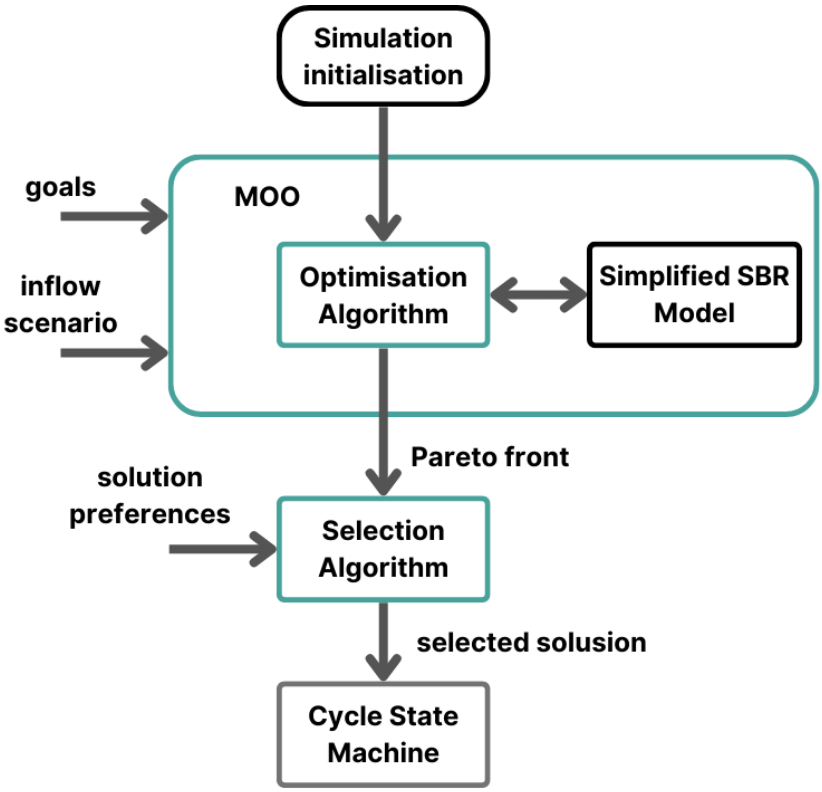

Figure 5.6: Cycle optimisation MOO

Application of stochastic methods to obtain a set of solutions

An elitist evolutionary algorithm based on the concept of ϵ-dominance, known as the ϵ-Multi-Objective Genetic Algorithm (ϵv-MOGA), was applied to solve the described problem. This algorithm, introduced by Afzalan and Joorabian (2013), is an extension of the basic MOGA approach developed by Martínez-Iranzo et al. (2009).

The ϵv-MOGA method is designed to efficiently approximate the Pareto-optimal solution set while operating under constrained memory resources. The algorithm aims to generate a solution set $\mathcal{X}_\mathrm{P}$ that accurately represents the Pareto front $F(\mathcal{X}_\mathrm{P})$ by strategically distributing solutions

across the front.

A distinctive feature of ϵv-MOGA is the partitioning of the objective space into a finite number of intervals (a so-called grid), where each interval (also called a box) can be represented by at most one solution. This prevents an excessive concentration of solutions in specific regions of the Pareto front and improves their overall distribution. Afzalan and Joorabian introduce ϵ-dominance in an analogous manner to the dominance relation presented in (5.24), but instead of considering individual solutions, they define dominance over boxes that represent the neighbourhood of a solution. Thus, a solution $\boldsymbol{\chi}'$ ϵ-dominates a solution $\boldsymbol{\chi}''$ if:

$$\text{box}\left(\boldsymbol{\chi}'\right) \prec \text{box}\left(\boldsymbol{\chi}''\right) \vee \left(\text{box}\left(\boldsymbol{\chi}'\right) = \text{box}\left(\boldsymbol{\chi}''\right) \text{ and } \boldsymbol{\chi}' \prec \boldsymbol{\chi}''\right). \tag{5.26}$$

ϵv-MOGA is a stochastic algorithm, meaning that the obtained solutions provide only an approximation of the true Pareto front, yielding suboptimal results. The dynamic adaptation of the Pareto front boundaries and the box widths enables efficient search-space management. However, it does not guarantee the identification of the exact set of Pareto-optimal solutions.

The algorithm structure consists of three populations: (I) the main population $P(t)$, which explores the solution space, (II) the archive $A(t)$, which stores the current approximation of the Pareto front, and (III) the auxiliary population $G(t)$, used to generate new candidate solutions. The set of solutions stored in the archive $A(t)$ is updated by selecting only those solutions that are not ϵ-dominated and that best represent a given box within the grid. The parameters of the considered algorithm are shown in Table 5.7.

Table 5.7: ϵv-MOGA parameters

Parameter Name	**Value**
Population size	100
Number of generations per function	50
Crossover rate	0.25
Mutation probability	0.2
Individuals for auxiliary population	8
Stopping criterion – number of generations without solution improvement	15
Initial crossover parameter	0.25
Final crossover parameter	0.1
Initial Gaussian mutation parameter	20
Final Gaussian mutation parameter	0.1

Since the algorithm produces an approximated Pareto front, an additional selection method is required to determine the final solution. This selection may involve a formal decision-making approach or direct feedback from a decision-maker, who specifies the priority objectives (goals) guiding the choice of the most suitable solution among the available options.

For further analysis, four selection scenarios were considered. The first three scenarios focus on solutions that best optimise specific objective functions, related to DO, TN, and TP. These scenarios correspond to economic treatment requirements, significant nitrogen reduction, and significant phosphorus reduction, respectively. During the study, it was observed that the designed system never approached the water-permit limit for COD; therefore, COD was excluded

from the selection criteria. The fourth scenario represents a balanced solution, obtained through an additional Pareto front analysis method, which is discussed in the following.

Method of selecting solutions from a given set of solutions

To select a balanced solution from the Pareto front, the Grey Relational Analysis (GRA) method was applied. This method was developed within the framework of Grey System Theory (GST), which was introduced by Julong et al. (1989).

GST provides an analytical approach for studying systems characterised by uncertainty and incomplete information. Within this framework, GRA serves as a technique for analysing and comparing multi-criteria data sets by evaluating the degree of similarity between candidate solutions and a reference solution.

The GRA procedure consists of several key steps. First, data normalisation is performed to scale the values within a comparable range (e.g., from 0 to 1), particularly when different criteria have different units. Next, a reference sequence is defined, representing the ideal solution with the best values for each criterion. This sequence serves as a benchmark for evaluating alternative solutions.

Subsequently, the Grey Relational Coefficient (GRC) (denoted as ξ) is calculated to quantify the proximity of each alternative to the reference sequence. It is determined for each alternative using the following formula:

$$\xi_i(k) = \frac{\Delta_{\min} + \zeta \cdot \Delta_{\max}}{\Delta_i(k) + \zeta \cdot \Delta_{\max}} \tag{5.27}$$

where $\Delta_i(k)$ represents the absolute difference between the actual and reference values, $\Delta_{\min}$ and $\Delta_{\max}$ denote the minimum and maximum differences within the set, and ζ is the distinguishing coefficient, typically set to 0.5.

The next step involves computing the Grey Relational Grade (GRG), which provides a comprehensive measure of similarity to the reference solution. The GRG is obtained as the weighted average of the GRC values across all criteria:

$$\gamma_i = \frac{1}{n} \sum_{k=1}^{n} \omega_k \cdot \xi_i(k) \tag{5.28}$$

where γ is GRG value and ω_k represents the weights assigned to individual criteria.

Finally, the ranking of alternatives is established, and the best solution is selected. The higher the GRG value, the closer the given alternative is to the ideal solution, enabling a structured selection process.

When applied to a set of Pareto-optimal solutions, GRA facilitates the identification of the most preferred alternative. The procedure follows three main steps. First, the reference point is defined. It can be assumed that this is the ideal solution, representing a hypothetical point with the best values across all criteria. Next, the GRG is calculated, allowing each Pareto-optimal solution to be evaluated in relation to the reference point. The final step is selecting the solution. The option with the highest GRG value is considered the most balanced, as it provides the best trade-off across all criteria.

A further improvement of GRA is introduced by Dynamic Grey Relational Analysis (DGRA),

proposed by Javed et al. (2022). In the original formulation, the distinguishing coefficient ζ is typically set to 0.5. However, this parameter may vary depending on the specific problem. DGRA addresses this limitation by introducing a dynamic distinguishing coefficient that is optimally determined for each problem instance, enhancing the accuracy and adaptability of the method.

The final form of the balanced solution to the MOO problem, obtained according to Fig. 5.6, employs the DGRA method with weight prioritisation for the objective functions. Weights are defined as $\boldsymbol{\omega} = [\omega_1, \omega_i, \ldots, \omega_{N_{\text{obj}}}]$, where ω_i denotes the priority associated with the i-th objective function in (5.21). The selected compromise solution provides a directly deployable cycle configuration that can be executed by the cycle state machine without further manual intervention. It should be emphasised that the weights used in the DGRA approach, unlike in the aggregation method used in the NMPC formulation, indicate the relative priorities of the objective functions rather than serving as weighting coefficients in a scalarised cost function.

Chapter 6

Manufacturing Execution System - Task Scheduling

The problem of TS in the context of WRRF constitutes the main subject of this chapter. The research work presented here corresponds to the objectives of RT 4 and builds upon the foundations established in RT 1. At this level of abstraction, scheduling represents the highest layer of the hierarchical control architecture (recall Subsection 4.2.4) considered in this dissertation (see Fig. 6.1), and provides the coordination framework that integrates individual cycle-level control strategies into a facility-wide operational plan.

At this level, a clear distinction can be introduced between the management layer (MES), which operates simultaneously across multiple reactors and coordinates the work of the entire facility, and the lower control layers, which act independently on individual reactors (see Fig. 6.2). In the previous chapters, the discussion was focused primarily on the control of a single reactor, where cycle parameters were determined locally and executed without explicit consideration of interactions with other units. In contrast, the scheduling layer addressed in this chapter extends the perspective to the facility scale: it not only ensures global coordination of reactor operations but also transmits to each reactor the cycle configuration parameters and the corresponding start times. In this way, scheduling provides the necessary link between individual process control and overall plant-level management.

As an initial step, two preliminary investigations were conducted to examine the applicability of TS concepts to wastewater treatment processes. The first investigation involved a systematic review of existing TS algorithms, with particular emphasis on their potential applicability and inherent limitations when transferred to the domain of WRRFs. This analysis revealed fundamental discrepancies between generic scheduling formulations and the technological characteristics of SBR-based systems. The second investigation focused on developing a simplified decision model explicitly tailored to wastewater treatment processes. This model aimed to link abstract scheduling representations with process-specific operational and regulatory constraints, providing an initial framework for subsequent model development. The insights derived from these preliminary studies have a significant impact on the scope and focus of the research and the selection of optimisation methods considered in this chapter. The results of these investigations were subsequently published in (Ujazdowski and Piotrowski, 2022a,b).

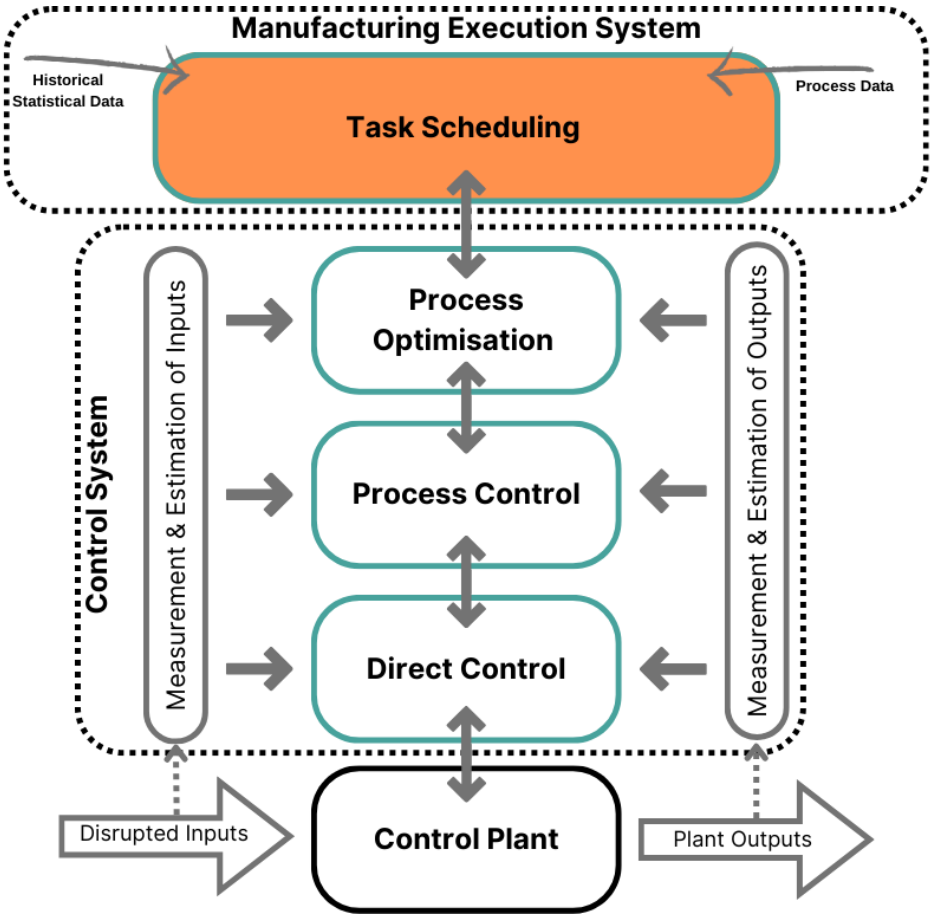

Figure 6.1: System architecture: integration of task scheduling within the hierarchical control framework

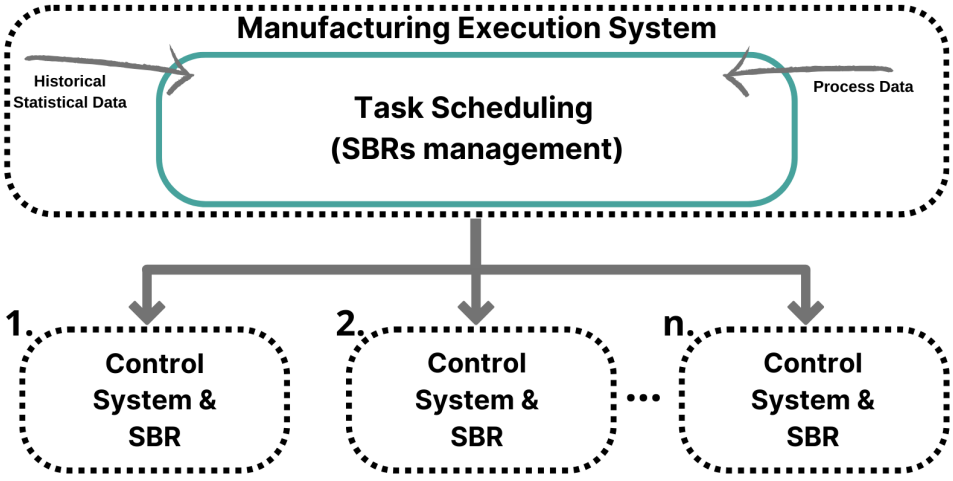

Figure 6.2: Management and control frameworks

From an operational standpoint, the management of a WRRF is required to guarantee that effluent pollutant concentrations remain within legally defined limits. These standards, defined both at the European level and within national regulations (Preisner et al., 2020), effectively impose upper bounds on key process variables, such as COD, TN, or TP. Consequently, the management strategy of a facility must combine expert assessments, historical and statistical

data, and real-time process information (Wodecka et al., 2022), which together determine the control and scheduling strategies adopted. In practice, this integration is essential not only to ensure compliance but also to balance operational costs, energy use, and treatment efficiency.

The remainder of this chapter is organised as follows. Section 6.1 formulates the optimisation problem for task scheduling in the WRRF context. Section 6.2 then introduces the selected optimisation algorithm designed to solve this problem.

6.1 Optimisation Problem Formulation

This section formulates the optimisation problem for the highest decision layer of the proposed hierarchical control system and clarifies its interfaces with the lower control layers. It presents the management perspective as opposed to local control and explains the role of scheduling as a coordination mechanism throughout the facility.

The TS problem formulated belongs to the class of *Unrelated Parallel Machine Scheduling Problems* (UPMSP) with *auxiliary resources* and *machine eligibility* constraints, according to the problem feature analysis carried out in the model section (Section 3.4), in the standard scheduling notation (Graham et al., 1979). Formally, the problem can be classified as:

$$R \mid \text{aux-res, eligibility, } |J| \text{ variable} \mid E(\mathcal{S}), \tag{6.1}$$

where R denotes unrelated parallel machines, auxiliary storage resources and eligibility describes considered feasibility constraints, and the number of scheduled jobs $K = |J|$.

The facility is represented as a set of reactors (machines) $\mathcal{M}$, each of which operates according to cyclic treatment processes. At the scheduling level, the central challenge is to coordinate the set $\mathcal{M}$ by determining a feasible and optimal schedule $\mathcal{S}^*$ that assigns treatment cycles to reactors while enforcing exclusivity, technological, and resource constraints:

$$\mathcal{S}^* \;=\; \arg\min_{\mathcal{S}\in\Omega_{\mathcal{TS}}} E\big(\mathcal{S}\big), \tag{6.2}$$

where $\Omega_{\mathcal{TS}}$ denotes the feasible set of schedules and $E\big(\mathcal{S}\big)$ is objective function defined over the horizon $\mathcal{T}$ and detailed in Subsection 6.1.2.

Remark: In the adopted interpretation of the problem under consideration, the scheduling horizon $\mathcal{T}$ refers only to the job start times, meaning that the execution or completion time of a job may exceed the assumed horizon[1].

For clarity and completeness, the schedule is defined as $\mathcal{S} = \{\tau_k\}_{k=1}^{K}$, where each element $\tau_k = (J_k, M_k, T_k)$ encodes the treatment cycle structure, the assigned reactor and the job starting time[2]. From $\mathcal{S}$, one can extract the sets of job and machine indices, and the corresponding start times, defined respectively as $\boldsymbol{J}_{\mathcal{S}} = \{J_k\}_{k=1}^{K}$ with $J_k \in \mathcal{J}$, $\boldsymbol{M}_{\mathcal{S}} = \{M_k\}_{k=1}^{K}$ with $M_k \in \mathcal{M}$, and $\boldsymbol{T}_{\mathcal{S}} = \{T_k\}_{k=1}^{K}$ with $T_k \in [0, \mathcal{T}]$.

[1] In the algorithm implementation, care was taken to ensure that the operational costs of such jobs are accounted for in the schedule evaluation (objective function). This prevents the algorithm from scheduling jobs at the end of the cycle that would reduce the storage volume while avoiding the associated aeration cost.

[2] The k index is not used here as a time step, as is assumed in the NMPC sense.

The optimal schedule can therefore be defined as:

$$\mathcal{S}^* = \big(\boldsymbol{J}^*_{\mathcal{S}}, \boldsymbol{M}^*_{\mathcal{S}}, \boldsymbol{T}^*_{\mathcal{S}}\big), \tag{6.3}$$

where $\boldsymbol{J}^*_{\mathcal{S}}$ and $\boldsymbol{M}^*_{\mathcal{S}}$ denote the optimal sets of job and machine indices, respectively, and $\boldsymbol{T}^*_{\mathcal{S}}$ denotes the corresponding optimal start times.

It is important to note that the procedure for selecting J_k can follow two alternative formulations. In the first case, the type of job is predetermined based on the assignment of a machine and a start time, reflecting predefined preferences regarding the choice of jobs. Alternatively, J_k may itself be treated as a decision variable, in which case, for a given starting time T_k and machine M_k, different types of jobs can be selected depending on the optimisation objective or process requirements. For the problem under consideration, the first approach was adopted:

$$\boldsymbol{J}^*_{\mathcal{S}} \xleftarrow{\text{selection}} \big(\boldsymbol{M}^*_{\mathcal{S}}, \boldsymbol{T}^*_{\mathcal{S}}\big). \tag{6.4}$$

Therefore, the decision variables of the problem are sets $\boldsymbol{M}^*_{\mathcal{S}}$ and $\boldsymbol{T}^*_{\mathcal{S}}$, and the (6.2) can be expressed as follows:

$$\begin{aligned} \big(\boldsymbol{M}^*_{\mathcal{S}}, \boldsymbol{T}^*_{\mathcal{S}}\big) &= \arg \min_{\boldsymbol{M}_{\mathcal{S}}(K), \boldsymbol{T}_{\mathcal{S}}(K)} E\big(\mathcal{S}\big), \\ \text{subject to:} \quad \mathcal{S} &= \big(\boldsymbol{J}_{\mathcal{S}}, \boldsymbol{M}_{\mathcal{S}}, \boldsymbol{T}_{\mathcal{S}}\big) \in \Omega_{\mathcal{TS}}. \end{aligned} \tag{6.5}$$

In the considered implementation of the scheduling problem, the number of jobs in schedule K, determining the number of decision variables included in sets $\boldsymbol{T}_{\mathcal{S}}$ and $\boldsymbol{M}_{\mathcal{S}}$. Thus, $\mathcal{S}$ is treated as the decision variable, formulated explicitly as a collection, where both the values of its elements and its length K determine the structure and dimensionality of the decision space.

Having defined the structure and dimensionality of the decision space at the scheduling level, it is necessary to address two fundamental properties of the formulated optimisation problem. First, the existence of feasible schedules must be established under the assumed operating conditions of the facility. Second, the relationship between feasibility at the scheduling level and implementability at the lower control layers must be clarified within the adopted hierarchical control architecture.

Under the assumption of normal facility operation (see Assumption 1.3), the inflow volume over the horizon $\mathcal{T}$ does not exceed the combined processing and storage capacity of the facility. Consequently, the feasible set $\Omega_{\mathcal{TS}}$ is non-empty. A feasible schedule can be constructed by sequentially assigning baseline jobs from $\mathcal{J}_{\text{base}}$ to machines in a round-robin fashion, starting at time $t = 0$, such that no machine overlap occurs and storage constraints are respected. Since baseline jobs were designed to satisfy technological constraints, this construction yields a feasible schedule.

The control architecture considered in this dissertation is based on a hierarchical decomposition in which regulatory compliance with effluent quality standards is enforced at the process control and process optimisation layers, while the TS layer focuses on cost-efficient coordination of treatment cycles and shared resources. It is assumed that for every treatment cycle type $j \in \mathcal{J}$ admissible at the scheduling level, there exists a corresponding control strategy at the lower layers such that, for all admissible initial reactor states and bounded disturbances, the

execution of job j guarantees compliance with all legal and technological constraints on effluent quality.

Consequently, the feasible set of schedules considered at the scheduling level is restricted to schedules composed exclusively of admissible cycle types whose execution is known to be implementable by the lower control layers. Under this assumption, any schedule declared feasible by the scheduling layer is guaranteed to be realisable without violation of effluent quality standards, provided that the stated modelling assumptions and disturbance bounds hold.

Thereafter, the computational properties of the resulting optimisation problem should be characterised. In particular, an assessment of the inherent complexity of the formulated TS problem provides justification for the choice of solution methods adopted in the subsequent sections. It is assumed that the formulated scheduling problem is NP-hard. By fixing the number of jobs K, removing storage constraints, and considering only machine assignment and sequencing, the proposed formulation reduces to $R||C_{\max}$ (Leung, 2004). Therefore, the problem generalises the UPMSP $R||C_{\max}$, which is NP-hard (Durasević and Jakobović, 2023). Then, since the proposed problem strictly contains this special case, it is also NP-hard.

Furthermore, in general, scheduling problems can be classified according to several criteria (Durasević and Jakobović, 2023). First, the distinction is made between deterministic and stochastic scheduling. In the deterministic case, all relevant parameters, such as processing times or setup times, are known with sufficient accuracy, independently of when they become available. Their values do not change throughout the execution of the system. In contrast, stochastic scheduling assumes that some parameter values are not precisely known in advance. For example, the processing time of a job might only become known once its execution on a machine is completed. Such uncertainty is usually represented through stochastic models or fuzzy sets.

A second distinction relates to the availability of information. In offline scheduling, all problem parameters, including the number of jobs, release times, and processing times, are known before execution begins. In online scheduling, this is not the case, and certain information only becomes available during execution. For instance, jobs may be released into the system at unknown times, and their properties are revealed gradually.

Finally, scheduling problems differ in terms of how the schedules are constructed. In static scheduling, a complete schedule is generated prior to execution, which requires full knowledge of all relevant parameters. Most metaheuristic approaches operate within this framework. In dynamic scheduling, by contrast, schedules are built incrementally in parallel with execution, usually by applying dispatching rules that select the immediate next decision rather than the entire sequence in advance.

The problem under consideration is addressed in a simplified form, namely under the deterministic assumption with a static scheduling procedure. Even this restricted variant already leads to a complex decision problem. However, the broader classification outlined above highlights substantial opportunities for future research in the area.

The following subsections provide the detailed formulation of the problem, including its description in Subsection 6.1.1, the objective function in Subsection 6.1.2, and the constraints in Subsection 6.1.3.

6.1.1 Problem Description

In the developed decision model, each job represents one cycle of SBR operation and contains information about the required number of reaction phases. A job consists of known operations performed according to a technological order. The job duration and resources needed for an operation depend on which machine performs it. The start time and the job assignment to the machine are the decision variables of the optimisation problem.

The scheduling problem considered in this work is characterised by the following features: (i) the inclusion of storage facilities, namely the retention tank and the stormwater lagoon, which imposes additional operational constraints that couple machine utilisation with the management of auxiliary resources; (ii) the number of jobs required to form a feasible schedule is not fixed a priori but depends on the total inflow volume over the scheduling horizon and on the effective storage capacity, such that the job count itself becomes a decision variable; (iii) the inflow to the facility is continuous and time-varying, yet it is assumed to be known over the considered horizon, which enables explicit modelling of the inflow–storage–processing interactions; (iv) the availability of a job at a given decision epoch depends directly on the instantaneous storage state, since each task consumes a portion of the available volume in the retention tank or lagoon; (v) the set of machines is heterogeneous, as certain reactors are restricted to processing only specific categories of jobs (e.g., small- or large-volume cycles), which induces eligibility constraints in the task–machine assignment; and (vi) the machines operate independently of each other.

Under Assumption 1.11, the TS layer is formulated based on deterministic abstraction of the wastewater treatment process. In this formulation, short-term disturbances and fast process dynamics are not represented explicitly at the scheduling level and are instead assumed to be compensated by the underlying control layers. Furthermore, the influent flow rate is assumed to be known deterministically over the scheduling horizon. Consequently, the impact of stochastic disturbances and uncertainty in influent forecasting is not taken into account.

Remark: This deterministic formulation constitutes a deliberate reduction of the problem scope and represents a main limitation of the proposed approach. Nevertheless, this simplification is introduced in order to focus the analysis on the structural complexity of the scheduling problem itself. As previously indicated, even under the deterministic assumption and with a static scheduling procedure, the resulting decision problem remains highly complex. The considered simplified formulation can be regarded as a well-defined baseline that highlights the potential for extending the proposed framework towards stochastic or robust scheduling formulations in future research.

The procedure described in Chapter 3 (Subsection 3.4.3), together with the application of cycle optimisation methods, based on the outcomes of RT 3 and described in Section 5.3, resulted in a set of twelve complete reactor operating cycles, optimised for selected influent conditions, thus forming the set $\mathcal{J}$. Only balanced solutions were selected (through GRA analysis). Therefore, each element of the set $\mathcal{J}$ corresponds to a component of the optimal decision vector $\boldsymbol{\chi}^*$ defining the Pareto-optimal solution $\mathcal{F}^*$. The jobs parameters, such as cycle durations and mean Q_{air} consumption in individual aeration phases, are presented in Table 6.1.

Remark: According to this deterministic interpretation of the problem and the cycle parameters selected for specific influent conditions, the optimum (in terms of the SBR cycle, i.e. job

execution) is fulfilled under conditions that correspond to the assumed influent. Any deviation from the specified influent parameters for a given job constitutes a sub-optimal outcome. Consequently, a sufficiently high density of job set ($\mathcal{J}$) for different influent conditions would minimise fluctuations from optimal conditions, as is the case in the gain scheduling approach.

The number of SBR units in the considered system is six, with three small and three large reactors, as mentioned in Chapter 2. Hence, the set of machines, according to the notation established in Subsection 3.4.3, is defined as $\mathcal{M} = \{1, 2, \ldots, 6\}$, where machines $\{1, 2, 3\} \in \mathcal{M}_{\text{small}}$, and $\{4, 5, 6\} \in \mathcal{M}_{\text{large}}$. Accordingly, the jobs with indexes $1, 2, \ldots, 6 \in \mathcal{J}_{\text{small}}$, and $7, 8, \ldots, 12 \in \mathcal{J}_{\text{large}}$.

Additionally, baseline jobs were designed for the development of reference schedules adopting parameters from the middle of the constraint set used in MOO problem in Section 5.3. Table 6.2 shows the parameters for these jobs, which constitute a set $\mathcal{J}_{\text{base}}$.

Table 6.1: Performance indicators under different scenarios for small and large machines. For $R_c = 3$ values of mean Q_{air} and phase duration are given for three aeration phases

$\mathcal{J}$	$\mathcal{M}$	R_C	Scenario	Cycle time [d]	Mean Q_{air} [m^3/d]	Phase duration [d]	Aeration time [d]
j_1	$\mathcal{M}_{small}$	1	Normal	1.11	32 549	0.32	0.32
j_2			Dry	1.66	42 871	0.40	0.40
j_3			Rain	1.24	27 248	0.24	0.24
j_4		3	Normal	1.71	42 593	0.02	0.33
					38 926	0.25	
					16 349	0.06	
j_5			Dry	1.72	81 231	0.13	0.38
					51 416	0.16	
					29 339	0.10	
j_6			Rain	1.39	49 786	0.02	0.29
					37 823	0.24	
					21 661	0.03	
j_7	$\mathcal{M}_{large}$	1	Normal	1.57	46 913	0.31	0.31
j_8			Dry	1.59	57 009	0.41	0.41
j_9			Rain	1.27	35 715	0.24	0.24
j_{10}		3	Normal	1.55	92 726	0.03	0.32
					60 535	0.25	
					30 452	0.04	
j_{11}			Dry	1.81	90 339	0.18	0.42
					65 047	0.12	
					39 150	0.12	
j_{12}			Rain	1.38	81 294	0.07	0.28
					39 087	0.16	
					16 187	0.05	

6.1.2 Objective Function

In classical scheduling formulations, the objective function is often expressed in terms of time-related performance indicators, such as makespan, number of jobs finished just in time, total weighted flow time, or total setup time. However, in the context of WRRF operation, these

Table 6.2: Performance indicators under baseline scenarios for small and large machines. For $R_c = 3$ values of mean Q_{air} and phase duration are given for three aeration phases

$\mathcal{J}_{\text{base}}$	$\mathcal{M}$	R_c	Scenario	Cycle time [d]	Mean Q_{air} [m^3/d]	Phase duration [d]	Aeration time [d]
$j_{b,1}$	$\mathcal{M}_{small}$	1	Normal	1.56	54 113	0.37	0.37
$j_{b,2}$		3	Normal	1.77	77 745	0.13	0.39
					56 872	0.13	
					34 163	0.13	
$j_{b,3}$	$\mathcal{M}_{large}$	1	Normal	1.62	72 190	0.37	0.37
$j_{b,4}$		3	Normal	1.84	105 492	0.13	0.39
					79 097	0.13	
					43 959	0.13	

metrics have limited relevance: they either do not directly affect the economic performance of the facility or cannot be meaningfully applied to the problem under consideration. Instead, the optimisation objectives must be aligned with the specific technological and regulatory requirements of wastewater treatment, capturing aspects such as process efficiency, storage utilisation, and operational safety.

The scheduling objective function is defined in a generic form as a weighted aggregation of cost, load balancing, terminal storage deviation, and feasibility penalties, consistent with the hierarchical control rationale:

$$E(\mathcal{S}) = w_{\text{c}} \cdot E_{\text{c}}(\mathcal{S}) + w_{\text{l}} \cdot E_{\text{l}}(\mathcal{S}) + w_{\text{v}} \cdot E_{\text{v}}(\mathcal{S}) + w_{\text{p}} \cdot E_{\text{p}}(\mathcal{S}) \tag{6.6}$$

where: $E_{\text{c}}(\mathcal{S})$ is the cost-related objective, $E_{\text{l}}(\mathcal{S})$ corresponds to balance machine load, $E_{\text{v}}(\mathcal{S})$ denotes the initial volume deviation objective, and $E_{\text{p}}(\mathcal{S})$ is the penalty related to constraint violation[3]. The elements $w_{\text{c}}, w_{\text{l}}, w_{\text{v}}, w_{\text{p}} \in \mathbb{R}_+$ represent the non-negative weights of each objective in the aggregated cost function.

The adopted formulation employs a weighted-sum aggregation, which is a classical approach in multi-objective optimisation. In this framework, each component explicitly depends on the scheduling decisions $\mathcal{S}$ while the weights determine their relative importance. In line with the hierarchical control architecture, a higher priority is assigned to economic efficiency, whereas the aspects of process quality are primarily safeguarded at lower control layers.

The cost-related objective $E_{\text{c}}(\mathcal{S})$ is obtained by computing the instantaneous blower power demand based on the air flow rate, $Q^h_{\text{air}}(t)$. In the proposed formulation, $Q^h_{\text{air}}(t)$ is assumed to remain constant within each aeration phase, with its value defined as the mean air flow (in m^3/h) measured for that specific phase in the reference trajectory used to generate the job model.

The procedure for obtaining the $E_{\text{c}}(\mathcal{S})$ value is as follows. First, the hydrostatic pressure at the effective depth is calculated as:

$$p_{\text{hyd}}(t) = \rho \cdot g \cdot h_{\text{eff}}(t), \tag{6.7}$$

[3] This term of the objective function corresponds to the introduction of a barrier function, allowing hard constraints to be converted into soft constraints, ensuring better algorithmic performance. The details of the barrier function are introduced by (6.20) and (6.21), while the hard constraint is introduced by (6.26) in Subsection 6.1.3.

where $\rho = 1150$ kg/m^3 is the density of the medium, $g = 9.81$ m/s^2 is the gravitational acceleration, and $h_{\text{eff}}(t) = h(t) - h_{\text{diff}}$ expressed in m is the effective depth. The total pressure difference is then expressed as:

$$\Delta p(t) = p_{\text{hyd}}(t) + p_{\text{diff}}, \tag{6.8}$$

where $p_{\text{diff}} = 2500$ Pa is the pressure in the aeration system, assuming minimum opening pressure of diffusers (Piotrowski and Ujazdowski, 2020). The blower power demand (in kW) is calculated as:

$$P(t) = \frac{1}{1000} \cdot \eta_b^{-1} \cdot \frac{Q_{\text{air}}^h(t)}{3600} \cdot \Delta p(t), \tag{6.9}$$

where $\eta_b^{-1} = 1.25$ is the inverse of blower efficiency and $Q_{\text{air}}^h(t)$ is expressed in m^3/h. The total cost is computed as the product of energy consumption and the electricity tariff $\zeta(t)$ from Energa (prices valid from 1 April 2025 for C12b tariff group). The tariff is time-dependent, distinguishing between peak and off-peak periods:

$$\zeta_{\text{peak}} = 1.0571 \text{ PLN/kWh}, \qquad \zeta_{\text{off}} = 0.7231 \text{ PLN/kWh}, \tag{6.10a}$$

$$\zeta(t) = \begin{cases} \zeta_{\text{off}}, & \text{for } T_h(t) \in [0, 6) \cup [13, 15) \cup [22, 24], \\ \zeta_{\text{peak}}, & \text{otherwise}, \end{cases} \tag{6.10b}$$

where $T_h(t)$ denotes the current simulation hour. Furthermore, as an additional parameter for evaluating the schedule, a fixed tariff (Energa C11) was applied with a value of $\zeta_{\text{con}} = 0.8960$ PLN/kWh (prices valid on 11 April 2025).

To express this objective per unit volume of treated wastewater, the total cost is divided by the effluent volume, calculated as the integral of the effluent flow rate $Q_{\text{eff}}(t)$:

$$V_{\text{eff}} = \int_0^{\mathcal{T}} Q_{\text{eff}}(t)\, dt, \tag{6.11}$$

thus yielding the final form:

$$E_{\text{c}}(\mathcal{S}) = \frac{\int_0^{\mathcal{T}} \zeta(t) \cdot P(t)\, dt}{V_{\text{eff}}}. \tag{6.12}$$

This formulation expresses the cost objective as the specific aeration cost in PLN/m^3 of treated wastewater. This representation is considered beneficial as it provides a direct comparison with the overall operational costs of the facility. The practice of expressing costs in terms of unit volume is a well-established convention within the relevant literature, as it facilitates benchmarking across a range of plants of differing scales and technologies. It should be noted, however, that the cost presented here does not account for the total energy consumption of the treatment process, since it excludes, for example, the operation of control cabinets, pumps, sensors, and auxiliary equipment. Consequently, the estimated value is regarded as a conservative, lower-bound cost of wastewater treatment, with a deliberate focus placed on aeration as the most energy-intensive component of the process.

The load-variability objective $E_{\text{l}}(\mathcal{S})$ penalises uneven utilisation of machines. Balanced reactor operation is motivated both by process and economic considerations. From the process perspective, activated sludge consists of living microorganisms that require a continuous supply

of substrate to remain viable and effective in wastewater treatment. Prolonged underloading of a reactor may therefore lead to deterioration of biomass activity. From the economic standpoint, uniform machine utilisation is also desirable to reduce wear, extend equipment lifespan, and improve the cost-effectiveness of plant operation.

Let $o_i(t;\mathcal{S}) \in \{0,1\}$ be an activity indicator (1 when machine i is active, 0 otherwise). The active time of machine i over the horizon $\mathcal{T}$ is:

$$\mu_i(\mathcal{S}) = \int_0^{\mathcal{T}} o_i(t;\mathcal{S})\,dt, \qquad i \in \mathcal{M}. \tag{6.13}$$

Let $\bar{\mu}(\mathcal{S})$ denote the mean active time:

$$\bar{\mu}(\mathcal{S}) = \frac{1}{M}\sum_{i=1}^{M} \mu_i(\mathcal{S}), \tag{6.14}$$

then, the (machines) variance of active times is:

$$\mathrm{var}_\mu(\mathcal{S}) = \frac{1}{M}\sum_{i=1}^{M} \big(\mu_i(\mathcal{S}) - \bar{\mu}(\mathcal{S})\big)^2, \tag{6.15}$$

and the load-variability objective is defined as the standard deviation:

$$E_\mathrm{l}(\mathcal{S}) = \sqrt{\mathrm{var}_\mu(\mathcal{S})}. \tag{6.16}$$

Next, the objective $E_\mathrm{v}(\mathcal{S})$ is responsible for maintaining the final state of the schedule close to the initial state. This aspect is important from the perspective of schedule repeatability and the continuity of WRRF operation. Alternatively, this aspect could be transferred to the problem constraints by requiring that the final states do not deviate from the initial state by more than a certain percentage or that they fall within a specified range. In the considered problem, however, no hard constraints were imposed; therefore, in order not to artificially restrict the set of feasible solutions, this requirement was incorporated into the objective function.

The desired terminal level of the retention tank, V_0^{tank}, is defined adaptively depending on the initial filling:

$$V_0^{\mathrm{tank}} \;=\; \begin{cases} V_{\mathrm{tank}}^{\mathrm{start}}, & \text{if } V_{\mathrm{tank}}^{\mathrm{start}} \le 0.35, \\ 0.35, & \text{otherwise,} \end{cases} \tag{6.17}$$

where V_0^{tank} denotes the filling level of the retention tank expressed relative to its maximum capacity. For the lagoon, it is always assumed that:

$$V_0^{\mathrm{lagoon}} = 0. \tag{6.18}$$

Let $V_{\mathrm{tank}}^{\mathrm{end}}$ and $V_{\mathrm{lagoon}}^{\mathrm{end}}$ denote the final filling levels for both tanks. The volume deviation measure is then defined as:

$$E_\mathrm{v}(\mathcal{S}) \;=\; \left(\frac{V_{\mathrm{tank}}^{\mathrm{end}}}{V_{\mathrm{tank}}^{\mathrm{max}}} - V_0^{\mathrm{tank}}\right) + \left(\frac{V_{\mathrm{lagoon}}^{\mathrm{end}}}{V_{\mathrm{lagoon}}^{\mathrm{max}}} - V_0^{\mathrm{lagoon}}\right). \tag{6.19}$$

The value of $E_{\mathrm{v}}(\mathcal{S})$ ranges from 0, in the case of ideal achievement of the target volumes, up to a maximum of $1 - V_0^{\mathrm{lagoon}} + 1 - V_0^{\mathrm{tank}}$, which under the adopted parameters corresponds to 1.65.

Last term of (6.6) is the barrier component. It is defined by penalising violations of volume constraints for both the retention tank and the stormwater lagoon. Let $V_{\mathrm{tank}}(t)$ and $V_{\mathrm{lagoon}}(t)$ denote the instantaneous volumes of the tank and lagoon, respectively. The safety threshold for the tank is defined as $\beta V_{\mathrm{tank}}^{\max}$ with $\beta = 0.05$. It is assumed that the reservoirs are connected to each other via a pumping station, and that excess water from the retention reservoir is directed directly to the lagoon. Similarly, the lagoon is emptied first, followed by the retention reservoir, so it can be assumed that the arrangement of these reservoirs forms a coherent storage space. The instantaneous penalty is given by:

$$\theta(t) \;=\; \begin{cases} \big(V_{\mathrm{lagoon}}(t) - V_{\mathrm{lagoon}}^{\max}\big)^2, & \text{if } V_{\mathrm{lagoon}}(t) > V_{\mathrm{lagoon}}^{\max}, \\ \big(\beta V_{\mathrm{tank}}^{\max} - V_{\mathrm{tank}}(t)\big)^2, & \text{if } V_{\mathrm{tank}}(t) < \beta V_{\mathrm{tank}}^{\max}, \\ 0, & \text{otherwise.} \end{cases} \tag{6.20}$$

The overall penalty component is then expressed as the time-weighted integral over the scheduling horizon $[0, \mathcal{T}]$, subject to an upper bound:

$$E_{\mathrm{p}}(\mathcal{S}) \;=\; \min\!\left(10,\; \int_0^{\mathcal{T}} \theta(t)\, dt\right). \tag{6.21}$$

The use of a barrier function is directly related to the stochastic mechanisms employed in the optimisation algorithm. The imposed upper bound of 10 primarily affects the presentation of the average fitness of the objective function values. This limitation is sufficient, since the remaining terms of the objective function typically attain values on the order of unity, ensuring that the penalty does not overwhelm the contribution of the other objectives while still effectively discouraging constraint violations.

The following weights were applied to the objective function: $[w_{\mathrm{c}},\, w_{\mathrm{l}},\, w_{\mathrm{v}},\, w_{\mathrm{p}}] = [10,\, 1,\, 1,\, 1]$. The cost-related term was assigned the highest weight due to its critical importance in the scheduling problem. For schedules without optimisation, the value of $E_{\mathrm{c}}(\mathcal{S})$ typically ranges from 0.15 to 0.20, which is considerably lower than the ranges observed for the other components of the objective function: $E_{\mathrm{v}}(\mathcal{S})$ varies from 0 to 1.65, $E_{\mathrm{p}}(\mathcal{S})$ ranges from 0 to 10, while the upper bound of $E_{\mathrm{l}}(\mathcal{S})$ is difficult to estimate precisely, but observations indicate it typically lies between 0 and 1.

Moreover, the objective function $E(\mathcal{S})$ defined in (6.6) is bounded from below on the feasible set $\Omega_{\mathcal{TS}}$. Each component of the objective function satisfies non-negativity or boundedness constraints, namely:

$$E_{\mathrm{c}}(\mathcal{S}) \geq 0, \quad E_{\mathrm{l}}(\mathcal{S}) \geq 0, \quad E_{\mathrm{v}}(\mathcal{S}) \geq 0, \quad 0 \leq E_{\mathrm{p}}(\mathcal{S}) \leq 10. \tag{6.22}$$

Since all weighting coefficients $w_{\mathrm{c}}, w_{\mathrm{l}}, w_{\mathrm{v}}$, and w_{p} are chosen to be non-negative, the resulting weighted sum is non-negative for all feasible schedules, which implies that $E(\mathcal{S})$ is bounded from below ($E(\mathcal{S}) \geq 0$).

Furthermore, knowing that the objective function is constructed as a weighted sum of multiple performance criteria $E_i(\mathcal{S})_{i=1}^4$ with strictly positive weights. Under this formulation, any schedule that minimises $E(\mathcal{S})$ corresponds to a Pareto-optimal solution of the associated multi-objective scheduling problem.

Indeed, if a feasible schedule were dominated by another schedule with respect to all considered criteria, at least one objective component would be strictly improved without deterioration of the remaining ones. In such a case, the weighted sum would attain a lower value, contradicting the optimality of the original solution.

6.1.3 Constraints

The constraints defining the feasible set $\Omega_{\mathcal{TS}}$ in the formulated optimisation problem are derived primarily from the underlying problem type, i.e. the UPMSP, as well as from problem-specific features related to machine capabilities and storage availability.

Firstly, each job must be allocated to exactly one machine[4]:

$$\sum_{M_k \in \boldsymbol{M}_{\mathcal{S}}} a(M_k, J_k) = 1, \qquad \forall J_k \in \boldsymbol{J}_{\mathcal{S}}, \tag{6.23}$$

where the binary assignment function $a(M_k, J_k)$ indicates whether job J_k is assigned to machine M_k, according to:

$$a(M_k, J_k) = \begin{cases} 1, & \text{if job } J_k \in \boldsymbol{J}_{\mathcal{S}} \text{ is assigned to machine } M_k \in \boldsymbol{M}_{\mathcal{S}}, \\ 0, & \text{otherwise.} \end{cases} \tag{6.24}$$

Then, mutual exclusivity must be ensured on the machines (no overlapping operations on a given machine). Consider two scheduled elements $\tau_i, \tau_j \in \mathcal{S}$, corresponding to jobs J_i, J_j and assigned to machines $M_i, M_j \in \mathcal{M}$, respectively. If both elements are assigned to the same machine, i.e. $M_i = M_j = m$, their execution intervals must not overlap. Let $T_i, T_j \in \boldsymbol{T}_{\mathcal{S}}$ denote the start times of τ_i and τ_j, respectively, and let $T_{\mathrm{p}}(J_i, m)$ denote the processing time of job J_i on machine m. The non-overlap condition can be written compactly as a disjunction:

$$\begin{aligned} &a(m, J_i) = 1 \wedge a(m, J_j) = 1 \implies \big(T_i + T_{\mathrm{p}}(J_i, m) \le T_j\big) \vee \big(T_j + T_{\mathrm{p}}(J_j, m) \le T_i\big), \\ &\forall \tau_i \neq \tau_j \in \mathcal{S},\ \forall m \in \mathcal{M} \end{aligned} \tag{6.25}$$

Another class of constraints concerns storage feasibility, often referred to as auxiliary resource constraints in the TS related literature. Let $V(t)$ denote the storage state (retention tank level) at time t and ΔV_j the volume consumed from the storage by job J_j. A job starting at time T_j is feasible only if it does not drive the storage below the minimum admissible level $V_{\min} = \beta V_{\mathrm{tank}}^{\max}$, which can be formalised as:

$$V\big(T_j^-\big) - \Delta V_j \ \ge\ V_{\min}, \qquad \forall T_j \in \boldsymbol{T}_{\mathcal{S}}, \tag{6.26}$$

[4] Under the deterministic formulation, the assignment of a job induces machine occupancy in the sense of its activity. In this context, allocating a job to a machine corresponds to activating that machine over the associated processing interval, consistently with the activity indicator $o_i(t; \mathcal{S})$ and the definition of active time given in (6.13).

where $V(T_j^-)$ denotes the storage level immediately before the start of job J_j. This constraint was transformed into a penalty function and described by (6.21).

In addition, job allocation depends on machine type. This machine eligibility condition, already introduced when defining the set $\mathcal{J}$, specifies that certain jobs can only be executed on a subset of machines. Denoting by $\mathcal{J}_{\text{small}}$ and $\mathcal{J}_{\text{large}}$ the job classes, and by $\mathcal{M}_{\text{small}}, \mathcal{M}_{\text{large}}$ the corresponding machine sets, eligibility is enforced as:

$$a(M_k, J_k) = 0, \quad \forall M_k \in \mathcal{M}_{\text{small}},\ \forall J_k \in \mathcal{J}_{\text{large}}, \tag{6.27a}$$

$$a(M_k, J_k) = 0, \quad \forall M_k \in \mathcal{M}_{\text{large}},\ \forall J_k \in \mathcal{J}_{\text{small}}. \tag{6.27b}$$

Finally, based on knowledge of the average daily inflow and the intended implementation of the optimisation procedure, the number of scheduled jobs is bounded. These bounds are determined through a static analysis of the system states under the assumed average inflow at steady-state conditions, providing an upper and lower estimate with a rationally chosen margin. This approach reduces the decision space and enhances the computational efficiency of the algorithm. Let $\underline{K}$ and $\overline{K}$ denote the minimum and maximum allowable number of jobs in the schedule (parameters of the optimisation algorithm). The number of scheduled jobs then satisfy:

$$\underline{K} \ \leq \ K \ \leq \ \overline{K}. \tag{6.28}$$

6.2 Optimisation Algorithm

To solve the scheduling problem under consideration, a metaheuristic approach was employed: the Memetic Algorithm (MA). The choice of a metaheuristic framework is primarily motivated by the computational complexity of the problem, which exhibits features of the UPMSP (Durasević and Jakobović, 2023). Moreover, based on the findings of the literature review presented in Subsection 1.1.3 and the results of preliminary research mentioned earlier (Ujazdowski and Piotrowski, 2022a,b), heuristic and metaheuristic methods are considered as a rational strategy for solving this type of planning problem, as they facilitate the identification of high-quality approximate solutions within an acceptable computational time.

The MA extends the evolutionary algorithm by incorporating a local search procedure. Consequently, a structure is created in which the exploitation capabilities of the algorithm are improved through local improvements to each individual. The GA and SA were selected as the constituent layers of MA (Pecháč and Saga, 2016). The structure of the algorithm includes all key steps of the evolutionary algorithm: population initialisation, evaluation of solution quality (fitness function), selection (with elitism), crossover and mutation operators, and local enhancement of each individual. The inclusion of SA as the local search component is motivated by its proven effectiveness in TS problems (Rudek, 2024). The pseudocode is shown as Algorithm 1.

As the selection mechanism, roulette-wheel selection with elitism was employed. In this approach, a subset of individuals with the best fitness values (the elite) is transferred directly to the next population and does not undergo crossover or mutation operators.

The crossover operation was implemented using the one-point crossover method. Prior to

Input: Population size N, crossover and mutation parameters, SA parameters, stopping criterion
Output: Best individual found

Initialise population $\mathcal{P}^{(0)}$ using predefined patterns
Evaluate fitness of all individuals using simulation-based evaluation in $\mathcal{P}^{(0)}$
$k \leftarrow 0$

while *stopping criterion not met* **do**
  Select elite individuals from $\mathcal{P}^{(k)}$ (elitism)
  Select parent individuals using roulette-wheel selection
  Apply crossover and mutation to generate offspring population
  foreach *individual i in offspring population* **do**
    Apply local search using Simulated Annealing to i
  end
  Apply local improvement using Simulated Annealing to all individuals in $\mathcal{P}^{(k)}$
  Insert offspring into new population $\mathcal{P}^{(k+1)}$
  Insert elite individuals into new population $\mathcal{P}^{(k+1)}$
  Evaluate fitness value of all individuals in the new population
  $k \leftarrow k + 1$
end

return *best individual*

Algorithm 1: Memetic Algorithm with Eliteism, Pattern-Based Initialisation and Simulated Annealing

selecting the crossover point, schedules are sorted with respect to job start times. In the case of schedules of unequal lengths, the offspring preserve the lengths of their respective parents, and the crossover point index cannot exceed the length of the shorter individual.

For the mutation operation, dedicated mechanisms were designed: (i) adding a job to the schedule with a random start time and a random machine, within the admissible set; (ii) removing a job from the schedule; (iii) changing the machine assigned to a random selected job (in the case of a transition from a small to a large machine, the job is also reassigned accordingly); and (iv) assigning a new random start time to a randomly selected job. The mutation operators used are subject to problem constraints. Adding or removing a job cannot exceed the constraints on variable K, while the randomly selected job time cannot exceed the schedule duration constraints $[0, \mathcal{T}]$.

In the initial development phase of the algorithm, the population was initialised through completely random schedule generation; however, this approach was problematic due to feasibility issues. To ensure feasible schedules in the initial population, a pattern-based generation mechanism was developed, inspired by operational practices of SBR under continuous inflow conditions. Each individual in the population represents a procedurally generated schedule, in which once the filling phase of one reactor is completed, the filling of the next reactor immediately begins. This approach can thus be described as pattern-driven population initialisation.

Several base patterns were defined to represent typical orders in which machines may be visited. Examples of such patterns are presented in Table 6.3, where each sequence indicates the order of machine utilisation. For each individual, one of these patterns was selected at random. To avoid uniformity across the population, a random offset was applied to the chosen

sequence, effectively shifting the starting point of the pattern. The resulting sequence was then repeated and truncated so that its length matched the number of jobs assigned to the individual. In this way, the base structural regularity introduced by the patterns was preserved, while the random offset ensured variation in the initial assignment. Finally, the constructed sequence was transformed into a continuous schedule and truncated to the admissible time horizon $\mathcal{T}$, forming a feasible initial solution.

The pattern-based initialisation procedure was introduced to generate feasible initial schedules consistent with continuous-inflow SBR operational practice, while maintaining population diversity through random offsets and truncation. It is worth mentioning that the indicated patern base must provide adequate density to ensure sufficient diversity for crossover operations in MA. If the base is too narrow, the role of mutation and local search, through SA operations, becomes a significant factor in the solutions obtained. Further investigation into the density of the initial solution base is beyond the scope of the present research work. However, this topic is worthy of consideration for future research.

Table 6.3: Examples of predefined machine visit patterns

Pattern ID	Machine sequence
1	1, 2, 3, 4, 5, 6
2	1, 3, 5, 2, 4, 6
3	1, 4, 2, 5, 3, 6
4	2, 4, 6, 1, 3, 5
5	2, 1, 4, 3, 6, 5
6	3, 1, 4, 2, 5, 6
7	6, 5, 4, 3, 2, 1

Alternatively, the generation of feasible schedules could be realised based on a set of rules and constraints, leading to the development of rule-based scheduling methods, such as Dispatching Rules (Đurasević and Jakobović, 2018).

Implemented as a local search method, SA operates on each newly created individual after the completion of crossover and mutation operations. At this stage, machine collision removal is applied, i.e., schedules in the new population are corrected in cases of collisions or constraint violations. Elitism is also preserved within the local search. Given the characteristic of SA that allows a non-zero probability of accepting a worse solution during the initial iterations of the algorithm, elite individuals are subject to the SA procedure but are overwritten only if an improvement in the fitness function occurs by the end of the algorithm.

The evaluation of an individual is performed using a MATLAB Simulink model, in which tanks, volumetric constraints, and models converting air consumption (Q_{air}) into electrical energy are implemented. The model accepts a schedule $\mathcal{S}$ as input and returns the objective function value $E(\mathcal{S})$, along with additional parameters including the operating time of each machine and data on electricity consumption.

For the purpose of schedule evaluation, the model was optimised using Simulink tools (Model Advisor and Performance Advisor), which reduced the evaluation time of a single schedule over a 14-day horizon from approximately 90 s to around 30 s. The selection of algorithm parameters, including population size and the number of generations, was guided by the computational cost

of schedule evaluation. Given that a single evaluation requires approximately 30 s, the evaluation within the SA algorithm is repeated 1 + number of iterations. For the chosen 8 iterations of SA, the evaluation of a single individual takes around 4.5 minutes. Considering a population of 24 individuals, the total evaluation time per generation amounts to approximately 108 minutes. Extending this to 16 generations results in an overall SA runtime of about 28.8 hours. In contrast, the evaluation of schedules within the GA is considerably shorter, requiring only 24 model calls per generation, or roughly 12 minutes, which corresponds to 3.2 hours for 16 generations. Consequently, the total runtime of the combined algorithm is approximately 32 hours on a mid-range personal computer. This analysis informed the selection of population size and number of generations, balancing computational feasibility with sufficient exploration of the solution space. The parameters applied in the scheduling problem solution are summarised in Table 6.4.

Table 6.4: Memetic Algorithm parameters

Parameter description	**Value / Range**
General	
Number of generations	16
Population size	24
Maximum scheduling horizon in days ($\mathcal{T}$)	14
Set of available machines	$\{1, 2, \ldots, 6\}$
Initial range of number of jobs ($\underline{K}$, $\overline{K}$)	$[16, 20]$
Stall generations without improvement	5
Number of elite individuals	4
Mutation probabilities	
Probability of removing a task	0.1
Probability of adding a task	0.1
Probability of shifting a task	0.3
Probability of changing machine assignment	0.3
Simulated Annealing	
Initial temperature	2.0
Cooling rate	0.8
Iterations per local search	8

The parameters of the SA algorithm were analysed with respect to the acceptance probability of new solutions, based on known objective function differences. Fig. 6.3 illustrates the dependence of the acceptance probability on the objective difference ΔE for various initial temperatures T_0 and cooling rates α. As expected, higher initial temperatures increase the likelihood of accepting worse solutions, thereby enhancing exploration in the early stages of the algorithm. Additionally, the effect of the cooling rate α is observed: slower cooling (higher α) maintains a higher acceptance probability for larger ΔE values over the course of the algorithm, supporting sustained exploration. Then, Fig. 6.4 presents the evolution of the acceptance probability over iterations for a fixed objective difference $\Delta E = 0.5$. The curves demonstrate that higher initial temperatures and slower cooling rates result in higher probabilities of accepting worse solutions in the initial iterations, gradually decreasing as the temperature decreases. This analysis confirms that the choice of T_0 and α significantly influences the balance between exploration and exploitation, which is critical for the convergence behaviour of the SA in the scheduling problem.

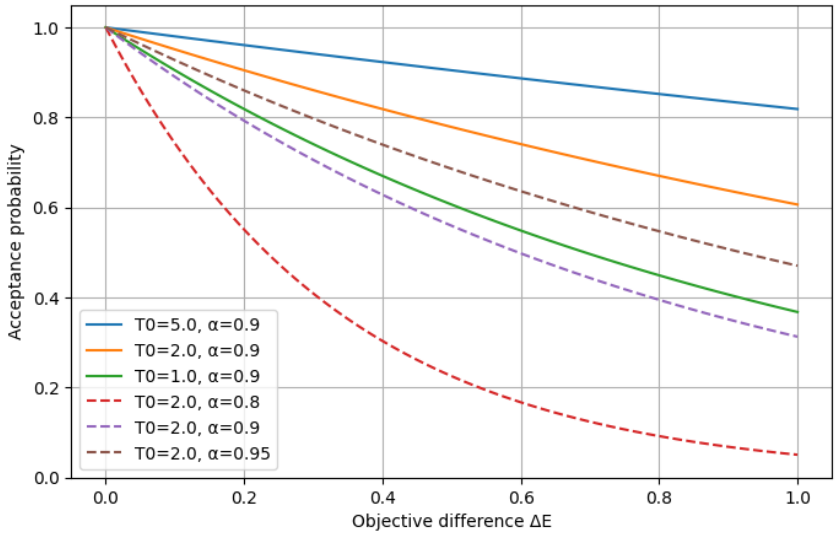

Figure 6.3: Probability vs ΔE

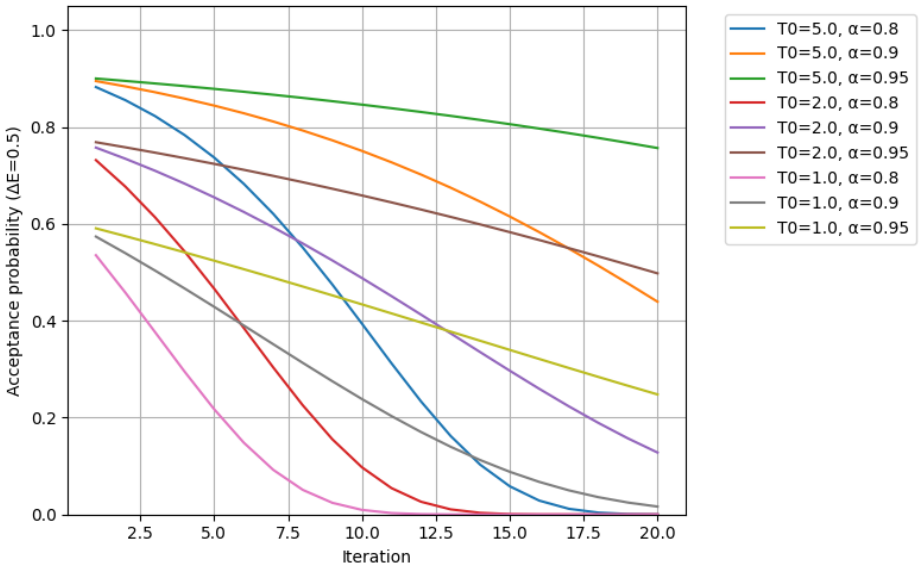

Figure 6.4: Probability vs Iteration for fixed ΔE

Chapter 7

Numerical Results

This chapter brings together the numerical results of the theoretical studies carried out for the developed system of a hierarchical layered control structure for a batch-type biological WWTP. The chapter is divided into sections closely related to the subsequent chapters of the dissertation and thus the layers of the system, as described in Chapter 4.

The research developed and presented in this chapter involved extensive computer simulations. The computer hardware facilitating this research is delineated in Section 7.1. Meanwhile, the aforementioned section contains a description of the scenarios and initial conditions for the computer simulations, forming the basis for the remaining sections of this chapter.

The results described in Section 7.2 relate to process control and support the research objectives set. Next, Section 7.3 addresses research objective O1, presenting the results of the multi-objective sensing optimisation considering the length of the different phases of the SBR cycle, the DO concentration level in each aerobic phase, and the considerations about the number of aerobic and anaerobic sequences. The highest control layer considered within this work concerns research objective O2, and the results for the experiments carried out are presented in Section 7.4. These are the results of the selected scenarios for the solution of the UPMSP.

A summary of the results, a discussion of the results obtained, as well as conclusions drawn from the performance of the individual layers of the system, as well as the full design and relationship of the layers to each other, are presented in the last section of this chapter (Section 7.5).

7.1 Experiment Setup

This section provides a detailed overview of the experimental setup used in this study. It includes a description of the software and hardware configuration (Subsection 7.1.1) and the simulation parameters (Subsection 7.1.2), which together define the operational environment for the optimisation framework.

7.1.1 Software and Hardware Setup

All simulations were performed using MATLAB Simulink R2022a, along with the Optimisation Toolbox and the Model Predictive Control Toolbox, where the models and algorithms were implemented. Additionally, the Python environment, via Google Colab, was employed for rapid

prototyping of utility functions, initial model testing, and visualisation of selected results.

A GitLab-based version control system was integrated with MATLAB to support reproducibility and collaborative development. This allowed for the consistent tracking of model changes, easy rollback to previous versions, and improved multi-device simulation workflows.

Simulations were executed on three categories of computing devices. The first was a desktop computer, the second was a standard laptop, and the third included multiple laboratory machines (divided into A and B, which means newer and older units). The specifications of the listed devices are shown in Table 7.1. The laboratory machines were from the Department of Intelligent Control and Decision Support Systems and were used primarily for parallel execution of evolutionary algorithm scenarios described in Chapter 5.

Table 7.1: Hardware specifications used for simulations

Specification	**Desktop**
Processor	AMD Ryzen 3 4300G
RAM	16 GB DDR4
GPU	AMD Radeon Graphics (integrated)
Operating System	Windows 10 Pro
Number of devices	1

Specification	**Laptop**
Processor	Intel Core i7-7700HQ
RAM	8 GB DDR4
GPU	NVIDIA GeForce GTX 1050
Operating System	Windows 10 Pro
Number of devices	1

Specification	**Lab Machines A**
Processor	Intel Core i5 12600K
RAM	16 GB DDR4
GPU	Intel UHD Graphics 770 (integrated)
Operating System	Windows 10 Pro
Number of devices	5

Specification	**Lab Machines B**
Processor	Intel Core i3-8100
RAM	8 GB DDR4
GPU	Intel UHD Graphics 630 (integrated)
Operating System	Windows 10 Pro
Number of devices	3

Table 7.2 summarises the average simulation times depending on the computing environment. These times were calculated for the execution of evolutionary algorithms across three solution phases defined in Chapter 6.

The complexity of the model, particularly in terms of the number of state variables, along with the use of population-based algorithms, had a significant impact on RAM utilisation during computations. The simulations imposed only a minor load on the CPU and GPU. To accelerate

Table 7.2: Average simulation times based on hardware type

Hardware Type	Total Time [h]	Phase I [h]	Phase II [h]
Overall average	24.51	15.28	8.03
Average with 16 GB RAM	18.05	11.39	5.86
Average with 8 GB RAM	36.31	22.47	12.00

the computational process, recommended memory optimisation techniques from MathWorks were applied, including avoiding dynamically sized arrays.

7.1.2 Simulation Parameters

The simulation parameters of the SBR model cover tank geometry and operational conditions, actuator-driven flows, switching-function parameters appearing in Eqs. (3.11) and (3.13), and additional model constants. All values are listed in Table 7.3.

Table 7.3: Model parameters for SBR system

Name	Symbol	Unit	Value
	Tank		
Cross section area of SBR (Small)	A	m^2	706
Cross section area of SBR (Large)	A	m^2	907
Height of SBR	h	m	7
Bottom layer volume	V_3	m^3	495
Initial tank volume	V_0	m^3	$0.35V_{max}$
	Flows & velocities		
Mean feed flow	Q_{in}	m^3/d	5000
Decant pump flow	Q_e	m^3/d	24 500
Ex. sludge pump flow	Q_w	m^3/d	12 000
Mixing flow	Q_m	m^3/d	80 000
Mixing velocity	v_{mx}	m/d	380
	SBR conditions		
Sludge volume index	SVI	mL/g	100
	Switching functions		
Lower effluent switch limit (V_1/V)	$rVe1_{min}$	-	0.05
Upper effluent switch limit (V_1/V)	$rVe1_{max}$	-	0.1
Lower effluent switch limit (V_2/V)	$rVe2_{min}$	-	0.025
Upper effluent switch limit (V_2/V)	$rVe2_{max}$	-	0.05
Lower sludge switch limit (V_1/V)	$rVw1_{min}$	-	0.05
Upper sludge switch limit (V_1/V)	$rVw1_{max}$	-	0.1
Lower sludge switch limit (V_2/V)	$rVw2_{min}$	-	0.025
Upper sludge switch limit (V_2/V)	$rVw2_{max}$	-	0.05
Settling velocity switch min (V_2/V)	$rV2_{min}$	-	0.025
Settling velocity switch max (V_2/V)	$rV2_{max}$	-	0.05
Settling velocity switch min (V_1/V)	$rV1_{min}$	-	0.15
Settling velocity switch max (V_1/V)	$rV1_{max}$	-	0.25
	Flow auxiliary variables		
Inflow clear water coefficient	c	-	0.0001
Max. hydraulic load	q_a	m/d	48
Return sludge coefficient	f_{by}	-	0

Initial state–fraction values for the ASM3e model are given in Table 7.4. These were used as the starting conditions for every simulated cycle (ifak system GmbH, 2001).

Table 7.4: Initial values of the ASM3e state variables

Fraction	**Symbol**	**Initial value**	**Unit**
$C_{(\cdot),1}$	S_{O}	0.1	g O_2/m^3
$C_{(\cdot),2}$	S_{S}	100	g COD/m^3
$C_{(\cdot),3}$	S_{NH}	14	g N/m^3
$C_{(\cdot),4}$	S_{NO}	0	g N/m^3
$C_{(\cdot),5}$	$S_{\mathrm{N_2}}$	0	g N/m^3
$C_{(\cdot),6}$	S_{ALK}	7	mol HCO_3^-/m^3
$C_{(\cdot),7}$	S_{I}	30	g COD/m^3
$C_{(\cdot),8}$	X_{I}	25	g COD/m^3
$C_{(\cdot),9}$	X_{S}	35	g COD/m^3
$C_{(\cdot),10}$	X_{H}	250	g COD/m^3
$C_{(\cdot),11}$	X_{STO}	1	g COD/m^3
$C_{(\cdot),12}$	X_{A}	50	g COD/m^3
$C_{(\cdot),13}$	X_{TSS}	2000	g TSS/m^3
$C_{(\cdot),14}$	$S_{\mathrm{PO_4}}$	1	g P/m^3
$C_{(\cdot),15}$	X_{PAO}	10	g COD/m^3
$C_{(\cdot),16}$	X_{PP}	2	g P/m^3
$C_{(\cdot),17}$	X_{PHA}	10	g COD/m^3
$C_{(\cdot),18}$	X_{EH}	25	g COD/m^3
$C_{(\cdot),19}$	X_{EA}	5	g COD/m^3

The NMPC parameters employed in the process control layer are summarised in Table 7.5. The parameters $C_{\mathrm{SO\,min}}$ and $C_{\mathrm{SO\,sat}}$ represent both $[\underline{y}, \overline{y}]$ and $[\underline{x}, \overline{x}]$. The parameters $Q_{\mathrm{air,min}}$ and $Q_{\mathrm{air,max}}$ represent $[\underline{u}, \overline{u}]$, while the $Q_{\mathrm{air,rate}}$ parameters correspond to $[\underline{\Delta u}, \overline{\Delta u}]$. The weights used in the objective function A, B, and Γ depend on the chosen scenario and will be provided together with the corresponding results. The prediction and control horizons were selected based on the dynamics of the system and simulation analyses, including experiments with step size optimisation and prediction horizon length, where various approaches were examined (for T_s in the range of 1 second to 10 minutes, and for N in the range of 5 minutes to 1 hour). However, these analyses are beyond the scope of this dissertation. Studies on the selection and adaptation of prediction and control horizons are the subject of numerous research efforts, conducted by, for example, (Krener, 2018) and (Ma et al., 2020).

Table 7.6 presents summary statistics of the influent under three scenarios-normal, dry, and rainy. Under *Normal* conditions, the mean flow of 20 465 m^3/d corresponds to moderate hydraulic loading, with total nitrogen and phosphorus averaging 40.13 g N/m^3 and 9.04 g P/m^3, respectively, while COD reaches a mean of 516.63 g COD/m^3. In the *Dry* scenario, inflow is reduced (mean 18 755 m^3/d), but nutrient concentrations are elevated (TN 49.85 g N/m^3, TP 11.41 g P/m^3), with a higher mean COD of 657.50 g COD/m^3. *Rain* events produce the highest hydraulic loads (mean 39 011.4 m^3/d) alongside lower nutrient concentrations (TN 23.81 g N/m^3, TP 5.53 g P/m^3) and a moderate COD level of 307.44 g COD/m^3. Temperature varies between 9.55 °C and 20.49 °C across all scenarios. Example influent time series for each scenario are depicted in Fig. 7.1. These plots illustrate the temporal variability of the influent parameters

Table 7.5: NMPC parameters for different reactor sizes

Parameter	**Variable Name**	**Unit**	**Value**	
Sample time	T_s	d	$\frac{1}{24 \cdot 60}$	
Prediction horizon	N	steps	30	
Control horizon	$\mathbf{M}$	steps	[1, 1, 1, 1, 1, 2, 3, 5]	
Max liquid level difference	h_{diff}	m	0.5	
Min airflow rate	$Q_{\text{air,min}}$	m^3/d	0	
Min state value	$C_{\text{SO min}}$	$g\,O_2/m^3$	0	
Max state value	$C_{\text{SO sat}}$	$g\,O_2/m^3$	8.63736	
			Small Reactor	**Large Reactor**
Max volume	$V_{\max}$	m^3	4948	6355
Max airflow rate	$Q_{\text{air,max}}$	m^3/d	115 200	144 000
Max airflow rate change	$Q_{\text{air,rate,max}}$	m^3/d^2	115 200	144 000
Min airflow rate change	$Q_{\text{air,rate,min}}$	m^3/d^2	−115 200	−144 000

during selected representative days, highlighting differences in dynamics between the considered conditions. To complement the statistical summary and time series examples, Fig. 7.2 presents boxplots of COD, TN, TP, and inflow rate across all scenarios.

It is noteworthy that the inflows obtained from the used BSM2 influent model significantly exceed those under *Normal* operating conditions of the treatment plant, as described in Chapter 2. Therefore, for the considered WRRF, an inflow reduction to one quarter of the presented original quantity was applied for all scenarios utilised. The chemical composition of the inflow remained constant.

Table 7.6: Summary statistics for influent parameters under different scenarios

Scenario	**Variable**	**Unit**	**Min**	**Mean**	**Max**
Normal	COD	g COD/m^3	127.73	516.63	913.48
	TN	g N/m^3	8.91	40.13	75.16
	TP	g P/m^3	2.28	9.04	15.47
	Flow	m^3/d	9162.04	20 465.44	34 486.91
	Temp	°C	9.55	13.38	20.47
Dry	COD	g COD/m^3	245.82	657.50	1095.68
	TN	g N/m^3	21.09	49.85	88.10
	TP	g P/m^3	4.75	11.41	21.80
	Flow	m^3/d	8333.25	18 755.91	34 260.19
	Temp	°C	11.46	17.37	20.37
Rain	COD	g COD/m^3	38.37	307.44	706.24
	TN	g N/m^3	5.06	23.81	57.71
	TP	g P/m^3	0.96	5.53	13.00
	Flow	m^3/d	14 226.96	39 011.42	63 992.25
	Temp	°C	12.66	16.92	20.49

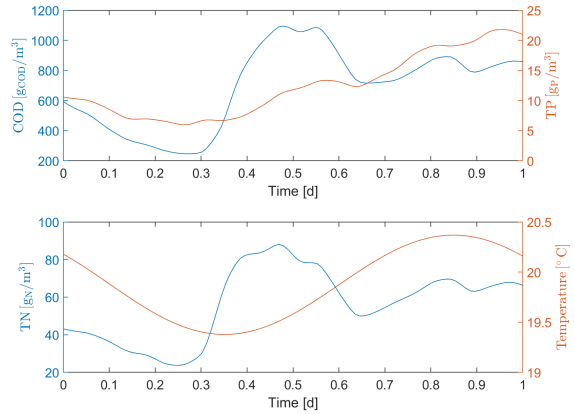

(a) Normal inflow quality

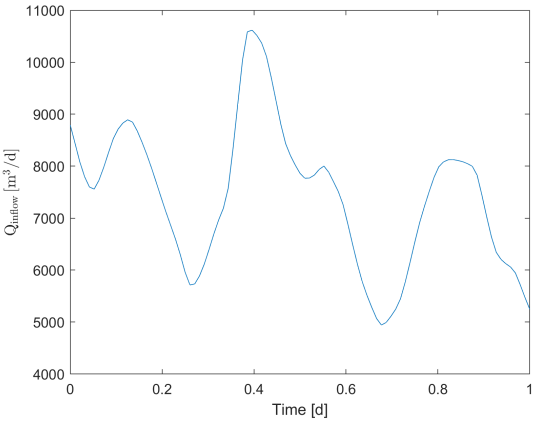

(b) Normal inflow quantity

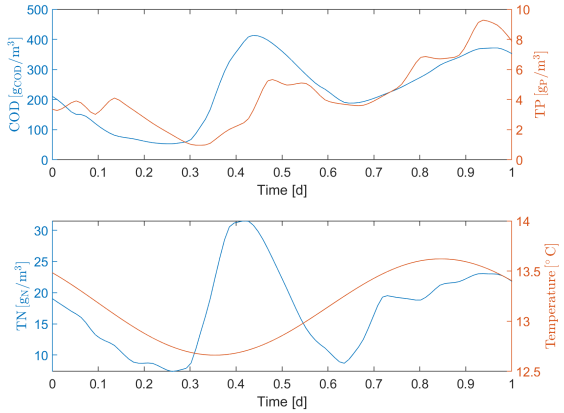

(c) Rain inflow quality

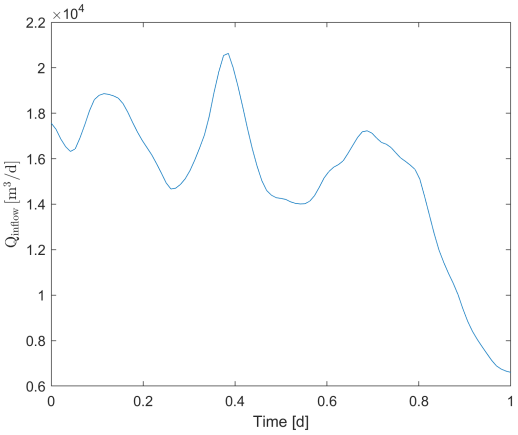

(d) Rain inflow quantity

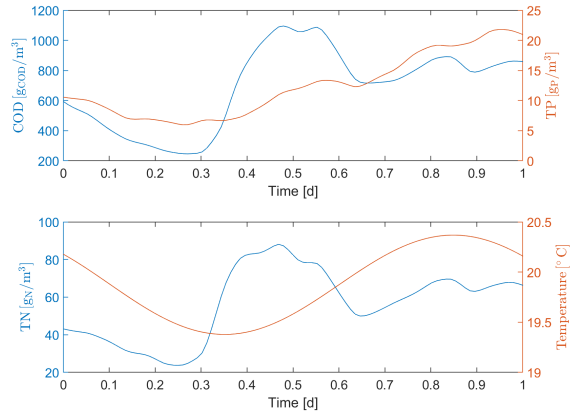

(e) Dry inflow quality

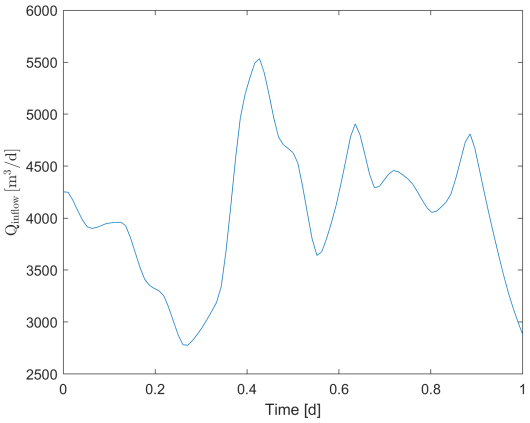

(f) Dry inflow quantity

Figure 7.1: Inflow characteristic for three different example scenario

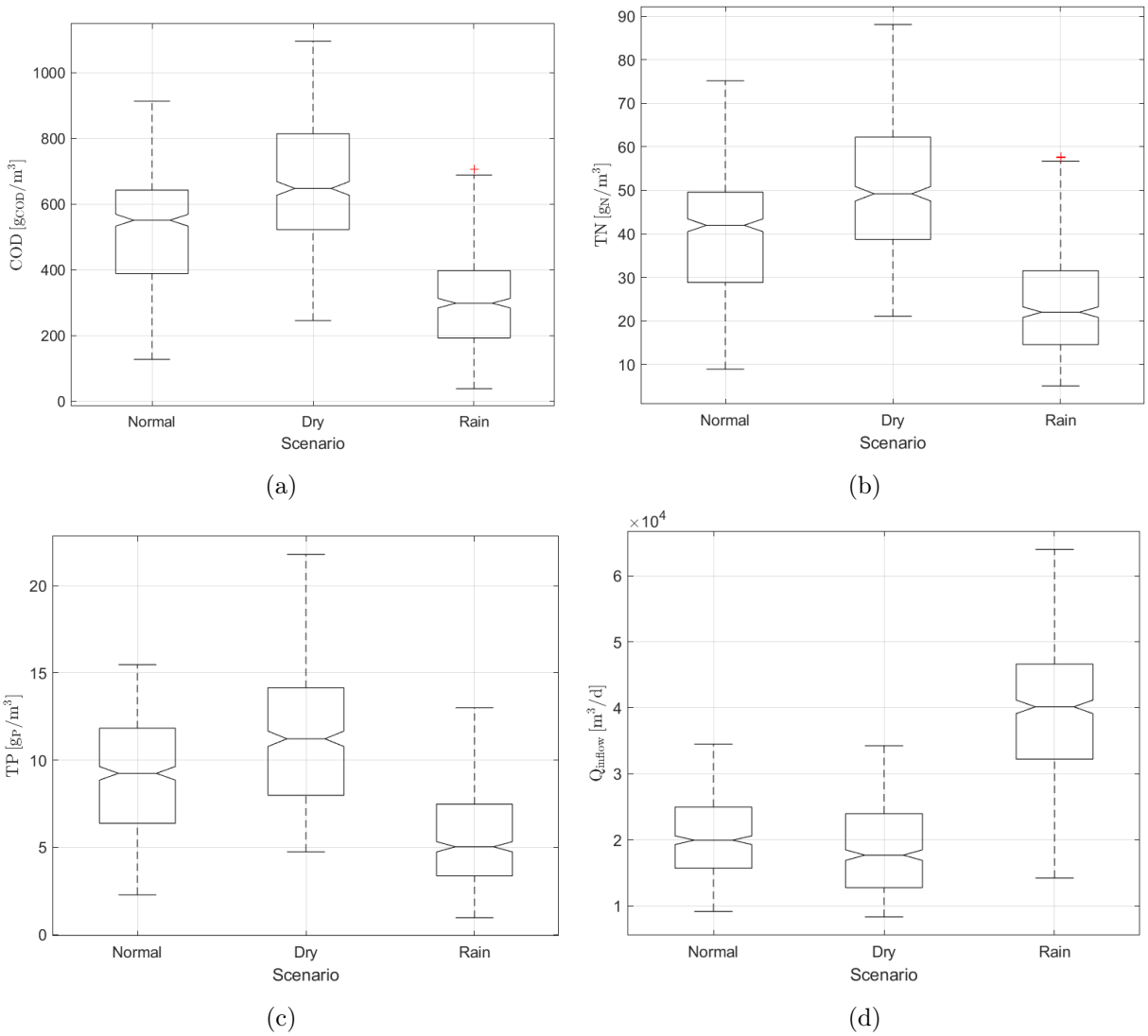

Figure 7.2: Comparison of influent characteristics across scenarios

7.2 Process Control Results

The following results correspond to the controller designed in Chapter 5, within the scope of RT2. The *Normal* scenario was selected to demonstrate the controller's performance, corresponding to day 20 of the full influent dataset. The simulation was conducted for the large reactor configuration, for three reaction cycles ($R_C = 3$).

At this stage of research, the cycle parameters were selected based on preliminary results (Ujazdowski and Piotrowski, 2024) of cycle optimisation studies, ensuring that the quality requirements for treated wastewater are met with the ideal implementation of the set trajectory. The characteristics of the influent during the filling phases for this scenario are shown in Fig. 7.3.

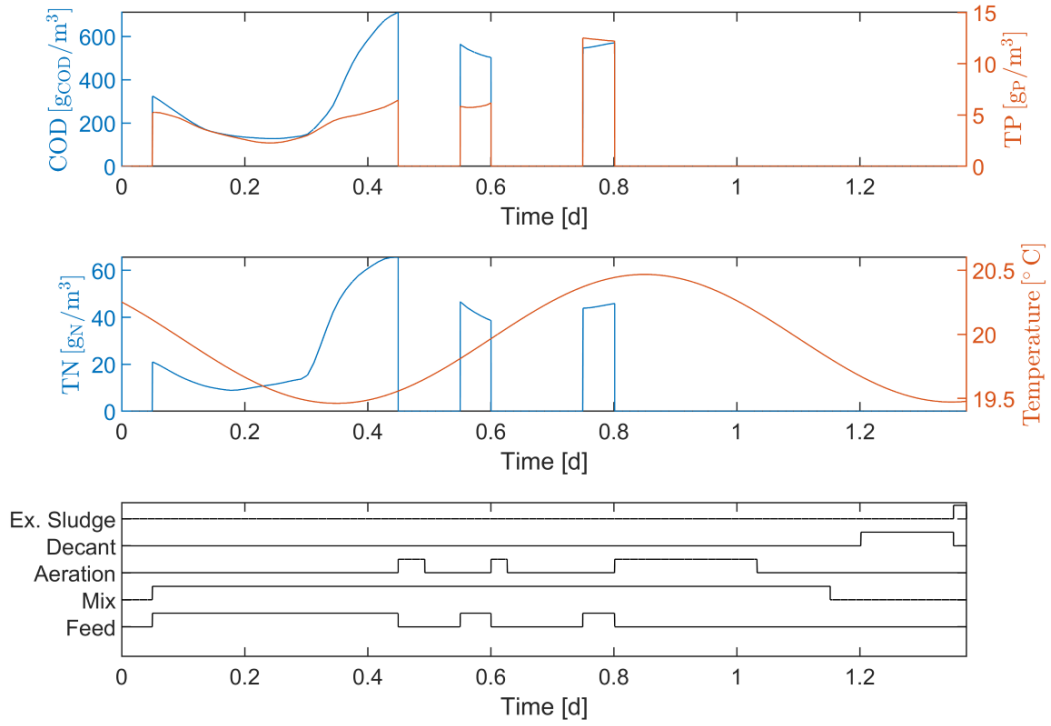

Figure 7.3: Inflow characteristic for *Normal* scenario, day 20, $R_C = 3$, large SBR

The performance of the proposed NMPC algorithm depends on the selected control strategy, which is implemented through the selection of weights. A series of simulations (66 possible strategies) was performed for common initial conditions and the same reference trajectory, with the sum of the weights equal to 1. Two ternary diagrams representing control energy and Integral Square Error (ISE) were obtained, as shown in Fig. 7.4a and Fig. 7.4b. These diagrams represent a discrete exploration of the normalised weight space, with the weights varied in increments of 0.1, according to the adopted aggregated formulation of the MOO problem. The resulting distributions provide a basis for analysing the selection of control strategies in terms of the trade-off between control cost and control performance.

Fig. 7.5 presents results for the vertices of the ternary plots presented (Fig. 7.4a and Fig. 7.4b). The upper graph presents a strategy for the best possible reference value tracking. The left graph

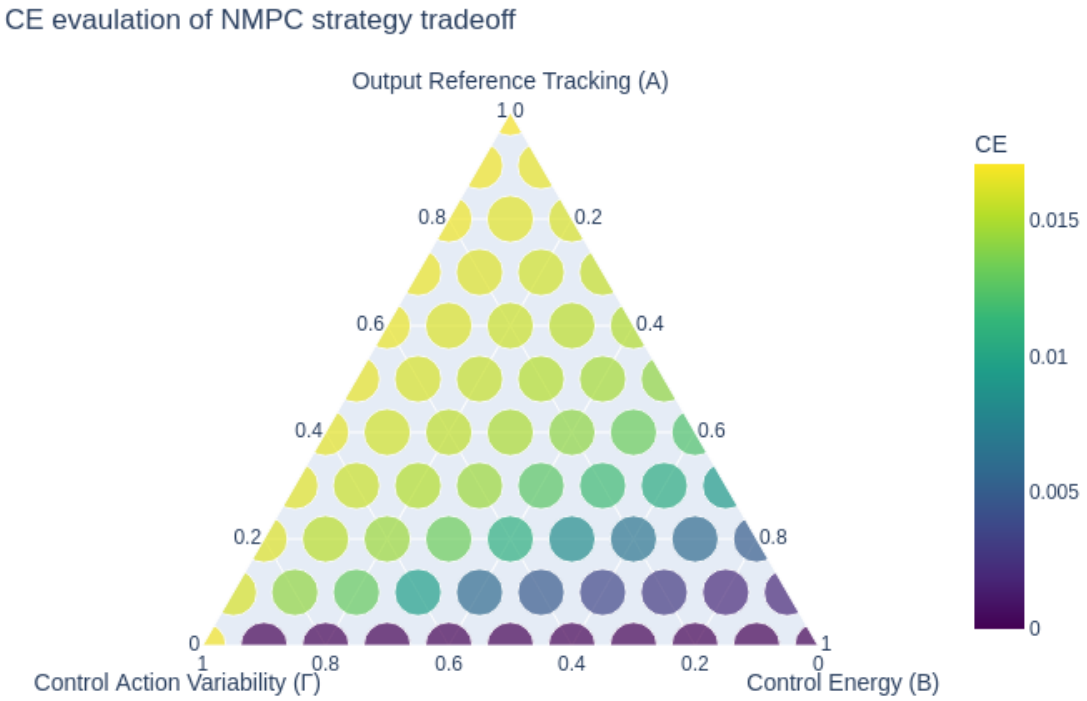

(a) Control Energy

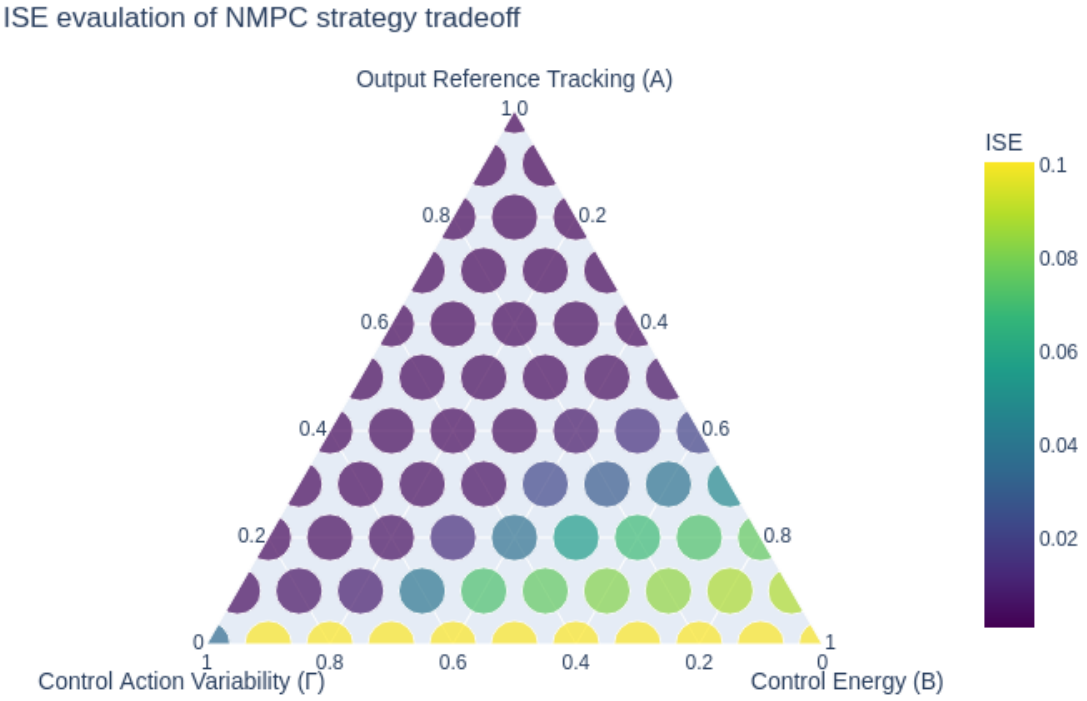

(b) Integral Square Error

Figure 7.4: Evaluation of NMPC strategy trade-off

shows the levels of pollution indicators in the upper layer of the reactor: COD, TP and TN, as well as DO for a clearer illustration of the oxygen phases. The right graph shows the control value ($Q_{\text{air}}(t)$), the change in the control value ($\Delta Q_{\text{air}}(t)$) and the DO level, together with the reference value. The results obtained are characterised by very aggressive initial controller action and a short control time. With this strategy, quality standards are met, as expected. The middle pair of graphs presents a strategy of the highest minimisation of control costs, which means that

the algorithm does not perform any control actions. The middle control signal graph shows only minor noise associated with the interference from the actuators. This is expected behaviour due to the lack of hard constraints related to the quality of the process in the adopted application. It can therefore be observed that in the absence of aeration, the phosphorus level in the reactor remains at 4 g P/m^3. Similarly, the upper layer of the reactor maintains a high COD level; only TN is partially reduced due to anaerobic processes. The bottom pair of graphs presents the results for the strategy responsible for minimising control changes, i.e. holding the controller output at the initial guess level. Due to the non-linearity of the process, maintaining a constant control output is insufficient to ensure that the reference DO level is achieved.

Based on a graphical analysis of the trajectories, a balanced solution with weights $A = 0.7$, $B = 0.1$, $\Gamma = 0.2$ was selected as a reasonable trade-off between control performance and cost. Then, Fig. 7.6 presents the results obtained for this configuration. The selected solution closely follows the reference trajectory while ensuring smoother control action, reduced energy consumption, and compliance with quality standards.

7.3 Process Optimisation Results

The MOO algorithm developed in Section 5.3 was executed multiple times for different sets of input data. Calculations were performed for three inflow scenarios, two cycle types, and two reactor sizes, resulting in a total of 12 variants for which optimisation was carried out. The applied algorithm enabled the approximation of Pareto fronts.

Preliminary studies (Ujazdowski and Piotrowski, 2024) demonstrated that COD reduction is always satisfied when the TP and TN objectives are fulfilled. Excluding COD also allows for improved graphical presentation, since only three objective functions were considered, thus forming a three-dimensional decision space. For the presentation of results, the following notation was adopted: J_1 denotes the DO objective (economic related), J_2 corresponds to TP, and J_3 represents TN.

As a baseline, cycles were prepared with aeration phases of 9 hours in the case of $R_C = 1$, and with three aeration phases of 3 hours each in the case of $R_C = 3$, with the DO setpoint fixed at 2 g O_2/m^3 for each phase. The J_2 and J_3 axes are normalised by the adopted constraints, while the J_1 axis represents an abstract measure of aeration performance, defined in accordance with (5.21).

Before discussing the results for individual cases, the aggregated Pareto fronts are presented in Fig. 7.7 and Fig. 7.8, which correspond to the small and large reactors, respectively. For the sake of clarity, these results have subsequently been decomposed into separate sets, which are described in the following.

Fig. 7.9 illustrates the Pareto front for the large reactor under the scenario with $R_C = 1$. The obtained data demonstrate a significant influence of the pollution load on the process performance. Under dry-weather conditions (characterised by a considerably higher load), even at high process costs, it is not possible to achieve the required level of TN removal without additional chemical enhancement. In contrast, under rain-weather conditions, both TP and TN targets are satisfied with a substantial margin, even at low energy costs during the aerated

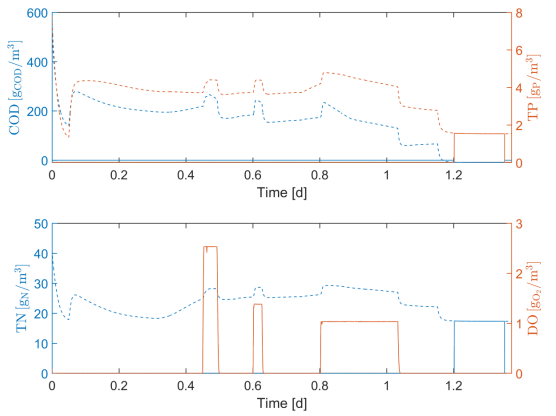

(a) Process ($A = 1.0$, $B = 0.0$, $\Gamma = 0.0$)

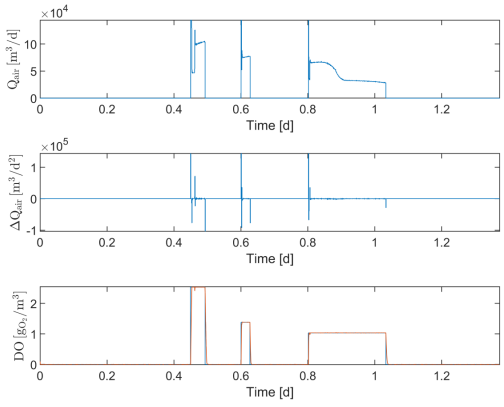

(b) Control ($A = 1.0$, $B = 0.0$, $\Gamma = 0.0$)

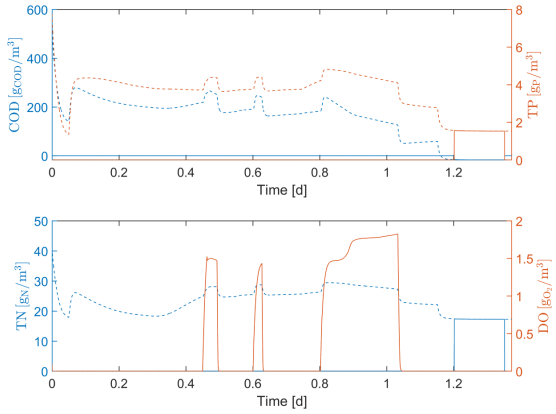

(c) Process ($A = 0.0$, $B = 1.0$, $\Gamma = 0.0$)

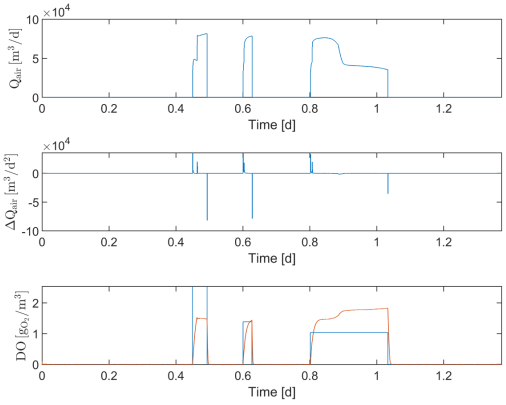

(d) Control ($A = 0.0$, $B = 1.0$, $\Gamma = 0.0$)

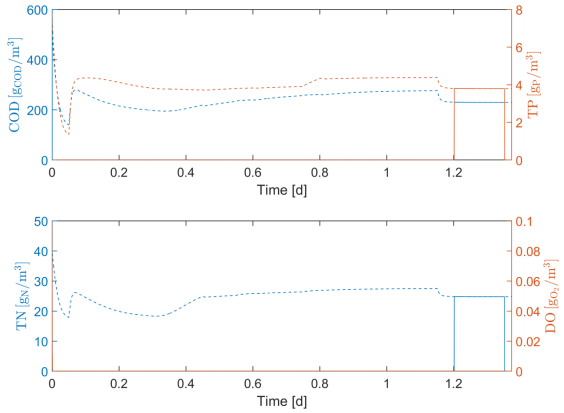

(e) Process ($A = 0.0$, $B = 0.0$, $\Gamma = 1.0$)

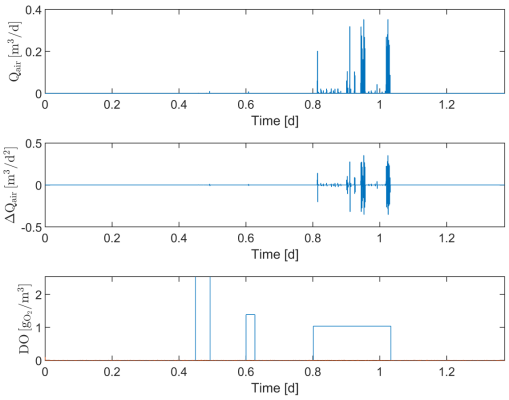

(f) Control ($A = 0.0$, $B = 0.0$, $\Gamma = 1.0$)

Figure 7.5: Composite plots showing for the vertices of the ternary plot NMPC control strategy weights, on the left side (a,c,e), the profiles of COD, TP, and TN during the cycle (dashed line) and during the decant phase (solid line), along with the DO level throughout the cycle (indicating aerobic phases). On the right side (b,d,f) are the corresponding Q_{air}, ΔQ_{air}, and DO (orange line), along with DO_{ref} (blue line)

phases. In the *Normal* inflow scenario (with medium load), the approximation of the Pareto front indicates that the required TP reduction is achieved, whereas the TN limit is slightly exceeded.

Subsequently, Fig. 7.10 presents the case for the large reactor with $R_C = 3$. With three

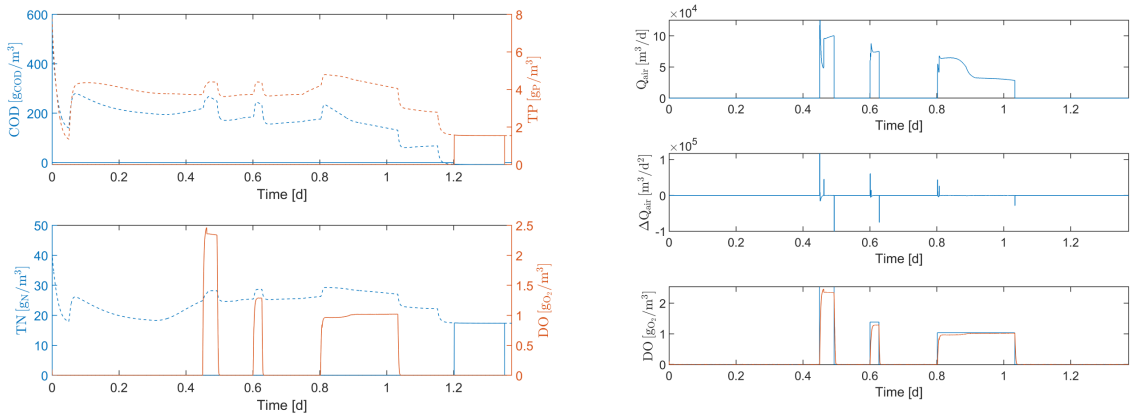

(a) Process ($A = 0.7$, $B = 0.1$, $\Gamma = 0.2$) (b) Control ($A = 0.7$, $B = 0.1$, $\Gamma = 0.2$)

Figure 7.6: Composite plots for selected NMPC control strategy weights, (a) the profiles of COD, TP, and TN during the cycle (dashed line) and during the decant phase (solid line), along with the DO level throughout the cycle (indicating aerobic phases), (b) the corresponding Q_{air}, ΔQ_{air}, and DO (orange line), along with DO_{ref} (blue line)

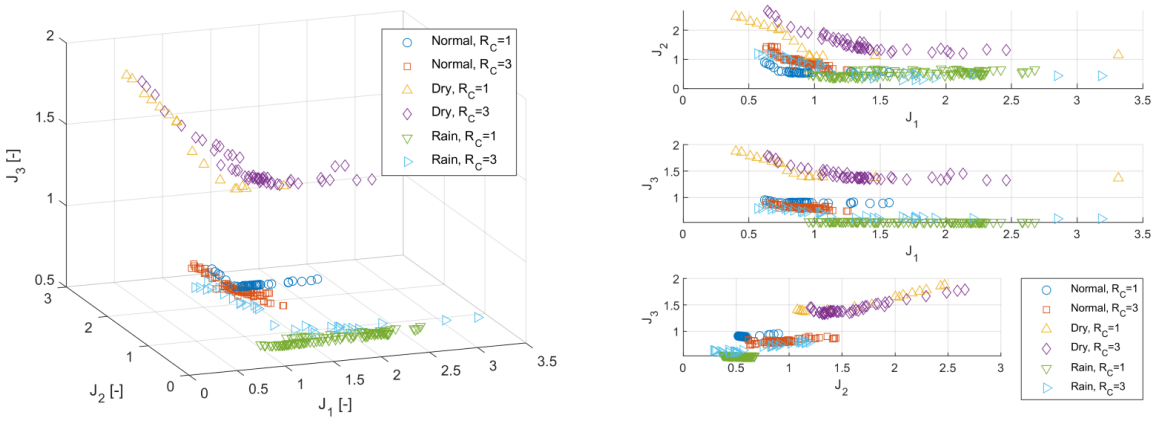

(a) (b)

Figure 7.7: All Pareto fronts for the small reactor, (a) 3D view, (b) projections

aerated phases, the intended reduction of both TN and TP is achieved under *Normal* and *Rain* conditions. As in the case of $R_C = 1$, *Dry* conditions would require chemical enhancement, which is not considered in this study. In this configuration, the Pareto front is also broader along the economic axis (J_1).

Experiments were also performed for the small reactor under the same inflow scenarios. The results for $R_C = 1$ are depicted in Fig. 7.11, and those for $R_C = 3$ in Fig. 7.12. The distribution of Pareto fronts for dry- and rain-weather conditions is very similar regardless of the reactor size. However, the results obtained for the *Normal* inflow scenario differ from this pattern: in the small reactor, better removal of both TN and TP was achieved compared with the large reactor. Regardless of the number of aerated phases, all TN-related results comply with the legal requirements without requiring chemical enhancement. Consequently, in the adopted configuration and under the assumed constraints, the small reactor ensures a more efficient treatment process.

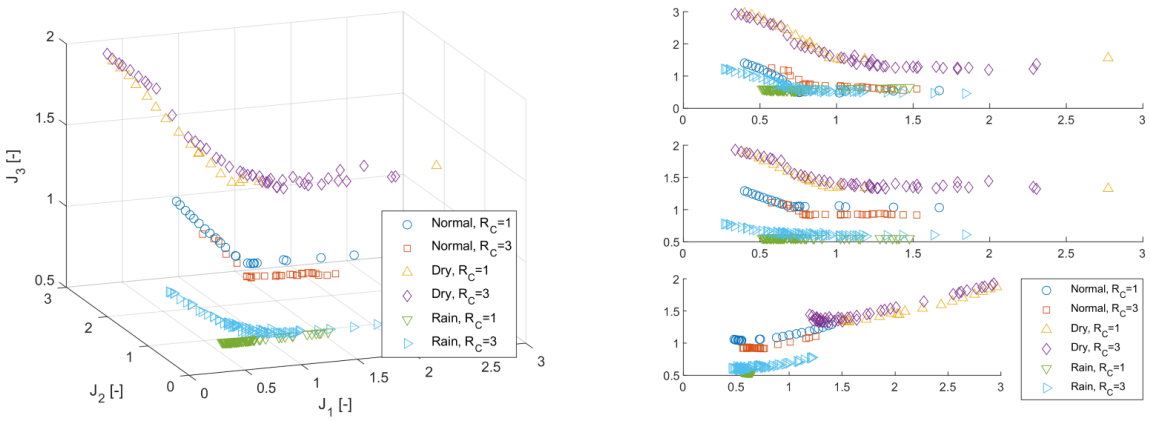

(a) (b)

Figure 7.8: All Pareto fronts for the large reactor, (a) 3D view, (b) projections

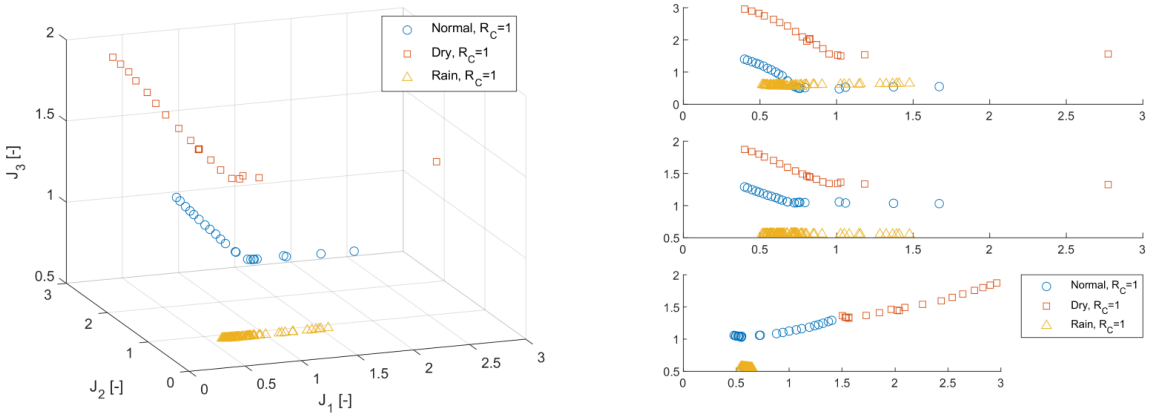

(a) (b)

Figure 7.9: Pareto front for the large reactor, $R_C = 1$ (a) 3D view, (b) projections

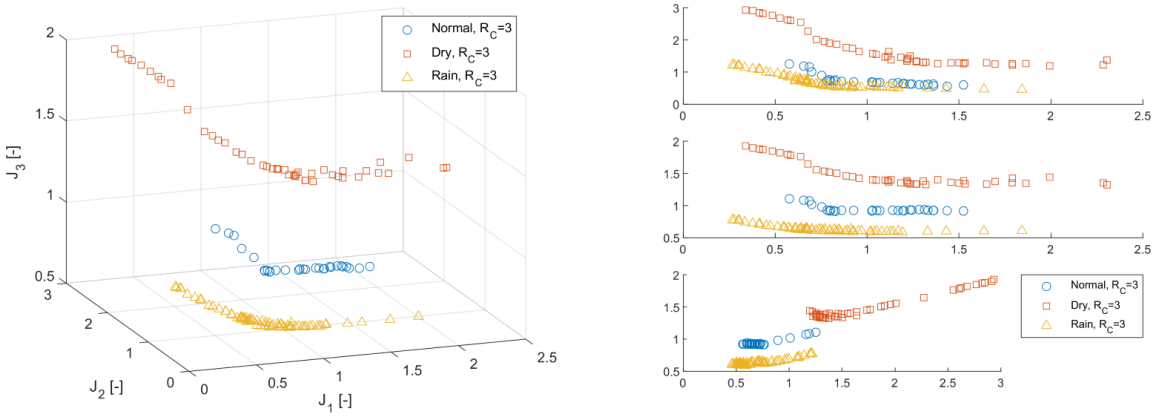

(a) (b)

Figure 7.10: Pareto front for the large reactor, $R_C = 3$ (a) 3D view, (b) projections

Then, the results obtained for uniform inflow conditions are compared, presenting the composition of Pareto fronts for both the large and small reactors, together with the indication of the

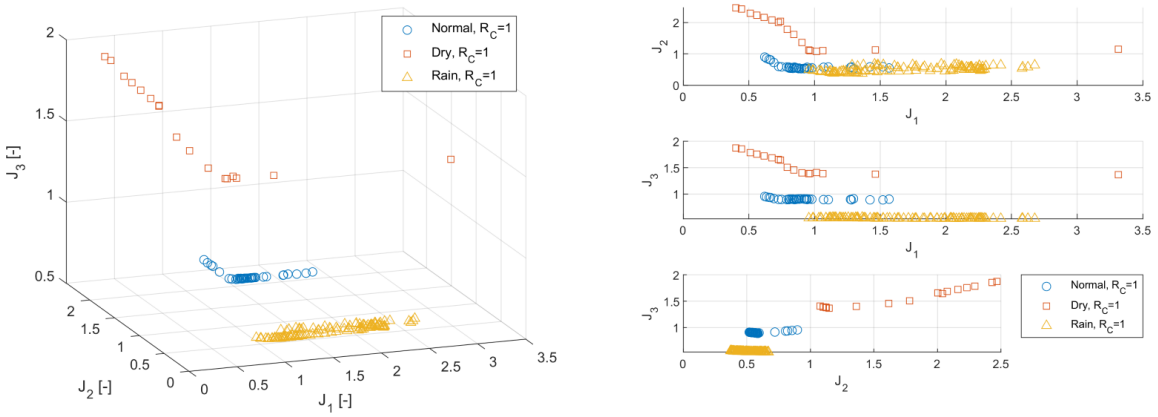

(a) (b)

Figure 7.11: Pareto front for the small reactor, $R_C = 1$ (a) 3D view, (b) projections

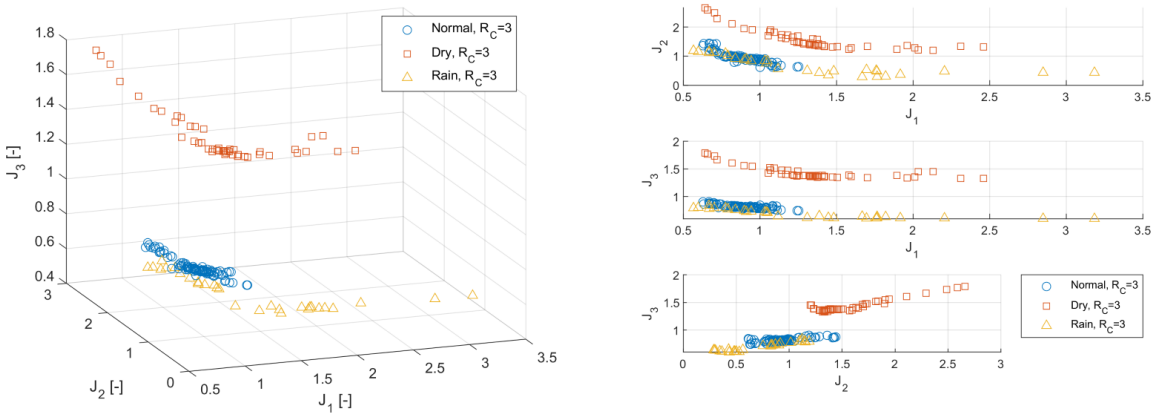

(a) (b)

Figure 7.12: Pareto front for the small reactor, $R_C = 3$ (a) 3D view, (b) projections

baseline outcomes. The baseline results, denoted on the figures with black symbols as *default*, were simulated separately for each inflow scenario in order to capture the reference treatment performance under specific operating conditions. This variant corresponds to the configuration introduced earlier, where the aeration strategy is fixed ($R_C = 1$ with a single aerated phase of 9 h, or $R_C = 3$ with three aerated phases of 3 h each), and the DO setpoint is maintained at 2 g O_2/m^3. Thus, the *default* points represent the performance of a system operating without optimisation, providing a benchmark against which the Pareto-optimal solutions can be evaluated. The obtained Pareto fronts for the *Normal* inflow conditions are presented in Fig. 7.13. In turn, Fig. 7.14 summarises the results for the *Dry* scenario, while Fig. 7.15 illustrates the case for *Rain* inflow conditions.

Most of the solutions obtained through optimisation require lower aeration intensity than the baseline cycles, and consequently lower energy costs. Approximately half of the optimised solutions also provide improved removal of both TP and TN. Particular attention should be given to the *default* results in Fig. 7.13, where it is evident that the application of a single aeration phase under *Normal* conditions yields higher phosphorus removal efficiency, whereas

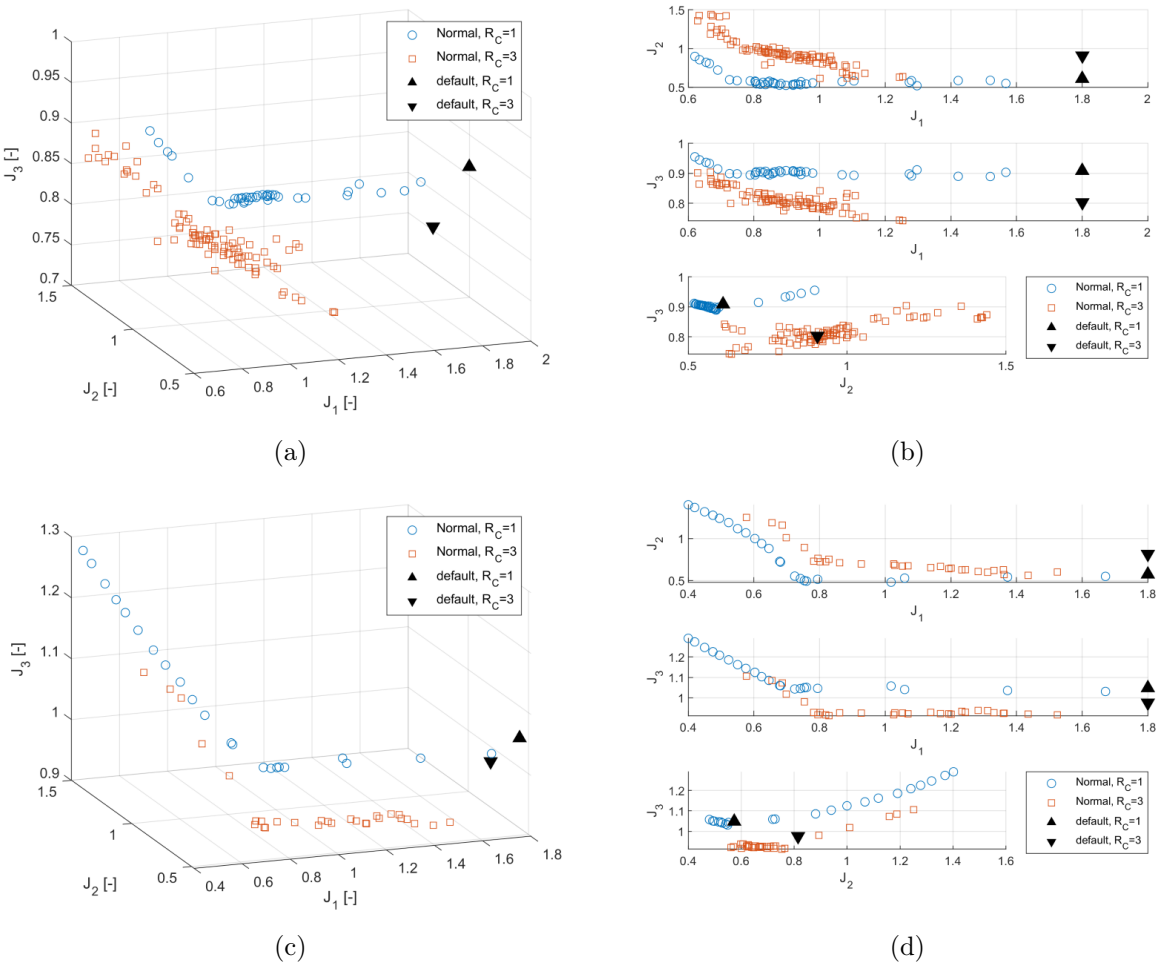

Figure 7.13: Pareto fronts for the *Normal* inflow scenario (a) 3D view for small reactor, (b) projections for small reactor, (c) 3D view for large reactor, (d) projections for large reactor

three aeration phases ensure more effective nitrogen removal. The situation is reversed for low chemical loads, i.e. the *Rain* inflow scenario (see Fig. 7.15).

Moreover, in the projections presenting the J_1–J_2 axes, it can be observed that the individuals forming the approximation of the blue Pareto front (corresponding to $R_C = 1$) are consistently below those of the orange front ($R_C = 3$), regardless of the inflow conditions. In the J_3–J_1 projections, the orange front performs better in terms of nitrogen removal under *Normal* conditions, while in the *Dry* scenario, both fronts align closely, and in the *Rain* scenario, the blue front lies lower along the J_3 axis. This outcome may indicate that the distribution of aeration phases has a stronger effect on phosphorus removal efficiency than on nitrogen removal, with the relative advantage shifting depending on the inflow scenario.

The selected individuals corresponding to the extreme solutions for the considered objectives, as well as the balanced solutions obtained through the GRA procedure, are presented in Table 7.7 and Table 7.8. A detailed analysis, based on the extreme points and the balanced solution, has been conducted using the tabulated data in the following manner.

For the identification of a balanced solution, a set of weights ensuring equal prioritisation of all objective functions was adopted, thereby avoiding arbitrary preference towards any particular

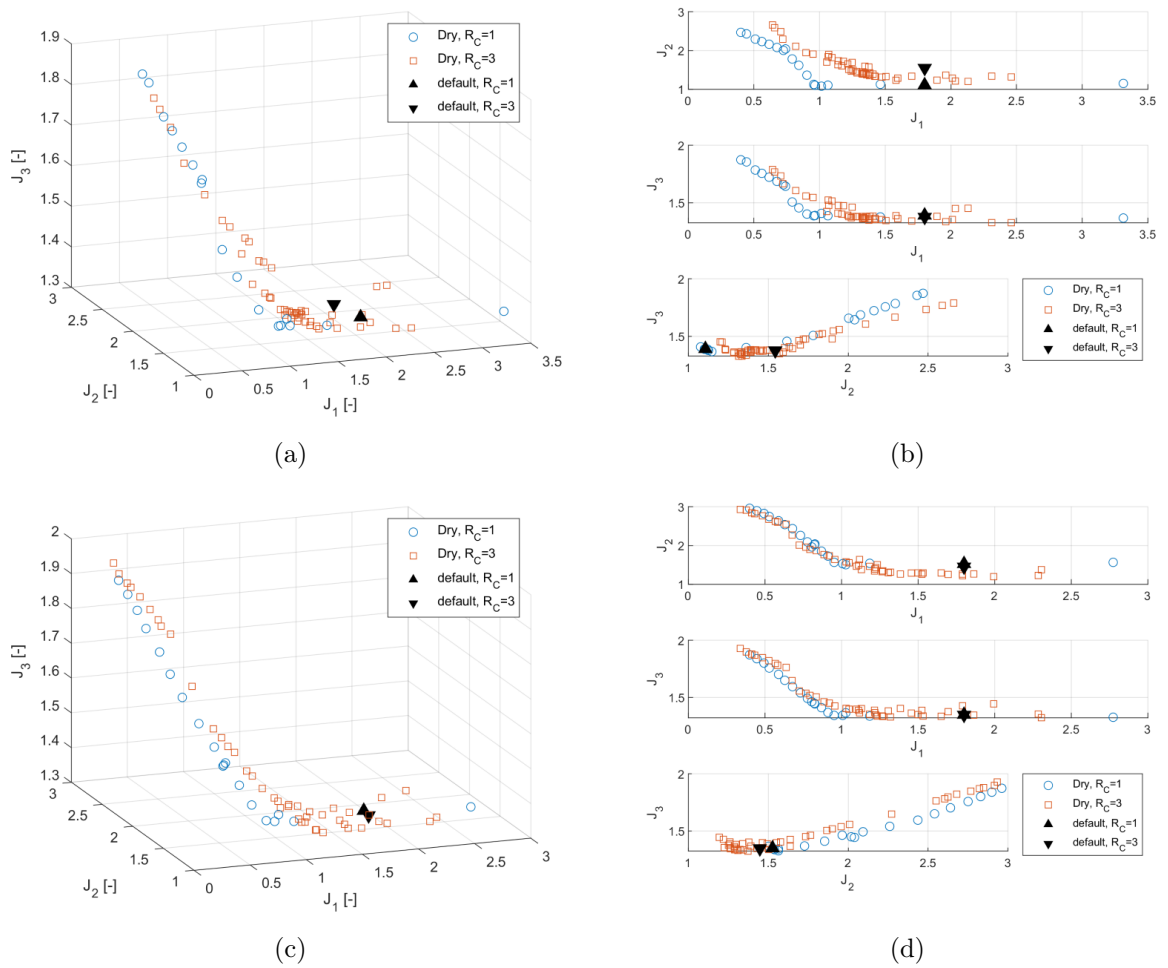

Figure 7.14: Pareto fronts for the *Dry* inflow scenario (a) 3D view for small reactor, (b) projections for small reactor, (c) 3D view for large reactor, (d) projections for large reactor

objective. The corresponding priority vector is defined as $\boldsymbol{\omega} = \begin{bmatrix} 0.25 & 0.25 & 0.25 & 0.25 \end{bmatrix}$.

It should be noted that, while equal weighting was adopted here to obtain a balanced solution, the selection of the priority vector may be defined arbitrarily from a technological perspective in practical applications. In such cases, specific objectives may be prioritised depending on operational requirements. For example, when chemical phosphorus removal is applied, the priority associated with the phosphorus-related objective function may be reduced, allowing greater emphasis to be placed on solutions balancing the trade-off between DO control and TN removal.

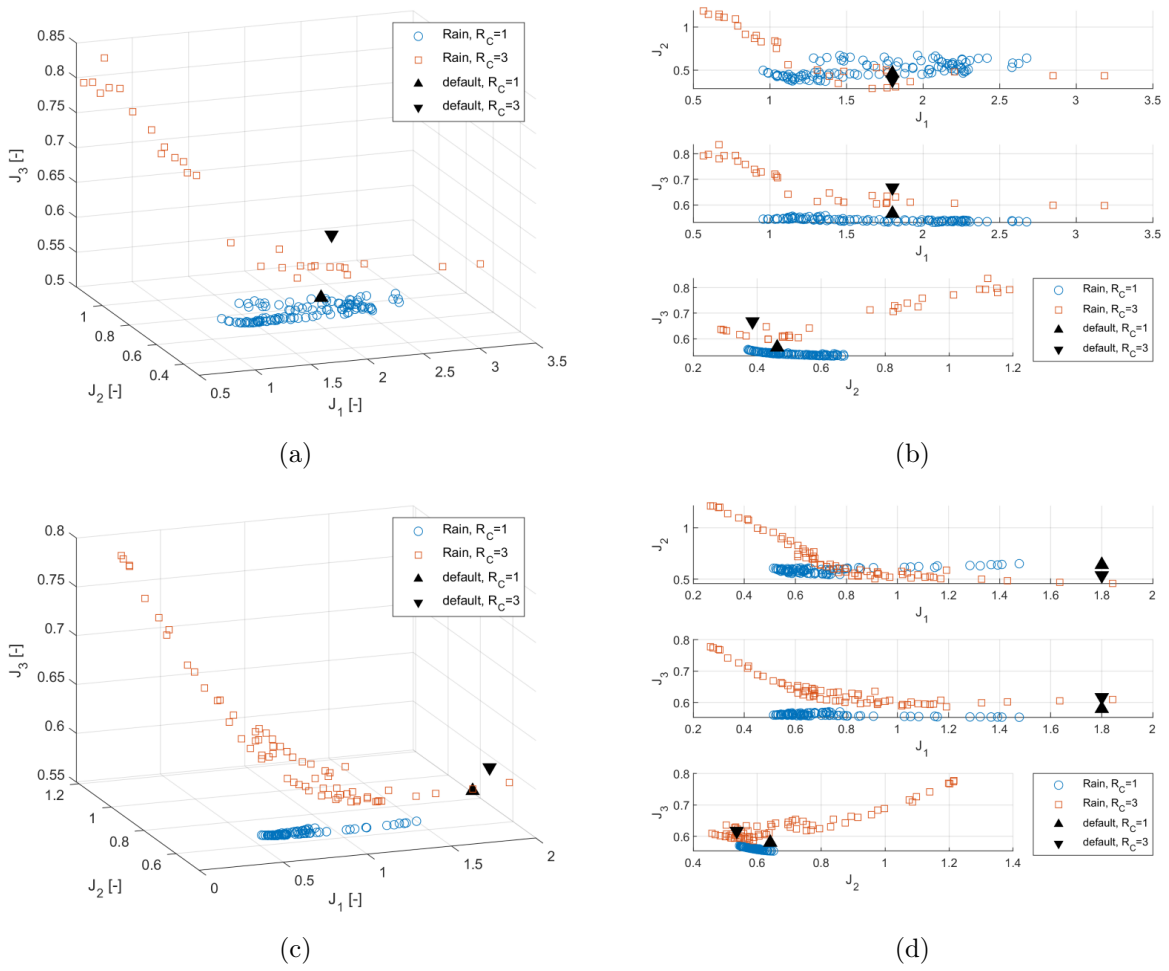

Figure 7.15: Pareto fronts for the *Rain* inflow scenario (a) 3D view for small reactor, (b) projections for small reactor, (c) 3D view for large reactor, (d) projections for large reactor

Table 7.7: Performance indicators under different scenarios for small SBR. For $R_c = 3$ values of mean Q_{air} and phase duration are given for three aeration phases; Aeration time is the total

R_C	Type	Scenario	Cycle time [d]	Mean Q_{air} [m^3/d]	Phase dur. [d]	Aeration time [d]	TN red.[%]	TP red.[%]	COD red.[%]
1	DO	Normal	1.10	38 548	0.22	0.22	74	71	99
	TP		1.45	41 186	0.27	0.27	75	82	100
	TN		1.11	40 550	0.32	0.32	75	80	100
	GRA		1.11	32 549	0.32	0.32	75	80	100
	DO	Dry	1.08	53 032	0.17	0.17	54	62	91
	TP		1.75	42 100	0.42	0.42	65	83	100
	TN		1.34	63 392	0.43	0.43	66	82	100
	GRA		1.66	42 871	0.40	0.40	65	83	100
	DO	Rain	0.88	29 428	0.20	0.20	45	78	98
	TP		1.28	28 414	0.24	0.24	44	83	100
	TN		0.82	40 437	0.19	0.19	46	78	100
	GRA		1.24	27 248	0.24	0.24	44	83	100
3	DO	Normal	1.23	45 946	0.03	0.18	71	49	96
				52 054	0.13				
				40 548	0.03				
	TP		1.18	63 995	0.02	0.29	73	76	100
				56 715	0.02				
				35 667	0.25				
	TN		1.72	41 460	0.02	0.33	76	75	100
				39 004	0.25				
				16 331	0.06				
	GRA		1.71	42 592	0.02	0.33	76	75	100
				38 926	0.25				
				16 349	0.06				
	DO	Dry	1.37	63 148	0.02	0.19	56	58	97
				59 769	0.02				
				55 785	0.15				
	TP		1.85	75 244	0.23	0.48	64	81	100
				35 645	0.20				
				21 594	0.06				
	TN		1.73	84 347	0.20	0.44	67	79	100
				89 745	0.02				
				34 042	0.22				
	GRA		1.72	81 231	0.13	0.38	67	79	100
				51 415	0.16				
				29 339	0.10				
	DO	Rain	0.83	68 592	0.02	0.06	22	37	79
				59 398	0.02				
				57 401	0.02				
	TP		1.13	75 676	0.03	0.36	36	84	100
				46 139	0.07				
				16 928	0.25				
	TN		0.88	48 596	0.02	0.26	40	76	100
				49 086	0.15				
				22v188	0.09				
	GRA		1.39	49 785	0.02	0.29	38	80	100
				37 823	0.24				
				21 661	0.03				

Table 7.8: Performance indicators under different scenarios for large SBR. For $R_c = 3$ values of mean Q_{air} and phase duration are given for three aeration phases; Aeration time is the total

R_C	Type	Scenario	Cycle time [d]	Mean Q_{air} [m^3/d]	Phase dur. [d]	Aeration time [d]	TN red.[%]	TP red.[%]	COD red.[%]
1	DO	Normal	1.33	58 340	0.17	0.17	65	61	96
	TP		1.64	52 602	0.31	0.31	71	86	100
	TN		1.28	57 416	0.35	0.35	72	84	100
	GRA		1.57	46 913	0.31	0.31	71	86	100
	DO	Dry	1.47	70 568	0.17	0.17	54	67	90
	TP		1.91	55 173	0.43	0.43	66	83	100
	TN		1.52	83 054	0.42	0.42	67	82	100
	GRA		1.59	57 009	0.41	0.41	67	83	100
	DO	Rain	1.12	37 527	0.21	0.21	58	78	99
	TP		1.37	39 974	0.23	0.23	57	80	100
	TN		0.93	59 804	0.21	0.21	58	76	100
	GRA		1.27	35 715	0.24	0.24	58	80	100
3	DO	Normal	1.31	72 883	0.06	0.21	70	62	98
				83 249	0.02				
				51 827	0.13				
	TP		1.55	92 726	0.03	0.32	75	82	100
				60 535	0.25				
				30 452	0.04				
	TN		1.66	63 761	0.06	0.34	75	76	100
				58 224	0.14				
				28 108	0.14				
	GRA		1.55	92 726	0.03	0.32	75	82	100
				60 535	0.25				
				30 452	0.04				
	DO	Dry	1.50	69 653	0.04	0.12	52	59	82
				89 099	0.04				
				68 019	0.04				
	TP		2.04	100 841	0.25	0.53	64	83	100
				51 618	0.07				
				27 929	0.20				
	TN		1.72	115 747	0.22	0.39	67	81	100
				84 459	0.04				
				50 260	0.14				
	GRA		1.81	90 339	0.18	0.42	67	81	100
				65 047	0.12				
				39 150	0.12				
	DO	Rain	0.90	58 299	0.02	0.09	23	50	88
				84 890	0.02				
				54 310	0.05				
	TP		1.51	64 540	0.03	0.33	38	80	100
				66 841	0.16				
				11 728	0.14				
	TN		1.35	79 100	0.07	0.28	41	76	100
				46 747	0.10				
				21 738	0.11				
	GRA		1.38	81 294	0.07	0.28	40	78	100
				39 087	0.16				
				16 187	0.05				

Optimisation with respect to minimising aeration intensity naturally leads to the shortest cycle times and the lowest aeration durations. At the same time, the efficiency of nutrient removal is significantly reduced. For example, in the small SBR under *Normal* inflow conditions, when prioritising the DO objective, the cycle length is approximately 1.10 d with aeration lasting 0.22 d, but TN removal is only about 74% and TP 71% (for the large SBR: TN ∼65%, TP ∼61%). In *Dry* and *Rain* scenarios, aeration demand decreases even further (0.17–0.21 d), resulting in dramatically low nitrogen removal (often below 50%) and phosphorus removal (e.g. in the *Rain* scenario: TN 22–58%, TP 37–78%).

When prioritising the objective related to TP, the system operates with longer cycles and higher aeration intensity. For instance, the small SBR under *Normal* conditions exhibits a cycle length of 1.45 d, aeration of 0.27 d, and TP removal of 82% (TN 75%). The large SBR reaches a cycle length of 1.64 d, aeration of 0.31 d, TP removal of 86%, and TN 71%. In all scenarios, phosphorus removal attains its highest values (80–86%), while COD removal remains practically complete (100%). The nitrogen removal objective produces results comparable to those obtained for TP. Cycle times and aeration durations are of similar magnitude (small SBR under *Normal* inflow: ∼1.11 d, aeration 0.32 d; TN 75%). As a result, TN removal reaches the highest values in each scenario (75–76% under *Normal* and *Dry* conditions, 38–46% under *Rain*), with TP removal also high (75–84%). In both *Dry* and *Rain* scenarios, TN and TP levels are slightly lower than those for the TP objective, yet still markedly higher than in the DO-focused optimisation.

The results obtained with the GRA method are comparable to the best outcomes of the TP and TN objectives. In most cases, TN and TP removal rates are about 75–76%, while aeration duration remains intermediate between TP- and TN-oriented cases. The GRA approach achieves complete COD removal (similarly to TP and TN), and typically results in moderate cycle times. This can be considered a balanced solution, offering good nutrient removal without the extreme energy savings observed in the DO-oriented case.

With $R_C = 3$, the system possesses greater flexibility in allocating aeration, which often enables shorter cycles or better adjustment of aeration across phases. However, the performance for the same objective type remains comparable. For TP/TN objectives, the number of phases does not substantially alter removal efficiencies (e.g. small SBR under *Normal* inflow for TP: $R_C = 1$ – TP 82%, $R_C = 3$ – 76%; for TN objective: 80% vs. 75%). Cycle length is sometimes slightly shorter for $R_C = 3$, yet total aeration demand frequently increases (more phases imply more aeration pulses).

The large SBR operates at higher aeration flow rates (average Q_{air} of 5–11 $\times 10^4$ m^3/d) than the small reactor (2–8$\times 10^4$ m^3/d) and usually with slightly longer cycles (e.g. DO objective under *Normal* inflow: 1.33 vs. 1.10 d). Higher airflow is required to achieve comparable performance in the larger volume. The overall trends remain consistent: for TP/TN objectives, TP removal reaches about 80–86% and TN 64–75% (depending on the scenario), comparable to the small SBR. Nevertheless, nutrient removal percentages are often slightly lower (e.g. large SBR under *Normal* inflow, DO objective: TN 65% vs. 74% for the small SBR). This suggests that larger-scale operation requires more aeration to achieve similar effluent concentrations.

The trade-off between energy efficiency and treatment performance is clearly visible. The DO objective minimises aeration time and intensity (shorter cycles, lower flow rates), which reduces

energy costs, but at the expense of lower nitrogen and phosphorus removal, and incomplete COD removal in some cases. Conversely, TP- and TN-oriented results extend cycle length and increase aeration demand, but achieve maximum removal of the targeted nutrient (phosphorus or nitrogen) as well as complete COD removal. For example, phosphorus removal exceeds 80% under the TP objective, while nitrogen removal surpasses 75% under the TN objective, across all inflow scenarios.

The compromise solution (by GRA) combines the features of TP and TN optimisation, achieving high (>75%) removal of both nutrients and complete COD removal, with moderate aeration demand (aeration time lying between TP and TN objectives).

The parameter R_C (number of aerated phases) does not substantially alter the overall findings. Increasing the number of phases mainly provides flexibility in distributing aeration but does not change the fundamental relationship between the optimisation objective and treatment performance. The most noticeable effect is the potential to shorten the cycle for TP/TN objectives or to achieve extremely low aeration for the DO objective (further reducing removal performance).

In both the small and large SBRs, the pattern remains consistent: minimisation of aeration reduces nutrient removal, while maximisation of nutrient removal increases aeration demand. The larger reactor requires higher aeration flow rates and slightly longer cycles, but the relative removal efficiencies are similar. This indicates that system scale affects absolute values (time, air volume), but does not alter the main conclusions.

COD removal is nearly complete (∼100%) for TP-, TN-, and GRA-oriented solutions. Only for the DO objective are slight decreases observed in certain cases (79–99%).

In summary, the presented data reveal a classical trade-off in SBR operation: energy savings versus treatment efficiency. Optimisation focused on aeration cost (DO objective) significantly reduces treatment performance, especially for nitrogen, whereas optimisation aimed at nutrient removal increases aeration demand. Compromise solutions (GRA) enable high treatment performance with moderate energy consumption.

The applied MOO approach, based on Pareto front approximation, clearly highlights the trade-off between treatment performance and operational costs in the analysed application. The obtained fronts provide a technologically relevant set of decision-making solutions, which may be directly applied in practice. This is particularly important in the context of balancing TP and TN removal, where different inflow scenarios reveal distinct equilibrium points. Consequently, the presented results confirm that the developed optimisation tool allows the adjustment of control strategies to diverse quality and economic requirements under real operating conditions.

In conclusion, the obtained results address the formulated research objective 1, concerning the design of a decision-support system for the operation of biological processes in a single sequential batch reactor (SBR), by solving the MOO problem of biological treatment in batch-type WRRF. The system enables the determination of both the duration of individual SBR phases and the number of aerobic and anoxic sequences.

7.4 Task Scheduling Results

In this section, the results obtained from the experiments with the proposed implementation of the MA applied to the considered UPMSP are presented and discussed. The results correspond to the execution of RT 4.

As the inflow scenario, a 14-day fragment from the inflow model was adopted, including rainfall events preceded by a period of increased load (see Section 3.5). The scenario was divided into the following periods: 3 days of increased load (yellow, denoted as *Dry*), followed by 3 days with rainfall (*Rain*, green), and the remaining days classified as *Normal* (blue). The average inflow for these two weeks was approximately 5000 m^3/d, which is comparable to the typical operating conditions in the Swarzewo facility. The inflow trajectory is shown in Fig. 7.16.

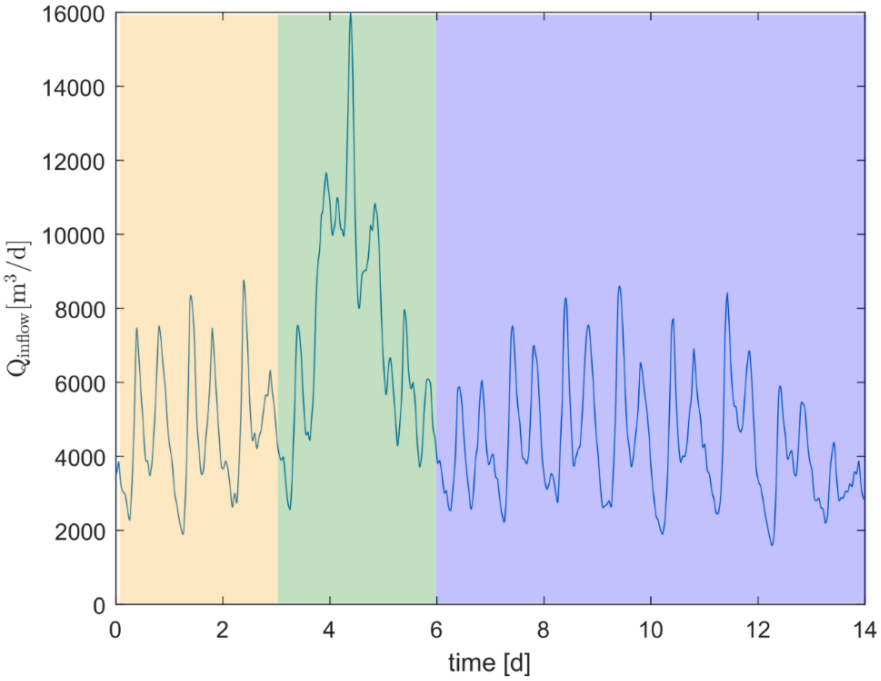

Figure 7.16: 14-day inflow scenario

The experiments were conducted over a 14-day horizon, starting from an initial filling level of 30% for the retention tank and 0% for the stormwater retention lagoon.

7.4.1 Baseline and Task-optimised Baseline Schedules

Since no similar solutions have been reported in the literature, baseline scenarios were prepared based on known operational practices, assuming continuous inflow to the reactors. Specifically, the shift of the filled reactor occurred at the end of the first filling phase. Excess inflow was directed to the retention tank, and in periods of insufficient inflow, the tank was additionally discharged.

Four preliminary experiments were carried out for the selected inflow scenario, considering one and three reaction phases. The first set corresponds to the baseline case, in which the schedules were generated with job types from $\mathcal{J}_{\text{base}}$ (introduced in Table 6.2 and additionally

described in Section 7.3). Subsequently, the obtained schedules were modified by replacing the job type with optimised ones, adapted to the respective inflow conditions ($\mathcal{J}$). This second set of experiments is referred to as the task-optimised baseline. Both variants were evaluated for one and three reaction phases.

The adopted approach provides a framework for evaluating the long-term operational costs of the WWTP when inflow-adapted cycles are introduced, as well as distinguishing the improvement obtained through solving the scheduling problem from that resulting from cycle optimisation. The baseline schedules were assessed using the same objective function (see Subsection 6.1.2) as that employed in solving the considered UPMSP.

Fig. 7.17 shows four schedules: those with a single aerobic phase are presented on the left, while the ones with three aerobic phases are on the right. The top pair of figures corresponds to baseline schedules, and the bottom pair to task-optimised baseline schedules.

Table 7.9 presents a comparison between the baseline and task-optimised baseline schedules for both cycle configurations ($R_C = 1$ and $R_C = 3$). The reported indicators include measures of machine workload ($\bar{t}$, $var(t)$), cost performance (C, C_{std}, C_{tar}), and the aggregated objective value J. The corresponding visual comparison of representative schedules is given in Fig. 7.18, where the effect of optimisation on the cycle durations can be directly observed.

The results indicate that the offline cycle optimisation procedure consistently reduces operating costs, with improvements of 44.0% and 38.3% in the cost per unit for $R_C = 1$ and $R_C = 3$, respectively. Similarly, the values of the objective function J decrease by 20.1% and 32.6%, confirming that the optimised schedules are not only more cost-effective but also better aligned with the defined multi-objective criteria. An increase in the variance of task durations can be observed in the $R_C = 1$ scenario, which reflects a greater flexibility in the optimised schedule. In contrast, the $R_C = 3$ case exhibits a substantially reduced variance, resulting in a more uniform distribution of task times. Importantly, all scenarios satisfy the imposed process constraints, as indicated by the penalty measure $P = 0$.

Table 7.9: Comparison of results for baseline (B) and task-optimised baseline (OB) schedules scenarios

Quantity	Symbol	Unit	B RC1	B RC3	OB RC1	OB RC3
Volume deviation	V_{dev}	–	0.8592	0.8593	0.8592	0.8593
Average time	$\bar{t}$	h	5.0083	5.1958	4.8584	5.3712
Time variance	$var(t)$	h^2	0.1053	0.1053	0.2423	0.0019
Time std. dev.	devstd(t)	h	0.3245	0.3245	0.4922	0.0431
Penalty	P	–	0	0	0	0
Cost per unit	C	PLN/m^3	0.1694	0.1891	0.0948	0.1168
Cost (standard)	C_{std}	PLN	10 305	11 748	5718	7251
Cost (tariff)	C_{tar}	PLN	10 780	12 034	6031	7435
Objective function	J	–	2.8780	3.0752	2.2994	2.0709
Improvement [C]		%			44.0%	38.3%
Improvement [J]		%			20.1%	32.6%

The applied scheduling approach resulted in a significant filling of the stormwater lagoon at the end of the simulation horizon, which is reflected by the high values of V_{dev}. To reduce the lagoon filling level at the end of the horizon, an additional job was introduced into the

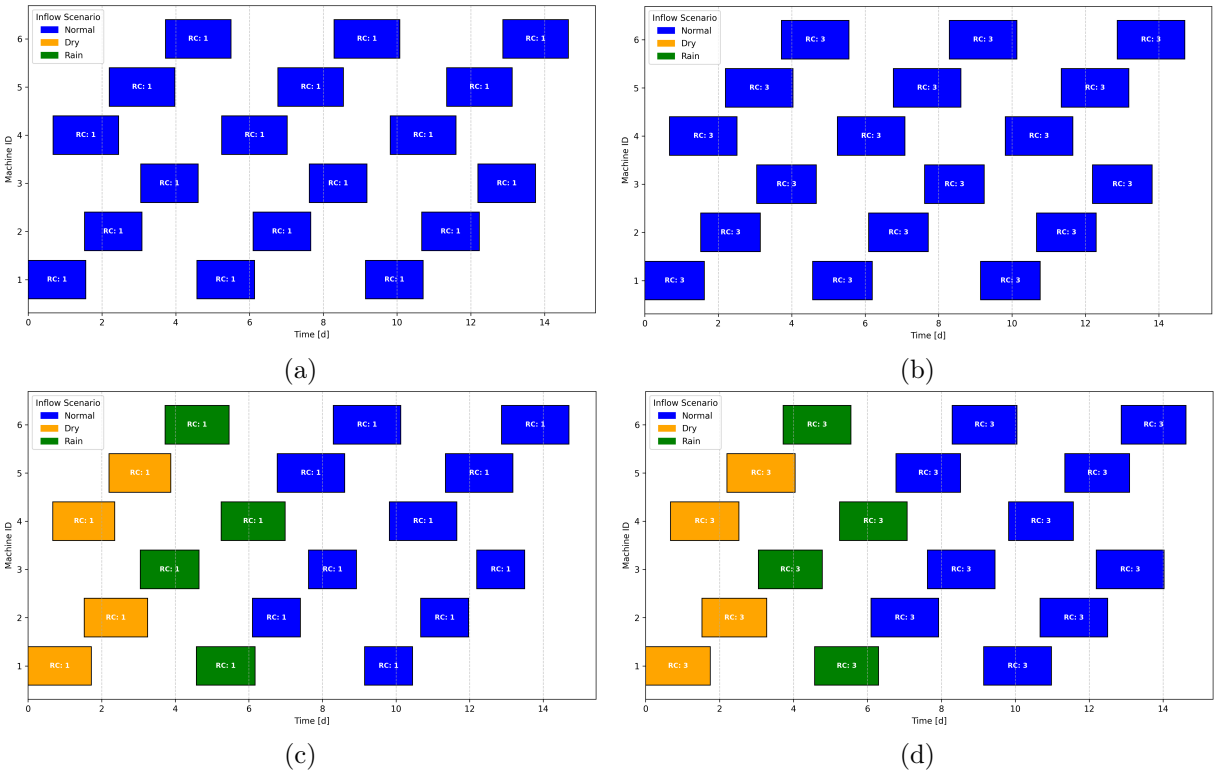

Figure 7.17: Baseline schedules: (a–b) correspond to the default job set $\mathcal{J}_{\text{base}}$, while (c–d) represent the optimised job set $\mathcal{J}$. Subfigures (a) and (c) illustrate the case $R_C = 1$, whereas (b) and (d) show $R_C = 3$

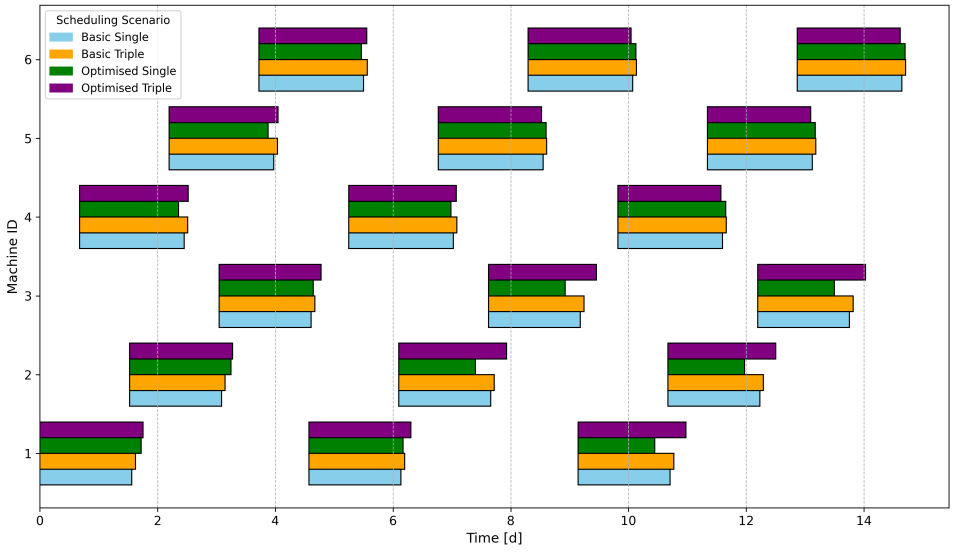

Figure 7.18: Comparison of baseline schedules

schedule. The placement of this job was arbitrarily chosen to occur after the rainfall period, using machine 5. The simulation was then repeated under the new conditions, and the results obtained are presented in Fig. 7.19 and summarised in Table 7.10.

The introduction of an additional job, whose purpose was to ensure the emptying of the stormwater lagoon at the end of the schedule, had a clear impact on the analysed indicators.

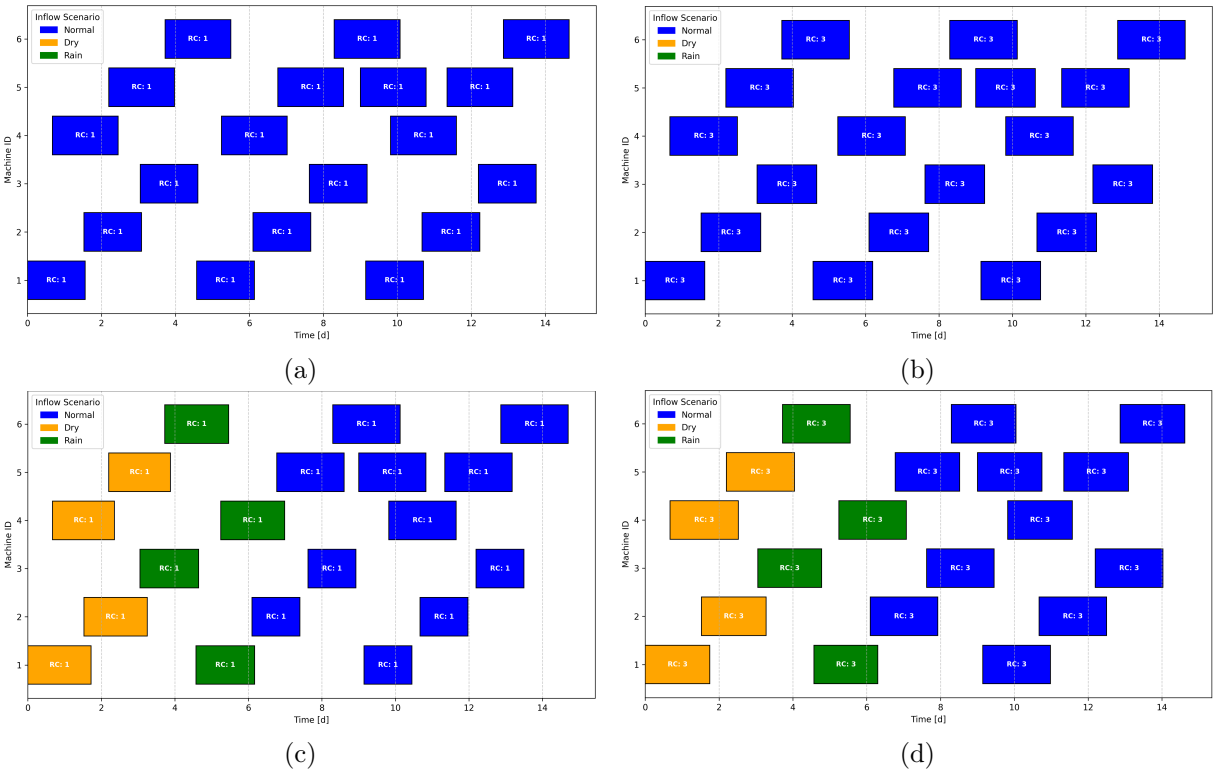

Figure 7.19: Comparison of baseline schedules with additional job: (a–b) correspond to the default job set $\mathcal{J}_{\text{base}}$, while (c–d) represent the optimised job set $\mathcal{J}$. Subfigures (a) and (c) illustrate the case $R_C = 1$, whereas (b) and (d) show $R_C = 3$

In particular, a noticeable decrease in the value of the volume deviation (V_{dev}) was observed compared to the scenarios without the lagoon (from approximately 0.86 to values in the range of 0.56–0.62). This indicates that the inclusion of the additional task improves the volume balance, allowing the system's desired final state to be more accurately represented.

At the same time, however, the cost of this improvement is clearly visible in the temporal characteristics. The time variance ($var(t)$) increased more than sevenfold in the single aeration case (from about 0.1 to 0.79–1.00) and several times in the triple aeration case (from about 0.1 to 0.70), which indicates a significant dispersion of cycle lengths between the reactors. This phenomenon directly translates into an increase in the value of the objective function J, whose components are sensitive to time heterogeneity. It is worth noting the importance of this parameter when the total number of scheduled jobs is not divisible by the number of available machines. In such a situation, if one machine is assigned one additional job compared to the others, a large imbalance occurs in the value of the objective function due to the term associated with the uniformity of machine utilisation. It should also be emphasised that the additional job had a significant impact on the total schedule cost (increase in both C_{std} and C_{tar}). However, when comparing the price relative to the amount of treated wastewater, no deterioration of economic efficiency is observed. In other words, the unit cost of treatment remained at a comparable level. At the same time, the main consequence of introducing the lagoon job is the increased time variability of cycles and the associated growth of the objective function.

Table 7.10: Comparison of results for baseline (B) and task-optimised baseline (OB) schedules with additional job to emptying lagoon

Quantity	Symbol	Unit	B RC1	B RC3	OB RC1	OB RC3
Volume deviation	V_{dev}	–	0.5587	0.6187	0.5587	0.5591
Average time	$\bar{t}$	h	5.1971	5.3486	5.1637	5.6628
Time variance	$var(t)$	h^2	0.7877	0.7037	1.0047	0.4136
Time std. dev.	devstd(t)	h	0.8875	0.8389	1.0024	0.6431
Penalty	P	–	0	0	0	0
Cost per unit	C	PLN/m^3	0.1676	0.1884	0.0942	0.1165
Cost (standard)	C_{std}	PLN	10 891	12 351	6073	7708
Cost (tariff)	C_{tar}	PLN	11 331	12 666	6369	7873
Objective function	J	–	3.1223	3.3418	2.5032	2.3669
Improvement [C]		%			43.8%	38.2%
Improvement [J]		%			19.9%	29.1%

7.4.2 Optimised Scheduling Scenarios

Subsequently, schedules were obtained through the optimisation procedure presented in Chapter 6. A population of 24 individuals was simulated over 16 generations. For the single-aeration case, the average evaluation time of one generation was 13 min 15 s, while the local search for a single individual lasted 4 min 29 s. The total simulation time was approximately 1 day and 7 hours. Simulations were performed using the first hardware configuration listed in Table 7.1.

The evolution of the fitness function across generations is presented in Fig. 7.20. Boxplots illustrate the variability within each generation, while the solid blue line indicates the best individual. The applied GA allows for sudden improvements in the best individual due to mutations and crossovers, while slight enhancements are achieved through the implemented SA-based local search and elitism. The initial average fitness value of the population is close to the baseline simulation results, which is expected due to the mechanism used to generate the initial schedules. The proposed algorithm effectively improves the objective function under the applied parameter settings.

Fig. 7.21 presents the obtained schedule. It can be observed that each large reactor is assigned three treatment cycles over the 14-day horizon, while small reactors receive four tasks on two machines and three on the remaining one. The resulting schedule assigns most of the large SBR jobs to the rainfall period, while under normal inflow conditions, mainly smaller reactors are utilised.

Fig.7.22 shows the economic analysis of the obtained schedule. The upper subplot presents the volume of treated wastewater and the electrical energy consumption for aeration. The lower subplot presents the total operational cost in PLN, considering both fixed and peak–off-peak tariffs.

The adopted optimisation approach and the proposed objective function provide very good results in terms of storage management. Figure 7.23 shows the filling levels of the two storage tanks considered in the problem. The stormwater lagoon is primarily used during rainfall events, and at the end of the horizon, the level of the retention tank is close to the initial filling of the reactor. The peak observed near the end of the 14th day is associated with the absence of

assigned jobs at the very end of the schedule.

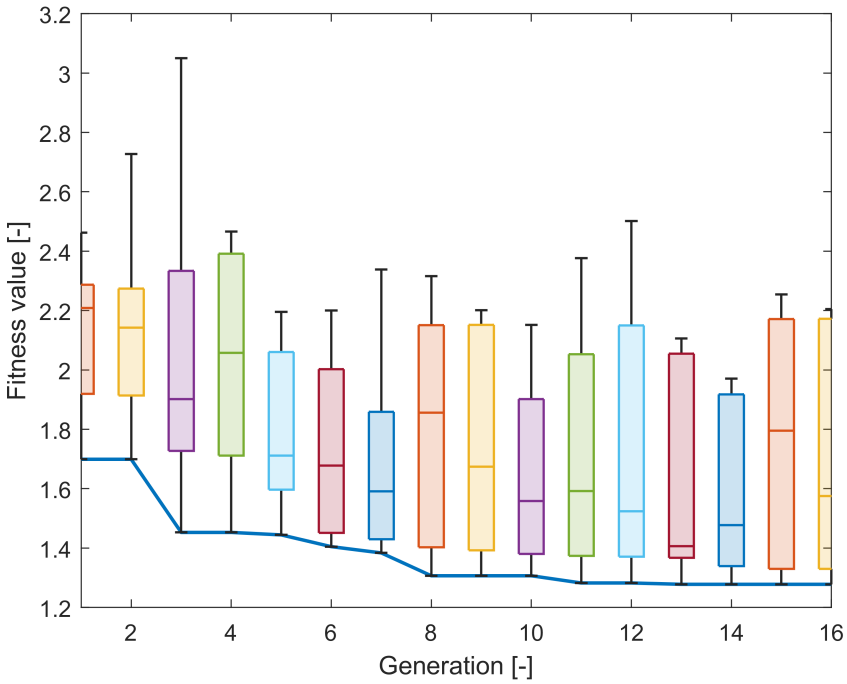

Figure 7.20: Distribution of the fitness function for $R_C = 1$

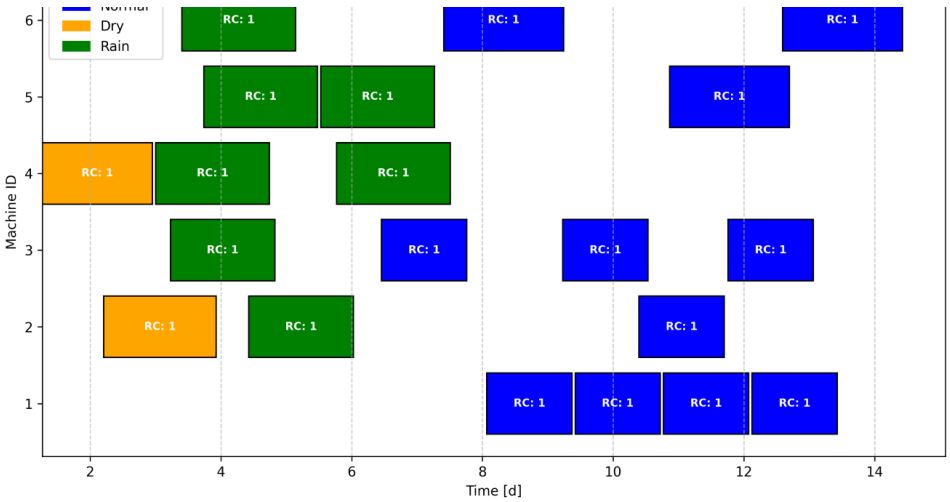

Figure 7.21: Obtained schedule for $R_C = 1$

The optimisation process for the configuration with three aeration phases ($R_C = 3$) was carried out using the same algorithmic parameters as in the single-phase case. The average evaluation time per generation was 13 min 53 s, and the local search for an individual took 4 min 38 s. In total, obtaining the 14-day schedule required approximately 1 day and 10 hours of computation.

The convergence of the optimisation process is illustrated in Fig. 7.24. The resulting schedule, presented in Fig. 7.25, reveals a more balanced distribution of jobs across the available machines. The obtained schedule features only a single operation during the period of increased loading,

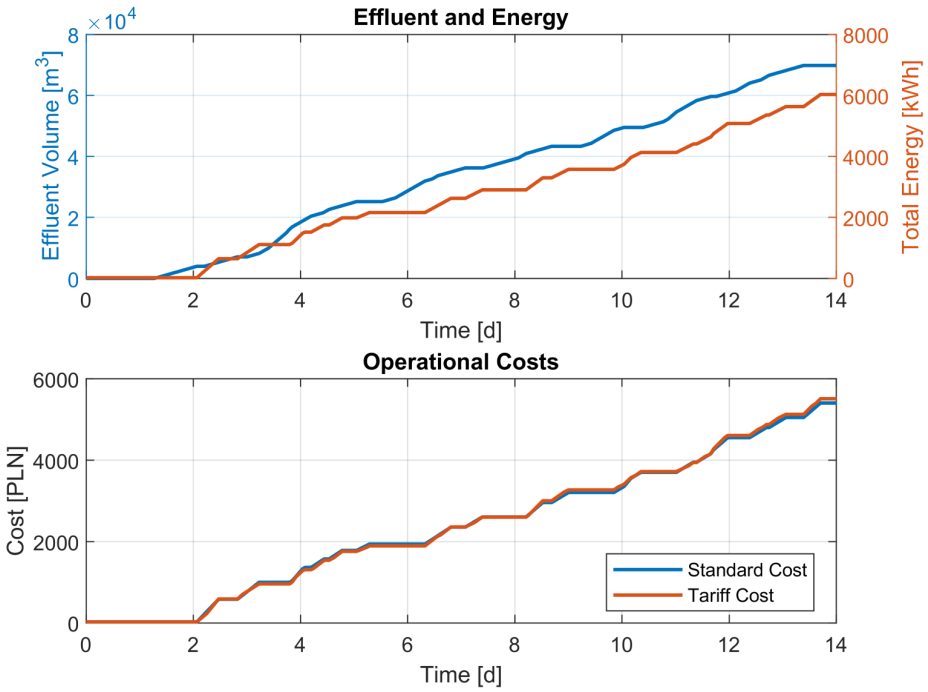

Figure 7.22: Economic analysis of the optimised schedule for $R_C = 1$: (top) treated wastewater volume and energy consumption for aeration, (bottom) operational costs with standard and peak–off-peak tariffs

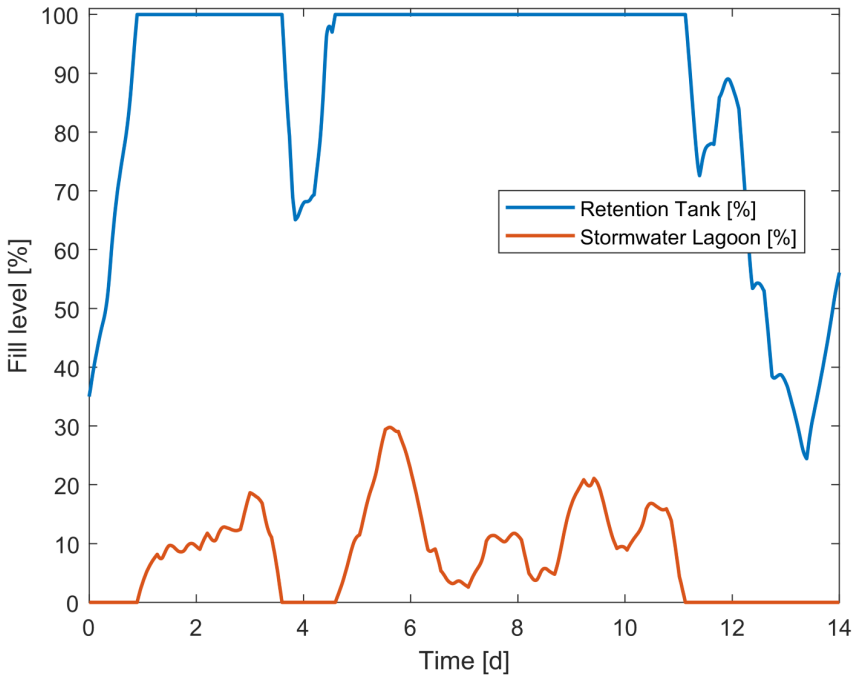

Figure 7.23: Filling levels of the retention tank and stormwater lagoon for $R_C = 1$ scenario

which could negatively affect the treatment quality in aspects not considered within the adopted approach. Subsequently, during the rainfall period, five reactors operate with similar job start times. In the first half of the schedule, significantly fewer jobs were allocated compared with the

single-aeration solution. In contrast, the second week contains a larger number of evenly distributed jobs, which results in the storage volume at the end of the simulation horizon being very close to its initial state. The economic and operational performance indicators are summarised in Fig. 7.26, while Fig. 7.27 shows the corresponding filling levels of the two storage tanks over the scheduling horizon.

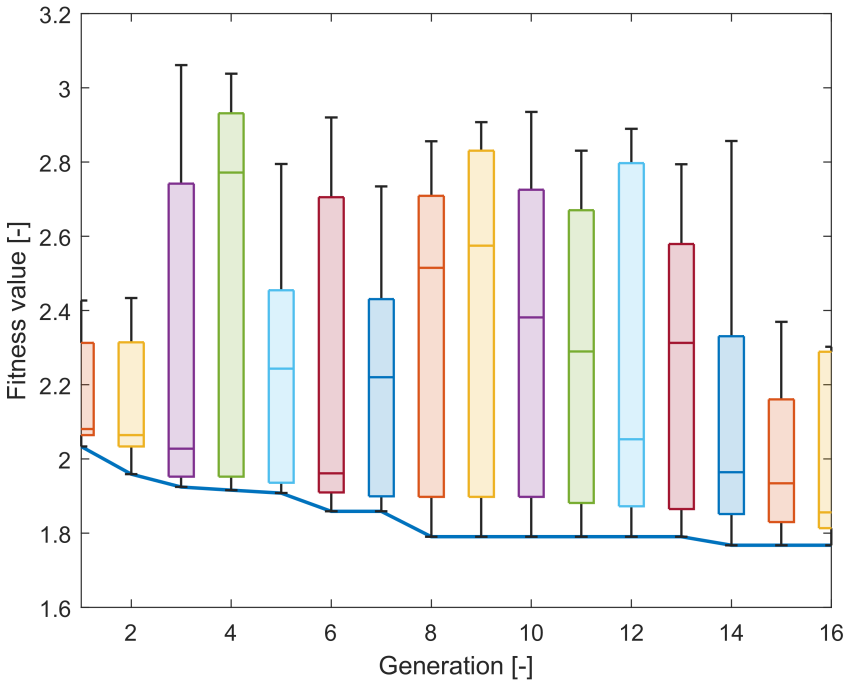

Figure 7.24: Distribution of the fitness function for $R_C = 3$

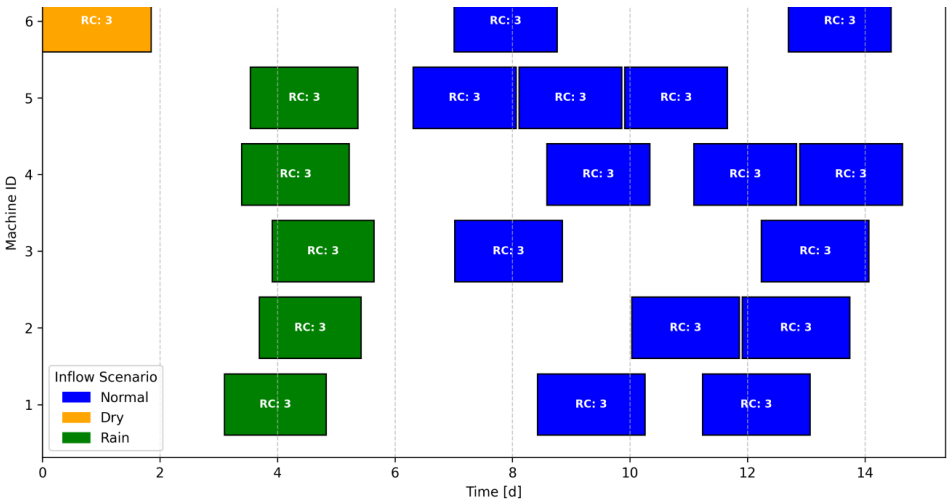

Figure 7.25: Obtained schedule for $R_C = 3$

Table 7.11 presents a summary of the obtained results for the optimised scenarios under $R_C = 1$ and $R_C = 3$, including the full calculation of energy costs for both constant and variable electricity tariffs. The results indicate that both configurations achieved satisfactory performance, maintaining zero penalty values and ensuring the fulfilment of all imposed constraints.

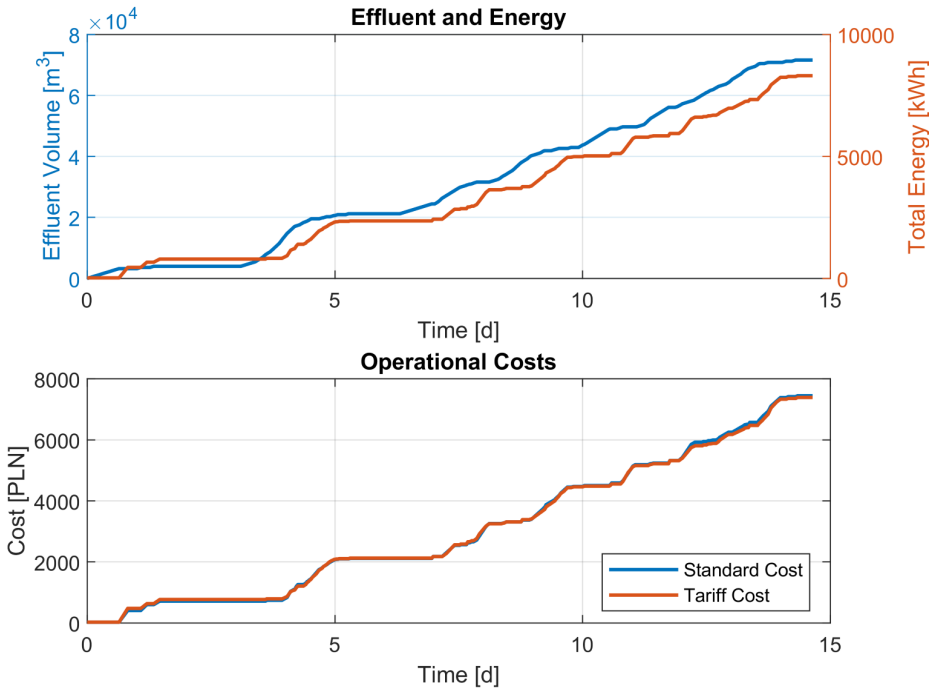

Figure 7.26: Economic analysis of the optimised schedule for $R_C = 3$: (top) treated wastewater volume and energy consumption for aeration, (bottom) operational costs with standard and peak–off-peak tariffs

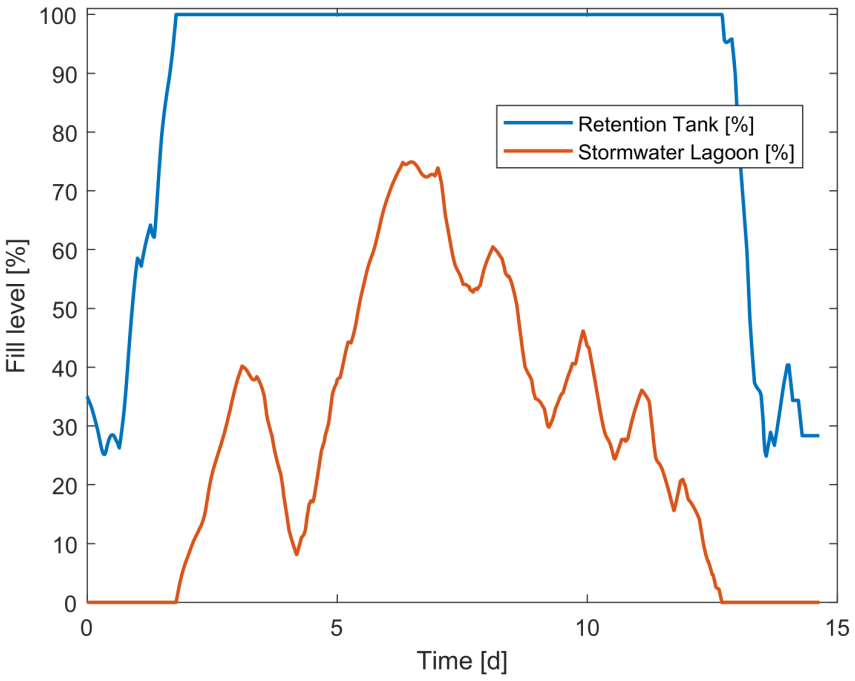

Figure 7.27: Filling levels of the retention tank and stormwater lagoon for $R_C = 3$ scenario

A clear difference can be observed in the value of the volume deviation (V_{dev}), which is close to zero for both cases, confirming the effective balancing of inflow and outflow volumes within the scheduling horizon. The three-aeration configuration ($R_C = 3$) achieved a slightly

better alignment with the desired final lagoon state, while the single-aeration variant ($R_C = 1$) demonstrated lower average machine operating time.

From an economic perspective, the total treatment cost increases with the number of aeration phases, which is consistent with the higher energy demand of more complex process sequences. Nevertheless, the unit treatment cost remains relatively low in both cases, approximately 0.079 PLN/m³ for $R_C = 1$ and 0.103 PLN/m³ for $R_C = 3$, confirming the overall energy efficiency of the proposed schedules. The objective function values (J) show an expected increase for the multi-aeration case, primarily due to its greater time dispersion, yet both configurations represent a substantial improvement compared with the baseline results presented earlier.

Table 7.11: Comparison of results for optimised scenarios

Quantity	Symbol	Unit	RC1	RC3
Volume deviation	V_{dev}	–	0.2110	-0.0665
Average time	$\bar{t}$	h	5.1303	5.9484
Time variance	$var(t)$	h^2	0.0770	0.6423
Time std. dev.	devstd(t)	h	0.2774	0.8015
Penalty	P	–	0	0
Cost per unit	C	PLN/m^3	0.0789	0.1033
Cost (standard)	C_{std}	PLN	5404.9	7444.5
Cost (tariff)	C_{tar}	PLN	5510.5	7390.7
Objective function	J	–	1.2777	1.7675

The presented results are provided in pairs corresponding to the two considered reactor cycle configurations: single and triple aeration phases ($R_C = 1$ and $R_C = 3$). This convention is maintained in the following discussion to ensure a clear comparison between the respective process configurations. The results clearly demonstrate a progressive improvement in operational performance and cost efficiency as the optimisation framework evolved from the baseline configuration to the full integration of TS and cycle optimisation. Each subsequent stage introduced an additional level of decision-making and coordination – from fixed cycle control, through cycle optimisation, to global management of multiple SBR within the defined time horizon.

The unit treatment cost decreased substantially from 0.1676 PLN/m^3 and 0.1884 PLN/m^3 in the baseline scenario to 0.0942 PLN/m^3 and 0.1165 PLN/m^3 after applying cycle optimisation. The final configuration, combining TS and cycle optimisation, achieved the lowest values of 0.0789 PLN/m^3 and 0.1033 PLN/m^3. The total operational cost, including peak and off-peak tariff rates, was reduced by nearly 50% compared with the baseline, from 11 331 and 12 666 PLN to 5510.5 and 7390.7 PLN.

The objective function values, which reflect the balance between treatment quality and operational cost, also confirm the improvement in overall system performance. Decrease of the value from 3.12 and 3.34 in the baseline configuration to 1.28 and 1.77 in the fully optimised case indicates a more favourable trade-off between process efficiency and energy expenditure.

A direct comparison between the partially optimised and fully optimised configurations reveals the additional benefit gained from incorporating TS. While cycle optimisation alone reduced unit costs by approximately 40%, the inclusion of scheduling led to a further 15–20% improvement, demonstrating that coordination of reactor operation in time is a key factor for

achieving global energy and cost efficiency. This highlights the importance of the scheduling layer as an integral part of the overall optimisation framework.

The obtained and presented results demonstrate that it is possible to efficiently and optimally manage the operation of multiple SBR over a given time horizon, while appropriately accounting for storage limitations and the availability of jobs, thereby confirming the fulfilment of the research objective O2.

7.5 Summary and Discussion

First of all, the purpose of this chapter was to illustrate the results obtained in relation to the research objectives 1 and 2, which were achieved through the implementation of RTs 1-4.

In the process control layer, the selected solution closely follows the reference trajectory while ensuring smoother control actions, reduced energy consumption, and compliance with quality standards. The proposed approach provides an alternative to commonly reported strategies in the literature, focusing on the flexibility in selecting control strategies. Then, the applied MOO methodology, based on Pareto front approximation, effectively captures the trade-off between treatment performance and operational costs in the considered application. The obtained fronts offer a technologically relevant set of solutions that can be directly applied in practice. This is particularly important when balancing TP and TN removal, as different inflow scenarios reveal distinct equilibrium points. Consequently, the results confirm that the developed optimisation tool enables the adjustment of control strategies to meet diverse quality and economic requirements under real operating conditions. The system allows the determination of both the duration of individual SBR phases and the number of aerobic and anoxic sequences.

The obtained and presented results demonstrate that it is possible to efficiently and optimally manage the operation of multiple SBR over a given time horizon, while appropriately accounting for storage limitations and the availability of jobs, thereby confirming the fulfilment of the research objective 2. A drawback of the applied approach is the tendency of the algorithm to avoid periods of increased energy demand, i.e., intervals in which *Dry*-type jobs are required. In baseline schedules, four *Dry* jobs were assigned, whereas in the optimised solutions, only two and one jobs were scheduled for single and triple aeration phases, respectively. These outcomes are related to the limitations of the adopted method and provide interesting directions for future research. It is suggested that job allocation should not be based solely on job availability windows, as in the current approach, but rather on more advanced observations of average inflows and pollutant concentrations in the storage units (retention tanks).

The lowest achieved aeration costs per m^3 of treated wastewater were 0.1807 kWh/m^3 and 0.2060 kWh/m^3 for the baseline schedules with single and triple aeration phases, respectively. For the optimised solutions, the corresponding values were 0.0864 kWh/m^3 and 0.1160 kWh/m^3. As previously noted, these results are slightly underestimated because only aeration costs were considered, although these can constitute more than 60% of the total operational costs of wastewater treatment. Nevertheless, the results are comparable with values reported in the literature. For instance, depending on the technology, plant configuration, and treated water quality, WWTP consume approximately 0.5–2.0 kWh/m^3 of treated water (Hamawand, 2023). In Polish condi-

tions, smaller plants with a capacity below 5000 m^3/d were characterised by energy efficiency in the range 0.264–1.422 kWh/m^3, with an average of 0.768 kWh/m^3, while larger systems above 5000 m^3/d showed a lower technological energy consumption range of 0.331–0.414 kWh/m^3 (Orchowski et al., 2018). Considering other European regions, the median energy consumption indicator for Italian plants, defined as the ratio of daily energy consumption to daily treated volume, is 0.45 kWh/m^3 (Vaccari et al., 2018).

The numerical results of the conducted studies confirm the effectiveness of the proposed approaches across all considered layers, from process control and process optimisation for a single reactor, to the optimisation of multiple reactors over the defined simulation horizon. The formulation and solution of the TS problem were successfully validated, demonstrating the ability of the developed system to support efficient, reliable, and economically feasible operations. Consequently, the numerical performance verification of the system under the design conditions can be considered accomplished, and the main theses put forward can be considered supported by the obtained results.

Chapter 8

Summary, Conclusions and Future Works

This dissertation has addressed the introduction of TS to water resource recovery management in a biological WWTP application, examining both the potential operational, economic and environmental benefits and the practical challenges associated with its implementation. In line with the objectives outlined in the introductory chapter, the research encompassed a broad spectrum of control engineering aspects, from process control and optimisation to the integration of scheduling mechanisms within the MES layer.

Based on the extensive literature review of the state-of-the-art scheduling applications in process industries, the gap in knowledge has been identified – namely, the lack of dedicated TS models for WRRF. To address this gap, the research thesis was formulated, asserting that the application of scheduling and optimisation methodologies can enhance the operational efficiency of wastewater treatment systems. To support this thesis, two principal research objectives, O1 and O2, were defined, followed by four detailed RTs (RT1–RT4), which were subsequently presented and discussed in Chapters 4–6. The completion of these RTs resulted in the development of a hierarchical control system comprising decomposed optimisation layers, each corresponding to different levels of decision-making, allowing for problem-specific optimisation and ensuring scalability of the proposed framework.

The fulfilment of the defined research objectives and the successful completion of the associated RTs provide support for the research thesis formulated in this dissertation. The numerical results obtained demonstrate that the integration of TS and optimisation mechanisms into the operational management of biological wastewater treatment systems enables a measurable improvement in both economic performance and operational efficiency, while maintaining compliance with treatment quality constraints. In this manner, the proposed hierarchical framework provides a theoretical contribution in addition to a decision-support structure that is applicable in practice for batch-type WRRFs.

The primary research effort was therefore concentrated on defining the object of study (a multi-SBR system) in the form of a TS problem and developing a dedicated stochastic optimisation framework to solve it. This constitutes the principal scientific contribution of this work, linking process-level optimisation with production-level scheduling in a hierarchical formulation.

Furthermore, a multi-objective approach to SBR cycle optimisation was proposed and evaluated, providing an additional dimension to process control and decision support in wastewater treatment management. The chosen stochastic approach for TS and MOO problems was determined by both the complexity of the issues and the computational complexity of the models employed.

Chapter 2 presented a detailed description of the Swarzewo WWTP, located in northern Poland, whose data served as the foundation for model development. Chapter 3 introduced the construction of layered SBR models within the MATLAB/Simulink environment. The model development was based on the ASM3 structure, extended with the BioP module and a lag-phase representation, which enabled accurate simulation of biological phosphorus removal processes. A non-linear oxygen dynamics model was also developed and later employed in the design of a predictive control strategy. A significant part of the modelling section was devoted to formulating the scheduling problem within the context of the WRRF, establishing the necessary link between the process control and operational management layers.

The subsequent part of the dissertation focused on the formulation of control and optimisation problems. Chapter 4 introduced the general architecture of the proposed system and described the exchange of information between the individual layers. The proposed decomposition of the control problem followed the hierarchical control structure commonly adopted in the literature. The following three chapters correspond to the control layers introduced in a bottom-up manner.

Process control (Section 5.1) was simplified to the task of maintaining the desired DO concentration level in the reactor during aeration phases, as this constitutes the most energy-intensive aspect of the treatment process. This task was addressed by defining a NMPC structure as part of the implementation of RT 2. Control costs, control variability, and control quality were considered in the optimisation objective function. Subsequently, the remainder of Chapter 5 concerned the search for the optimal SBR operational cycle under defined inflow conditions and was divided into two main parts. The first part (Section 5.2) dealt with the interpretation of the SBR cycle management problem using a state machine formalism. The second part (Section 5.3) introduced multi-objective optimisation approach and the decision-support procedure for selecting preferred solutions from approximated Pareto fronts. The multi-objective approach focused on objective functions related to treatment quality (mainly nitrogen and phosphorus) as well as economic factors.

The core scientific subject of the dissertation, the management of multiple reactors, was discussed in Chapter 6, which focused on the definition and solution of the scheduling problem. This chapter presented the optimisation problem formulation and the proposed approach for representing SBR cycles as jobs within the scheduling domain. It also described the author's implementation of a metaheuristic optimisation algorithm (MA) constructed by combining a modified GA with a SA local search procedure.

Numerical results obtained from the experiments verifying the operation of the designed control layers were collectively presented in Chapter 7. The results demonstrated that reactor scheduling can yield measurable economic benefits. The use of optimised operational cycles improved aeration-related costs by approximately 40%, while the inclusion of the scheduling mechanism provided an additional improvement of 15–20%. The obtained results were verified through multiple simulation scenarios representing various inflow and operational conditions,

ensuring the robustness of the proposed approach. The quality of the treatment process was assessed using standards from water law permits and restrictions adopted in BSM2 models.

The author considers the following to be the most significant achievements of this dissertation:

- the development and implementation of layered SBR models in MATLAB/Simulink environment based on the ASM3 and BioP structure, extended with a lag-phase dynamic,
- the development of a hierarchical control and optimisation framework integrating process control, MOO, and TS for biological batch-type wastewater treatment systems,
- the formulation of a novel scheduling-oriented representation of multi-reactor operation in WRRF, bridging the gap between process-level and production-level decision-making,
- the design and validation of a NMPC strategy for DO control in the aeration phase, ensuring improved control performance and energy efficiency,
- the definition and solution of a MOO problem for SBR treatment cycle optimisation, providing trade-off analysis between effluent quality and operational costs through Pareto-based decision support,
- the formulation, development and implementation of a stochastic metaheuristic algorithm (MA – a hybrid of a GA and SA), to solve the reactor scheduling problem.

The presented research constitutes an opening of this subject area, leaving numerous aspects for further investigation. Future studies may include the development of scheduling strategies based on predictive inflow models that take into account industrial discharges and meteorological conditions. A natural and complex continuation of the current work would be to incorporate inflow uncertainty and to propose a control system capable of responding dynamically to deviations from the predefined schedule.

From the implementation perspective, an important step would be the transfer of the developed models to a high-performance, low-level computing environment, enabling periodic optimisation based on weekly or seasonal inflow patterns. Another promising research direction lies in the interpretation of SBR management as a state machine problem, which could facilitate the application of algorithms derived from graph theory. Such developments would further extend the applicability of the proposed framework and move it towards real-time decision support in full-scale wastewater treatment operations.

The interpretation of the WRRF developed in this dissertation for scheduling purposes may also be extended to include additional functional aspects, such as biogas production, SBR maintenance scheduling, or other operational constraints and objectives that would enrich the formulation of the scheduling problem with further multi-criteria considerations.

In conclusion, the research presented in this dissertation has contributed to bridging the gap between process control and optimisation of a single reactor with the management of multiple SBRs in water resource recovery systems. The integration of a hierarchical structure that combines TS with optimisation-based control has yielded novel insights into the operational dynamics of WWTP. The proposed methods and models provide a basis for the further development of intelligent decision support and effective resource management. The findings substantiate the considerable potential of TS techniques in the domain of biological wastewater treatment, providing a promising direction for future research and practical implementation in WRRF systems.

Bibliography

Aerzen USA Corporation (2025). Aerzen Turbo Blowers. https://catalog.aerzen.com/viewitems/blowers-compressors-spare-parts/turbo-blowers. [accessed December 12, 2025].

Afzalan, E. and Joorabian, M. (2013). Emission, reserve and economic load dispatch problem with non-smooth and non-convex cost functions using epsilon-multi-objective genetic algorithm variable. *International Journal of Electrical Power & Energy Systems*, 52:55–67.

Akça, L., Kinaci, C., and Karpuzcu, M. (1993). A model for optimum design of activated sludge plants. *Water Research*, 27(9):1461–1468.

Alex, J. (2011). A simple three-layer clarifier model. In *Proceedings of the 8th IWA Symposium on Systems Analysis and Integrated Assessment, June 20-22, San Sebastian, Spain*. Watermatex.

Alex, J., Holm, N. C., and Rönner-Holm, S. G. (2009). Lag phase, dynamic alpha factor and ammonium adsorption behaviour: Introduction of special activated sludge characteristics in the ASM3+ EAWAG-BioP-model. *Water Science and Technology*, 59(1):133–140.

Alex, J., Rönner-Holm, S. G., Hunze, M., and Holm, N. C. (2011). A combined hydraulic and biological SBR model. *Water Science and Technology*, 64(5):1025–1031.

Alex, J., Tschepetzki, R., and Jumar, U. (2002). Predictive control of nitrogen removal in WWTPs using parsimonious models. *IFAC Proceedings Volumes*, 35(1):405–410.

Ali, S. I., Moustafa, M. H., Nwery, M. S., Farahat, N. S., and Samhan, F. (2022). Evaluating the performance of sequential batch reactor (SBR & ASBR) wastewater treatment plants, case study. *Environmental Nanotechnology, Monitoring & Management*, 18:100745.

Arica, E. and Powell, D. J. (2017). Status and future of manufacturing execution systems. In *Proceedings of the 2017 IEEE International Conference on Industrial Engineering and Engineering Management (IEEM)*, pages 2000–2004. IEEE.

Bakiri, Z., Chebli, D., and Nacef, S. (2012). Dynamic modelling of the secondary settler of a wastewater treatment via activated sludge to low-load. *Energy Procedia*, 18:1–9.

Banach, M., Kolankowski, M., Piotrowski, R., and Ujazdowski, T. (2023). Employment of a nonlinear adaptive control system for improved control of dissolved oxygen in sequencing batch reactor. In *Proceedings of the XXI Polish Control CXXI Polish Control Conferenceconference, Gliwice, Poland*, pages 155–164. Springer.

Belotti, P., Kirches, C., Leyffer, S., Linderoth, J., Luedtke, J., and Mahajan, A. (2013). Mixed-integer nonlinear optimization. *Acta Numerica*, 22:1–131.

Beraud, B., Lemoine, C., and Steyer, J.-P. (2009). Multiobjective genetic algorithms for the optimisation of wastewater treatment processes. In *Computational Intelligence Techniques for Bioprocess Modelling, Supervision and Control*, pages 163–195. Springer.

Boruah, N. and Roy, B. K. (2019). Event triggered nonlinear model predictive control for a wastewater treatment plant. *Journal of Water Process Engineering*, 32:100887.

Brdys, M., Grochowski, M., Gminski, T., Konarczak, K., and Drewa, M. (2008). Hierarchical predictive control of integrated wastewater treatment systems. *Control Engineering Practice*, 16(6):751–767.

Chen, K., Wang, H., Valverde-Pérez, B., Zhai, S., Vezzaro, L., and Wang, A. (2021). Optimal control towards sustainable wastewater treatment plants based on multi-agent reinforcement learning. *Chemosphere*, 279:130498.

Chen, T., Zhang, B., Hao, X., and Dai, Y. (2006). Task scheduling in grid based on particle swarm optimization. In *Proceedings of the 2006 Fifth International Symposium on Parallel and Distributed Computing*, pages 238–245. IEEE.

Cheng, X., Guo, Z., Shen, Y., Yu, K., and Gao, X. (2023). Knowledge and data-driven hybrid system for modeling fuzzy wastewater treatment process. *Neural Computing and Applications*, 35:7185–7206.

Ching, P. M., So, R. H., and Morck, T. (2021). Advances in soft sensors for wastewater treatment plants: A systematic review. *Journal of Water Process Engineering*, 44:102367.

Chitra, M., Pappa, N., and Abraham, A. (2018). Dissolved oxygen control of batch bioreactor using model reference adaptive control scheme. *IFAC-PapersOnLine*, 51(4):13–18.

Coats, E. R. and Wilson, P. I. (2017). Toward nucleating the concept of the water resource recovery facility (WRRF): perspective from the principal actors. *Environmental Science & Technology*, 51(8):4158–4164.

Cornejo, P. K., Becker, J., Pagilla, K., Mo, W., Zhang, Q., Mihelcic, J. R., Chandran, K., Sturm, B., Yeh, D., and Rosso, D. (2019). Sustainability metrics for assessing water resource recovery facilities of the future. *Water Environment Research*, 91(1):45–53.

Costa, A. L., de Medeiros, J. L., and Pessoa, F. L. (2001). Global optimization of water distribution networks through a reduced space branch-and-bound search. *Water Resources Research*, 37(4):1083–1090.

Costa, L., Santo, I. A. E., and Fernandes, E. M. (2011). Using a genetic algorithm to solve a bi-objective WWTP process optimization. In *Operations Research Proceedings 2010: Selected Papers of the Annual International Conference of the German Operations Research Society*, pages 359–364. Springer, Berlin, Heidelberg.

Cristea, V. M., Pop, C., and Agachi, P. S. (2008). Model Predictive Control of the waste water treatment plant based on the Benchmark Simulation Model No.1-BSM1. *Computer Aided Chemical Engineering*, 25:441–446.

Cupek, R., Ziebinski, A., Huczala, L., and Erdogan, H. (2016). Agent-based manufacturing execution systems for short-series production scheduling. *Computers in Industry*, 82:245–258.

Czyżniewski, M., Łangowski, R., and Piotrowski, R. (2023). Respiration rate estimation using non-linear observers in application to wastewater treatment plant. *Journal of Process Control*, 124:70–82.

Daigger, G. T. (1995). Development of refined clarifier operating diagrams using an updated settling characteristics database. *Water Environment Research*, 67(1):95–100.

Daigger, G. T. and Roper, R. E. (1985). The relationship between SVI and activated sludge settling characteristics. *Journal of the Water Pollution Control Federation*, 57(8):859–866.

Dionisi, D. (2017). *Biological wastewater treatment processes: mass and heat balances*. CRC press.

Directive, E. (1991). Council Directive of 21. May 1991 concerning urban waste water treatment (91/271/EEC). *European Journal of Communication*, 34:40.

Du, S., Yan, Q., and Qiao, J. (2020). Event-triggered PID control for wastewater treatment plants. *Journal of Water Process Engineering*, 38:101659.

Durasević, M. and Jakobović, D. (2023). Heuristic and metaheuristic methods for the parallel unrelated machines scheduling problem: a survey. *Artificial Intelligence Review*, 56(4):3181–3289.

Dutta, A. and Sarkar, S. (2015). Sequencing batch reactor for wastewater treatment: recent advances. *Current Pollution Reports*, 1:177–190.

Egea, J. A. and Gracia, I. (2012). Dynamic multiobjective global optimization of a waste water treatment plant for nitrogen removal. *IFAC Proceedings Volumes*, 45(2):374–379.

Ekama, G. A., Barnard, J. L., and Günthert, F. W. (1997). *Secondary settling tanks: theory, modelling, design and operation*. Scientific and Technical Report Series.

Fan, L. and Boshnakov, K. (2010). Fuzzy logic based dissolved oxygen control for SBR wastewater treatment process. In *Proceedings of the 8th World Congress on Intelligent Control and Automation*, pages 4142–4146. IEEE.

Fan, L. and Xie, Y. (2011). Optimization control of SBR wastewater treatment process based on pattern recognition. *Procedia Environmental Sciences*, 10:20–25.

Francisco, M., Skogestad, S., and Vega, P. (2015). Model predictive control for the self-optimized operation in wastewater treatment plants: Analysis of dynamic issues. *Computers & Chemical Engineering*, 82:259–272.

Francisco, M., Vega, P., and Revollar, S. (2011). Model predictive control of BSM1 benchmark of wastewater treatment process: A tuning procedure. In *Proceedings of the IEEE Conference on Decision and Control*, pages 7057–7062. IEEE.

Gernaey, K. V. and Jeppsson, U. (2014). *Benchmarking of control strategies for wastewater treatment plants*. IWA publishing.

Gernaey, K. V., Van Loosdrecht, M. C., Henze, M., Lind, M., and Jørgensen, S. B. (2004). Activated sludge wastewater treatment plant modelling and simulation: state of the art. *Environmental Modelling & Software*, 19(9):763–783.

Grabowski, J. and Pempera, J. (2000). Sequencing of jobs in some production system. *European Journal of Operational Research*, 125(3):535–550.

Graham, R. L. (1966). Bounds for certain multiprocessing anomalies. *Bell System Technical Journal*, 45(9):1563–1581.

Graham, R. L., Lawler, E. L., Lenstra, J. K., and Kan, A. R. (1979). Optimization and approximation in deterministic sequencing and scheduling: a survey. *Annals of Discrete Mathematics*, 5:287–326.

Guerrero, J., Guisasola, A., Comas, J., Rodríguez-Roda, I., and Baeza, J. (2012). Multi-criteria selection of optimum WWTP control setpoints based on microbiology-related failures, effluent quality and operating costs. *Chemical Engineering Journal*, 188:23–29.

Gujer, W., Henze, M., Mino, T., and Van Loosdrecht, M. (1999). Activated sludge model No. 3. *Water Science and Technology*, 39(1):183–193.

Gujer, W. and Larsen, T. A. (1995). The implementation of biokinetics and conservation principles in ASIM. *Water Science and Technology*, 31(2):257–266.

Haimi, H., Mulas, M., Corona, F., and Vahala, R. (2013). Data-derived soft-sensors for biological wastewater treatment plants: An overview. *Environmental Modelling & Software*, 47:88–107.

Hamawand, I. (2023). Energy consumption in water/wastewater treatment industry—optimisation potentials. *Energies*, 16(5):2433.

Han, H. and Qiao, J. (2014). Nonlinear model-predictive control for industrial processes: An application to wastewater treatment process. *IEEE Transactions on Industrial Electronics*, 61(4):1970–1982.

Han, H. G., Wang, C. Y., Sun, H. Y., and Qiao, J. F. (2022). Data-based robust model predictive control for wastewater treatment process. *Journal of Process Control*, 118:115–125.

Hansen, L. D., Veng, M., and Durdevic, P. (2021). Compressor scheduling and pressure control for an alternating aeration activated sludge process—a simulation study validated on plant data. *Water*, 13(8):1037.

Harja, G., Vlad, G., and Nascu, I. (2016). MPC advanced control of dissolved oxygen in an activated sludge wastewater treatment plant. In *Proceeding of the 20th IEEE International Conference on Automation, Quality and Testing, Robotics*. IEEE.

Hauduc, H., Rieger, L., Oehmen, A., Van Loosdrecht, M., Comeau, Y., Héduit, A., Vanrolleghem, P., and Gillot, S. (2013). Critical review of activated sludge modeling: state of process knowledge, modeling concepts, and limitations. *Biotechnology and Bioengineering*, 110(1):24–46.

Hedayati Moghaddam, A. and Sargolzaei, J. (2015). Application of a new type of dispersed particles-stabilized biomass in aerobic sequencing batch reactor (SBR) for treating starchy wastewater. *Journal of Dispersion Science and Technology*, 36(4):563–568.

Henze, M., Grady Jr, L., Gujer, W., Marais, G., and Matsuo, T. (1987). Activated Sludge Model No. 1. *International Association on Water Pollution Research and Control Scientific and Technical Reports*.

Henze, M., Gujer, W., Mino, T., Matsuo, T., Wentzel, M. C., Marais, G. v. R., and Van Loosdrecht, M. C. (1999). Activated sludge model No. 2d, ASM2d. *Water Science and Technology*, 39(1):165–182.

Hreiz, R., Roche, N., Benyahia, B., and Latifi, M. (2015). Multi-objective optimal control of small-size wastewater treatment plants. *Chemical Engineering Research and Design*, 102:345–353.

ifak - Institut für Automation und Kommunikation e. V. (2024). SIMBA#: Modelling and simulation software. https://www.ifak.eu/en/produkte/simba, Accessed: 2024-11-22.

ifak system GmbH (2001). Simba 4.0 simulation of biological wastewater treatment.

Iqbal, J. and Guria, C. (2009). Optimization of an operating domestic wastewater treatment plant using elitist non-dominated sorting genetic algorithm. *Chemical Engineering Research and Design*, 87(11):1481–1496.

Javed, S. A., Gunasekaran, A., and Mahmoudi, A. (2022). DGRA: Multi-sourcing and supplier classification through dynamic grey relational analysis method. *Computers & Industrial Engineering*, 173:108674.

Jiang, L.-M., Zhang, W., Li, Y., Shao, Y., Zhang, Z., Zhang, M., He, J., Qiu, J., Li, W., Wang, J., et al. (2023). Applying mass flow analysis and aeration optimization strategy to reduce energy consumption of a full-scale anaerobic/anoxic/oxic system. *Journal of Water Process Engineering*, 54:104037.

Jouglet, A., Oğuz, C., and Sevaux, M. (2009). Hybrid flow-shop: a memetic algorithm using constraint-based scheduling for efficient search. *Journal of Mathematical Modelling and Algorithms*, 8:271–292.

Julong, D. et al. (1989). Introduction to grey system theory. *The Journal of Grey System*, 1(1):1–24.

Kandare, G. and Reviriego, A. N. (2011). Adaptive predictive expert control of dissolved oxygen concentration in a wastewater treatment plant. *Water Science and Technology*, 64(5):1130–1136.

Kashani, M. H. and Jahanshahi, M. (2009). Using simulated annealing for task scheduling in distributed systems. In *Proceedings of the 2009 International conference on computational intelligence, modelling and simulation*, pages 265–269. IEEE.

Katoch, S., Chauhan, S. S., and Kumar, V. (2021). A review on genetic algorithm: past, present, and future. *Multimedia Tools and Applications*, 80:8091–8126.

Kawail, F., Nakazawa, C., Fukuyama, Y., and Ueno, T. (2006). An aeration control for advanced wastewater treatment processes. In *Proceedings of the 2006 SICE-ICASE International Joint Conference*, pages 4078–4082.

Keller, J., Watts, S., Battye-Smith, W., and Chong, R. (2001). Full-scale demonstration of biological nutrient removal in a single tank SBR process. *Water Science and Technology*, 43(3):355–362.

Keshanchi, B. and Navimipour, N. J. (2016). Priority-based task scheduling in the cloud systems using a memetic algorithm. *Journal of Circuits, Systems and Computers*, 25(10):1650119.

Klawikowska, Z. and Grochowski, M. (2024). Optimizing control of wastewater treatment plant with reinforcement learning: Technical evaluation of twin-delayed deep deterministic policy gradient agent. *IEEE Access*, 12:130318–130333.

Kolankowski, M., Banach, M., Piotrowski, R., and Ujazdowski, T. (2023). A new approach to designing control of dissolved oxygen and aeration system in sequencing batch reactor by applied backstepping control algorithm. *Acta Mechanica et Automatica*, 17(4):605–612.

Krawczyk, W., Piotrowski, R., Brdys, M. A., and Chotkowski, W. (2007). Modelling and identification of aeration systems for model predictive control of dissolved oxygen – Swarzewo wastewater treatment plant case study. *IFAC Proceedings Volumes*, 40(4):43–48.

Krener, A. J. (2018). Adaptive horizon model predictive control. *IFAC-PapersOnLine*, 51(13):31–36.

Kuba, T., Van Loosdrecht, M., and Heijnen, J. (1997). Biological dephosphatation by activated sludge under denitrifying conditions ph influence and occurrence of denitrifying dephosphatation in a full-scale waste water treatment plant. *Water Science and Technology*, 36(12):75–82.

Lee, B. X., Kjaerulf, F., Turner, S., Cohen, L., Donnelly, P. D., Muggah, R., Davis, R., Realini, A., Kieselbach, B., MacGregor, L. S., et al. (2016). Transforming our world: implementing the 2030 agenda through sustainable development goal indicators. *Journal of Public Health Policy*, 37:13–31.

Leung, J. Y. (2004). *Handbook of scheduling: algorithms, models, and performance analysis*. Chapman and Hall/CRC.

Li, F., Su, Z., and Wang, G. M. (2021). An effective integrated control with intelligent optimization for wastewater treatment process. *Journal of Industrial Information Integration*, 24:100237.

Li, J.-q. and Han, Y.-q. (2020). A hybrid multi-objective artificial bee colony algorithm for flexible task scheduling problems in cloud computing system. *Cluster Computing*, 23:2483–2499.

Li, J.-W. and Qu, C.-W. (2016). Cloud computing task scheduling based on cultural genetic algorithm. *MATEC Web of Conferences*, 40:09008.

Li, W.-W., Yu, H.-Q., and Rittmann, B. E. (2015). Chemistry: Reuse water pollutants. *Nature*, 528(7580):29–31.

Liu, X. and Yu, W. (2017). Research of dissolved oxygen concentration control strategy based on the fuzzy self-tuning PID parameter. In *Proceedings of the 2017 29th Chinese Control And Decision Conference (CCDC)*, pages 5928–5932. IEEE.

Liwarska-Bizukojć, E. (2014). *Modelowanie procesów oczyszczania ścieków metodą osadu czynnego (in Polish)*. Seidel-Przywecki.

Ma, A., Liu, K., Zhang, Q., Liu, T., and Xia, Y. (2020). Event-triggered distributed MPC with variable prediction horizon. *IEEE Transactions on Automatic Control*, 66(10):4873–4880.

Mamandipoor, B., Majd, M., Sheikhalishahi, S., Modena, C., and Osmani, V. (2020). Monitoring and detecting faults in wastewater treatment plants using deep learning. *Environmental Monitoring and Assessment*, 192(2):148.

Mang, N. Z. L., Hwang, Y., and Lee, T.-J. (2022). Optimization of the step feeding ratio for nitrogen removal by SBR using technique for order preference by similarity to ideal solution (TOPSIS). *Environmental Engineering Research*, 27(3):200685.

Martínez-Iranzo, M., Herrero, J. M., Sanchis, J., Blasco, X., and García-Nieto, S. (2009). Applied pareto multi-objective optimization by stochastic solvers. *Engineering applications of artificial intelligence*, 22(3):455–465.

Masoudi, S. M. A., Hedayati Moghaddam, A., Sargolzaei, J., Darroudi, A., and Zeynali, V. (2018). Investigation and optimization of the SND–SBR system for organic matter and ammonium nitrogen removal using the central composite design. *Environmental Progress & Sustainable Energy*, 37(5):1638–1646.

Monday, C., Zaghloul, M. S., Krishnamurthy, D., and Achari, G. (2025). Incremental machine learning and genetic algorithm for optimization and dynamic aeration control in wastewater treatment plants. *Journal of Water Process Engineering*, 69:106600.

Mousavi, S. A. and Khodadoost, F. (2019). Effects of detergents on natural ecosystems and wastewater treatment processes: a review. *Environmental Science and Pollution Research*, 26:26439–26448.

Olsson, G. and Newell, B. (2005). *Wastewater Treatment Systems: Modelling, Diagnosis and Control*. Water Intelligence Online, IWA Publishing.

Orchowski, M., Masłoń, A., and Heidrich, Z. (2018). Energochłonność oczyszczalni ścieków w Sandomierzu (in Polish). *Gaz, Woda i Technika Sanitarna*, 2:68–73.

Ozinsky, A. E. and Ekama, G. A. (1995). Secondary settling tank modelling and design part 2: Linkage sludge settleability measures. *Water SA*, 21(4):333–349.

Palma-Flores, O. and Ricardez-Sandoval, L. A. (2022). Simultaneous design and nonlinear model predictive control under uncertainty: A back-off approach. *Journal of Process Control*, 110:45–58.

Pecháč, P. and Saga, M. (2016). Controlling of local search methods' parameters in memetic algorithms using the principles of simulated annealing. *Procedia Engineering*, 136:70–76.

Piotrowski, R., Brdys, M., Konarczak, K., Duzinkiewicz, K., and Chotkowski, W. (2008). Hierarchical dissolved oxygen control for activated sludge processes. *Control Engineering Practice*, 16(1):114–131.

Piotrowski, R., Brdys, M., and Miotke, D. (2010). Centralized dissolved oxygen tracking at wastewater treatment plant: Nowy Dwor Gdanski case study. *IFAC Proceedings Volumes*, 43(8):292–297.

Piotrowski, R., Hirsch, P., and Lorenc, J. (2018). Comparison of algorithms for hybrid nonlinear optimization problem in biological wastewater treatment plant. In *Proceedings of the 2018 International Interdisciplinary PhD Workshop (IIPhDW)*, pages 45–50. IEEE.

Piotrowski, R. and Ujazdowski, T. (2020). Model of aeration system at biological wastewater treatment plant for control design purposes. In *Advanced, Contemporary Control: Proceedings of KKA 2020—The 20th Polish Control Conference, Łódź, Poland, 2020*, pages 349–359. Springer, Cham.

Popp, D. (2024). New EU rules to improve urban wastewater treatment and reuse. *European Parliament: Strasbourg, France*.

Preisner, M., Neverova-Dziopak, E., and Kowalewski, Z. (2020). An analytical review of different approaches to wastewater discharge standards with particular emphasis on nutrients. *Environmental Management*, 66(4):694–708.

Puig, S., Corominas, L., Traore, A., Colomer, J., Balaguer, M., and Colprim, J. (2006). An on-line optimisation of a SBR cycle for carbon and nitrogen removal based on on-line ph and our: the role of dissolved oxygen control. *Water Science and Technology*, 53(4-5):171–178.

Qambar, A. S. and Al Khalidy, M. M. (2022). Optimizing dissolved oxygen requirement and energy consumption in wastewater treatment plant aeration tanks using machine learning. *Journal of Water Process Engineering*, 50:103237.

Quevauviller, P., Thomas, O., and Beken, A. V. D. (2007). *Wastewater Quality Monitoring and Treatment*. John Wiley & Sons, Ltd.

Ratkevičius, D., Ratkevičius, Č., and Skyrius, R. (2012). ERP selection criteria: theoretical and practical views. *Ekonomika*, 91(2):97–116.

Richalet, J., Rault, A., Testud, J. L., and Papon, J. (1978). Model predictive heuristic control: Applications to industrial processes. *Automatica*, 14(5):413–428.

Rieger, L., Koch, G., Kuhni, M., Gujer, W., and Siegrist, H. (2001). The eawag bio-p module for activated sludge model no. 3. *Water Research*, 35(16):3887–3903.

Rudek, R. (2024). A neighborhood search relaxation towards railway maintenance optimization. In *2024 28th International Conference on Methods and Models in Automation and Robotics (MMAR)*, pages 405–410. IEEE.

Rönner-Holm, S. G., Mennerich, A., and Holm, N. C. (2006). Specific SBR population behaviour as revealed by comparative dynamic simulation analysis of three full-scale municipal SBR wastewater treatment plants. *Water Science and Technology*, 54(1):71–80.

San Martín, J. A. D., Bournazou, M. N. C., Neubauer, P., and Barz, T. (2014). Mixed integer optimal control of an intermittently aerated sequencing batch reactor for wastewater treatment. *Computers & Chemical Engineering*, 71:298–306.

Scholten, B. (2007). *The road to integration: A guide to applying the ISA-95 standard in manufacturing*. International Society of Automation.

Sekulski, Z. (2012). *Wybrane problemy optymalizacji wielokryterialnej we wstępnym projektowaniu konstrukcji kadłuba statków morskich (in Polish)*. Wydawnictwo Uczelniane Zachodniopomorskiego Uniwersytetu Technologicznego.

Setty, K., Jiménez, A., Willetts, J., Leifels, M., and Bartram, J. (2020). Global water, sanitation and hygiene research priorities and learning challenges under sustainable development goal 6. *Development Policy Review*, 38(1):64–84.

Shen, W., Chen, X., Pons, M. N., and Corriou, J. P. (2009). Model predictive control for wastewater treatment process with feedforward compensation. *Chemical Engineering Journal*, 155(1-2):161–174.

Shojaeinasab, A., Charter, T., Jalayer, M., Khadivi, M., Ogunfowora, O., Raiyani, N., Yaghoubi, M., and Najjaran, H. (2022). Intelligent manufacturing execution systems: A systematic review. *Journal of Manufacturing Systems*, 62:503–522.

Silverstein, J. and Schroeder, E. (1983). Performance of SBR activated sludge processes with nitrification/denitrification. *Water Pollution Control Federation*, 55(4):377–384.

Simon, J., Wiese, J., and Steinmetz, H. (2006). A comparison of continuous flow and sequencing batch reactor plants concerning integrated operation of sewer systems and wastewater treatment plants. *Water Science and Technology*, 54(11):241–248.

Simon-Várhelyi, M., Cristea, V. M., and Luca, A. V. (2020). Reducing energy costs of the wastewater treatment plant by improved scheduling of the periodic influent load. *Journal of Rnvironmental Management*, 262:110294.

Spanjers, H. and Vanrolleghem, P. (1995). Respirometry as a tool for rapid characterization of wastewater and activated sludge. *Water Science and Technology*, 31(2):105–114.

Spółka Wodno-Ściekowa "SWARZEWO" (2025). About the Company - Spółka Wodno-Ściekowa "SWARZEWO" (in Polish). https://www.sws-swarzewo.pl/. [accessed December 12, 2025].

Stare, A., Hvala, N., and Vrečko, D. (2006). Modeling, identification, and validation of models for predictive ammonia control in a wastewater treatment plant—a case study. *ISA Transactions*, 45(2):159–174.

Stebel, K., Pospiech, J., Nocon, W., Czeczot, J., and Skupin, P. (2021). Boundary-based predictive controller and its application to control of dissolved oxygen concentration in activated sludge bioreactor. *IEEE Transactions on Industrial Electronics*, 69(10):10541–10551.

Stentoft, P. A., Munk-Nielsen, T., Møller, J. K., Madsen, H., Valverde-Pérez, B., Mikkelsen, P. S., and Vezzaro, L. (2021). Prioritize effluent quality, operational costs or global warming? – Using predictive control of wastewater aeration for flexible management of objectives in WRRFs. *Water Research*, 196:116960.

Takacs, I., Patryioand, G., and Nolasco, D. (1991). A dynamic model of the clarification-thickening process. *Water Research*, 25(10):1263–1271.

Tatjewski, P. (2007). Model-based predictive control. In *Advanced Control of Industrial Processes: Structures and Algorithms*, Advances in Industrial Control, pages 107–271. Springer.

Thangavel, S., Subramanian, S., and Engell, S. (2019). Robust NMPC using a model-error model with additive bounds to handle structural plant-model mismatch. *IFAC-PapersOnLine*, 52(1):592–597.

Therrien, J.-D., Nicolaï, N., and Vanrolleghem, P. A. (2020). A critical review of the data pipeline: how wastewater system operation flows from data to intelligence. *Water Science and Technology*, 82(12):2613–2634.

Torfs, E., Nicolaï, N., Daneshgar, S., Copp, J. B., Haimi, H., Ikumi, D., Johnson, B., Plosz, B. B., Snowling, S., Townley, L. R., et al. (2022). The transition of wrrf models to digital twin applications. *Water Science and Technology*, 85(10):2840–2853.

Trelles, I. J., Mahamud, M. M., Lavín, A. G., and Díaz, M. (2017). Sludge settling prediction in sequencing batch reactor plants. *Journal of Cleaner Production*, 152:115–124.

Turmel, V. J., Williams, D., and Jones, K. O. (1997). Dissolved oxygen control strategies in an activated sludge process. *IFAC Proceedings Volumes*, 30(6):1569–1573.

Ujazdowski, T. and Piotrowski, R. (2022a). Development of a decision model for solving the task scheduling of multiple sequential batch reactors. In *Proceedings of the 26th International Conference on Methods and Models in Automation and Robotics (MMAR)*, pages 59–63. IEEE.

Ujazdowski, T. and Piotrowski, R. (2022b). Task scheduling–review of algorithms and analysis of potential use in a biological wastewater treatment plant. *IEEE Access*, 10:45230–45240.

Ujazdowski, T. and Piotrowski, R. (2024). Optimising sequencing batch reactor operation cycle planning using evolutionary algorithm. In *Proceedings of 28th International Conference on Methods and Models in Automation and Robotics (MMAR)*, pages 41–46. IEEE.

Ujazdowski, T., Piotrowski, R., and Banach, M. (2024). A stochastic approach for the solution of single and multi-objective optimisation problems of biological processes in sequencing batch reactor. *Journal of Process Control*, 140:103266.

Ujazdowski, T., Zubowicz, T., and Piotrowski, R. (2023). A comprehensive approach to SBR modelling for monitoring and control system design. *Journal of Water Process Engineering*, 53:103774.

Đurasević, M. and Jakobović, D. (2018). A survey of dispatching rules for the dynamic unrelated machines environment. *Expert Systems with Applications*, 113:555–569.

Vaccari, M., Foladori, P., Nembrini, S., and Vitali, F. (2018). Benchmarking of energy consumption in municipal wastewater treatment plants–a survey of over 200 plants in Italy. *Water Science and Technology*, 77(9):2242–2252.

Van Loosdrecht, M., Lopez-Vazquez, C., Meijer, S., Hooijmans, C., and Brdjanovic, D. (2015). Twenty-five years of ASM1: past, present and future of wastewater treatment modelling. *Journal of Hydroinformatics*, 17(5):697–718.

Verma, S., Kuila, A., and Jacob, S. (2023). Role of biofilms in waste water treatment. *Applied Biochemistry and Biotechnology*, 195(9):5618–5642.

Vetter, P. B., Stentoft, P. A., Munk-Nielsen, T., Madsen, H., and Møller, J. K. (2024). Toward smart wastewater treatment plants: a novel data-driven sludge blanket model based on stochastic differential equations. *Water Science & Technology*, 90(5):1397–1415.

Vrečko, D., Hvala, N., and Stražar, M. (2011). The application of model predictive control of ammonia nitrogen in an activated sludge process. *Water Science and Technology*, 64(5):1115–1121.

Wahl, S., Gahm, C., and Tuma, A. (2024). Serial-and hierarchical-batch scheduling: a systematic review and future research directions. *International Journal of Production Research*, 63(11):4238–4268.

Wahlberg, E. J. and Keinath, T. M. (1988). Development of settlung flux curves using SVI. *Journal of the Water Pollution Control Federation*, 60(12):2095–2100.

Wang, L., Zhou, G., Xu, Y., Wang, S., and Liu, M. (2012). An effective artificial bee colony algorithm for the flexible job-shop scheduling problem. *The International Journal of Advanced Manufacturing Technology*, 60:303–315.

Wang, T., Gao, H., and Qiu, J. (2016). A combined adaptive neural network and nonlinear model predictive control for multirate networked industrial process control. *IEEE Transactions on Neural Networks and Learning Systems*, 27(2):416–425.

Wang, Z., Gu, D., Lu, J., Zhang, N., Liu, Y., and Li, G. (2022). Scheduling of batch operation for a wastewater treatment plant under time-of-use electricity pricing. *ACS Omega Journal*, 7(32):28525–28533.

Watts, R. W., Svoronos, S. A., and Koopman, B. (1996). One-dimensional clarifier model with sludge blanket heights. *Journal of Environmental Engineering*, 122(12):1094–1100.

Wiese, J., Schmitt, S., Bergmann, R., and Schmitt, T. (2003). A case-based predictive sequencing batch reactor controller. In *Proceedings of the 18TH International Joint Conference on Artificial Intelligence, Workshop on Environmental Decision Support Systems (EDSS'2003)*. Morgan Kaufmann Publishers Inc.

Wodecka, B., Drewnowski, J., Białek, A., Łazuka, E., and Szulżyk-Cieplak, J. (2022). Prediction of wastewater quality at a wastewater treatment plant inlet using a system based on machine learning methods. *Processes*, 10(1):85.

Wu, C., Chen, Z., Liu, X., and Peng, Y. (2007). Nitrification–denitrification via nitrite in SBR using real-time control strategy when treating domestic wastewater. *Biochemical Engineering Journal*, 36(2):87–92.

Yuan, X., Nie, H., Yuan, Y., Su, A., and Wang, L. (2009). Hydrothermal systems generation scheduling using cultural algorithm. *Journal of Hydroinformatics*, 11(1):65–78.

Zaburko, J., Głowienka, R., Widomski, M. K., Szulżyk-Cieplak, J., Babko, R., and Łagód, G. (2020). Modeling of the aeration system of a sequencing batch reactor. *Journal of Ecological Engineering*, 21(7):249–256.

Zhong, R. Y., Dai, Q., Qu, T., Hu, G., and Huang, G. Q. (2013). Rfid-enabled real-time manufacturing execution system for mass-customization production. *Robotics and Computer-Integrated Manufacturing*, 29(2):283–292.

Zubowicz, T., Ujazdowski, T., Klawikowska, Z., and Piotrowski, R. (2024). An optimized dissolved oxygen concentration control in SBR with the use of adaptive and predictive control schemes. In *Proceedings of the 2024 European Control Conference (ECC)*, pages 1214–1221. IEEE.

Appendix A

Description of the DO model based on the mass balance

The concentration change in the control volume can be described by the mass balance with the reaction part (A.1).

$$\frac{\partial n(t)}{\partial t} = F_{\text{in}}(t) - F_{\text{out}}(t) + r(t) \tag{A.1}$$

where:

$n(t)$ - mass $[M]$,

$F_{\text{in}}(t)$ - input mass flow $[M\ T^{-1}]$,

$F_{\text{out}}(t)$ - output mass flow $[M\ T^{-1}]$,

$r(t)$ - production/consumption rates from bio-chemical conversion $[M\ T^{-1}]$.

To determine the derivative of concentration, mass is split into volume and concentration (A.2).

$$\frac{\partial n(t)}{\partial t} = \frac{\partial C(t) \cdot V(t)}{\partial t} = C(t) \cdot \frac{\partial V(t)}{\partial t} + V(t) \cdot \frac{\partial C(t)}{\partial t} \tag{A.2}$$

where:

$C(t)$ - concentrations of substances in an SBR $[M\ L^{-3}]$,

$V(t)$ - volume $[L^3]$.

Substituting (A.2) into (A.1) we obtain the following notation:

$$V(t) \cdot \frac{\partial C(t)}{\partial t} = F_{\text{in}}(t) - F_{\text{out}}(t) + r(t) - C(t) \cdot \frac{\partial V(t)}{\partial t} \tag{A.3}$$

Then, on the assumption that the concentration under consideration is dissolved oxygen, the below assumptions can be made. There is no effluent discharge or inflow during the reaction phase under aerobic conditions. Therefore, the flow rates as well as the volume change are zero. Thus, the equation (A.3) is simplified only to production/consumption rates from bio-chemical conversions.

$$\frac{\partial DO(t)}{\partial t} = \frac{1}{V} \cdot r(t) \tag{A.4}$$

During the reaction phase under aerobic conditions, air is supplied to the SBR, so r can be decomposed into the rate of oxygen transfer to SBR and the rate of oxygen uptake by micro-organisms (respiration) (Spanjers and Vanrolleghem (1995)).

$$r(t) = r_{in}(t) - r_{out}(t) \tag{A.5}$$

where:

$r_{in}(t)$ - rate of oxygen transfer,

$r_{out}(t)$ - rate of oxygen uptake by micro-organisms (respiration).

Oxygen is injected into the tank through a flow of air, distributed in the tank by a diffuser unit. The air, in the form of bubbles, rises, and the oxygen dissolves in the water. In addition, the saturation coefficient of dissolved oxygen is known to affect the dissolution rate of oxygen. According to Olsson and Newell (2005), the oxygen transfer function can be described as:

$$r_{in}(t) = K_L(Q_{air}(t)) \cdot (DO_{sat} - DO(t)) \tag{A.6}$$

where:

K_L - aeration coefficient,

$Q_{air}(t)$ - airflow rate,

$DO(t)$ - dissolved oxygen concentration,

DO_{sat} - saturated dissolved oxygen concentration.

Substituting (A.5) and (A.6) into (A.4) and assuming that the equation is considered for a control volume unit we obtain the following notation:

$$\frac{\partial DO(t)}{\partial t} = K_L(Q_{air}(t)) \cdot (DO_{sat} - DO(t)) - r_{out}(t) \tag{A.7}$$

Appendix B

Respiration rate for ASM3 with BioP

The starting point for the analysis is the form of the dissolved oxygen (DO) equation derived from the ASM3 with BioP model. The dynamics of oxygen concentration are expressed as a linear combination of process rates $r_i(t)$ (for clarity, the time dependency for process rates has been omitted) and their corresponding stoichiometric coefficients p_i:

$$\begin{aligned}\frac{dDO(t)}{dt} &= p_{13}\cdot r_{13} + p_2\cdot r_2 + p_4\cdot r_4 + p_6\cdot r_6 + p_8\cdot r_8 \\ &+p_{10}\cdot r_{10} + p_{11}\cdot r_{11} + p_{15}\cdot r_{15} + p_{17}\cdot r_{17} + p_{19}\cdot r_{19} + p_{23}\cdot r_{23}.\end{aligned} \tag{B.1}$$

In this formulation, the element $p_{13}\cdot r_{13}$ corresponds to the aeration process, while the remaining terms represent oxygen consumption by biochemical reactions such as substrate storage, heterotrophic and autotrophic growth, decay, and phosphorus-related processes. For clarity, the equation can also be expressed in the compact form:

$$\frac{dDO(t)}{dt} = DO_{inf}(t) + R(t) \tag{B.2}$$

where $DO_{inf}(t)$ describes oxygen inflow due to aeration, and $R(t)$ represents the total oxygen consumption by biological reactions.

The stoichiometric coefficients p_i used in the model are summarised in Table B.1. Subsequently, the forms of the process rate equations for ASM3 and BioP models, as well as the oxygen transfer equation, are presented in Table B.2. For the sake of clarity, the tables below do not include time-dependent notation. Temperature correction factors (fT_1, fT_2, fT_3, fT_4) account respectively for hydrolysis and heterotroph decay, autotrophic processes, and oxygen transfer. By isolating the common saturation terms, the DO equation can be reformulated in a more compact structure. This step reveals the relationship between measurable variables and respiration rates:

$$\begin{aligned}\frac{dDO(t)}{dt} &= p_{13}\, r_{13}(t) + \frac{DO(t)}{a+DO(t)}\hat{R}_1(t) + \\ &\frac{DO(t)}{a+DO(t)}\left(\frac{ALK(t)}{b+ALK(t)}\frac{PO_4(t)}{c+PO_4(t)}\left(\hat{R}_2(t) + \frac{NH(t)}{d+NH(t)}\,\hat{R}_3(t)\right)\right)\end{aligned} \tag{B.3}$$

where the constants a, b, c, and d are defined as: $a = 0.2,\ b = 0.1,\ c = 0.01,\ d = 0.01$.

This transformation enables the separation of measurable quantities (DO, ALK, PO_4, NH) from grouped respiration components. The latter can be defined as follows:

$$\hat{R}_1(t) = p_2 \cdot \bar{r}_2 + p_6 \cdot \bar{r}_6 + p_8 \cdot \bar{r}_8 + p_{11} \cdot \bar{r}_{11} + p_{19} \cdot \bar{r}_{19} + p_{23} \cdot \bar{r}_{23} \tag{B.4}$$

$$\hat{R}_2(t) = p_{15}\, \bar{r}_{15}(t) \left(\frac{c + PO_4(t)}{0.2 + PO_4(t)} \right) \tag{B.5}$$

$$\begin{aligned} \hat{R}_3(t) =& p_4 \cdot \bar{r}_4 + p_{17} \cdot \bar{r}_{17} \left(\frac{d + NH(t)}{0.05 + NH(t)} \right) \\ &+ p_{10} \cdot \bar{r}_{10} \left(\frac{a + DO(t)}{0.5 + DO(t)} \right) \left(\frac{b + ALK(t)}{0.5 + ALK(t)} \right) \left(\frac{d + NH(t)}{1 + NH(t)} \right) \end{aligned} \tag{B.6}$$

The grouped respiration terms $\hat{R}_1(t)$, $\hat{R}_2(t)$, and $\hat{R}_3(t)$ capture the contributions of heterotrophic, phosphorus-related, and nitrification processes, respectively.

By introducing the numerical values of the stoichiometric coefficients from the ASM3 with BioP model, the simplified set of equations (Table B.3) is converted into its numerical form (Table B.4b), based on data from (Rieger et al., 2001) and (Henze et al., 1999). This highlights the specific contributions of different respiration pathways, where the saturation coefficients differ from the generalised measurements.

Finally, the overall structure of the oxygen dynamics can be expressed as a saturation-dependent respiration model:

$$\overline{R}(t) = \frac{DO(t)}{K + DO(t)} R(t) \tag{B.7}$$

with the grouped respiration rate:

$$R(t) = \hat{R}_1(t) + \frac{ALK(t)}{b + ALK(t)} \frac{PO_4(t)}{c + PO_4(t)} \left(\hat{R}_2(t) + \frac{NH(t)}{d + NH(t)}\, \hat{R}_3(t) \right) \tag{B.8}$$

This final form clearly separates the measurable inputs (DO, ALK, PO_4, NH) from grouped respiration processes, thereby facilitating further analysis of the oxygen dynamics in the ASM3 with BioP model.

Table B.1: Parameters of the DO equation in ASM3+BioP model

Parameter	Definition
p_2	$YSTO_{O2} - 1$
p_4	$1 - \left(\frac{1}{YH_{O2}}\right)$
p_6	$-1 \cdot (1 - fXI)$
p_8	-1
p_{10}	$\left(-\frac{64}{14 \cdot YA}\right) + 1$
p_{11}	$-1 \cdot (1 - fXI)$
p_{13}	1
p_{15}	$-Y_{PHA}$
p_{17}	$1 - \left(\frac{1}{YPAO_{O2}}\right)$
p_{19}	$-(1 - fXI)$
p_{23}	-1

Table B.2: Equations of the ASM3+BioP respiration model

(a) ASM3 model equations

Model	*Equation*
r_2	$fT2 \cdot k_{sto} \cdot \frac{DO}{KHO2+DO} \cdot \hat{r}_2$
r_4	$fT2 \cdot \mu_H \cdot \frac{DO}{KHO2+DO} \cdot \frac{NH}{KHNH4+NH} \cdot \frac{ALK}{KHALK+ALK} \cdot \frac{PO4}{KHPO4+PO4} \cdot \hat{r}_4$
r_6	$fT2 \cdot b_H \cdot \frac{DO}{KHO2+DO} \cdot \hat{r}_6$
r_8	$fT2 \cdot b_H \cdot \frac{DO}{KHO2+DO} \cdot \hat{r}_8$
r_{10}	$fT3 \cdot \mu_A \cdot \frac{DO}{KNO2+DO} \cdot \frac{NH}{KNNH4+NH} \cdot \frac{ALK}{KNALK+ALK} \cdot \frac{PO4}{KAPO4+PO4} \cdot \hat{r}_{10}$
r_{11}	$fT3 \cdot b_{AUT} \cdot \frac{DO}{KHO2+DO} \cdot \hat{r}_{11}$

(b) Oxygen transfer equation

Model	*Equation*
r_{13}	$fT_4 \cdot \alpha \cdot R_{air} \cdot \frac{h-h_{\text{diff}}}{DO_{\text{sat}} \cdot V_{\max}} \cdot Q_{\text{air}} \cdot (DO_{\text{sat}}(T) - DO)$

(c) BioP model equations

Model	*Equation*
r_{15}	$fT1 \cdot q_{PP} \cdot \frac{DO}{KPAOO+DO} \cdot \frac{PO4}{KPPPO4+PO4} \cdot \frac{ALK}{KPAOALK+ALK} \cdot \hat{r}_{15}$
r_{17}	$fT2 \cdot \mu_{PAO} \cdot \frac{DO}{KPAOO+DO} \cdot \frac{NH}{KPNH4+NH} \cdot \frac{PO4}{KPAOPO4+PO4} \cdot \frac{ALK}{KPAOALK+ALK} \cdot \hat{r}_{17}$
r_{19}	$fT2 \cdot b_{PAO} \cdot \frac{DO}{KPAOO+DO} \cdot \hat{r}_{19}$
r_{23}	$fT2 \cdot b_{PHA} \cdot \frac{DO}{KPAOO+DO} \cdot \hat{r}_{23}$

Table B.3: Simplified equations with grouped respiration terms

(a) ASM3 model (simplified form)

Model	*Equation*
r_2	$\frac{DO}{KHO2+DO} \cdot \bar{r}_2$
r_4	$\frac{DO}{KHO2+DO} \cdot \frac{NH}{KHNH4+NH} \cdot \frac{ALK}{KHALK+ALK} \cdot \frac{PO4}{KHPO4+PO4} \cdot \bar{r}_4$
r_6	$\frac{DO}{KHO2+DO} \cdot \bar{r}_6$
r_8	$\frac{DO}{KHO2+DO} \cdot \bar{r}_8$
r_{10}	$\frac{DO}{KNO2+DO} \cdot \frac{NH}{KNNH4+NH} \cdot \frac{ALK}{KNALK+ALK} \cdot \frac{PO4}{KAPO4+PO4} \cdot \bar{r}_{10}$
r_{11}	$\frac{DO}{KHO2+DO} \cdot \bar{r}_{11}$

(b) BioP model (simplified form)

Model	*Equation*
r_{15}	$\frac{DO}{KPAOO+DO} \cdot \frac{PO4}{KPPPO4+PO4} \cdot \frac{ALK}{KPAOALK+ALK} \cdot \bar{r}_{15}$
r_{17}	$\frac{DO}{KPAOO+DO} \cdot \frac{NH}{KPNH4+NH} \cdot \frac{PO4}{KPAOPO4+PO4} \cdot \frac{ALK}{KPAOALK+ALK} \cdot \bar{r}_{17}$
r_{19}	$\frac{DO}{KPAOO+DO} \cdot \bar{r}_{19}$
r_{23}	$\frac{DO}{KPAOO+DO} \cdot \bar{r}_{23}$

Table B.4: Numerical form of the simplified equations

(a) ASM3 model (numerical values)

Model	*Equation*
r_2	$\frac{DO}{0.2+DO} \cdot \bar{r}_2$
r_4	$\frac{DO}{0.2+DO} \cdot \frac{NH}{0.01+NH} \cdot \frac{ALK}{0.1+ALK} \cdot \frac{PO4}{0.01+PO4} \cdot \bar{r}_4$
r_6	$\frac{DO}{0.2+DO} \cdot \bar{r}_6$
r_8	$\frac{DO}{0.2+DO} \cdot \bar{r}_8$
r_{10}	$\frac{DO}{0.5+DO} \cdot \frac{NH}{1.0+NH} \cdot \frac{ALK}{0.5+ALK} \cdot \frac{PO4}{0.01+PO4} \cdot \bar{r}_{10}$
r_{11}	$\frac{DO}{0.2+DO} \cdot \bar{r}_{11}$

(b) BioP model (numerical values)

Model	*Equation*
r_{15}	$\frac{DO}{0.2+DO} \cdot \frac{PO4}{0.2+PO4} \cdot \frac{ALK}{0.1+ALK} \cdot \bar{r}_{15}$
r_{17}	$\frac{DO}{0.2+DO} \cdot \frac{NH}{0.05+NH} \cdot \frac{PO4}{0.01+PO4} \cdot \frac{ALK}{0.1+ALK} \cdot \bar{r}_{17}$
r_{19}	$\frac{DO}{0.2+DO} \cdot \bar{r}_{19}$
r_{23}	$\frac{DO}{0.2+DO} \cdot \bar{r}_{23}$

Appendix C

Single-objective optimisation of SBR operation cycle

The problem under consideration is defined as the minimisation of the objective function using stochastic optimisation methods. The developed solution provides optimal values for the DO concentration, the number of reaction cycles, the duration of aerobic phases, and the duration of anaerobic phases. Thus, the solution obtained represents the parameters of the SBR cycle. The decision variables used in the objective function, representing specific process parameters, are summarised in Table C.1.

Table C.1: Decision variables for the SOO task.

Symbol	**Description**	**Type**	**Unit**
x_1	Duration of aerobic phase	Real	$[d]$
x_2	Duration of anaerobic phase	Real	$[d]$
x_3	Number of reaction cycles	Integer	$[-]$
x_4	DO concentration set point, $DO_{\text{ref}}(t)$	Real	[g O_2/m^3]
x_5	TN at the end of the cycle	Real	[g N/m^3]
x_6	TP at the end of the cycle	Real	[g P/m^3]
x_7	COD at the end of the cycle	Real	[g O_2/m^3]

The optimisation task is addressed by simulating a simplified ASM2d model as SBR. The model was derived in a similar way to that described for the ASM3e (see Section 3.3). These simulations estimate the values of x_5, x_6, and x_7 during the decanting phase. This approach provides a straightforward method for evaluating the level of pollution reduction while not requiring difficult online measurements to be provided.

Therefore, for the model under consideration and the given decision variables, the designed optimisation task takes the form of a mixed-integer non-linear optimisation problem. The solution to such problems is not trivial and is often computationally demanding (Belotti et al. (2013)). This complexity arises from the combination of mixed decision variables (integer and real in this example) and non-linear relationships (both in the model and the cost function), which significantly increases the solution space and the difficulty of finding a global optimum.

Details of the objective function used are presented in Section C.1. Next, Section C.2 extends the optimisation problem with constraints on the decision variables. The algorithms used

to obtain the solution to the optimisation problem are presented in Section C.3. The SOO approach forms the basis for the MOO problem used and complements the content of the research. However, as previously mentioned, the models used in this appendix are inconsistent with those adopted in the rest of the research. To maintain model consistency across the dissertation, detailed results of this auxiliary study are omitted and referenced to the corresponding publication. Instead, the reader is referred to the source paper (Ujazdowski et al. (2024)).

C.1 Objective Function

Using the decision variables presented in Table C.1, an optimisation problem was proposed:

$$\min J(\boldsymbol{x}) = \underbrace{1000 \cdot x_1 x_3 x_4}_{\text{aeration}} + \underbrace{x_5^3 + 0.1 \cdot x_6^3 + 10^{-3} \cdot x_7}_{\text{quality indicators}} + \underbrace{p_{\text{TN}}(x_5) + p_{\text{TP}}(x_6) + p_{\text{COD}}(x_7)}_{\text{penalty functions}}, \quad \text{(C.1)}$$

where:

$$p_{\text{TN}}(x_5) = \begin{cases} 1000, & x_5 < 0, \\ 0, & 0 \leq x_5 \leq 10, \\ 0.4 \cdot (x_5 - 10)^2 + 0.15, & 10 < x_5 \leq 15, \\ 1000, & x_5 > 15, \end{cases} \quad \text{(C.2a)}$$

$$p_{\text{TP}}(x_6) = \begin{cases} 1000, & x_6 < 0, \\ 0, & 0 \leq x_6 \leq 1, \\ 0.02 \cdot (x_6 - 1)^2 + 0.01, & 1 < x_6 \leq 2, \\ 1000, & x_6 > 2, \end{cases} \quad \text{(C.2b)}$$

$$p_{\text{COD}}(x_7) = \begin{cases} 1000, & x_7 < 0, \\ 0.01 \cdot (x_7 - 80)^2 + 0.01, & 80 < x_7 \leq 125, \\ 1000, & x_7 > 125. \end{cases} \quad \text{(C.2c)}$$

The objective function of the formulated optimisation problem consists of three main elements. The first term, $x_1 x_3 x_4$, represents the cost of aeration, calculated as the product of the duration of the aerobic phase, their number, and the corresponding $DO_{\text{ref}}(t)$.

The next terms are related to the measured quality indicators of the wastewater treatment process. The decision variables x_5, x_6, and x_7, along with their respective weights, aim to minimise the concentrations of TN, TP, and COD, respectively.

The third element of the objective function is the penalty function, consisting of $p_{\text{TN}}(x_5)$, $p_{\text{TP}}(x_6)$, and $p_{\text{COD}}(x_7)$, as defined in (C.2a)–(C.2c). This term imposes additional costs if specific TN, TP, and COD concentration requirements are unmet.

The resulting optimisation problem is complex, characterised by non-linearity and non-convexity, as the Hessian matrix of (C.1) is not positive semidefinite. Additionally, it is hybrid in nature due to the presence of decision variables of different types.

C.2 Constraints

The decision variables x_1, x_2, x_3, and x_4 were subjected to constraints based on both theoretical insights into the process and outcomes from simulation studies. The minimum values for x_1 and x_2, representing the shortest allowable durations for the aerobic and anaerobic phases within a sequence, were determined by analysing the dynamics of DO and the performance of the aeration system. The batch process phase lengths used in practice determined the upper limits for these variables. The range for x_3, the number of phases, was set according to empirical observations. It is acknowledged that the absence of a relationship between the maximum phase length and the number of reaction cycles characterises this approach. Consequently, this approach is limited to increasing reaction cycle numbers rather than utilising longer cycles. Next, for the variable x_4, corresponding to the reference oxygen concentration DO_{ref}, the theoretical minimum value of 0.5 g O_2/m^3 was established, while the theoretical maximum value was constrained by the saturation concentration $C_{\text{SO}}(20°\text{C})$. To maintain operational efficiency and economic feasibility, the range of x_4 was narrowed to values commonly observed in practice, as aeration near the saturation limit is not cost-effective.

The specific constraints imposed on the decision variables were as follows:

$$0.02 \leq x_1 \leq 0.10, \tag{C.3a}$$

$$0.02 \leq x_2 \leq 0.10, \tag{C.3b}$$

$$1 \leq x_3 \leq 7, \tag{C.3c}$$

$$1.00 \leq x_4 \leq 3.00. \tag{C.3d}$$

C.3 Algorithms

When designing the process optimisation layer, a stochastic population-based method was chosen to address the formulated SOO problem. This approach was selected because such algorithms, relying on probabilistic techniques, are better equipped to handle the non-convex nature of the objective function, thereby reducing the risk of becoming trapped in local extrema. Given the hybrid nature of the optimisation problem, including the presence of an integer-type decision variable, modifications to the standard optimisation algorithm were required to incorporate integer programming capabilities.

A schematic representation of the proposed process optimisation system is provided in Fig. C.1. The SOO problem is solved for a given influent scenario by calling in each iteration a simplified SBR model. The optimisation algorithm employed a combination of the GA (Katoch et al. (2021)) and the B&B methods (Costa et al. (2001)). This hybrid strategy first uses the B&B method to divide the decision space into smaller sub-problems and then applies GA to search for solutions within these subsets.

The B&B algorithm operates by constructing a tree that represents the solution space of the optimisation problem and systematically exploring it to identify the optimal solution. The algorithm involves two main steps: branching, where the solution space is divided into smaller subsets, forming branches of the tree, and bounding, where branches that cannot contain the

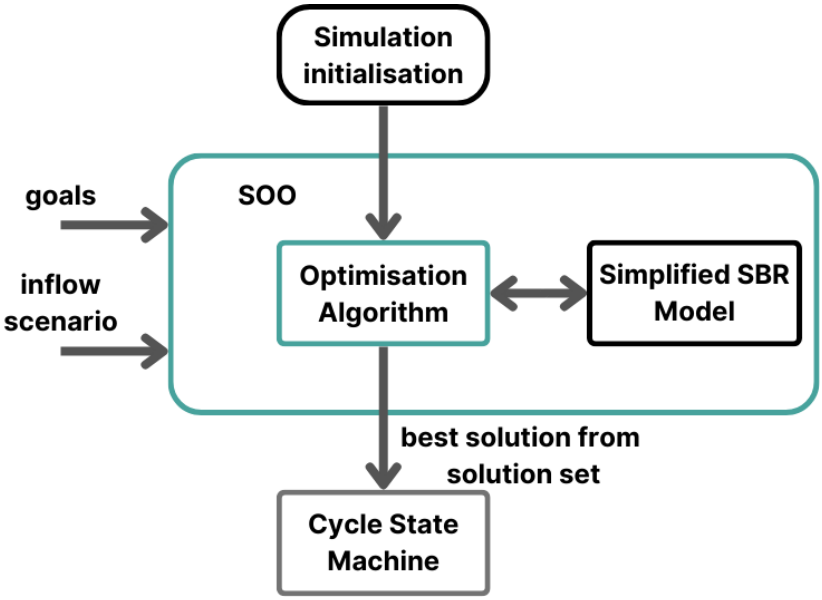

Figure C.1: Cycle optimisation SOO

optimal solution are identified and eliminated based on bounds.

The B&B method is classified as an exact algorithm, meaning it searches all possible and feasible solutions to guarantee to find the optimal solution. However, this rigorous approach comes with significant computational demands. For complex optimisation problems, the B&B method can be to slow, requiring substantial computational resources and time, even to verify the existence of an optimal solution. In the case under consideration, getting an exact solution in a reasonable time becomes challenging, even with strong constraints on the decision variables.

One way to address this challenge is through a hybrid approach similar to MA. A stochastic method is introduced to locally enhance the branches of the tree, where a local search that considers each subset's constraints is implemented. The drawback of this solution is that it drifts away from the notion of exactness of the B&B algorithm, and there is no guarantee of obtaining an optimal solution (the solutions found are close to optimal, i.e. suboptimal).

A classical GA was chosen as the stochastic algorithm running in each iteration of the B&B method (see Fig. C.2). The GA starts with the random initialisation of individuals in binary form, evaluated based on the fitness function. The process involves selecting the best-adapted individuals, incorporating elitism, and creating the next generation through crossover and mutation operations. This cycle continues until a specified stopping criterion is met. The algorithm provides an approximate solution to the formulated problem with well-chosen parameters. The parameters of the implemented GA are presented in Table C.2

Table C.2: GA parameters

Parameter Name	**Value**
Population size	80
Elite individuals	2
Crossover rate – fraction of the next generation created by crossover	0.90
Number of generations	30
Stopping criterion – execution time without solution improvement [s]	120
Stopping criterion – number of generations without solution improvement	15

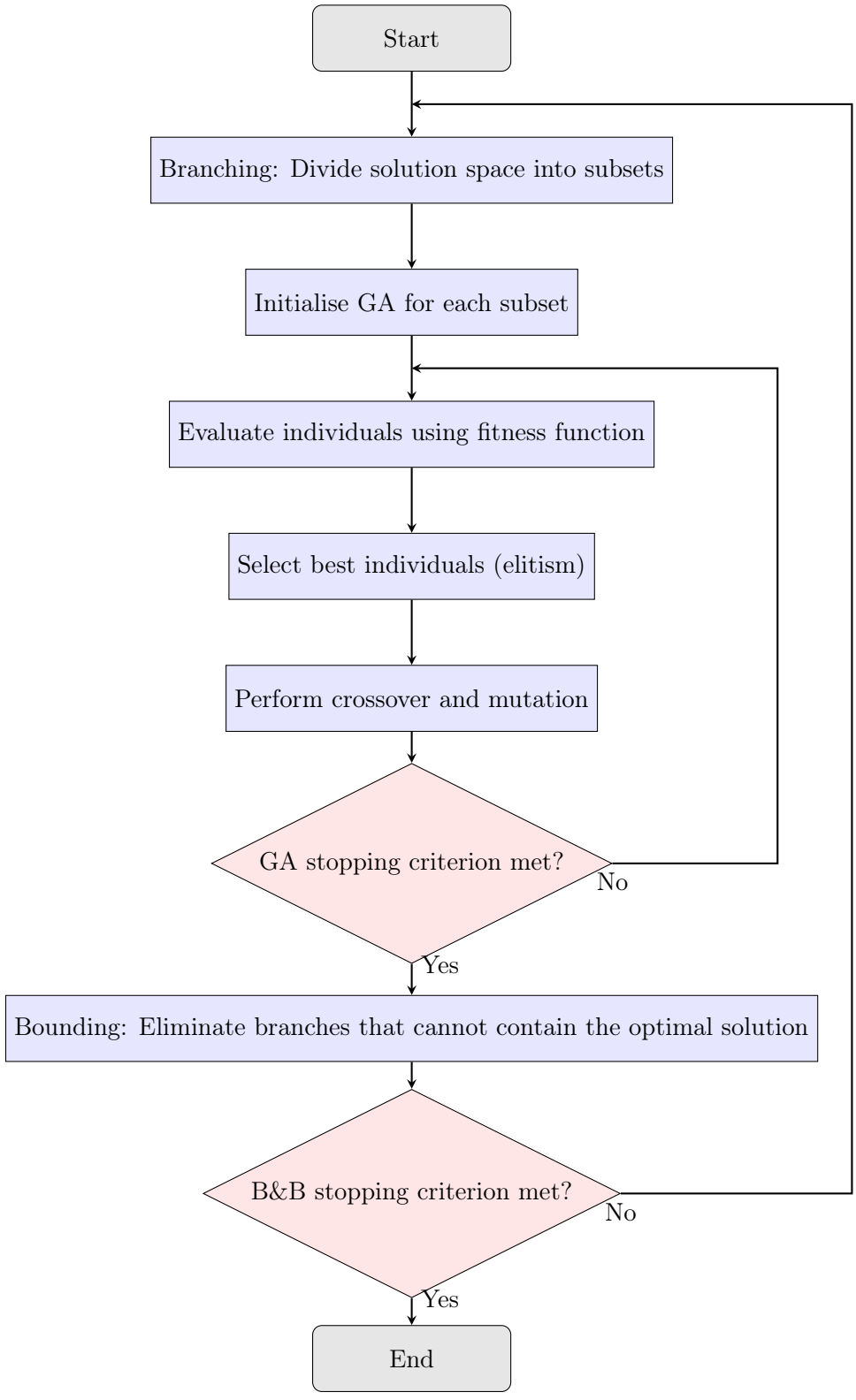

Figure C.2: B&B and GA optimisation algorithm